

Bacterial Degradation of Isoprene in the Terrestrial Environment

Myriam El Khawand

A thesis submitted to the University of East Anglia in
fulfillment of the requirements for the degree of Doctor of Philosophy

School of Environmental Sciences

November 2014

©This copy of the thesis has been supplied on condition that anyone who consults it is understood to recognise that its copyright rests with the author and that use of any information derive there from must be in accordance with current UK Copyright Law. In addition, any quotation or extract must include full attribution.

Abstract

Isoprene is a climate active gas emitted from natural and anthropogenic sources in quantities equivalent to the global methane flux to the atmosphere. 90 % of the emitted isoprene is produced enzymatically in the chloroplast of terrestrial plants from dimethylallyl pyrophosphate via the methylerythritol pathway. The main role of isoprene emission by plants is to reduce the damage caused by heat stress through stabilizing cellular membranes. Isoprene emission from microbes, animals, and humans has also been reported, albeit less understood than isoprene emission from plants. Despite large emissions, isoprene is present at low concentrations in the atmosphere due to its rapid reactions with other atmospheric components, such as hydroxyl radicals. Isoprene can extend the lifetime of potent greenhouse gases, influence the tropospheric concentrations of ozone, and induce the formation of secondary organic aerosols. While substantial knowledge exists about isoprene production and atmospheric chemistry, our knowledge of isoprene sinks is limited. Soils consume isoprene at a high rate and contain numerous isoprene-utilizing bacteria. However, *Rhodococcus* sp. AD45 is the only terrestrial isoprene-degrading bacterium characterized in any detail. A pathway for isoprene degradation involving a putative soluble monooxygenase has been proposed. In this study, we report the isolation of two novel isoprene-degrading bacteria and characterization of the isoprene gene clusters in their draft genomes. Using marker exchange mutagenesis, transcription assays and proteomics analyses, we provide conclusive evidence that isoprene is metabolized in *Rhodococcus* sp. AD45 through the induced activity of soluble isoprene monooxygenase, a close relative to well known soluble diiron center monooxygenase enzymes. Metabolic gene PCR assays based on a key component of isoprene monooxygenase were also developed to detect isoprene degraders in the environment. The diversity of active isoprene degraders in the terrestrial environment was investigated using DNA-stable isotope probing experiments combined with 454 pyrosequencing.

Dedicated to my loving parents

Table of contents

Abstract	2
List of tables	9
List of figures	11
List of abbreviations	15
Acknowledgements	16
Chapter 1	17
Introduction	17
1.1 Isoprene	18
1.2 Isoprene and atmospheric chemistry	18
1.3 Isoprene production	22
1.3.1 Isoprene biosynthesis by plants	24
1.3.1.1 Environmental factors influencing isoprene emission from leaves	28
1.3.1.2 The role of isoprene in plant protection	32
1.3.2 Isoprene production by microbes.....	35
1.3.3 Isoprene production by animals and humans.....	36
1.3.4 Isoprene production in the marine environment	38
1.4 Isoprene and climate change	40
1.5 Bacterial degradation of isoprene	41
1.6 Project aims	46
Chapter 2	48
Materials and Methods	48
2.1 General purpose buffer and solutions.....	52
2.2 Cultivation of <i>Rhodococcus sp.</i> strains AD45, LB1 and SC4.....	53
2.3 Purity checks and maintenance of bacterial strains	54
2.4 Quantification of headspace concentration of isoprene.....	55

2.5	Extraction of nucleic acids	55
2.5.1	Extraction of genomic DNA	55
2.5.2	Small-scale plasmid extraction	57
2.5.3	RNA extraction	57
2.6	Nucleic acid manipulation methods	58
2.6.1	Quantification of DNA and RNA	58
2.6.2	Nucleic acid purification.....	58
2.6.3	DNA restriction digests	58
2.6.4	Polymerase chain reaction (PCR)	58
2.6.5	Cloning of PCR products.....	59
2.6.6	Clone library construction and Restriction Fragment Length Polymorphism (RFLP) assays	59
2.6.7	DNA ligations	59
2.6.8	Agarose gel electrophoresis	59
2.6.9	Reverse transcription PCR (RT-PCR)	60
2.6.10	Quantitative Reverse Transcription - PCR (qRT-PCR).....	60
2.6.11	DNA sequencing.....	61
2.7	Antibiotics	61
2.8	Preparation of SOC medium	62
2.9	Transformation of chemically competent <i>E. coli</i>	62
2.10	Preparation and transformation of electrocompetent <i>E.coli</i>	62
2.11	Conjugual transfer of pMEK plasmid from <i>E. coli</i> to <i>Rhodococcus AD45</i> ...	63
2.12	Preparation and transformation of electrocompetent <i>Rhodococcus sp. AD45</i>	64
2.13	Sucrose selection for double cross-over mutants	64
2.14	Analysis of proteins.....	65
2.14.1	Harvesting of cells and preparation of cell-free extracts	65
2.14.2	Protein quantification.....	65

2.14.3 Sodium Dodecyl Sulfate-Polyacrylamide Gel Electrophoresis (SDS-PAGE).....	65
2.14.4 Mass spectrometry analysis of polypeptides	66
2.15 DNA- Stable Isotope Probing (DNA- SIP)	67
2.16 Denaturing gradient gel electrophoresis (DGGE)	67
2.17 Bacterial community analysis by 454 pyrosequencing	68
Chapter 3	69
Isolation of novel terrestrial isoprene degrading bacteria and preliminary analyses of the genome sequences of <i>Rhodococcus</i> AD45, <i>Rhodococcus</i> SC4 and <i>Rhodococcus</i> LB1	69
3.1 Introduction	70
3.2 Enrichment and isolation of two novel terrestrial isoprene degraders	70
3.3 The two new isolates were identified as <i>Rhodococcus</i> strains	71
3.4 Growth profile of <i>Rhodococcus</i> strains AD45, LB1, SC4 on selected substrates	74
3.5 General genome features	75
3.6 Overview of the potential metabolic pathways of <i>Rhodococcus</i> strains AD45, SC4 and LB1	76
3.7 Isoprene oxidation pathway.....	82
3.8 Isoprene monooxygenase is a soluble diiron centre monooxygenase	87
3.9 Glutathione as a cofactor in the isoprene oxidation pathway.....	95
3.10 Pathways of alkane oxidation in <i>Rhodococcus</i> strains AD45, LB1 and SC4	96
3.11 Terminal versus subterminal oxidation of propane in <i>Rhodococcus</i> SC4 and <i>Rhodococcus</i> LB1.....	102
3.12 Rubber degradation	103
Chapter 4	105
Mutagenesis and regulation of <i>isoA</i> in <i>Rhodococcus</i> AD45.....	105
4.1 Introduction	106

4.2 Mutagenesis of <i>isoA</i> in <i>Rhodococcus</i> AD45	107
4.2.1 Antibiotic sensitivity of <i>Rhodococcus</i> AD45	107
4.2.2 Construction of a pK18 <i>mobsacB</i> -based plasmid for mutagenesis of <i>isoA</i>	108
4.2.3 Transfer of DNA into <i>Rhodococcus</i> AD45.....	112
4.2.4 Screening for <i>IsoA</i> single cross-over mutant	115
4.2.5 Assessment of selective pressure on the single cross-over mutant.....	118
4.2.6 Selection for <i>isoA</i> double cross-over mutants.....	119
4.3 Assays of <i>isoA</i> transcription using quantitative RT-PCR.....	123
4.3.1 <i>isoA</i> is transcribed during growth on isoprene as shown by RT-PCR....	123
4.3.2 <i>isoA</i> transcription is upregulated during growth on isoprene as shown by quantitative RT-PCR.....	125
4.4 The isoprene gene cluster is induced by growth on isoprene.....	129
4.5 Discussion	131
Chapter 5	134
Design and evaluation of primers for the detection of genes encoding isoprene monooxygenase alpha subunit in the environment	134
5.1 Introduction	135
5.2 Design of primers targeting <i>isoA</i> gene which encodes the alpha subunit of the isoprene monooxygenase	135
5.3 Optimization of PCR protocol for <i>isoA</i> amplification.....	141
5.4 Evaluation and validation of the primers	143
5.5 Discussion	154
Chapter 6	159
Identification of active bacterial isoprene degraders in environmental soil samples	159
6.1 Introduction	160
6.2 DNA-SIP experiments with partially labelled ¹³ C-isoprene	161

6.2.1 Experimental set-up	161
6.2.2 DNA extraction from soil, density gradient ultracentrifugation and fractionation	162
6.2.3 Analysis of the bacterial community profile by 16S rRNA gene profiling using Denaturing Gradient Gel Electrophoresis (DGGE)	162
6.2.4 Identification of active isoprene degraders by 454 16S rRNA amplicon sequencing	165
6.2.5 Analysis of <i>isoA</i> amplicon sequences	172
6.3 DNA-SIP experiments with fully labelled ¹³ C-isoprene	173
6.3.1 Experimental set-up	173
6.3.2 Processing of the SIP incubations.....	174
6.3.3 DGGE profiles of 16S rRNA genes amplified from DNA extracted from heavy and light fractions of the ¹³ C-incubated microcosms	174
6.3.4 Analysis of 454 pyrosequencing data	177
6.3.5 Analysis of <i>isoA</i> amplicon sequences	186
6.4 Discussion	189
Chapter 7	191
Final discussion	191
References	196

List of tables

Table 2.1 List of bacterial strains	49-50
Table 2.2 List of plasmids used in this study	51
Table 3.1 Growth profile of <i>Rhodococcus strains</i> AD45, SC4 and LB1.....	74
Table 3.2 Summary of genome content of <i>Rhodococcus</i> AD45, <i>Rhodococcus</i> SC4 and <i>Rhodococcus</i> LB1.....	75
Table 3.3 Comparison of <i>Rhodococcus</i> AD45, <i>Rhodococcus</i> LB1 and <i>Rhodococcus</i> SC4 genomes with those of selected <i>Rhodococcus</i> strains.....	76
Table 3.4 The isoprene gene cluster present in the <i>Rhodococcus</i> AD45 megaplasmid.....	83
Table 3.5 The isoprene gene cluster present in the genome of <i>Rhodococcus</i> LB1...84	
Table 3.6 The isoprene gene cluster present in the genome of <i>Rhodococcus</i> SC4...85	
Table 3.7 Propane monooxygenase gene clusters of <i>Rhodococcus sp.</i> SC4 and <i>Rhodococcus sp.</i> LB1	98
Table 4.1 Testing for antibiotic sensitivity of <i>Rhodococcus</i> AD45.....	108
Table 4.2 List of primers used in these experiments.....	109
Table 4.3 Electroporation of <i>Rhodococcus</i> AD45 with pNV18.....	114
Table 4.4 Electroporation of <i>Rhodococcus</i> AD45 with pNV18.....	115
Table 4.5 Assessment of selective pressure on the single cross-over mutant.....	119
Table 4.6 List of primers used for RT-PCR.....	124
Table 4.7 List of primers used for quantitative RT-PCR.....	125
Table 4.8 Determination of the efficiency of the qRT-PCR amplification of <i>isoA</i> and <i>rpoB</i>	127
Table 4.9 qRT-PCR data	128
Table 4.10 Polypeptides identified in the bands excised from the gel in Figure 4.15	131
Table 5.1 <i>isoA</i> degenerate primers	140
Table 5.2 TouchDown PCR protocol for <i>isoA</i> amplification	142
Table 5.3 List of the non-isoprene degrading <i>isoA</i> ⁻ bacteria tested	152

Table 5.4 Marine isoprene-degrading bacteria used in the validation of <i>isoA</i> primers.....	155
Table 6.1 Primers used for the amplification of 16S rRNA genes from the fractionated samples.....	163
Table 6.2 Primers used for 454 16S rRNA amplicon sequencing	166
Table 6.3 Bacterial composition of the light fraction (¹² C-DNA) and heavy fraction (¹³ C-DNA) of the ¹³ C-isoprene enriched microcosms, at the phylum level.....	167
Table 6.4 Bacterial composition of the isoprene-enriched microcosms at the order, family or genus level.....	169-170-171
Table 6.5 Number of 454 reads that passed quality control for each sample.....	178
Table 6.6 Bacterial composition of T ₀ and T ₁ microcosms as well as the heavy and light fractions of the SIP incubations, at the phylum level.....	181
Table 6.7 Bacterial composition of the samples, at the genus level.....	183-184-185
Table 6.8 Analysis of 454 <i>isoA</i> sequences from the ¹³ C-isoprene enriched microcosms and comparison of representative IsoA sequences with IsoA of <i>Rhodococcus</i> AD45.....	187-188

List of figures

Figure 1.1 Isoprene structure	18
Figure 1.2 Possible products of the reaction of isoprene with OH radicals.....	19
Figure 1.3 Secondary organic particles are key component of atmospheric aerosols.....	21
Figure 1.4 Estimated global isoprene emission for 2003.....	23
Figure 1.5 Isoprene synthesis reaction.....	26
Figure 1.6 Methylerythritol phosphate (MEP) pathway of isoprenoid biosynthesis.....	27
Figure 1.7 Isoprene emission (measured as a flux) in oak leaves as a function of temperature.....	29
Figure 1.8 Possible scenarios of the role of isoprene in protecting photosynthetic membranes.....	33
Figure 1.9 Endogenous production of isoprene as a by-product of the mevalonate pathway of cholesterol biosynthesis.....	38
Figure 1.10 Organisation of the <i>isoABCDEFGHIJ</i> gene cluster from <i>Rhodococcus sp.</i> AD45.....	42
Figure 1.11 Proposed pathway of isoprene metabolism in <i>Rhodococcus sp.</i> AD45.....	45
Figure 2.1 <i>Rhodococcus sp.</i> AD45 genomic DNA in comparison to <i>HindIII</i> -digested Lambda DNA standard.....	56
Figure 3.1 Neighbour-joining phylogenetic tree (Bootstrap 100) based on the alignment of 16S rRNA gene sequences (1,437 bp).....	72-73
Figure 3.2 KEGG recruitment plot of the genes involved in the TCA cycle in <i>Rhodococcus sp.</i> SC4.....	77
Figure 3.3 KEGG recruitment plot of the genes involved in the TCA cycle <i>Rhodococcus sp.</i> AD45.....	78
Figure 3.4 KEGG recruitment plot of the genes involved in nitrogen metabolism in <i>Rhodococcus sp.</i> SC4.....	79
Figure 3.5 KEGG recruitment plot of the genes involved in nitrogen metabolism in <i>Rhodococcus sp.</i> LB1.....	80

Figure 3.6 KEGG recruitment plot of the genes involved in nitrogen metabolism in <i>Rhodococcus sp</i> AD45.....	81
Figure 3.7 Comparison of the isoprene gene clusters across the terrestrial isoprene degrading <i>Rhodococcus</i> strains.....	86
Figure 3.8 Phylogenetic relationships between IsoA and hydroxylase α -subunits of other representative SDIMOs.....	89
Figure 3.9 Partial alignment of deduced amino acid sequences of isoprene monooxygenase α -subunit and hydroxylase α -subunits of representative SDIMOs from different groups.....	90-91-92
Figure 3.10 Gene organisation of operons encoding soluble diiron centre monooxygenases of different groups of SDIMO enzymes.....	93-94
Figure 3.11 Glutathione biosynthesis pathway.....	96
Figure 3.12 Gene organization of the propane monooxygenase gene operons in <i>Rhodococcus</i> SC4, <i>Rhodococcus</i> LB1, and other known propane-oxidizing bacteria.....	99
Figure 3.13 Schematic view of the <i>alkB</i> gene cluster from <i>Rhodococcus</i> strains AD45, LB1 and SC4 and other known alkane-utilizing <i>Rhodococcus</i> strains.....	101
Figure 3.14 Pathway of propane oxidation in <i>Gordonia sp.</i> TY5.....	103
Figure 4.1 Construction of plasmid pMEK for mutagenesis of <i>isoA</i> in <i>Rhodococcus</i> AD45.....	111
Figure 4.2 <i>EcoRI</i> digest of plasmid pMEK.....	112
Figure 4.3 Screening for <i>isoA</i> single cross-over mutant by PCR using the primer set 3723F / 5296R.....	116
Figure 4.4 Colony PCR using primers 3723F and 5296R to screen for homologous recombination between the <i>Rhodococcus</i> AD45 genome and pMEK plasmid.....	117
Figure 4.5 Screening for <i>isoA</i> single cross-over mutant by PCR using the primers 3723F and GmR.....	118
Figure 4.6 Screening for <i>isoA</i> double cross-over mutant by PCR using the primer set 3723F / 5296R.....	120
Figure 4.7 Primers 3723F and 5296R were used to screen for the replacement of the targeted <i>isoA</i> region with gentamicin resistance cassette.....	120
Figure 4.8 Screening for the loss of the pMEK plasmid backbone after sucrose counter selection using primers KmF and KmR (kanamycin resistance).....	121

Figure 4.9 GmF and GmR primers were used to screen for the insertion of the gentamicin resistance cassette into the genome of <i>Rhodococcus</i> AD45 mutant strain.....	122
Figure 4.10 Growth curves of the <i>isoA</i> mutant strain and the wild type	123
Figure 4.11 PCR of <i>isoA</i> gene from cDNA generated from mRNA and DNA control.....	124
Figure 4.12 Standard curve plot for <i>isoA</i> gene.....	126
Figure 4.13 Standard curve plot for <i>rpoB</i> gene	127
Figure 4.14 The standard curve, obtained by Bio-Rad Protein Assay, for the quantification of solubilized protein concentrations.....	129
Figure 4.15 SDS-PAGE of cell-free extract	130
Figure 5.1 Alignment of the deduced IsoA sequences from the isoprene-degrading isolates.....	137-138-139
Figure 5.2 Test of the new primers using genomic DNA from <i>Rhodococcus</i> AD45, <i>Rhodococcus</i> SC4 and <i>Rhodococcus</i> LB1 strains.....	143
Figure 5.3 Alignment of the <i>isoA</i> nucleotide sequences with the forward <i>isoA</i> primer.....	146
Figure 5.4 Alignment of the <i>isoA</i> nucleotide sequences with the reverse <i>isoA</i> primer.....	147
Figure 5.5 Partial alignment of deduced amino acid sequences of the α -subunit of the hydroxylases.....	148-149-150
Figure 5.6 Neighbour-joining phylogenetic tree of deduced IsoA sequences (338 amino acids) from the oak, poplar and garden soil <i>isoA</i> clone libraries.....	151
Figure 5.7 The designed primers are specific for the <i>isoA</i> gene.....	153
Figure 5.8 No PCR inhibitors in the genomic DNA from <i>isoA</i> ⁻ bacteria.....	153
Figure 5.9 Neighbour-joining phylogenetic tree of deduced IsoA sequences (338 amino acids) from terrestrial and marine isolates and clone libraries.....	157-158
Figure 6.1 Experimental set up of the SIP incubations.....	161
Figure 6.2 Density gradients of CsCl measured from each fraction of T ₁ samples 3, 5 and 6.....	162
Figure 6.3 DGGE analysis of 16S rRNA genes in fractions 8 to 15 from microcosm 5 incubated with ¹³ C-isoprene.....	164

Figure 6.4 DGGE analysis of 16S rRNA genes in fractions 2 to 15 from microcosm 3 incubated with ^{12}C -isoprene.....	164
Figure 6.5 DGGE analysis of 16S rRNA genes in fractions 8 to 12 from microcosm 8 (T ₂) incubated with ^{13}C -isoprene.....	165
Figure 6.6 Bar graphs displaying the bacterial community composition at the phylum level of the light fraction (LF, ^{12}C -DNA) and heavy fraction (HF, ^{13}C -DNA) of the ^{13}C -isoprene incubations.....	168
Figure 6.7 Neighbour-joining phylogenetic tree of deduced IsoA sequences (111 amino acids) from the 454 pyrosequencing of <i>isoA</i> amplicons from the ‘heavy DNA’ of the ^{13}C -isoprene SIP incubations.....	172
Figure 6.8 Consumption of isoprene in the SIP incubations spiked for the first time with 8 µl of isoprene i.e. 0.5% isoprene (v/v).....	173
Figure 6.9 DGGE profile of 16S rRNA genes amplified from DNA extracted from heavy and light fractions (6 to 12) of ^{13}C -incubated sample 2.....	175
Figure 6.10 DGGE profile of 16S rRNA genes amplified from DNA extracted from heavy fraction (HF, fraction 7) and light fraction (LF, fraction 11) of ^{13}C -incubated samples 1 and 3.....	176
Figure 6.11 DGGE profile of 16S rRNA genes amplified from DNA extracted from fractions 12 to 6 of ^{12}C -isoprene incubated sample 4.....	177
Figure 6.12 Bar graphs displaying the bacterial community composition at the phylum level.....	180
Figure 6.13 Bar graphs displaying the bacterial community composition at the Order level.....	182

List of abbreviations

SDIMO	Soluble diiron monooxygenase
KEGG	Kyoto Encyclopedia of Genes and Genomes
OTU	Operational taxonomic unit
PCR	Polymerase chain reaction
RNA	Ribonucleic acid
rRNA	Ribosomal RNA
μ	Micro
TCA	Tricarboxylic acid
bp	Base pairs
FISH	Fluorescent <i>in situ</i> hybridization
kDa	Kilo dalton
v / v	Volume to volume
w / v	Weight to volume
RT-PCR	Reverse transcriptase PCR

Acknowledgements

First of all, I am extremely grateful to my advisor Professor Colin Murrell for his excellent supervision throughout my PhD. Being a member of your research group has been a privilege and this work would not have been possible without your immense knowledge and true guidance. I am also very grateful to Dr Yin Chen for his insightful advice, discussions and comments which brought an added value to this work. I thank Dr Terry McGenity and Professor Andy Johnston for the interesting and valuable meetings we had, discussing my project and future plans. Andrew, thank you for being around to give advice and motivation. You have definitely inspired all the members of the laboratory including myself to commit to hard work and perseverance.

I would also like to thank DuPont Industrial Biosciences for their technical, financial, and scientific support and the University of Warwick and the Earth and Life Systems Alliance at the University of East Anglia for funding this research.

I would like to thank the past and current members of the Murrell group as well as my fellow PhD students that I have got to know at UEA and Warwick. I would specially like to thank Alex, Andrea, Antonia, Basti, Dani, Ian, Jason, Jean, and Ollie. Thank you all for your support, friendship, and encouragement and for making the time I spent at UEA and Warwick very memorable. Antonia, I want to thank you for being a lovely housemate and a great team member.

Finally, I thank my parents, sisters and brother for their unequivocal support and faith in me.

Chapter 1

Introduction

1.1 Isoprene

Isoprene or 2-methyl-1,3-butadiene is an unsaturated hydrocarbon (Figure 1.1) with low water-solubility and a greasy smell (Sharkey *et al.*, 1996a). It belongs to the family of volatile organic compounds (VOC) due to its low boiling temperature of 33 °C (Sharkey *et al.*, 1996a). Isoprene units (C₅) are common structural motifs for isoprenoid compounds such as carotenoids, natural rubber and steroids (Taalman, 1996). Studies conducted in rodents have shown that isoprene possesses carcinogenic properties (Watson *et al.*, 2001).

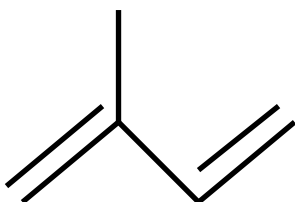


Figure 1.1 Isoprene structure

1.2 Isoprene and atmospheric chemistry

Isoprene influences the chemistry of the atmosphere primarily through its reactions with hydroxyl radicals (OH), nitrate radicals (NO₃) and ozone (O₃) molecules in the troposphere (Atkinson & Arey, 1998). Isoprene has a short lifetime which varies between 1.3 days and less than a few hours depending on the identity and concentration of the atmospheric component it is reacting with (Atkinson & Arey, 2003). Almost 85 % of atmospheric isoprene is removed by OH radicals during the daytime (Miyoshi *et al.*, 1994). This reaction consists of the addition of OH to one of the two C = C double bonds. Depending on the addition site, four different hydroxyalkyl radicals are produced. These primarily react with O₂ and form hydroxy-peroxy radicals. From this step, different reaction scenarios occur, whereby the possible end-products include organic nitrates (isoprene nitrate), HO₂ radicals, formaldehyde, and NO₂ (Fehsenfeld *et al.*, 1992, Fan & Zhang, 2004) (Figure 1.2). Depending on the final product, together with the condition of the light and the levels of NO_x, the reaction of isoprene with OH can influence the tropospheric concentrations of ozone either negatively or positively. In their free form, NO₂

molecules represent a source of tropospheric ozone formation through photolysis (Stone *et al.*, 2012). Organic nitrates (RONO_2), however, sequester NO_2 molecules and subsequently preclude their photolysis. HO_2 reacts with NO , when the latter is present in high levels, and produce NO_2 . At low concentrations of NO_x , HO_2 will instead react with HO_2 and RO_2 to produce H_2O_2 and RO_2H with no NO_2 molecules being generated, effectively suppressing ozone formation (Fehsenfeld *et al.*, 1992). Tropospheric ozone can equally be depleted as a result of its direct reaction with isoprene. The reaction of isoprene with O_3 , however negligible at daylight, accelerates considerably at night (Fehsenfeld *et al.*, 1992). In addition to influencing ozone levels, isoprene modulates the concentrations of other key climate active gases. Given that the reaction of isoprene with OH is rapid ($k = 1 \times 10^{-10} \text{ cm}^3 \text{ molecule}^{-1} \text{ s}^{-1}$), it acts as a sink for OH radicals and extends the lifetime of less reactive greenhouse gases such as methane (Atkinson *et al.*, 2006, Poisson *et al.*, 2000).

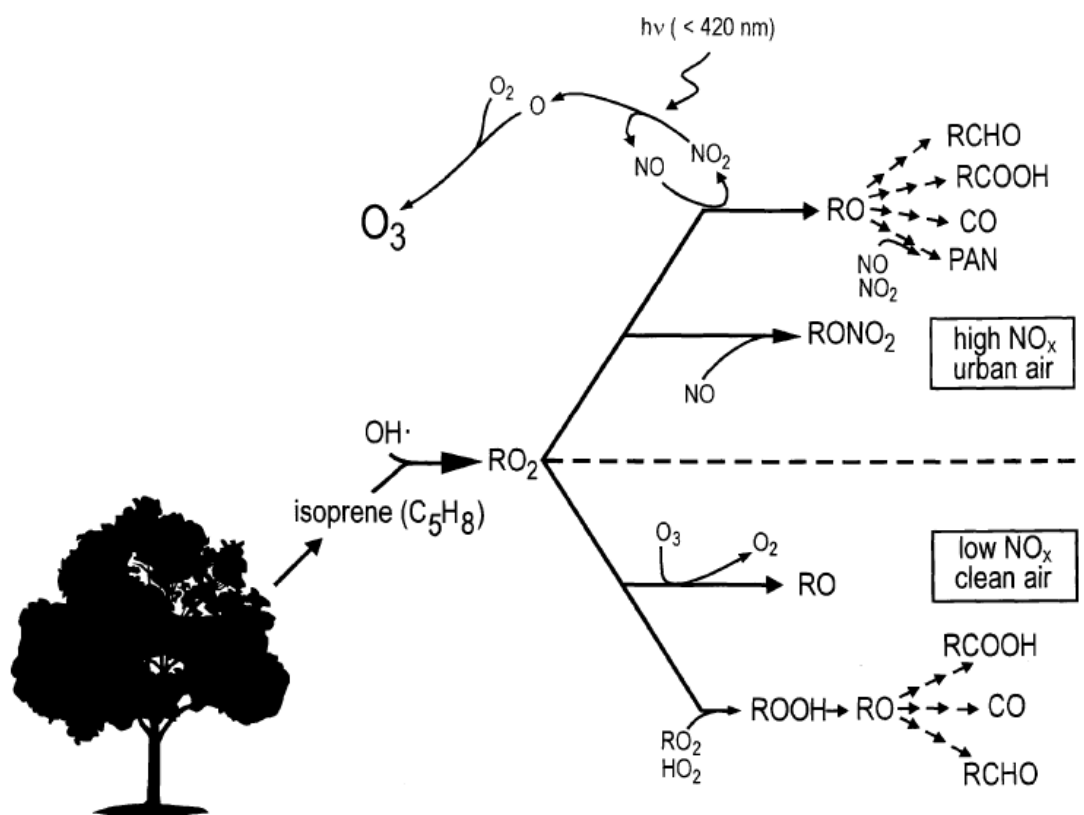


Figure 1.2 Possible products of the reaction of isoprene with OH radicals. Taken from Harley *et al.*, 1999.

It is now widely accepted that isoprene acts as a precursor of secondary organic aerosol (SOA) formation (Carlton *et al.*, 2009). A finding strongly suggested by Claeys *et al.*, (2004) following the detection in aerosols samples collected from an Amazonian forest of large amounts of 2-methylthreitol and 2-methylerythritol, both of which are isoprene oxidation products. Secondary organic aerosols constitute an important component of atmospheric aerosols that modulate solar radiation (Hallquist *et al.*, 2009) (Figure 1.3). They derive from the atmospheric oxidation of volatile organic compounds into semi- or non-volatile gaseous products which then partition into the aerosol phase (Ziemann & Atkinson, 2012). The annual amount of SOA that is produced from isoprene was estimated to account for 22 % of the global SOA budget (Engelhart *et al.*, 2011). Secondary organic aerosols, including isoprene SOA, can produce a cooling effect by acting as cloud condensation nuclei and inducing cloud formation (Engelhart *et al.*, 2011). In summary, all of the facts above indicate that isoprene has a major role in the regulation of global cooling and warming.

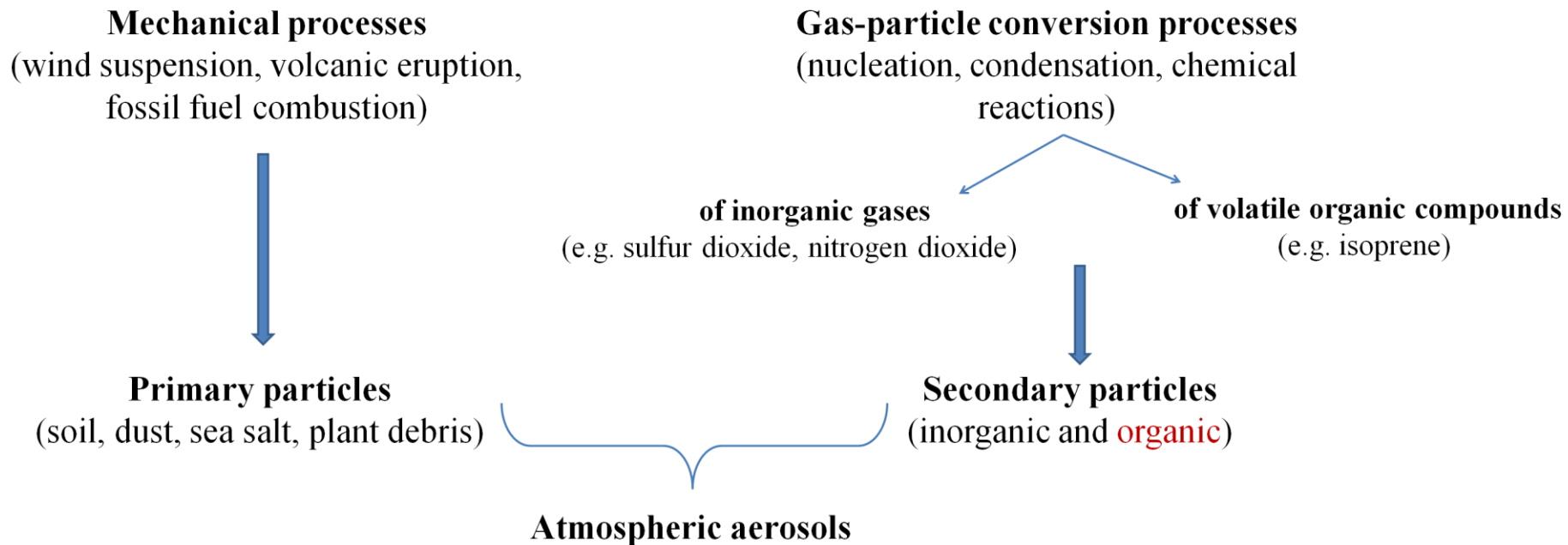


Figure 1.3 Secondary organic particles, highlighted in red, are key component of atmospheric aerosols. Based on the review by Hallquist *et al.*, 2009.

1.3 Isoprene production

Anthropogenic sources, such as fossil fuel combustion and industrial activities, supply 83 – 178 Tg C of non-methane volatile organic compounds (NMVOC) to the atmosphere per year (Nakicenovic *et al.*, 2000). This is a quantity approximately ten-fold lower than the biogenic input of NMVOC estimated at 1,150 Tg C / year (Guenther *et al.*, 1995, Atkinson & Arey, 2003). Isoprene accounts for 44 % of total NMVOC flux with an annual emission of 400 – 600 Tg C, which is equivalent if not greater than the total methane flux to the atmosphere (Guenther *et al.*, 1995, Arneth *et al.*, 2008, Dlugokencky *et al.*, 2011, Kirschke *et al.*, 2013). The terrestrial environment is the main source of biogenic isoprene, however marine sources of isoprene have also been identified and characterized (Pacifico *et al.*, 2009, Moore *et al.*, 1994, Shaw *et al.*, 2003). Isoprene emission displays geographic and temporal variations controlled by the type of vegetation, the climate and the seasonal changes in temperature (Figure 1.4) (Guenther *et al.*, 2006, Arneth *et al.*, 2011). While estimations of global biogenic isoprene emission vary depending on the model used for calculation, the tropics are consistently reported as the region of the Earth which is the largest contributor to isoprene production (Arneth *et al.*, 2011). The tropical climate is characterized by a high humidity which reduces evaporative cooling, exposing tropical plants to increased heating (Sharkey & Yeh, 2001). Since heat induces isoprene emission (see section 1.3.1.1), cold regions have the lowest emission and tropical regions the highest (Figure 1.4).

The anthropogenic contribution to the global budget of isoprene (mainly from car exhausts) has also been recognized, but it remains quantitatively less important than natural production (Reimann *et al.*, 2000, Borbon *et al.*, 2001, Wagner & Kuttler, 2014). Several different industrial processes contribute to the production of synthetic isoprene for the manufacturing of commercial rubber, polymers (used for example in tyres and paint resins), and terpenes (e.g. sweeteners) (Taalman, 1996). However despite large emissions, isoprene is present in the atmosphere at low concentrations, not exceeding 16 parts per billion (ppbv), due to its high reactivity (Donoso *et al.*, 1996, Goldstein *et al.*, 1998, Fuentes *et al.*, 1999, Rinne *et al.*, 2002, Greenberg *et al.*, 2004).

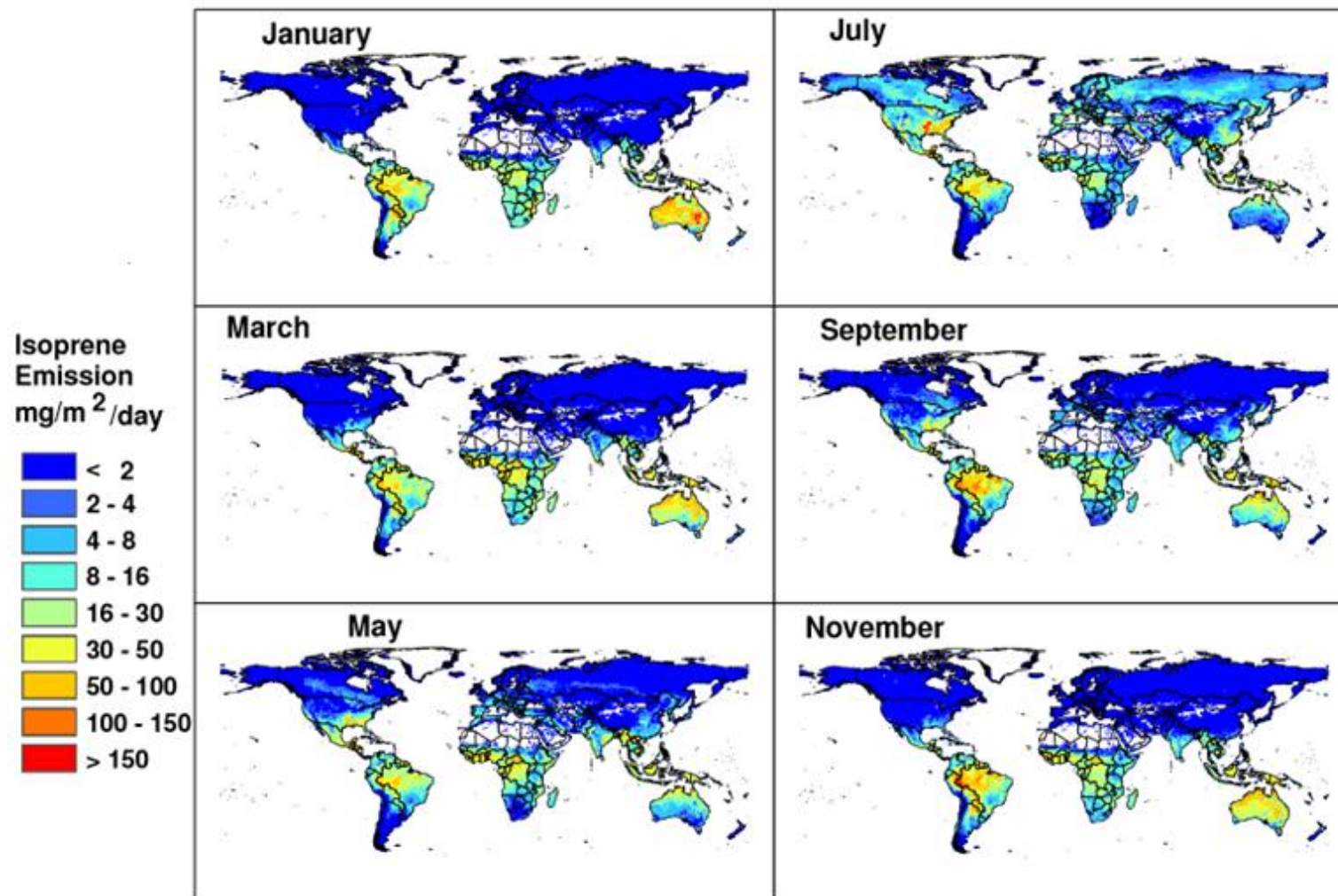


Figure 1.4 Estimated global isoprene emission for 2003. Taken from Guenther *et al.*, 2006

1.3.1 Isoprene biosynthesis by plants

More than 90 % of isoprene that is supplied to the atmosphere originates from terrestrial plants (Guenther *et al.*, 2006). Isoprene emission from plants, or the “isoprene effect” as it was then named, was discovered as early as 1957 by Sanadze *et al.*, who found that, when exposed to light, poplar, oak, willow, acacia, and boxwood leaves released isoprene amongst other volatile compounds (Sanadze, 1991, Sanadze, 2004). Nearly a decade after, Rasmussen and Went (1965) reported that gas chromatography measurements of air samples collected from bags in which plants were enclosed matched with the data on air samples collected from the general atmosphere outside the bags. This suggested that the volatile organic compounds present in the atmosphere, including isoprene, originate from plants. Mass spectrometric analyses carried out by the same group a few years later supported their previous work and identified isoprene as a natural plant product (Rasmussen *et al.*, 1970). Not all plant species produce isoprene and those which do belong to phylogenetically diverse groups, including mosses, ferns and angiosperms (Evans *et al.*, 1982, Monson & Fall, 1989, Sharkey *et al.*, 2008, Tingey *et al.*, 1987, Hanson *et al.*, 1999). Guenther *et al.*, (1995) reported that woody species emit at least 3 times more isoprene than shrubs and 15 times more than crops. A compiled list of isoprene-emitting plants was published by the group of Professor Nick Hewitt (Lancaster University) and included eucalyptus, oak, willow, and poplar species having variable emission potentials (Sharkey *et al.*, 2008, <http://www.es.lancs.ac.uk/cnhgroup/iso-emissions.pdf>). Hanson *et al.*, (1999) postulated that isoprene emission is an adaptive trait that has evolved in the first plants to colonize land to allow them to cope with relatively more pronounced temperature changes than those encountered in water. This trait has since been lost and replaced in a number of plants by other response mechanisms to heat stress such as the mechanism of heat shock protein synthesis. However, Harley and colleagues (1999) suggested that emitting plant species have separately gained the capacity for isoprene emission at different times throughout history. Regardless of the evolutionary origin of isoprene emission, it is reasonable to suggest that the gene pool required for isoprene production is only retained or acquired by plants to which this compound is beneficial. This suggestion is supported by the following facts. Firstly, plants invest 6 carbons, 20 ATP and 14 NADH to produce isoprene via the

methylerythritol phosphate pathway (Sharkey & Yeh, 2001). This represents quite a high energy and carbon expenditure for the plants to waste. In addition, within the same species, some plants emit isoprene while others do not, depending on the geographical location and the environmental conditions of their habitats (Sharkey *et al.*, 2008). Furthermore, Monson *et al.*, 2013 reported that losing or gaining the capacity for isoprene synthesis is a question of a small number of mutations within the genetic machinery required to produce isoprene.

Isoprene is synthesized in chloroplasts then released to the atmosphere through the stomata (Sharkey, 1991, Sanadze, 2004). The amount of isoprene exiting the leaf is not however subject to a stomatal control, and is only a function of how much isoprene is actually being synthesized (Sharkey & Yeh, 2001). No significant isoprene storage capacity was found in leaves (Sharkey & Yeh, 2001). The isoprene flux from leaves is therefore regulated on the basis of its synthesis, which itself is regulated primarily by temperature and light, as will be discussed in the following section. It is now very widely accepted that the carbon atoms of the isoprene molecule derive mainly from photosynthesis. The previous statement was clearly demonstrated by the $^{13}\text{CO}_2$ labelling experiment conducted by Delwiche and Sharkey (1993) who showed that upon feeding $^{13}\text{CO}_2$ to photosynthesizing *Quercus rubra* leaves placed in an illuminated chamber at 32 °C, they rapidly retrieved the ^{13}C isotope in the isoprene molecules that were sampled from the leaf chamber and analyzed by mass spectrometry. Isoprene emission can effectively cost the plants about 2 % of their photosynthetically-fixed carbon (Monson & Fall, 1989, Loreto & Sharkey, 1990).

Silver & Fall (1991) have shown that isoprene is formed enzymatically in plants from DMAPP (dimethylallyl pyrophosphate) substrate by adding aspen leaf extract to a reaction containing DMAPP and Mg^{2+} then detecting isoprene formation by gas chromatography combined with mass spectrometry. These researchers later managed to purify the enzyme, termed isoprene synthase IspS, that catalyses isoprene production in aspen leaves and to assay its activity (Silver & Fall, 1995). On the basis of these assays, isoprene was thought to be formed following the enzyme-mediated cleavage of the diphosphate group from the DMAPP molecule (Figure 1.5).

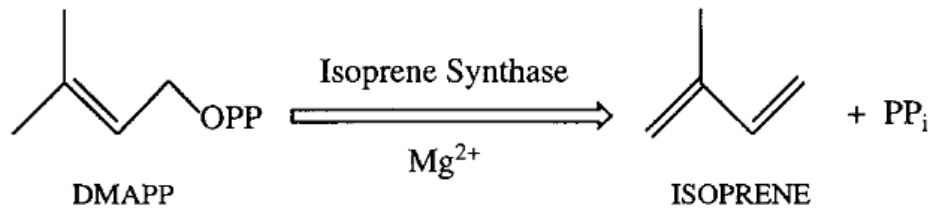


Figure 1.5 Isoprene synthesis reaction. Taken from Silver & Fall, 1995.

There are two sources of DMAPP in plant cells: the mevalonate pathway taking place in the cytosol and the methylerythritol (MEP) pathway (or the non-mevalonate pathway) occurring in the chloroplast (Pulido *et al.*, 2012). Loreto *et al.*, (2004) demonstrated the existence of a DMAPP pool in plant cells that is not involved in isoprene synthesis by showing that as opposed to the 90 % labelling of isoprene emitted from ¹³CO₂-fed poplar leaves, less than half of the DMAPP isolated from the leaves were labelled. It is now well accepted that only the DMAPP pool that derives from the MEP pathway is used for isoprene synthesis. The MEP pathway is widely used amongst plants, including the non-isoprene emitters, for the synthesis of isoprenoids, such as monoterpenes (Lichtenthaler, 1999) (Figure 1.6). It starts with glyceraldehyde-3-phosphate which is found in the chloroplast as an end-product of photosynthesis, further confirming the relation between photosynthesis and isoprene production.

Photosynthesis is the primary but not the only source of carbon for isoprene formation. This discovery was preceded by several experimental evidence that hinted at the existence of another carbon source. For instance, isoprene that was formed in the dark or under CO₂-free air could not have derived from photosynthesis (Affek & Yakir, 2003). The most obvious evidence was that young oak plants emitted ¹³C-labelled isoprene after being fed [U- ¹³C] glucose into their xylem, suggesting that carbons deriving from glucose metabolism contributed to isoprene formation (Kreuzwieser *et al.*, 2002). In addition to the glyceraldehyde-3-phosphate source of DMAPP and isoprene, it is now well established that isoprene is also formed from pyruvate which constitutes a second substrate for the MEP pathway (Figure 1.6) (Schnitzler *et al.*, 2004, Trowbridge *et al.*, 2012). Pyruvate is produced in the chloroplast from phosphoenolpyruvate, a product of glycolysis.

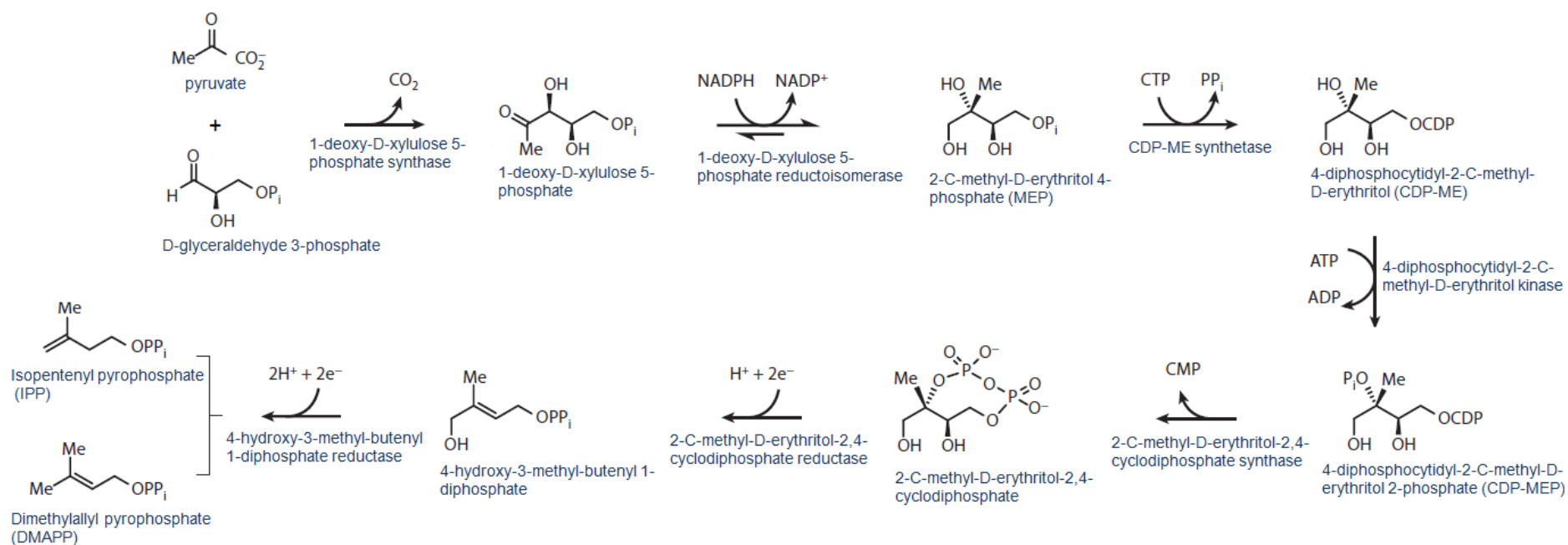


Figure 1.6 Methylerythritol phosphate (MEP) pathway of isoprenoid biosynthesis. Modified from Zhao *et al.*, 2013

Isoprene synthase requires an alkaline milieu (pH 8.0) and the presence of Mg^{2+} ions (optimum concentration ranging between 10 and 20 mM) for its catalytic activity (Fall & Wildermuth, 1998). This is in agreement with the fact that isoprene biosynthesis takes place in the chloroplast where the pH is 8.0 and the concentration of Mg^{2+} is high during photosynthesis (Silver & Fall, 1995). Isoprene emission by plants is tightly regulated. Regulation can occur at the level of the transcription and expression of the isoprene synthase gene, the availability of DMAPP substrate through the regulation of the MEP pathway, or the catalytic activity of isoprene synthase (Fall & Wildermuth, 1998, Sharkey & Yeh, 2001, Rosenstiel *et al.*, 2002, Wolfertz *et al.*, 2004, Vickers *et al.*, 2010). Miller and colleagues (2001) were the first to identify and characterize the gene encoding isoprene synthase enzyme from the leaves of a hybrid poplar species (*Populus alba* x *Populus tremula*). On the basis of this finding, Sasaki *et al.*, (2005) showed that transcription of the isoprene synthase gene was upregulated in poplar leaves when exposed to constant light and heated at 40 °C. Vickers *et al.*, (2010) reported, however, that the increase in isoprene emission from stressed mature poplar leaves was not induced by an increase in the expression of the gene coding isoprene synthase given that stressed and unstressed leaves contained similar amounts of isoprene synthase proteins. They subsequently suggested that this increase in emitted isoprene might be due to an increase in the DMAPP supply. The high K_m value of the isoprene synthase enzyme indicates that the conversion rate of DMAPP to isoprene is actually affected by the availability and concentration of the DMAPP substrate (Silver & Fall, 1995, Wiberley *et al.*, 2009).

1.3.1.1 Environmental factors influencing isoprene emission from leaves

The rate of isoprene emission from leaves is influenced by several environmental factors, in particular temperature, light, and ambient CO_2 concentration. The observation that an increase in the leaf temperature stimulates an increase in isoprene emission goes back to the early stages of the discovery of isoprene emission from plants. Rasmussen and Went (1965) observed a fluctuation in the rate of VOC emission from plants in response to seasonal variations: the rate decreased by at least 10-fold in winter compared to summer. Several studies have since shown that the

rate of isoprene emission is temperature-dependent. These studies investigated isoprene emission either at the leaf scale (e.g. aspen, kudzu, and oak) or at the field scale, confirming temperature dependence in both cases (Monson & Fall, 1989, Loreto & Sharkey, 1990, Sharkey & Loreto, 1993, Singaas & Sharkey, 2000, Potosnak *et al.*, 2013). There exists a threshold temperature (around 20 °C) above which isoprene emission is triggered in isoprene-emitting plants then the emission starts to increase with increased temperature (Figure 1.7) (Sharkey & Loreto, 1993). As temperature continues to rise beyond the optimal temperature for photosynthesis, carbon assimilation starts slowing while more isoprene molecules are needed for plant protection (Rasulov *et al.*, 2010). This causes an increase in the loss of photosynthetically fixed carbons from the typical 2 % to as high as 20 % under excessive heat (Harley *et al.*, 1996, Sharkey & Yeh, 2001). Isoprene emission typically peaks at 40 °C – 42 °C then starts diminishing when temperature reaches higher values (Rasulov *et al.*, 2010).

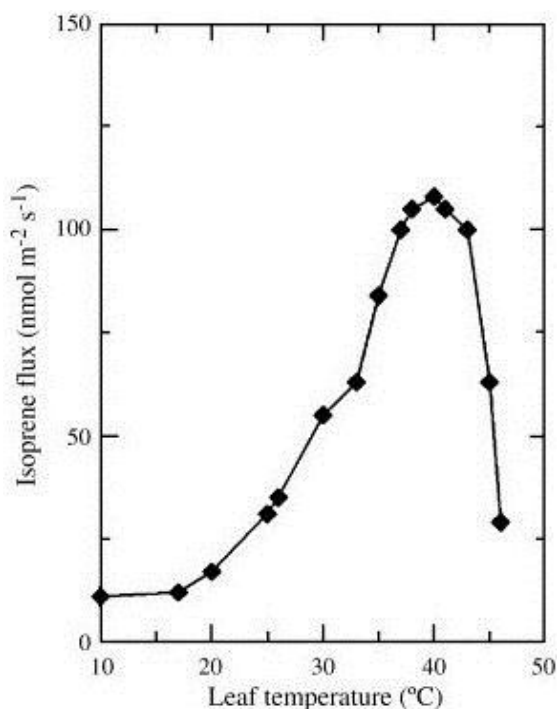


Figure 1.7 Isoprene emission (measured as a flux) in oak leaves as a function of temperature. Taken from Siwko *et al.*, 2007

Monson and colleagues (1992) showed that isoprene emission, in response to increased temperature, was congruent with isoprene synthase activity in velvet bean leaves. On the basis of their work, the authors presented two important observations, one of which was later rejected. The first observation, which holds valid, is that isoprene emission is influenced by the activity of isoprene synthase which is in turn influenced by temperature. This is in good agreement with the results obtained by Rasulov *et al.*, (2010). The second observation was that the decline in isoprene emission recorded when the velvet bean leaves were treated with temperatures higher than 45 °C was due to the denaturation of the isoprene synthase protein. It was later known that temperature does not cause the denaturation of isoprene synthase, but regulates its activity through inducing changes to its kinetic properties (e.g. post-translational modifications) (Sharkey & Yeh, 2001, Singsaas & Sharkey, 2000).

Light is also a rate-determining factor in isoprene emission. The effect of light on isoprene emission is comparable to that on photosynthesis in that isoprene emission rate increases with an increase in light (Tingey *et al.*, 1981, Monson & Fall, 1989, Sharkey & Loreto, 1993). However, unlike photosynthesis, isoprene emission drops to significantly lower levels in the dark, but does not completely cease. It is now well established that light regulates how much isoprene is being synthesized directly at the level of the isoprene synthase enzyme, rather than controlling how much ATP and NADPH are being generated in the cell and are therefore available as energy and reducing power, as it was previously assumed (Logan *et al.*, 2000). A set of hypotheses has been put forward for explaining the light effect on isoprene synthase, including that light can enhance the activity of the isoprene synthase by increasing the levels of Mg²⁺ in the chloroplast (Logan *et al.*, 2000). Light can also regulate genes involved in the MEP pathway for DMAPP synthesis or activate the transcription and expression of the gene encoding isoprene synthase (Loivamäki *et al.*, 2007, Rasulov *et al.*, 2009). All of the above possibilities suggest that the type of regulation that light exhibits on isoprene synthase is not be restricted to one mechanism but rather influenced by the leaf species and stage of development, the presence of other environmental factors, and by whether light is applied to the plant in a steady or transient state (Rasulov *et al.*, 2009).

Given that isoprene emission is regulated by light and temperature, it is not surprising that the significant changes in temperature and light that occur throughout the day are paralleled by a diurnal variation in isoprene flux. Isoprene emission measurements made on oak leaves at different time points throughout the day showed that isoprene emission started at 6:00 am, increased throughout the morning hours until midday, when it reached its peak then started decreasing in the evening (Geron *et al.*, 2000). The highest concentration of isoprene released from cottonwood, oak and eucalyptus, was also reported at mid-day (~ 1:00 pm) when the temperature and light intensity are supposedly the highest throughout the day (Funk *et al.*, 2003).

While it is agreed amongst scientists that atmospheric concentrations of CO₂ influence isoprene emission, the effect of high CO₂ levels on isoprene biosynthesis remains debatable. This is mainly due to the fact that different isoprene-emitting plant species respond differently to elevated CO₂ concentrations (Sun *et al.*, 2013). Many studies have shown that elevated ambient CO₂ levels, unlike elevated temperature, suppress isoprene emission from leaves (Arneeth *et al.*, 2007). This phenomenon was explained by Rosenstiel and colleagues (2003) as follows. There are several routes of phosphoenolpyruvate (PEP) metabolism in plants, including PEP carboxylation to produce oxaloacetic acid or dephosphorylation to produce pyruvate, one of the two substrates for the MEP pathway for DMAPP synthesis. The presence of high concentrations of CO₂ activates the former route, thus hinders pyruvate formation. This consequently leads to less DMAPP being produced and converted to isoprene. Another explanation was suggested and consisted in that under high CO₂ conditions, the levels of intracellular ATP generated through photosynthesis are not sufficient to meet the high energy demands of the isoprene synthesis pathway (Rasulov *et al.*, 2009). The finding that isoprene emission is inhibited by high levels of CO₂ while enhanced by high temperature represents a challenge for future predictions of isoprene flux in light of the simultaneous increase in global temperature and atmospheric CO₂ (Heald *et al.*, 2009).

1.3.1.2 The role of isoprene in plant protection

Experimental evidence is emerging, attributing a role for isoprene in protecting the photosynthetic apparatus in plants from a heat-induced damage. Kudzu leaves treated with fosmidomycin, an inhibitor of isoprene emission through targeting the 1-deoxy-D-xylulose 5-phosphate reductoisomerase enzyme of the MEP pathway (Zeidler *et al.*, 1998), were exposed together with untreated leaves to a temperature of 46 °C for a short period, followed by a recovery period at the initial growth temperature. Fosmidomycin-treated leaves recovered 56 % of their original photosynthesis activity compared to an 87 % recovery for untreated leaves (Sharkey *et al.*, 2001). Non-isoprene emitting plants supplied with exogenous isoprene (22 µl/l) had their photosynthesis recovery rate improved by at least 20 % after a brief heat shock at 46 °C (Sharkey *et al.*, 2001). Behnke and co-workers (2007) generated transgenic poplar trees whose ability to produce isoprene was suppressed using RNA interference. Both the transgenic trees and the wild type controls were exposed to a heat cycle and showed reduced photosynthetic activity. However, photosynthesis was two-fold lower in the transgenic plants compared to wild type plants. Sharkey and colleagues (1996) measured the rate of isoprene emission from white oak leaves located at the bottom (6 m height), middle (20 m) and top of the tree canopy (30 m height). Isoprene emission was the lowest for the bottom leaves and increased gradually towards the top. According to the explanation put forward in a later publication by the same group (Sharkey *et al.*, 2008), under standard conditions, top canopy leaves, which are naturally more susceptible to solar heat, are adapted to produce isoprene in amounts considerably greater than the shadowed bottom leaves.

Several explanations were proposed as to how isoprene provides thermotolerance to photosynthesis (Velikova *et al.*, 2011). Impairment of the photosynthetic apparatus under high temperatures is generally caused by leakiness of the thylakoid membrane (Schrader *et al.*, 2004). At 45°C and higher, chloroplast membranes can even segregate and lose their functional structure (Gounaris *et al.*, 1984). Owing to its lipophilic and hydrophobic nature, isoprene can intercalate into the chloroplast membrane, fill any potential leaky space, tether the lipid layers together, and strengthen the adhesion of the membrane proteins to each other and to the bilayer (Figure 1.8) (Sharkey *et al.*, 1996a, Singaas *et al.*, 1997, Velikova *et al.*, 2011). A

molecular dynamics simulation study of the interaction of isoprene with lipid membranes showed the congregation of isoprene molecules at the centre of the interface between the phospholipid layers (Siwko *et al.*, 2007). It is worth noting that while isoprene is effective in alleviating heat stress over short periods, it plays no role in the case of constant exposure to heat. In this context, desert plants do not emit isoprene (Sharkey & Yeh, 2001, Sharkey *et al.*, 2008).

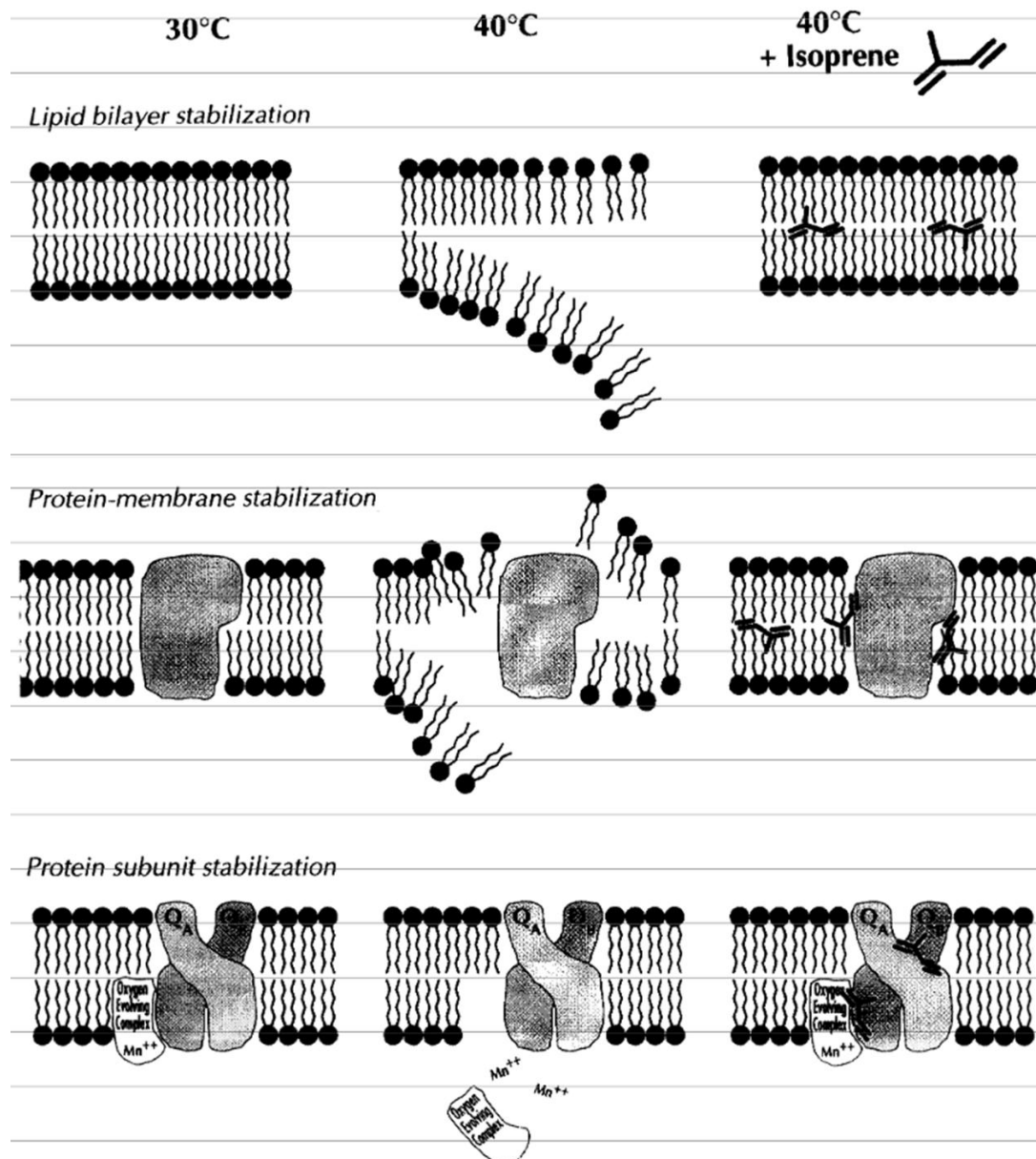


Figure 1.8 Possible scenarios of the role of isoprene in protecting photosynthetic membranes. Figure taken from Sharkey *et al.*, 1996a.

Another set of hypotheses has been proposed, including that isoprene confers to plants a protection against oxidative damage. Ozone-induced production of reactive oxygen species (e.g. H₂O₂) can cause the denaturation of plant cellular membranes. Loreto *et al.*, (2001) showed that supplying exogenous isoprene to naturally non-emitting tobacco leaves mitigated the damage caused by ozone exposure. This experiment did not however conclusively determine if isoprene reduces oxidative damage by efficiently engaging in scavenging mechanisms or rather by intercalating into the membrane to prevent its disassociation (Sharkey & Yeh, 2001). Loreto and Velikova (2001) reported that following an 8 hour exposure to ozone (100 ppb), reed leaves whose capacity for isoprene production has been impaired by treatment with fosmidomycin contained more H₂O₂ than the untreated isoprene-emitting leaves. They therefore argued that isoprene quenches oxidative products. This experiment was consistent with the results later obtained by Vickers *et al.*, (2009) showing that after 5 days of fumigation with ozone (120 ppb), H₂O₂ molecules were significantly more abundant in wild type non-isoprene emitting tobacco leaves compared to the tobacco leaves that were transformed with an isoprene synthase gene and were capable of emitting isoprene.

In the event that the cell supply of DMAPP would exceed the demand, DMAPP will accumulate in the cell, sequestering phosphates. It was therefore suggested that isoprene formation allows the cell to metabolize the surplus of DMAPP and liberate the diphosphate group (Logan *et al.*, 2000). The main argument against this suggestion is that the MEP pathway of DMAPP synthesis, similarly to other metabolic pathways, is strictly regulated to prevent such event from occurring (Cordoba *et al.*, 2009, Banerjee & Sharkey, 2014).

In addition to the abiotic stresses, plants are equally affected by biotic stresses such as pathogens. VOC emission plays a role in the defence mechanism of plants against herbivores. Infested plants release VOCs as repelling odours or as attractants to draw parasitic predators (the 'plant bodyguards') towards infesting herbivores (Laothavornkitkul *et al.*, 2008). The likelihood that isoprene might be implicated in these plants-insects interactions has been investigated. Transgenic isoprene-emitting tobacco plants were less susceptible to an infestation by the caterpillar, *Manduca sexta*, than their wild type non-emitting counterparts (Laothavornkitkul *et al.*, 2008).

However, the outcome of this experiment was challenged by another experiment carried out by Loivamaki *et al.*, (2008) which showed that isoprene emission was rather damaging for herbivore attack on a transgenic isoprene-emitting *Arabidopsis thaliana* plant because isoprene repelled the predator and not the infesting herbivore. Available information on the ecological role of isoprene synthesis remains limited and further studies in this area are well worth considering (Gershenzon, 2008).

1.3.2 Isoprene production by microbes

Kuzma *et al.*, (1995) showed that bacteria grown in batch cultures emitted isoprene. *Escherichia coli*, *Bacillus subtilis*, *Bacillus amyloliquefaciens* and *Acinetobacter calcoaceticus* were all reported as bacterial isoprene emitters. However, the level of isoprene detected from *Escherichia coli* and *Acinetobacter calcoaceticus* cultures was very low. *Bacillus subtilis* displayed the highest isoprene emission rate ranging between 7 to 13 nmol. (g cell)⁻¹. h⁻¹, depending on the growth conditions. Out of 26 *Streptomyces* strains tested for VOC emission, 22 strains produced isoprene (Schöller *et al.*, 2002). Cultures of *Pseudomonas putida* KT2442, *Pseudomonas fluorescens* R2F, *Pseudomonas aeruginosa* ATCC10145, *Serratia liquefaciens* SM 1302, and *Enterobacter cloacae* SM 639 grown with 1 % (w/v) citrate were surveyed for the identity of the volatile compounds they release during growth using mass spectrometry and gas chromatography (Schöller *et al.*, 1997). All five Gram-negative bacteria emitted isoprene which effectively dominated the VOCs released from three of the cultures. The answer to what role isoprene plays in bacteria which produce it, remains unclear (Sivy *et al.*, 2002). Several suggestions were presented, including a potential role for isoprene in signaling pathways (Julsing *et al.*, 2007). Another suggestion was put forward by Wagner and colleagues (1999, 2000) who showed that *Bacillus subtilis* produces isoprene from DMAPP substrates supplied to the bacterial cells via the MEP pathway. The main use of DMAPP in bacteria is as an intermediate in the formation of isoprenoids, similar to that in plants. Therefore, Wagner and colleagues suggested that by emitting isoprene, bacteria can safely metabolize the excess of DMAPP that is not used for isoprenoid synthesis and recycle the diphosphate group. The fact that plants and bacteria share the same pathway for DMAPP synthesis was of primary importance in the field of

biotechnology because it allows the engineering of transgenic isoprene-emitting bacterial strains through transformation of bacterial cells with an isoprene synthase gene from plants. This would ensure a sustainable and environmentally sound production of isoprene for industrial and commercial use (Zhao *et al.*, 2011, Lindberg *et al.*, 2010). This approach has already been successfully tested by Zhao and co-workers (2011).

Serious efforts are being lately invested into finding a suitable volatile compound released from pathogenic bacteria to be used as a biomarker for bacterial infection. This diagnostic approach is non-invasive and could offer substantial clinical advantages. Isoprene was identified as a potential candidate given that it was emitted from virtually all tested pathogens and in significant amounts, making it easily identified (Filipiak *et al.*, 2012, Bos *et al.*, 2013). However, the difficulty with using isoprene as a biomarker for bacterial infection is that it is endogenously retrieved in the breath of healthy uninfected individuals (see section 1.3.3) (Filipiak *et al.*, 2012, Bos *et al.*, 2013).

1.3.3 Isoprene production by animals and humans

Humans exhale isoprene along with other organic compounds such as methanol, acetone, and ethanol (Conkle *et al.*, 1975, DeMaster & Nagasawa 1978). Isoprene was estimated to be one of the most abundant hydrocarbons in human breath with a concentration ranging from 12 to 580 parts per billion (ppb), effectively accounting for 30 to 70 % of all hydrocarbons found in human breath (Gelmont *et al.*, 1981, Fenske & Paulson, 1999). In total, 4 mg of isoprene are exhaled from an average individual, daily (Sharkey, 1996a). However, there are no accurate estimations of what proportion of the total isoprene flux, this source of isoprene represents. Smoking and exercising can influence the amount of isoprene that is exhaled (Karl *et al.*, 2001, Euler *et al.*, 1996). Conversely, breath isoprene levels did not seem to vary with gender or different types of diets (DeMaster & Nagasawa, 1978, Gelmont *et al.*, 1981). The question of whether the age factor has an effect on the concentration of isoprene in human breath was tackled by several research groups, controversial findings were however reported (Nelson *et al.*, 1998, Kushch *et al.*, 2008). Cailleux and Allain (1989) clearly showed that isoprene exhalation effectively depended on

whether the individual was awake or asleep. DeMaster and Nagasawa (1978) showed that breath isoprene concentrations varied considerably throughout the day, with the highest concentrations recorded during the night hours when individuals were presumably asleep. This is consistent with the observation by King *et al.*, (2012) of enhanced isoprene exhalation coupled with frequent isoprene peaks during sleep. Rats and mice also produce isoprene at a rate estimated to be 1.9 and 0.4 $\mu\text{mol/kg/h}$, respectively (Peter *et al.*, 1987). This production rate, however, is not indicative of the emission rate of isoprene because, unlike plant cells, rodent cells have the capacity to remetabolize isoprene (Peter *et al.*, 1987, Sharkey, 1996a).

Isoprene is thought to be produced in the liver of humans and animals through a non-enzymatic breakdown of DMAPP, an intermediate metabolite of the mevalonate pathway used in the synthesis of cholesterol (Figure 1.9) (Deneris *et al.*, 1984). Isoprene emission is therefore expected to decrease in individuals that are given drugs to lower cholesterol (Sharkey, 1996a). Surprisingly, Sharkey and colleagues reported that there was no significant difference in breath isoprene levels for drug treated individuals compared to untreated ones.

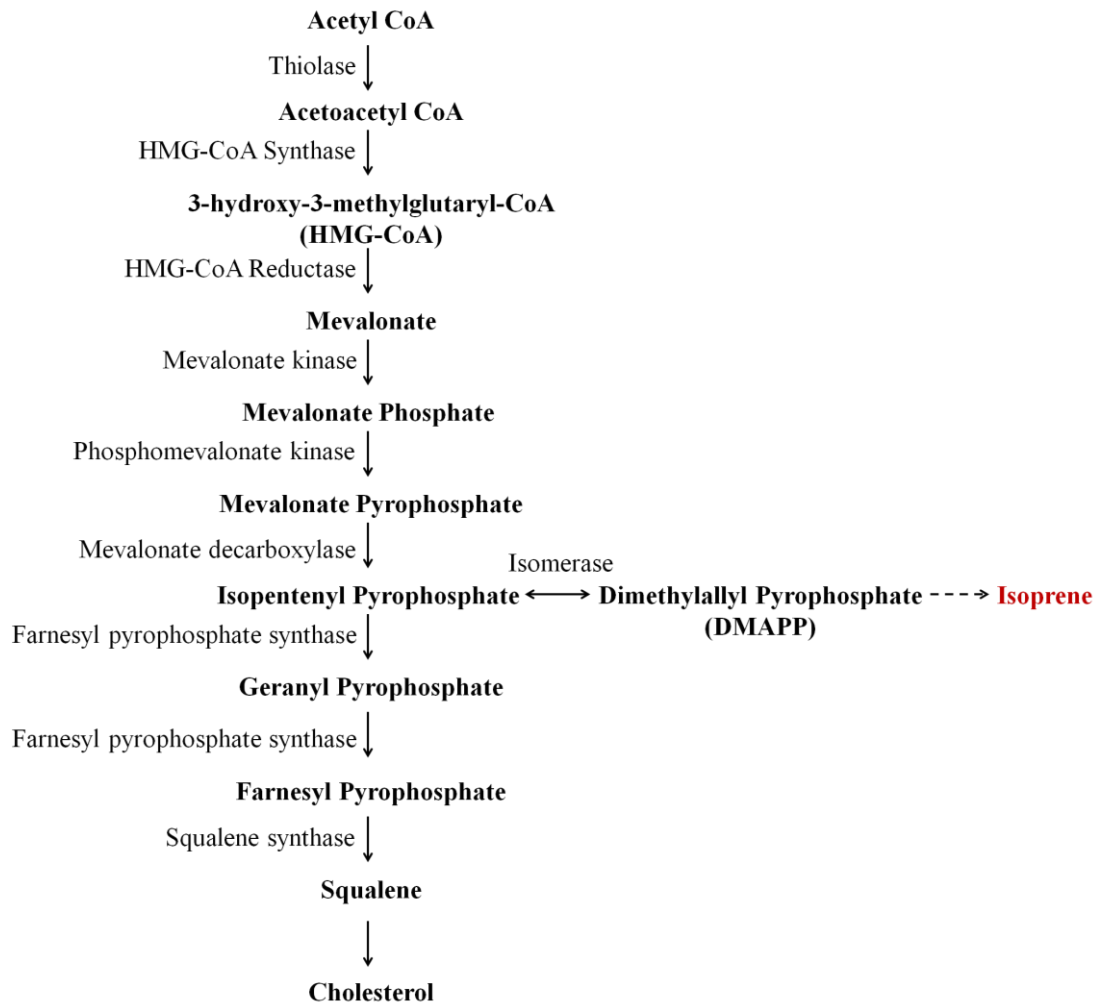


Figure 1.9 Endogenous production of isoprene as a by-product of the mevalonate pathway of cholesterol biosynthesis. The dashed arrow represents a non-enzymatic reaction. Adapted from Salerno-Kennedy & Cashman, 2005.

1.3.4 Isoprene production in the marine environment

The question of how much isoprene is emitted from the marine environment remains controversial. While some studies estimate the total isoprene flux from oceans to be 0.1 Tg C/year (Palmer & Shaw, 2005), others extrapolate it to 10-fold (Bonsang *et al.*, 1992) and 100-fold higher (Shaw *et al.*, 2010). Independently-led observations of a striking correlation between the levels of isoprene emitted and chlorophyll concentrations have prompted the belief that isoprene production in the marine environment is carried out by photosynthetic organisms (Milne *et al.*, 1995, Baker *et al.*, 2000). The main marine producers of isoprene include seaweed, and phytoplankton (e.g. diatoms, cyanobacteria, dinoflagellates, coccolithophores)

(Moore *et al.*, 1994, Broadgate *et al.*, 2004, Shaw *et al.*, 2003, Bonsang *et al.*, 2010). *Prochlorococcus*, the most abundant marine photosynthetic prokaryote, was shown to emit isoprene at an estimated rate of 9×10^{-9} mol/g dry weight/day, a rate 1000 times lower than that of terrestrial plants, such as oak (Shaw *et al.*, 2003, Partensky *et al.*, 1999). Bonsang *et al.*, (2010) reported that isoprene production rates vary from one phytoplankton group to another, with cyanobacteria showing the highest rates. Laboratory cultures of different species of seaweed were also shown to produce isoprene in a species-dependent manner (Broadgate *et al.*, 2004). Shaw and colleagues (2003) investigated whether the rate at which isoprene is emitted from phytoplankton changes when the environmental conditions change and how do these changes compare to those observed in the terrestrial environment. They showed that isoprene emission from *Prochlorococcus* cultures scaled positively with increased light and temperature. However, the temperature value (23 °C) at which isoprene emission peaked was considerably lower than that for terrestrial isoprene production and corresponded to the optimal growth temperature. At temperatures higher than 23 °C, isoprene emission decreased. This finding challenged the relevance of the thermotolerance hypothesis to marine ecosystems, especially that temperature fluctuations are less frequent in the marine ecosystem and do not impose a selective pressure on marine organisms as they do on terrestrial ones (Shaw *et al.*, 2003). Furthermore, the loss of fixed carbons for isoprene is negligible (10^{-4} %) in phytoplankton compared to terrestrial plants (2 %), raising the possibility that isoprene might simply represent a waste with no determined metabolic or physiological role (Shaw *et al.*, 2003, 2010). In addition to phytoplankton and seaweed, other sources of marine isoprene flux to the atmosphere include higher aquatic plants (e.g. sedges, mosses) from wetlands (Hellén *et al.*, 2006, Haapanala *et al.*, 2006, Ekberg *et al.*, 2009, Shaw *et al.*, 2010). Several field measurements showed that isoprene production from aquatic environments displays sharp seasonal and diurnal variations (Broadgate *et al.*, 1997, Lewis *et al.*, 1999, Lewis *et al.*, 2001, Shaw *et al.*, 2010). However a clear interpretation of this pattern is still lacking (Lewis *et al.*, 2001).

1.4 Isoprene and climate change

Due to its abundance and high atmospheric reactivity, isoprene is inevitably factored into climate change models. This justifies the need for accurate quantification of current isoprene flux and predictions of future changes in the global isoprene budget (Monson *et al.*, 2007). Isoprene is influenced by several environmental factors, including land use, productivity, temperature, and CO₂ levels, as discussed earlier. This implies that a realistic estimation of a future isoprene budget should account for all of these factors (Arneth *et al.*, 2007). Several models that predict future changes in isoprene emission already exist in the literature. These models however mostly account for global rise in temperature and overlook other less obvious factors that might influence isoprene emission, such as plant pathogens (Anderson *et al.*, 2000). For instance, wide areas of oak trees in Texas (USA) are being infected with a fungus-mediated disease, so-called oak wilt. A study conducted by Anderson *et al.*, (2000) showed that isoprene emission from leaves was reduced by approximately half in infected oak trees compared to healthy ones. Planting biofuel crops might also have future implications on the isoprene flux to the atmosphere considering that some of the biofuel crops that are being grown have the capacity to emit isoprene (Hewitt *et al.*, 2009). The substantial increase in isoprene production predicted by some scenarios which rely primarily on changes in temperature and biomass productivity (Sanderson *et al.*, 2003, Wiedinmyer *et al.*, 2006, Guenther *et al.*, 2006) is severely criticized by other scenarios which take into consideration the inhibitory effect of high CO₂ levels on isoprene emission (Arneth *et al.*, 2007, Monson *et al.*, 2007, Pacifico *et al.*, 2009, Pacifico *et al.*, 2012). The latter scenarios expect that the ongoing rise in CO₂ concentrations will effectively reduce global isoprene emissions or at the very least will counteract the effect of global warming. Another pressing issue with regard to predicting future changes in total isoprene budget is the limited information available on isoprene consumption. Compared to our knowledge on isoprene sources, our knowledge on isoprene sinks, consumption rates and mechanisms is restricted to a few studies.

1.5 Bacterial degradation of isoprene

Cleveland and Yavitt (1997) were the first to suggest that not all the isoprene that is being synthesized gets depleted in the atmosphere through chemical reactions with other atmospheric components. A portion of the isoprene produced is depleted through metabolic reactions by soil microorganisms which utilize it as a growth substrate. The authors incubated different soil samples (including samples collected from tropical, temperate, and boreal forests) with 508 ppbv isoprene in sealed vessels at 25 °C in the dark, then monitored isoprene uptake by gas chromatography. Isoprene concentrations in the headspace decreased throughout incubation at a soil type-specific rate. Appropriate controls were included and ruled out the possibility of isoprene depletion being caused by leakage or chemical oxidation. On the basis of these laboratory incubations, Cleveland & Yavitt estimated a global uptake of 20.4 Tg / year (~5 %) of atmospheric isoprene by soils. It is worth emphasising, however, that this estimate might not be very accurate given that it was based on a small scale study, better estimates have not since been reported. *In situ* field studies were also conducted, showing that temperate forest soil exposed to isoprene in field chambers consumed isoprene at a rapid rate (Cleveland & Yavitt, 1998). 1 gram of this soil was estimated to harbour 10^5 isoprene-utilizing bacteria, members of the *Arthrobacter* genus. Bacteria capable of utilizing isoprene as their sole source of carbon and energy, including *Nocardia*, *Rhodococcus* and *Alcaligenes* species, have previously been isolated, albeit briefly characterized (van Ginkel *et al.*, 1987, Ewers *et al.*, 1990).

Researchers in the laboratory of Professor Dick Janssen have led pioneering investigations concerning isoprene degradation by bacteria. They isolated an isoprene-utilizing bacterium from an isoprene enrichment culture of freshwater sediment (Vlieg *et al.*, 1998). This bacterium was identified as *Rhodococcus sp.* AD45, a Gram-positive strain of the phylum *Actinobacteria*. Members of this phylum have long been known for their importance in the healthcare and biotechnology industries as they include human pathogens, antibiotic-producing bacteria and extremophiles that represent a source of highly stable enzymes (Gao & Gupta, 2012). *Rhodococcus* AD45 grown on isoprene produces 3, 4-epoxy-3-methyl-1-butene as the first product in the isoprene degradation pathway (Vlieg *et al.*, 1998). This product is acted upon by a glutathione S-transferase which was

purified and characterized by the same group, a year later (Vlieg *et al.*, 1999). The purification of glutathione S-transferase allowed for the design of primers targeting the gene encoding this enzyme. These primers were used to construct a gene library of *Rhodococcus* AD45 which led to the identification of an 8.5 kb gene cluster involved in isoprene degradation pathway in *Rhodococcus* AD45 (Vlieg *et al.*, 2000). The operon encodes a putative multicomponent monooxygenase, two glutathione S-transferases, a dehydrogenase, and a racemase (Figure 1.10).

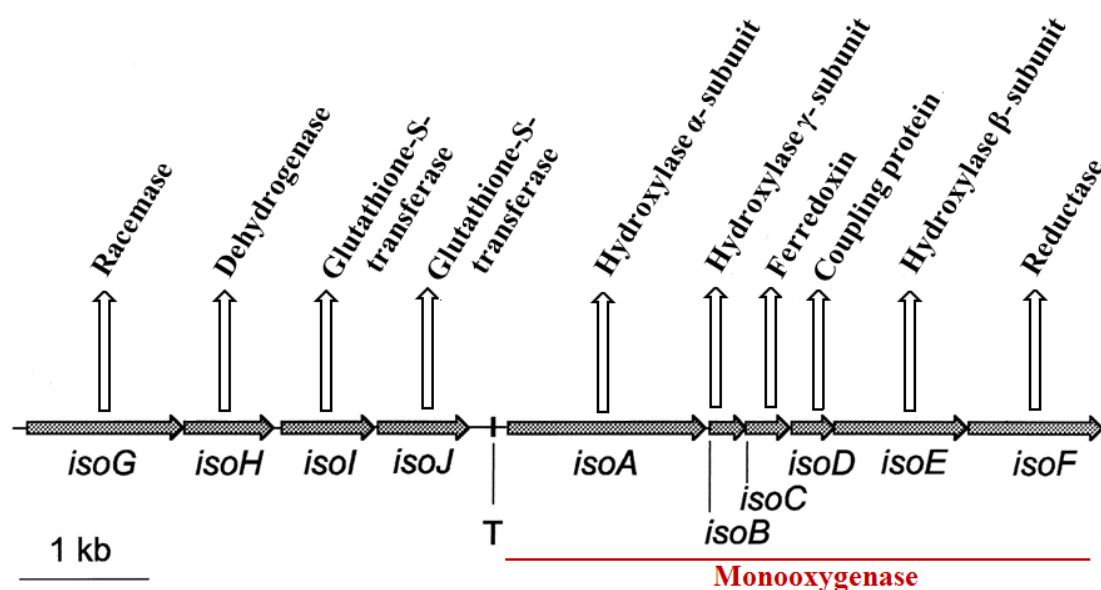


Figure 1.10. Organisation of the *isoABCDEFGHIJ* gene cluster from *Rhodococcus* *sp.* AD45. Modified from Vlieg *et al.*, 2000. T: putative *rho*-independent transcription terminator.

Isoprene monooxygenase was found to have significant levels of homology to enzymes of the soluble diiron centre monooxygenase (SDIMO) family (Vlieg *et al.*, 2000). This family of enzymes, of which the soluble methane monooxygenase (sMMO) is a well known example, has been extensively studied for its role in hydrocarbon oxidation. As the name indicates, SDIMO enzymes contain a diiron centre coordinated by conserved histidine and glutamate residues (Sazinsky & Lippard, 2006). The three core components of the SDIMO multi-component protein include: a hydroxylase consisting of two or three subunits, a reductase, and a regulatory protein (Merkx *et al.*, 2001, Sazinsky & Lippard, 2006). The hydroxylase harbours in its α -subunit the diiron centre to which electrons are transferred from

NAD(P)H by the reductase. Following electron transfer, the regulatory protein changes conformation and allows the reduced diiron active site to have access to and to bind molecular oxygen and hydrocarbon substrate, thus initiating the hydroxylation reaction (Wang & Lippard, 2014). Six groups of SDIMO enzymes have been identified to date (see Chapter 3) (Coleman *et al.*, 2006). Enzymes pertaining to the same group share same phylogeny, identical number of hydroxylase subunits, and similar gene organisation of the SDIMO operon. The SDIMO operon is usually located on the bacterial chromosome (Notomista *et al.*, 2003, Leahy *et al.*, 2003). However, there have been cases where it was found on plasmids as is the case for the alkene-oxidizing bacterium, *Xanthobacter sp.* PY2 (Krum & Ensign, 2001). The rich diversity of the SDIMO enzymes found in nature reflects a wide substrate range. This characteristic of the SDIMOs is particularly relevant in bioremediation and clean technology applications (Holmes, 2009). Chlorinated compounds are prominent soil and water pollutants which, if untreated, can remain in the environment for a very long period of time. Hydrocarbon-oxidizing bacteria can co-metabolize chlorinated alkanes and alkenes in the presence of the appropriate hydrocarbon growth substrate through the catalytic activity of their SDIMO enzymes. Numerous studies have already provided solid experimental evidence that soluble monooxygenases can readily oxidize halogenated compounds. These studies mainly consisted in monitoring the depletion of halogenated compounds in bioreactors containing pure or mixed hydrocarbon-oxidizing bacterial cultures, purifying and assaying the catalytic activity of soluble monooxygenases towards selected chlorinated compounds, or evaluating the diversity of metabolic genes and bacteria in contaminated sites (Fox *et al.*, 1990, Ensley, 1991, Taylor *et al.*, 1993, Holmes, 2009).

A pathway for isoprene degradation has been proposed based on sequence information from *Rhodococcus sp.* AD45 and the purification of glutathione S-transferase and dehydrogenase proteins with high activity to intermediate products of the breakdown of isoprene (Vlieg *et al.*, 1999, 2000) (Figure 1.11). In brief, molecular oxygen is introduced into isoprene by the catalytic activity of the isoprene monooxygenase IsoABCDEF. The oxidation reaction yields an epoxide which is detoxified following conjugation to glutathione, a reaction catalysed by the glutathione S-transferase enzyme IsoI. Subsequently, the glutathione conjugate, 1-

hydroxy-2-glutathionyl-2-methyl-3-butene, undergoes a two-step oxidation reaction mediated by the dehydrogenase IsoH which converts the hydroxyl group to carboxyl, thus producing 2-glutathionyl-2-methyl-3-butenic acid. The latter will ultimately feed into central metabolism for carbon and energy assimilation through as of yet unknown reactions likely to involve the activity of the racemase IsoG and the second glutathione S-transferase IsoJ.

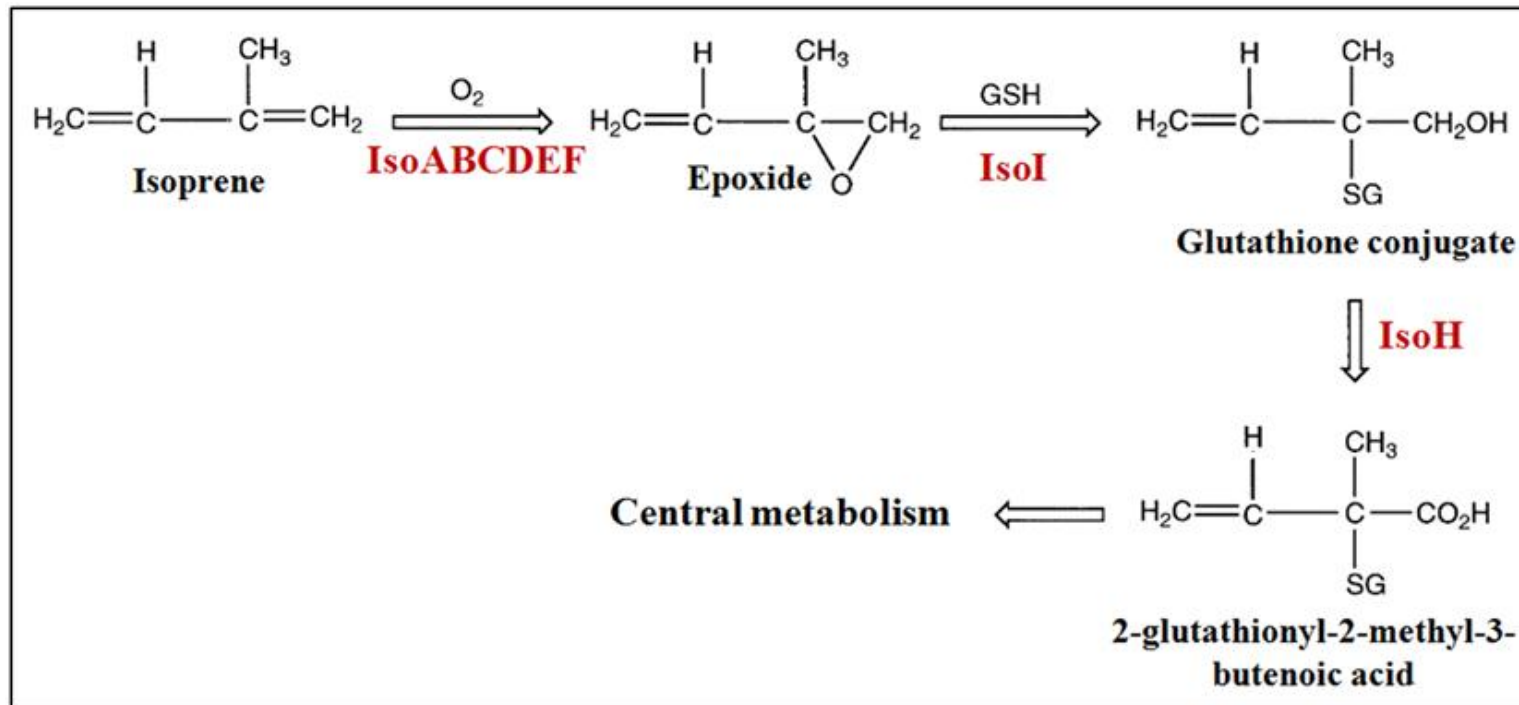


Figure 1.11 Proposed pathway of isoprene metabolism in *Rhodococcus sp.* AD45. Modified from Fall & Copley, 2000.

Efforts led by the group of Terry McGenity at the University of Essex identified several marine strains capable of growing solely on isoprene, including members of different genera, *Leifsonia*, *Gordonia*, *Rhodococcus*, *Dyadobacter*, and *Xanthobacter* (Alvarez *et al.*, 2009). When tested, these strains were capable of utilizing isoprene produced by phytoplankton cultures of *Dunaliella tertiolecta* and *Phaeodactylum tricornutum*, suggesting that isoprene producers and consumers coexist in marine ecosystems. Alvarez and colleagues (2009) showed that tropical (Indonesia), Mediterranean (Etang de Berre), and estuarine (Colne estuary) waters can degrade isoprene. Estuarine sediments were also capable of consuming isoprene at a higher rate compared to water samples. Using denaturing gradient gel electrophoresis (DGGE) and 454 pyrosequencing of 16S rRNA gene amplicons, the authors showed the diversity of the isoprene-utilizing bacterial community of the water and sediment cultures enriched with unlabeled isoprene. Phylotypes affiliated with *Actinobacteria* dominated the total 16S rRNA gene sequences from the isoprene enriched estuarine and Mediterranean waters. On the other hand, *Alphaproteobacteria* dominated the isoprene-degrading bacterial community in the tropical Indonesian water.

Our knowledge of bacterial degradation of isoprene remains, however, limited to the few studies mentioned above, with *Rhodococcus* AD45 being the only well characterized terrestrial isoprene-degrading bacterium. This calls for further research to elucidate the identity and diversity of bacteria and genes involved in the isoprene oxidation pathway.

1.6 Project aims

Using cultivation-dependent and independent methods, the aim was to investigate the bacterial degradation of isoprene in terrestrial environments, characterize the isoprene-degrading bacterial communities, and identify key genes in the isoprene degradation pathway. The cultivation independent methods included DNA-stable isotope probing (see Chapter 6), 454 pyrosequencing, and functional gene biomarkers (see Chapter 5). The specific aims of this study are listed below.

1. Isolate and characterize novel isoprene-degrading bacteria from the terrestrial environment.
2. Characterize new isoprene gene clusters through sequencing and analyzing the genomes of *Rhodococcus* AD45 and new isolates.
3. Develop a PCR-based approach to detect and investigate the diversity of genes encoding the α -subunit of the hydroxylase component of the isoprene monooxygenase in enrichments and environmental samples.
4. Identify uncultivated active isoprene-utilizing bacteria by combining DNA-SIP and 454 pyrosequencing technology.
5. Develop a genetics system in *Rhodococcus* AD45 to investigate the requirement for the isoprene monooxygenase during growth on isoprene.

Chapter 2

Materials and Methods

Table 2.1 List of bacterial strains

Strains	Description	Reference/source
<i>Rhodococcus sp.</i> AD45	Wild type	Vlieg <i>et al.</i> , 1998
<i>Rhodococcus sp.</i> AD45 Δ IsoA	<i>Rhodococcus sp.</i> AD45 with deletion of isoprene monooxygenase α -subunit	This study
<i>Rhodococcus sp.</i> SC4	Wild type, soil isolate	This study
<i>Rhodococcus sp.</i> LB1	Wild type, leaf isolate	This study
<i>Rhodococcus opacus</i> PD630	Wild type	Alvarez <i>et al.</i> , 1996
<i>Mycobacterium hodleri</i> i29a2*	Wild type, marine isolate. For <i>isoA</i> primer design	Dr Terry McGenity
<i>Gordonia polyisoprenivorans</i> i37	Wild type, marine isolate. For <i>isoA</i> primer design	Alvarez <i>et al.</i> , 2009
<i>Methylococcus capsulatus</i> Bath	Non-isoprene degrading strain, negative control for testing the specificity of <i>isoA</i> primers	Stainthorpe <i>et al.</i> , 1990
<i>Methylocella silvestris</i> BL2	Non-isoprene degrading strain, negative control for testing the specificity of <i>isoA</i> primers	Theisen <i>et al.</i> , 2005

<i>Mycobacterium sp.</i> NBB4	Non-isoprene degrading strain, negative control for testing the specificity of <i>isoA</i> primers	Coleman <i>et al.</i> , 2011
<i>Pseudomonas putida</i> ML2	Non-isoprene degrading strain, negative control for testing the specificity of <i>isoA</i> primers	Tan <i>et al.</i> , 1993
<i>Rhodococcus aetherivorans</i> I24	Non-isoprene degrading strain, negative control for testing the specificity of <i>isoA</i> primers	Priefert <i>et al.</i> , 2004
<i>Rhodococcus jostii</i> RHA1	Non-isoprene degrading strain, negative control for testing the specificity of <i>isoA</i> primers	Sharp <i>et al.</i> , 2007
<i>Rhodococcus opacus</i> DSM1069	Non-isoprene degrading strain, negative control for testing the specificity of <i>isoA</i> primers	Trojanowski <i>et al.</i> , 1977
<i>Rhodococcus rhodochrous</i> B276	Non-isoprene degrading strain, negative control for testing the specificity of <i>isoA</i> primers	Saeki & Furuhashi, 1994
<i>Rhodococcus rhodochrous</i> PNKb1	Non-isoprene degrading strain, negative control for testing the specificity of <i>isoA</i> primers	Woods & Murrell, 1989
<i>Escherichia coli</i> S17.1 λ pir	For the conjugal transfer of pMEK plasmid	Simon <i>et al.</i> , 1983
<i>Escherichia coli</i> TOP10	For cloning and plasmid preparation	Invitrogen
<i>Escherichia coli</i> JM109	For cloning and plasmid preparation	Promega

Table 2.2 List of plasmids used in this study

Plasmids	Description	Reference/source
pGEM-T Easy	Ap ^R , cloning vector	Promega
p34S-Gm	Contains Gm ^R cassette	Dennis & Zylstra, 1998
pK18 <i>mobsacB</i>	Km ^R , RP4- <i>mob</i> , mobilizable cloning vector containing <i>sacB</i> from <i>Bacillus subtilis</i>	Schäfer <i>et al.</i> , 1994
pNV18	Km ^R , broad host range vector	Chiba <i>et al.</i> , 2007
pMEK	pK18 <i>mobsacB</i> containing arm A and arm B of <i>isoA</i> ligated to Gm ^R cassette	This study

2.1 General purpose buffer and solutions

LB (Luria Bertani) medium

Tryptone 10 g

Yeast extract 5 g

NaCl 10 g

Volume adjusted to 1 litre with deionized water

Tris-borate-EDTA (TBE) buffer 10 X

Tris base 108 g / l

Orthoboric acid 55 g / l

0.5 M Sodium EDTA (pH 8.0) 40 ml / l

Tris-acetate-EDTA (TAE) buffer 50 X

Tris 242 g / l

Glacial acetic acid 57.1 ml / l

0.5 M Sodium EDTA (pH 8.0) 100 ml / l

Tris-EDTA (TE) buffer pH 8.0

Tris-HCl 10 mM

Na₂EDTA 1 mM

Prepared from 1 M Tris-HCl (pH 8.0) and 0.5 M Na₂EDTA (pH 8.0)

SET buffer

EDTA	40 mM
Tris-HCl pH 9.0	50 mM
Sucrose	0.75 M

2.2 Cultivation of *Rhodococcus sp.* strains AD45, LB1 and SC4

Rhodococcus sp. strains LB1, SC4 and AD45 were routinely cultivated on CBS minimal medium with an appropriate carbon source. 1 litre of CBS minimal medium, previously described by Boden *et al.*, 2008, was prepared from solutions 1 and 2, autoclaved separately for 15 minutes at 15 psi, 121 °C, cooled then mixed aseptically. The solutions were prepared as follows:

Solution 1:

MgSO ₄ .7H ₂ O	0.1 g
NH ₄ Cl	0.8 g
Trace element solution	10 ml

Dissolved in sterile deionized water, total volume of the solution being 800 ml

Solution 2: Phosphate buffer

KH ₂ PO ₄	1.5 g
Na ₂ HPO ₄	6.3 g

Dissolved in sterile deionized water, total volume of the solution being 200 ml

Trace element solution: stored at 4 °C, in the dark, contained the following components dissolved in sterile deionized water in 1 litre total volume:

Na ₂ – EDTA	50 g
NaOH	11 g

ZnSO ₄ . 7H ₂ O	5 g
CaCl ₂ . 2H ₂ O	7.34 g
MnCl ₂ . 4H ₂ O	2.5 g
CoCl ₂ . 6H ₂ O	0.5 g
(NH ₄) ₂ MoO ₄	0.5 g
FeSO ₄ . 7H ₂ O	5 g
CuSO ₄ . 5H ₂ O	0.2 g
H ₃ BO ₃	0.05 g
NH ₄ VO ₃	0.01 g

For growth with gaseous substrates, cultures were set up in 125 ml sterile serum vials sealed with grey butyl rubber seals or in Quickfit flasks (250 ml or 2 L) fitted with SubaSeal stoppers (Sigma-Aldrich), shaking at 150 rpm, at 30 °C. For growth with isoprene on solid medium, CBS mineral medium agar plates were prepared by adding 1.5 % (w/v) of bacteriological agar (Oxoid, UK), inoculated, and incubated in a desiccator in an isoprene-rich atmosphere which was created by placing inside the desiccator a sterile glass universal containing a piece of glass wool to which 1 ml of isoprene was added. The desiccator was placed at 30 °C.

2.3 Purity checks and maintenance of bacterial strains

Cultures were regularly checked for purity by phase contrast microscopy at 1,000 x magnification (Zeiss Axioscop, UK) and plating on nutrient-rich R2A agar plates. Glycerol stocks of the *Rhodococcus* isolates were prepared by adding 200 µl of sterile 20 % (v/v) glycerol to 800 µl of *Rhodococcus sp.* cells grown in LB medium. The stocks were drop frozen in liquid nitrogen and stored at – 80 °C.

2.4 Quantification of headspace concentration of isoprene

The headspace concentration of isoprene in pure cultures and enrichments was measured by gas chromatography using Agilent 7890A GC: Column (Porapak Q, 530 μm), carrier gas (He, 20 ml / min), detector (FID). The temperature of the column, injector and detector was set to 175 °C, 250 °C, and 300 °C, respectively. The retention time of isoprene at these settings was 4.7 min. The headspace concentration of isoprene was determined by injection of 100 μl of headspace gas into the gas chromatograph and comparison with standards prepared in 125 ml sealed serum vials by dilution of pure isoprene in air, thus containing a known quantity of isoprene in air.

2.5 Extraction of nucleic acids

2.5.1 Extraction of genomic DNA

Genomic DNA to be used for standard downstream applications, such as PCR amplification of genes of interest, was extracted from pure cultures or enrichments using the FastDNA Spin Kit for Soil (MP Biomedicals). 500 mg of soil or 500 μl of concentrated cell suspension were initially added to the supplied Lysing Matrix E tube. The cell suspension was prepared from cells grown on 1 % (v/v) isoprene in 50 ml CBS minimal medium to an optical density of 0.6 at 540 nm, harvested by centrifugation at 14,000 x g for 20 min, and suspended in minimum volume of sterile CBS medium. The rest of the procedure was conducted according to the manufacturer's manual.

For genome sequencing, high-molecular mass genomic DNA was extracted from cultures of *Rhodococcus sp.* strains AD45, LB1 and SC4 following the Marmur extraction method (1961) with modifications. 500 ml cultures of *Rhodococcus sp.* SC4, LB1 and AD45 were grown to an OD of 0.7 (540 nm). Cells were pelleted by centrifugation at 8,700 x g for 30 min, washed and resuspended in 2 ml SET buffer (section 2.1). 100 μl of lysozyme solution (5 mg/ml) was added to the cell suspension and incubated at 37 °C for 30 min. 50 μl of proteinase K solution (20 mg/ml) and 200 μl of 20 % (w/v) SDS were added to the cells before incubation at

55 °C for half an hour. After adding 4 ml of SET buffer and 400 µl of 20 % (w/v) SDS, the cells were re-incubated at 55 °C for 5 to 10 hours. Two phenol washes (6 ml of Phenol: Chloroform: Isoamyl alcohol 25:24:1) and one chloroform wash (6 ml of Chloroform: Isoamyl alcohol 24:1) were subsequently carried out. The aqueous phase was transferred to a clean tube and incubated at - 20 °C overnight with 2 volumes of 95 % (v/v) ethanol and 1/10 volume of 3.0 M sodium acetate (pH: 4.8). DNA was obtained after a 20 min centrifugation at 14,000 x g followed by 75 % (v/v) ethanol wash and suspension in 100 µl of TE buffer. The quality of the DNA was assessed by running it on a 1 % (w/v) agarose gel against a *Hind*III- digested Lambda-DNA ladder for comparison (Figure 2.1).

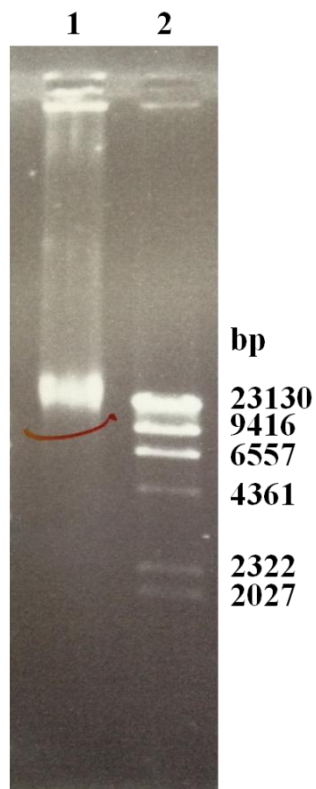


Figure 2.1 *Rhodococcus sp.* AD45 genomic DNA (10 µl, lane 1) in comparison to *Hind*III-digested Lambda DNA standard (lane 2). The top 23,130 bp band of standard contains 250 ng DNA. The mass of the DNA band > 23,130 bp in lane 1 was estimated to be 520 ng.

2.5.2 Small-scale plasmid extraction

Plasmids were extracted from *E. coli* cells using GeneJET Plasmid Miniprep Kit (Fermentas) according to the manufacturer's protocol. *E. coli* cells were grown overnight in 5 ml sterile LB medium in 20 ml sterile universals, shaking at 150 rpm, at 37 °C.

2.5.3 RNA extraction

Rhodococcus sp. AD45 was grown in 250 ml sterile flasks containing 50 ml of CBS minimal medium with either 10 mM glucose or 1 % (v/v) isoprene in the headspace, in triplicate. The cultures were harvested at mid-late exponential phase. With a 1 ml syringe, 1ml of the culture was removed from each flask and aliquoted into (2 x) 0.5 ml volume placed into RNase- free microcentrifuge tubes already containing 1 ml of RNa protect Bacteria Reagent (Qiagen) for RNA stabilization. After mixing by vortexing for 5 s, the tubes were incubated at 21 °C for 5 min prior to centrifugation for 10 min at 5,000 x g. The supernatant was then discarded and the cell pellet was placed on ice for RNA extraction using RNeasy Lipid Tissue Mini Kit (Qiagen) with modification of the initial steps in the manufacturer's protocol. The cell pellet was carefully resuspended in 100 µl TE buffer (prepared with DEPC-treated water) to which lysozyme (15 mg/ml) was added. After mixing by vortexing for 5 s, the tubes were incubated at 21 °C for 10 min, mixing every 2 min. 1 ml of pre-heated Qiazol Lysis Reagent supplied in the kit was added to the cell suspension then briefly mixed by vortexing. The cell suspension was incubated for 1 min at 65 °C, mixed by vortexing for 3 min then incubated at 21 °C for 5 min. The cells were subsequently lysed by bead-beating (FastPrep-24 beadbeater, MP Biomedicals) for 30 s at a speed of 6.0 m/s. The remaining steps in the RNA extraction procedure were conducted according to the manufacturer's protocol.

DNA contamination was removed by two consecutive treatments of the RNA using Qiagen RNase- free DNase according to the manufacturer's protocol. The absence of a 16S rRNA PCR product in PCR reactions (section 2.6.4) using 1- 4 µl of RNA template, 27f and 1492r primers (Lane, 1991), and 35 PCR cycles confirmed that the purified RNA is DNA-free.

2.6 Nucleic acid manipulation methods

2.6.1 Quantification of DNA and RNA

NanoDrop 2000 spectrophotometer (Thermo Fisher Scientific) was used to measure the concentration of DNA and RNA samples.

2.6.2 Nucleic acid purification

PCR products were purified using QIAquick PCR Purification kit (Qiagen) as instructed by the manufacturer. For DNA fragments excised from agarose gels, the purification was carried out using QIAquick Gel Extraction Kit (Qiagen), according to the manufacturer's protocol.

2.6.3 DNA restriction digests

Restriction enzymes were purchased from Invitrogen or Fermentas. The digestion reactions were prepared as specified by the manufacturers.

2.6.4 Polymerase chain reaction (PCR)

PCR amplification reactions were prepared in 50 µl total volume. A typical PCR mixture consisted of 10 x DreamTaq buffer (Fermentas), 0.07 % (w/v) BSA, 2.5 units of DreamTaq *Taq* DNA polymerase (Fermentas), 0.2 µM of forward and reverse primers, 0.2 mM of each dNTP, and 2 – 20 ng of DNA template. Standard PCR conditions consisted of: initial denaturation at 95 °C for 5 min, followed by 30 cycles of denaturation at 95 °C for 30 s, annealing at a primer-dependent temperature for 30 s, and extension at 72 °C for 1 min/kb and final extension at 72 °C for 7 min. In the case of PCR from colonies, 2.5 % (v/v) of DMSO was added to the PCR mixture and the duration of the initial denaturation was extended from 5 min to 10 min. A Tetrad thermal cycler (Bio-Rad) was used for all the PCR reactions.

2.6.5 Cloning of PCR products

Purified PCR products were cloned into pGEM-T Easy vector (Promega) as instructed in the manufacturer's manual. Inserts were sequenced (section 2.6.11) using both M13 forward and reverse primers (Invitrogen).

2.6.6 Clone library construction and Restriction Fragment Length Polymorphism (RFLP) assays

Clone libraries were constructed using *isoA* PCR products amplified from DNA purified from isoprene enrichments (see Chapter 5). The PCR products were purified and cloned as described in section 2.6.5. Inserts were amplified directly from colonies using M13 forward and reverse primers. The amplicons were then digested with *EcoRI* and *MspI* restriction enzymes (Fermentas) in a 10 µl final volume. The double digestion reactions comprised 300 ng of PCR product, 2 U of *EcoRI*, 4 U of *MspI* and 2 x Tango buffer. Digested DNA fragments from each clone were separated on a 2 % (w/v) agarose gel and the clones were grouped based on the restriction pattern. One representative clone from each group was sequenced with primers M13F/M13R for phylogenetic analysis.

2.6.7 DNA ligations

Ligation reactions of DNA fragments into plasmid vector were typically set up in 10 µl total volume using T4 DNA ligase (Fermentas) according to the instruction manual.

2.6.8 Agarose gel electrophoresis

1 % (w/v) agarose gels containing 0.5 µg/ml ethidium bromide were cast and run using 1 x TBE buffer. For RFLP analysis, DNA fragments were separated on 2 % (w/v) agarose gels for better resolution. The sizes of DNA fragments were estimated using GeneRuler™ 1 kb DNA ladder (Fermentas). Gels were visualized on a UV

transilluminator (Molecular Imager® Gel Doc™ XR+ System, Bio-Rad) and photographed using the embedded Image Lab™ software.

2.6.9 Reverse transcription PCR (RT-PCR)

cDNA was synthesized from DNA-free RNA isolated from *Rhodococcus* AD45 cells grown on isoprene or glucose (section 2.5.3) using SuperScript II (Invitrogen) and random hexamers, according to the manufacturer's instructions. 60 - 530 ng of RNA and 200 ng of random hexamers were used for first-strand cDNA synthesis at 42°C in 20 µl total volume. cDNA synthesis reactions in which the reverse transcriptase was omitted and substituted with water were included and used as negative controls. 2 µl of the synthesized cDNA were used as template for PCR amplification of *isoA*. PCR reactions with *Rhodococcus* AD45 genomic DNA template and reactions with no-template were also included as controls.

2.6.10 Quantitative Reverse Transcription - PCR (qRT-PCR)

cDNA was synthesized as described in section 2.6.9. Quantitative reverse transcription PCR reactions were set up in a 96-well plate. Each reaction was prepared in a final volume of 20 µl, comprising 2 µl of cDNA, 0.25 µM of forward and reverse primers, and 2 x Fast SYBR Green Master Mix (Applied Biosystems). Two sets of primers were used separately: one targeting *isoA* gene (the gene of interest) and the other targeting *rpoB* gene ('housekeeping' reference gene for normalization). Five standards were prepared for calibration purposes with cDNA generated from isoprene grown *Rhodococcus* AD45 cells and subjected to serial dilutions (to 10⁻⁴). Negative control reactions, which consisted of 2 µl of cDNA-synthesis reactions in which the reverse transcriptase was not added, were included. Quantitative amplification was carried out using StepOnePlus Real - Time PCR System (Applied Biosystems) at the following settings: 95 °C, 20 s (polymerase activation), then 95 °C, 3 s; 60 °C, 30 s for 40 cycles, then 95° C, 15 s; then a melt curve 60° C to 95° C in 0.3° C increments (1 min each). StepOne software v 2.2.2 was used for data analysis.

2.6.11 DNA sequencing

Routine DNA sequencing service was provided by the University of Warwick Genomics Facility (Coventry, UK) and Source BioScience (Cambridge, UK). DNA samples were submitted for sequencing with the appropriate primers. The concentrations of the DNA and the primers complied with the provider's specifications. Sequences were analysed and aligned using Chromas (Technelysium Pty Ltd) and ClustalW available on MEGA versions 5 (Tamura *et al.*, 2011) and 6 (Tamura *et al.*, 2013). Sequence alignments were checked manually for accuracy. *isoA* and 16S rRNA gene amplicons amplified from isoprene SIP incubations were sequenced using 454 pyrosequencing at MR DNA (Texas, USA). 454 sequences were checked for chimeras and quality and analysed using Qiime available on Bio-Linux.

The genomes of *Rhodococcus* SC4 and *Rhodococcus* LB1 were sequenced using Illumina GAIIx at the University of Warwick Genomics Facility (Coventry, UK). The run produced 70 bp paired-end reads that we assembled using the CLC Genomics Workbench for *de novo* assembly provided by CLCbio. The genome sequences were uploaded to RAST (Rapid Annotation using Subsystem Technology) for annotation. Genome sequencing of *Rhodococcus* sp. AD45 was carried out at DuPont Industrial Biosciences (California, USA) by Gregg Whited and colleagues using Illumina's 5 kb mate pair sequencing platform. The genome of *Rhodococcus* AD45 was annotated using Prodigal and the Prokka software (this work was done by Gregg Whited *et al.*). RAST and BioEdit (Ibis Biosciences, USA) software were used for the analysis of all three genomes.

2.7 Antibiotics

Stock solutions of antibiotics were prepared, filter sterilized, and stored at -20 °C. Selective growth media, either liquid or solid (agar), were prepared by adding the filter sterilized antibiotic solutions to the autoclaved medium, after cooling. The stock and working concentrations of the antibiotic solutions used in this project are as follows:

	Antibiotics		
	Ampicillin	Kanamycin	Gentamicin
Stock concentration (mg/ml)	100	50	10
Working concentration (µg/ml)	100	100	5

2.8 Preparation of SOC medium

SOC medium was prepared from SOB medium by adding 20 mM (final concentration) of filter sterilized glucose. SOB medium contained (per 1 litre): 5 g yeast extract, 20 g tryptone, 0.5 g NaCl, and 10 ml of 250 mM KCl solution. The pH was adjusted to 7.0 with 5.0 M NaOH. 2.0 M sterile MgCl₂ solution was added to 10 mM, directly prior to use.

2.9 Transformation of chemically competent *E. coli*

Chemically competent *E. coli* Top10 or JM109 cells (Promega) were thawed on ice, gently mixed with 2 µl of plasmid DNA or ligation mix, and incubated on ice for 20 min. After incubation, cells were subjected to a heat shock at 42 °C for 50 seconds then cooled on ice for 2 min. 950 µl of SOC medium were added to the cells prior to incubation for 1.5 h at 37 °C, shaking at 150 rpm. 50 µl – 100 µl aliquots were then spread onto selective LB agar plates and incubated at 37 °C overnight.

2.10 Preparation and transformation of electrocompetent *E. coli*

5 ml of sterile LB were inoculated with a fresh colony of *E. coli* S17.1 and incubated at 37 °C overnight. 500 µl of the overnight culture were then used to inoculate 500 ml of sterile LB. The cells were grown at 37 °C and harvested at OD₅₄₀ of 0.4 – 0.5. Cells were cooled on ice for 15 min prior to centrifugation for 15 min at 8,000 x g,

4°C. Cells were then washed twice with cold sterile deionised water and once with cold 10 % (v/v) glycerol. The cell pellet was resuspended in 2.5 ml of cold 10 % (v/v) glycerol. 50 µl aliquots of cells were placed into pre-chilled 1.5 ml microcentrifuge tubes and immediately stored at -80 °C for later use.

50 µl of electrocompetent *E. coli* S17.1 cells were gently mixed (on ice) with 2 µl of plasmid DNA and incubated on ice for 1 min. Cells and DNA were transferred into pre-chilled 1 mm electroporation cuvette and subjected to an electric pulse at 1.8 kV, 25 µF, and 200 Ω by GenePulser Xcell™ (Bio-Rad). Quickly after electroporation, the cells were added to 950 µl of SOC medium in 15 ml Falcon tube and incubated for 1 hour, at 37 °C, shaking at 150 rpm. 50 µl – 100 µl aliquots were then spread onto LB agar plates containing the appropriate antibiotic and incubated overnight at 37 °C.

2.11 Conjugal transfer of pMEK plasmid from *E. coli* to *Rhodococcus* AD45

Rhodococcus AD45 and *E. coli* S17.1 which contained the pMEK plasmid (section 2.10) were grown overnight in 5 ml sterile LB medium with no added antibiotic. The cells were separately harvested the following day by centrifugation for 15 min at 4,000 x g, 15 °C. *Rhodococcus* AD45 cells were harvested at mid-exponential phase (OD₅₄₀: 0.4 – 0.5). Each of the cell pellets was washed in 5 ml LB medium before being mixed together in a total volume of 10 ml in a sterile Falcon tube. The mixture was centrifuged for 15 min at 4,000 x g, 15 °C and the pellet was re-suspended in 0.5 ml sterile LB medium. 0.25 ml of the cell suspension was placed at the center of a 0.2 µm nitrocellulose filter (Millipore, USA) on LB agar plate and incubated at 30 °C overnight. Following incubation, the cells were washed off the filter with 1 ml sterile LB medium. 50 – 100 µl aliquots were then spread onto LB agar plates containing gentamicin (5 µg/ml) and nalidixic acid (10 µg/ml) and incubated at 30 °C for five to seven days. Nalidixic acid at 10 µg/ml concentration was found to selectively inhibit the growth of *E.coli* cells on LB agar plates and in liquid LB medium.

2.12 Preparation and transformation of electrocompetent *Rhodococcus sp.* AD45

A single colony of *Rhodococcus sp.* AD45 was picked from a fresh plate and inoculated into 5 ml of CBS minimal medium with 10 mM sodium succinate. The culture was grown overnight at 30 °C, shaking at 150 rpm. The following day, 500 µl of the overnight culture were used to inoculate 50 ml of CBS minimal medium with 10 mM succinate in a sterile 250 ml flask. The cells were grown to an OD₅₄₀ of 0.4 – 0.5 (mid exponential phase), cooled on ice for 15 min then harvested by centrifugation for 15 min at 2,500 x g, 4 °C. The cells were washed once with cold sterile water then washed with cold sterile 10 % (v/v) glycerol. Subsequently, the cells were resuspended in 1 ml of 10 % (v/v) glycerol and used fresh for transformation.

100 µl of cells were transferred to 1.5 ml microcentrifuge tubes. 4 µl of plasmid DNA (279 ng) was added to the cells and incubated on ice for 10 min. Cells and DNA were transferred to a cold 2 mm gap electroporation cuvette (VWR, Taiwan) and subjected to an electric pulse using GenePulser Xcell™ (Bio-Rad). Several electroporation settings were tried. Best results were obtained at the following setting: 2.5 kV, 25 µF, 800 Ω. Immediately after electroporation, cells were recovered in 1 ml CBS medium with 10 mM succinate and incubated with shaking at 30 °C for 4 – 6 hours. 50 µl aliquots of cells were plated onto LB plates with gentamicin (5 µg/ml) and incubated at 30 °C for 3 -5 days.

2.13 Sucrose selection for double cross-over mutants

Rhodococcus AD45 cells which contained the *sacB* gene (i.e., the pMEK plasmid) were grown in 5 ml LB medium with no added antibiotic at 30 °C, overnight. The culture was diluted to 10⁻⁴ – 10⁻⁵, and 100 µl aliquot of the dilution were spread onto LB agar plates containing 10 % (w/v) sucrose and gentamicin (5 µg/ml). The plates were incubated at 30 °C for 3 – 5 days.

2.14 Analysis of proteins

2.14.1 Harvesting of cells and preparation of cell-free extracts

Rhodococcus AD45 cells were grown in 2 L sterile flasks containing 500 ml CBS minimal medium with 10 mM glucose or 1 % (v/v) isoprene. The flasks were incubated at 30°C, shaking at 150 rpm. Cells were harvested at late exponential phase (OD₅₄₀: 0.8 - 1) by centrifugation for 30 min at 14,000 x g, 4 °C. After decanting the supernatant, the cells were washed with CBS minimal medium containing no substrate then resuspended in 3 ml of 50 mM PIPES buffer (pH 7.4). The cells were subjected to three passages through a French pressure cell (American Instrument Company, USA) at 110 MPa (on ice). Cell-free extracts were prepared by removing cell debris via centrifugation for 15 min at 14,000 x g, 4 °C.

2.14.2 Protein quantification

The concentration of proteins in the cell-free extracts was estimated using the Bio-Rad Protein Assay (Bio- Rad) whereby bovine serum albumin was used for the preparation of standards, according to the manufacturer's protocol.

2.14.3 Sodium Dodecyl Sulfate-Polyacrylamide Gel Electrophoresis (SDS-PAGE)

Polypeptides in the cell-free extracts were separated by SDS-PAGE using an X-Cell II Mini-Cell apparatus (Novex). A 4% (w/v) stacking gel and a 12.5 % (w/v) resolving gel were prepared as follows:

	4 % stacking gel	12.5 % resolving gel
40 % (w/v) acrylamide/bis (37.5:1)	0.5 ml	3.125 ml
Tris 0.5 M pH 6.8	1.25 ml	-
Tris 3.0 M pH 8.8	-	1.25 ml
10 % (w/v) SDS	50 μ l	100 μ l
10% (w/v) Ammonium persulfate	25 μ l	75 μ l
TEMED	5 μ l	5 μ l
Water	3.17 ml	5.44 ml
Total	5 ml	10 ml

Protein samples were prepared in a total volume of 15 μ l for loading into the wells. The samples contained x volume of cell-free extract (15 μ g of protein) and 5 x loading buffer. The loading buffer consisted of 63 mM Tris-HCl (pH 6.8), 2 % (w/v) SDS, 10 % (v/v) glycerol, 5 % (v/v) β - mercaptoethanol, and 0.001 % (w/v) bromophenol blue. The prepared samples were immediately boiled for 8 min in a boiling water bath, cooled on ice, and loaded into the wells. Samples were run in 5 x running buffer at 90 V through the stacking gel and 120 V through the resolving gel. The 5 x running buffer consisted of (per 500 ml): 7.5 g Tris base, 36 g glycine and 25 ml of 10 % SDS. After electrophoresis, gels were stained with Coomassie Brilliant Blue staining solution prepared by dissolving 0.1 % (w/v) Coomassie Brilliant Blue R-250 in 40 % (v/v) methanol, 10 % (v/v) acetic acid and 50 % water. The gels were then destained in 40 % (v/v) methanol and 10 % (v/v) acetic acid.

2.14.4 Mass spectrometry analysis of polypeptides

The bands of interest were excised from the gel and 200 μ l of deionized water were added to each excised band prior to submission for analysis at the Centre for BioMedical Mass Spectrometry and Proteomics at the University of Warwick (Coventry, UK). The samples were digested with trypsin and analysed by means of nano liquid-chromatography electrospray-ionization tandem mass spectrometry (LC-ESI-MS/MS) using the NanoAcquity/Synapt HDMS instrumentation (Waters) using a 45 minute LC gradient. The MS data were used to interrogate the database of predicted amino acid sequences derived from the genome sequence of *Rhodococcus*

AD45 for polypeptide identification, using ProteinLynx Global Server v2.4. Dr Susan Slade and colleagues at the Center carried out the mass spectrometry analysis described in this section.

2.15 DNA- Stable Isotope Probing (DNA- SIP)

DNA- SIP was conducted according to Neufeld *et al.*, 2007. 5 g of wet soil samples were incubated with 0.1 – 0.5 % (v/v) labelled (^{13}C) or unlabelled (^{12}C) isoprene. The partially-labelled (2 out of 5 carbons were labelled) isoprene incubations were set up in 2 L sterile sealed Quickfit flasks placed at 30 °C whereas fully-labelled isoprene SIP incubations were set up in sterile 125 ml serum vials, sealed and placed at room temperature, in the dark. Control incubations with autoclaved soil were also prepared. The headspace concentrations of isoprene were regularly measured by gas chromatography (section 2.4). After sufficient consumption (see Chapter 6), the incubation was terminated and DNA was extracted from the soil sample using the FastDNA Spin Kit for Soil (MP Biomedicals) as described in section 2.5.1.

1 - 2 μg of extracted DNA were added to caesium chloride solutions (1.725 g/ml density) and subjected to a density gradient ultracentrifugation in a Beckman Vti 65.2 rotor at $177,000 \times g_{\text{av}}$, 20 °C for 40 hours, under vacuum. The samples were then fractionated, as described in the published protocol by Neufeld *et al.*, (2007), into 12 to 15 fractions of 300- 400 μl . The caesium chloride density of each fraction was measured using a Reichert AR200 digital refractometer. DNA was precipitated from each fraction and suspended in 30 to 50 μl of nuclease-free water (Ambion®). DNA was then quantified (section 2.6.1), run on a 1 % (w/v) agarose gel and stored at - 20 °C to be used for downstream applications (see Chapter 6).

2.16 Denaturing gradient gel electrophoresis (DGGE)

16S rRNA gene PCR products were run on an 8 % (w/v) polyacrylamide gel with a 30 % - 70 % linear denaturant gradient. A 100 % denaturant solution contains 7.0 M urea and 40 % UltraPure™ formamide (Invitrogen). 1 x TAE was used as buffer and the electrophoresis was carried out for 16 h, at 80 V, 60 °C using the DCode™

Universal Mutation Detection System (Bio-Rad). The DGGE gels were then stained with 3 µl of SYBR® Gold Nucleic Acid Gel Stain (Invitrogen) in 250 ml of 1 x TAE for one hour. The gels were washed three times with distilled water prior to being photographed using a BioRad GelDoc imaging system.

2.17 Bacterial community analysis by 454 pyrosequencing

16S rRNA and *isoA* gene amplicons were sequenced using the 454 pyrosequencing platform at MR DNA Molecular Research (Texas, USA). The 454 reads were quality checked and analyzed using QIIME pipeline available on BioLinux. Only reads sized between 200 and 1000 bp with an average score above 25 and presenting no ambiguous base calls and no mismatches in the primer sequence were further processed and split into separate libraries based on the sequence of their barcode. The reads were then assigned to OTUs defined at a cutoff of 97 % similarity. Representative sequences were picked for each OTU and assigned to taxonomic groups based on the curated GreenGenes reference database (DeSantis *et al.*, 2006), which is embedded in QIIME. The OTU representative sequences were also aligned and used to generate phylogenetic trees.

Chapter 3

Isolation of novel terrestrial isoprene degrading bacteria and preliminary analyses of the genome sequences of *Rhodococcus* AD45, *Rhodococcus* SC4 and *Rhodococcus* LB1

3.1 Introduction

It has been known for over a decade that bacteria in soil ecosystems are capable of consuming atmospheric isoprene (Cleveland & Yavitt, 1997, Fall & Copley, 2000). Nonetheless, at the start of this project, *Rhodococcus sp.* AD45 was the only well characterized terrestrial isoprene degrader reported in the literature. *Rhodococcus* AD45 was isolated from a freshwater sediment by Janssen's group in The Netherlands (Vlieg *et al.*, 1998). This chapter describes the isolation and characterisation of *Rhodococcus* SC4 and *Rhodococcus* LB1, two novel isoprene degrading bacteria from the terrestrial environment. It also reports the draft sequence of *Rhodococcus* AD45, *Rhodococcus* SC4 and *Rhodococcus* LB1 genomes and gives insight into the metabolic potential of these isoprene degrading strains.

Genomic DNA was extracted from 500 ml pure cultures of *Rhodococcus* strains AD45, SC4 and LB1 grown on 1 % (v/v) isoprene, as described in the Materials and Methods section 2.5.1. The genomes of *Rhodococcus* SC4 and *Rhodococcus* LB1 were sequenced using Illumina GAIIX (70 bp paired-end reads) at the Genomics Facility at the University of Warwick, Coventry, UK. The genome data were then assembled using the CLC Genomics Workbench for *de novo* assembly provided by CLCbio. The assembled data were uploaded to the RAST website (available at <http://rast.nmpdr.org>) for annotation. The genome of *Rhodococcus* AD45 was sequenced using Illumina's 5 kb mate pair sequencing platform and annotated by our collaborators at DuPont Industrial Biosciences (Dr Gregg Whited *et al.*) using Prodigal and the Prokka program (Seemann *et al.*, 2014). The genome analysis was carried out using RAST and BioEdit software.

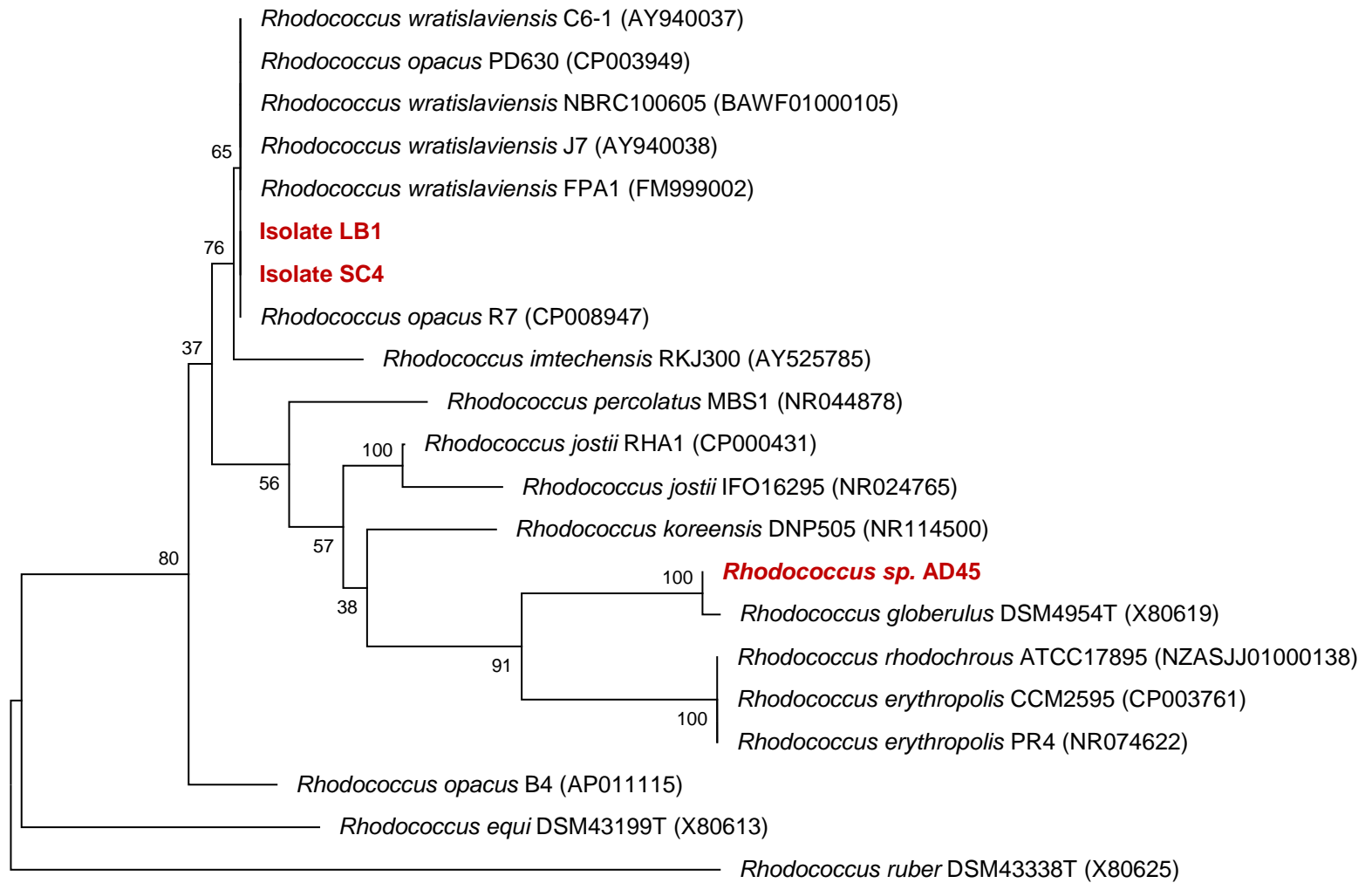
3.2 Enrichment and isolation of two novel terrestrial isoprene degraders

Isoprene enrichment cultures were set up in sealed sterile 250 ml Quickfit flasks using a soil sample collected from Leamington Spa (Warwickshire, UK) and leaves of a Horse Chestnut tree located adjacent to the laboratory at the University of Warwick (Coventry, UK). 0.6 % (v/v) isoprene was added to the 250 ml Quickfit flasks containing 50 ml CBS minimal medium (prepared as detailed in Materials and Methods section 2.2) inoculated with either 0.3 g soil or with one Horse Chestnut leaf, cut into small pieces. The cultures were incubated at 30 °C, shaking at 150 rpm.

The optical density of cultures was followed spectrophotometrically at 540 nm and showed an increase during enrichment. Isoprene uptake was monitored by gas chromatography (GC) (Materials and Methods section 2.4). Enrichment cultures were then inoculated onto CBS agar plates which were incubated at 30 °C in an isoprene rich atmosphere, as described in section 2.2 of Chapter 2. Colonies appeared on the plates after five days of incubation. Single colonies were transferred onto new fresh CBS agar plates and incubated with isoprene as many times as necessary until only colonies of same morphology were seen on the plates. Single colonies were then checked for purity by streaking them onto R2A agar plate, a low nutrient medium, which allows the recovery of slow growing heterotrophic contaminants. Further purity checks included growing the colonies in liquid in 50 ml CBS minimal medium in 250 ml Quickfit flasks with 0.6 % (v/v) isoprene at 30 °C and checking them under a phase contrast microscope at 1,000 x magnification. Two strains were isolated from the enrichment cultures: a leaf isolate (SC4) and a soil isolate (LB1). Isolates SC4 and LB1 grew on isoprene as the sole source of carbon and energy at growth rates of 0.308 hr⁻¹ and 0.307 hr⁻¹, respectively.

3.3 The two new isolates were identified as *Rhodococcus* strains

Genomic DNA was extracted from isoprene-grown isolate cells using the FastDNA spin kit for soil (MP Biomedicals), as detailed in the Material and Methods section 2.5.1. Genomic DNA was then used as template in the PCR amplification reactions targeting bacterial 16S rRNA gene (Materials and Methods section 2.6.4). The 27f/1492R primer set (Lane, 1991) was used for the amplification reactions. 16S rRNA gene amplicons from both isolates were purified, cloned into the pGEMT-easy vector (Promega), and sequenced with M13 primers (Invitrogen). Based on 16S rRNA gene sequencing, strains SC4 and LB1 were phylogenetically associated with the genus *Rhodococcus* of the phylum *Actinobacteria* (Figure 3.1). The full-length 16S rRNA gene sequences (1,521 bp) of isolates SC4 and LB1 were identical and closely affiliated with *Rhodococcus opacus* (100 % sequence identity).



0.005

Figure 3.1 Neighbour-joining phylogenetic tree (Bootstrap 100) based on the alignment of 16S rRNA gene sequences (1,437 bp). The 16S rRNA genes of *Rhodococcus* strains AD45, SC4 and LB1 (shown in red) were sequenced in this study. The 16S rRNA sequences of the reference *Rhodococcus* strains were obtained from GenBank (the accession numbers are displayed between brackets). The tree was constructed using MEGA6 (Tamura *et al.*, 2013).

3.4 Growth profile of *Rhodococcus* strains AD45, LB1, SC4 on selected substrates

Members of the genus *Rhodococcus* are known for their versatile metabolic reactions (Bell *et al.*, 1998, Larkin *et al.*, 2005). It seemed worthwhile, therefore, to investigate the growth of *Rhodococcus* strains AD45, SC4 and LB1 on selected substrates. For growth on gaseous substrates, 25 ml of CBS minimal medium contained in 125 ml sterile serum vials were inoculated with isoprene-grown isolate cultures (5 % final concentration). The sealed vials were supplied with 10 % (v/v) gaseous substrates and incubated at 30 °C, shaking at 150 rpm. For growth on liquid substrates (10 mM final concentration), cultures were set up in 20 ml sterile universals containing 5 ml sterile CBS minimal medium inoculated with 5 % final concentration of isolate cultures grown in liquid on isoprene. All three isolates grew on fructose, succinate, glucose, and acetate. However, only *Rhodococcus* SC4 and *Rhodococcus* LB1 were capable of growing on propane and butane as sole source of carbon and energy (Table 3.1).

Table 3.1 Growth profile of *Rhodococcus* strains AD45, SC4 and LB1. + indicates growth.

	AD45	SC4	LB1
Isoprene	+	+	+
Succinate	+	+	+
Glucose	+	+	+
Fructose	+	+	+
Acetate	+	+	+
Methane	-	-	-
Ethane	-	-	-
Propane	-	+	+
Butane	-	+	+
Ethene	-	-	-
Propene	-	-	-
Trans-2 butene	-	-	-

3.5 General genome features

Rhodococcus AD45 genome is considerably smaller than the genomes of *Rhodococcus* SC4 and *Rhodococcus* LB1 (Table 3.2). A 300 kbp circular plasmid was also found in the genome of *Rhodococcus sp.* AD45. The high GC - content of *Rhodococcus* AD45, *Rhodococcus* SC4 and *Rhodococcus* LB1 genomes is characteristic for *Rhodococcus* strains (Table 3.3).

Table 3.2 Summary of genome content of *Rhodococcus* AD45, *Rhodococcus* SC4 and *Rhodococcus* LB1

	<i>R. AD45</i>	<i>R. SC4</i>	<i>R. LB1</i>
Size (Mbp)	6.5 ^a / 0.34 ^b	10.6	10.7
GC content (%)	61.8 / 60.6	66.7	66.6
Number of contigs	9	345	448
Number of predicted coding sequences	6,173 / 409	10,075	10,242
Number of rRNA genes	16	3	3
Number of tRNA genes	50	49	44

^aChromosome, ^b megaplasmid

Table 3.3 Comparison of *Rhodococcus* AD45, *Rhodococcus* LB1 and *Rhodococcus* SC4 genomes with those of selected *Rhodococcus* strains

Organism	Size (Mbp)	G + C %	Reference
<i>Rhodococcus</i> AD45	6.5 / 0.34	61.8 / 60.6	This study
<i>Rhodococcus</i> LB1	10.7	66.6	This study
<i>Rhodococcus</i> SC4	10.6	66.7	This study
<i>Rhodococcus jostii</i> RHA1	9.7	67	McLeod <i>et al.</i> , 2006
<i>Rhodococcus</i> sp. R04	9.1	69.6	Yang <i>et al.</i> , 2011
<i>Rhodococcus equi</i> 103S	5	68.8	Letek <i>et al.</i> , 2013
<i>Rhodococcus pyridinovorans</i> AK37	5.2	67.8	Kriszt <i>et al.</i> , 2012
<i>Rhodococcus opacus</i> B4	8.8	67.6	NITE *
<i>Rhodococcus erythropolis</i> PR4	6.9	62.3	NITE *

* Published online by the Japanese National Institute for Technology and Evaluation (NITE) available at <http://www.nite.go.jp/index-e.html>

3.6 Overview of the potential metabolic pathways of *Rhodococcus* strains AD45, SC4 and LB1

Local nucleotide database files of the genome sequences were created using BioEdit software. Based on BLAST searches against these databases and using the KEGG (Kyoto Encyclopedia of Genes and Genomes) recruitment plots provided by the RAST server, the potential metabolic pathways of *Rhodococcus* strains AD45, LB1 and SC4 were analyzed. The genes reported in this section were solely deduced from the genome sequence and were not supported by further experimental evidence.

Rhodococcus AD45, *Rhodococcus* SC4 and *Rhodococcus* LB1 genomes encode all the enzymes required for complete TCA (Tricarboxylic acid) cycle (Figures 3.2, 3.3). These enzymes include citrate synthase (EC 2.3.3.1), aconitase (EC 4.2.1.3), isocitrate dehydrogenase (EC 1.1.1.42), α -ketoglutarate dehydrogenase (EC 1.2.4.2), succinyl-CoA synthetase (EC 6.2.1.5), succinate dehydrogenase (EC 1.3.99.1), fumarase (EC 4.2.1.2), and malate dehydrogenase (EC 1.1.1.37). The TCA cycle enzyme 2-oxoglutarate synthase (EC 1.2.7.3) was present in *Rhodococcus* SC4 and LB1, but absent in *Rhodococcus* AD45 (Figures 3.2, 3.3).

The genomes of *Rhodococcus* AD45, *Rhodococcus* SC4 and *Rhodococcus* LB1 code for all the necessary enzymes involved in the glycolysis and gluconeogenesis pathways. All tRNA encoding regions have been identified in the draft genomes. Genes encoding nitrate reductase (EC 1.7.99.4) and nitrite reductase (EC 1.7.1.4), enzymes involved in the nitrogen metabolism, are present in the genomes of *Rhodococcus* strains SC4, LB1 and AD45 (Figures 3.4, 3.5, 3.6). This suggests that these strains are capable of utilizing nitrate and nitrite as a source of nitrogen. The genomes do not contain genes encoding the nitrogenase enzyme (EC 1.18.6.1 / EC 1.19.6.1) responsible for nitrogen fixation (Figures 3.4, 3.5, 3.6).

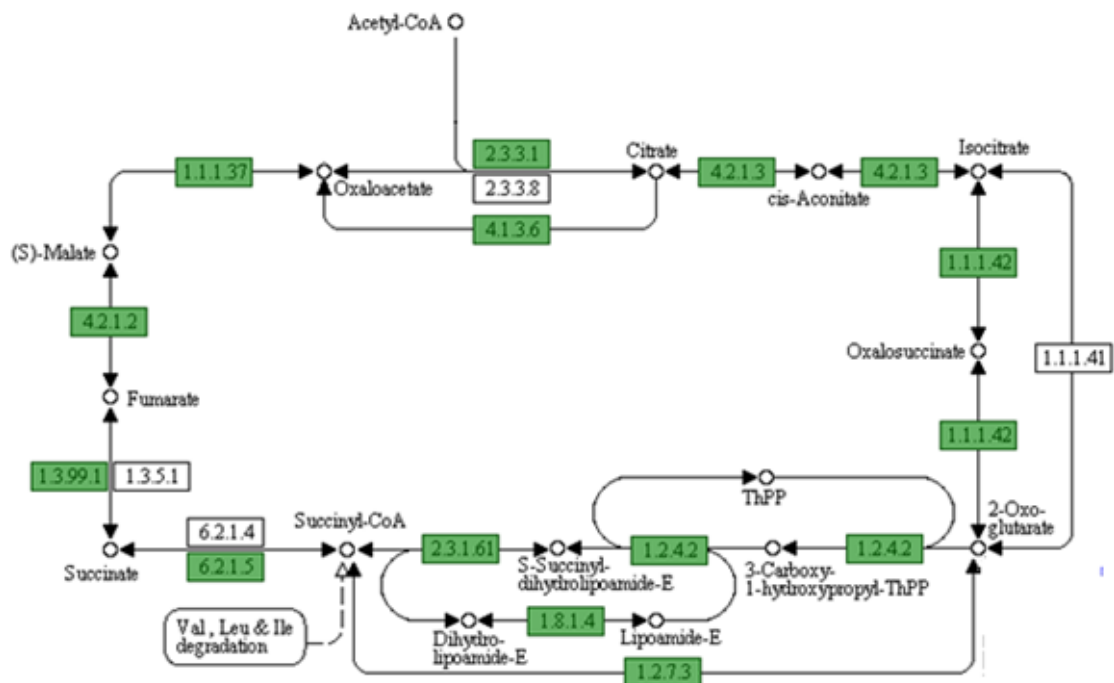


Figure 3.2 KEGG recruitment plot of the genes involved in the TCA cycle. Highlighted in green are the enzymes that are encoded by genes present in the *Rhodococcus* SC4 genome. The genome of *Rhodococcus* LB1 generated a KEGG recruitment plot of the genes involved in the TCA cycle which was identical to that from *Rhodococcus* SC4 genome.

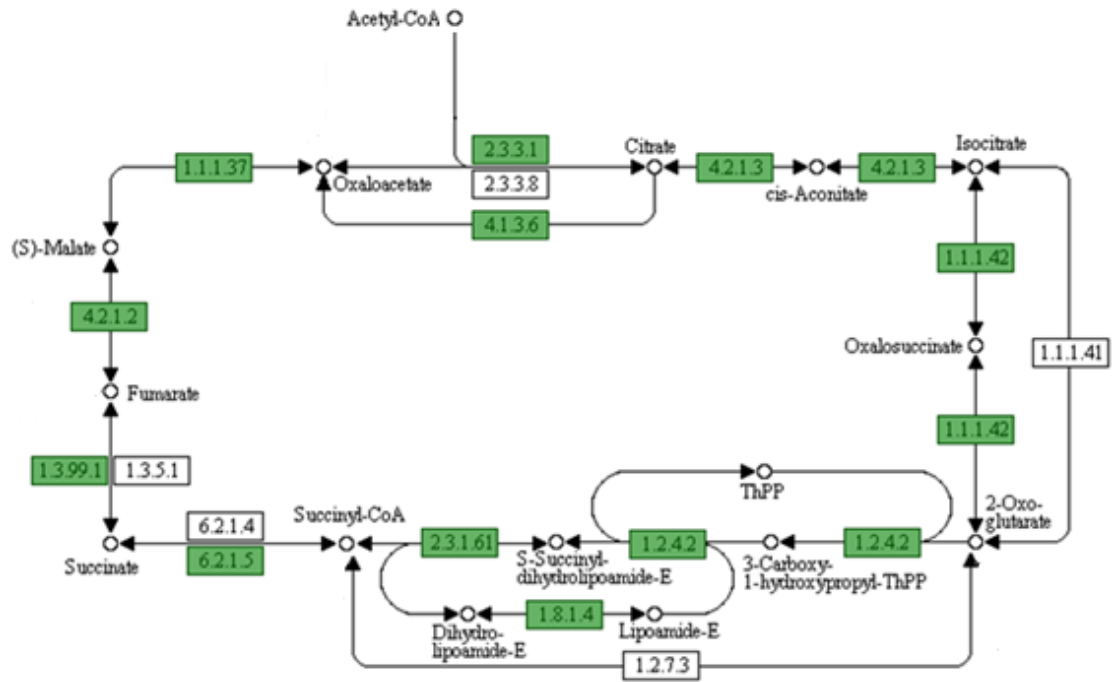


Figure 3.3 KEGG recruitment plot of the genes involved in the TCA cycle. Highlighted in green are the enzymes that are encoded by genes present in the *Rhodococcus* AD45 genome.

3.7 Isoprene oxidation pathway

Through cloning and sequence analysis, an 8.5 kbp DNA region has been previously identified as being involved in isoprene degradation in *Rhodococcus* AD45 (Vlieg *et al.*, 2000). This region contains 10 genes, six of which (*isoABCDEF*) encode the soluble isoprene monooxygenase. *Rhodococcus* AD45, *Rhodococcus* SC4 and *Rhodococcus* LB1 genomes all contain one copy of the isoprene monooxygenase genes. These genes are part of a gene cluster (Tables 3.4, 3.5, 3.6). The isoprene gene cluster in *Rhodococcus* AD45 resides on the 0.34 Mbp megaplasmid. The layout of the genes encoding the isoprene monooxygenase is conserved across the three *Rhodococcus* strains (Figure 3.7). Blast P searches against the NCBI database with the *isoABCDEF* gene products as query sequences consistently showed a high percent identity to sequences from *Rhodococcus opacus* PD630, a triacylglycerol-synthesizing bacterium with a genome sequence available in the database (Alvarez *et al.*, 1996; Holder *et al.*, 2011). *Rhodococcus opacus* PD630 strain was obtained from the German Collection of Microorganisms and Cell Cultures (DSMZ) and the ability of *Rhodococcus opacus* PD630 to grow on isoprene was tested. Growth tests confirmed that *Rhodococcus* PD630 is capable of growing on isoprene as sole source of carbon and energy. The genes encoding the enzymes involved in later steps in isoprene oxidation pathway were also identified in the genomes of *Rhodococcus* strains SC4, AD45 and LB1. These enzymes include a putative racemase (IsoG), a hydrogenase (IsoH) and two glutathione-S-transferases (IsoI and IsoJ) (Figure 3.7).

Table 3.4 The isoprene gene cluster present in the *Rhodococcus* AD45 megaplasmid

Gene	Start	Finish	Size (bp)	Product	Size (aa)
<i>isoG</i>	278948	280165	1,218	Racemase	405
<i>isoH</i>	280182	280862	681	Dehydrogenase	226
<i>isoI</i>	280929	281645	717	Glutathione-S-transferase	238
<i>isoJ</i>	281680	282381	702	Glutathione-S-transferase	233
<i>isoA</i>	282708	284231	1,524	Hydroxylase α -subunit	507
<i>isoB</i>	284267	284551	285	Hydroxylase γ -subunit	94
<i>isoC</i>	284544	284888	345	Ferredoxin	114
<i>isoD</i>	284907	285239	333	Coupling protein	110
<i>isoE</i>	285236	286264	1,029	Hydroxylase β -subunit	342
<i>isoF</i>	286425	287315	891	Reductase	296
<i>isoG-2</i>	267775	268992	1,218	Racemase	405
<i>isoH-2</i>	269009	269689	681	Dehydrogenase	226
<i>isoI-2</i>	269748	270464	717	Glutathione-S-transferase	238
<i>isoJ-2</i>	270499	271200	702	Glutathione-S-transferase	233

Table 3.5 The isoprene gene cluster present in the genome of *Rhodococcus* LB1

Gene	Contig	Start	Finish	Size (bp)	Product	Size (aa)	% identity to <i>R. AD45</i> (aa)
<i>isol</i>	110	59380	58664	717	Glutathione-S-transferase	238	87
<i>isoJ</i>	110	58628	57927	702	Glutathione-S-transferase	233	78
<i>isoA</i>	110	56432	54909	1,524	Hydroxylase α -subunit	507	91
<i>isoB</i>	110	54870	54586	285	Hydroxylase γ -subunit	94	83
<i>isoC</i>	110	54593	54249	345	Ferredoxin	114	86
<i>isoD</i>	110	54230	53898	333	Coupling protein	110	96
<i>isoE</i>	110	53901	52879	1,023	Hydroxylase β -subunit	340	84
<i>isoF</i>	110	52855	51830	1,026	Reductase	341	81
<i>isoG</i>	83	35150	34632	519	Racemase	172	83
<i>isoH</i>	83	34617	33937	681	Dehydrogenase	226	87
<i>isol-2</i>	83	33878	33162	717	Glutathione-S-transferase	238	76
<i>isoJ-2</i>	83	33127	32426	702	Glutathione-S-transferase	233	90

Table 3.6 The isoprene gene cluster present in the genome of *Rhodococcus* SC4

Gene	Contig	Start	Finish	Size (bp)	Product	Size (aa)	% identity to <i>R. AD45</i> (aa)
<i>isoG</i>	339_323	15	467	453	Racemase	150	81
<i>isoH</i>	66	43	663	621	Dehydrogenase	206	87
<i>isoI</i>	66	730	1446	717	Glutathione-S-transferase	238	87
<i>isoJ</i>	66	1482	2183	702	Glutathione-S-transferase	233	78
<i>isoA</i>	66	3678	5201	1,524	Hydroxylase α -subunit	507	91
<i>isoB</i>	66	5240	5524	285	Hydroxylase γ -subunit	94	84
<i>isoC</i>	66	5517	5861	345	Ferredoxin	114	86
<i>isoD</i>	66	5880	6212	333	Coupling protein	110	98
<i>isoE</i>	66	6209	7231	1,023	Hydroxylase β -subunit	340	84
<i>isoF</i>	66	7255	8280	1,026	Reductase	341	81
<i>isoI-2</i>	245	141	857	717	Glutathione-S-transferase	238	75
<i>isoJ-2</i>	245	892	1593	702	Glutathione-S-transferase	233	90

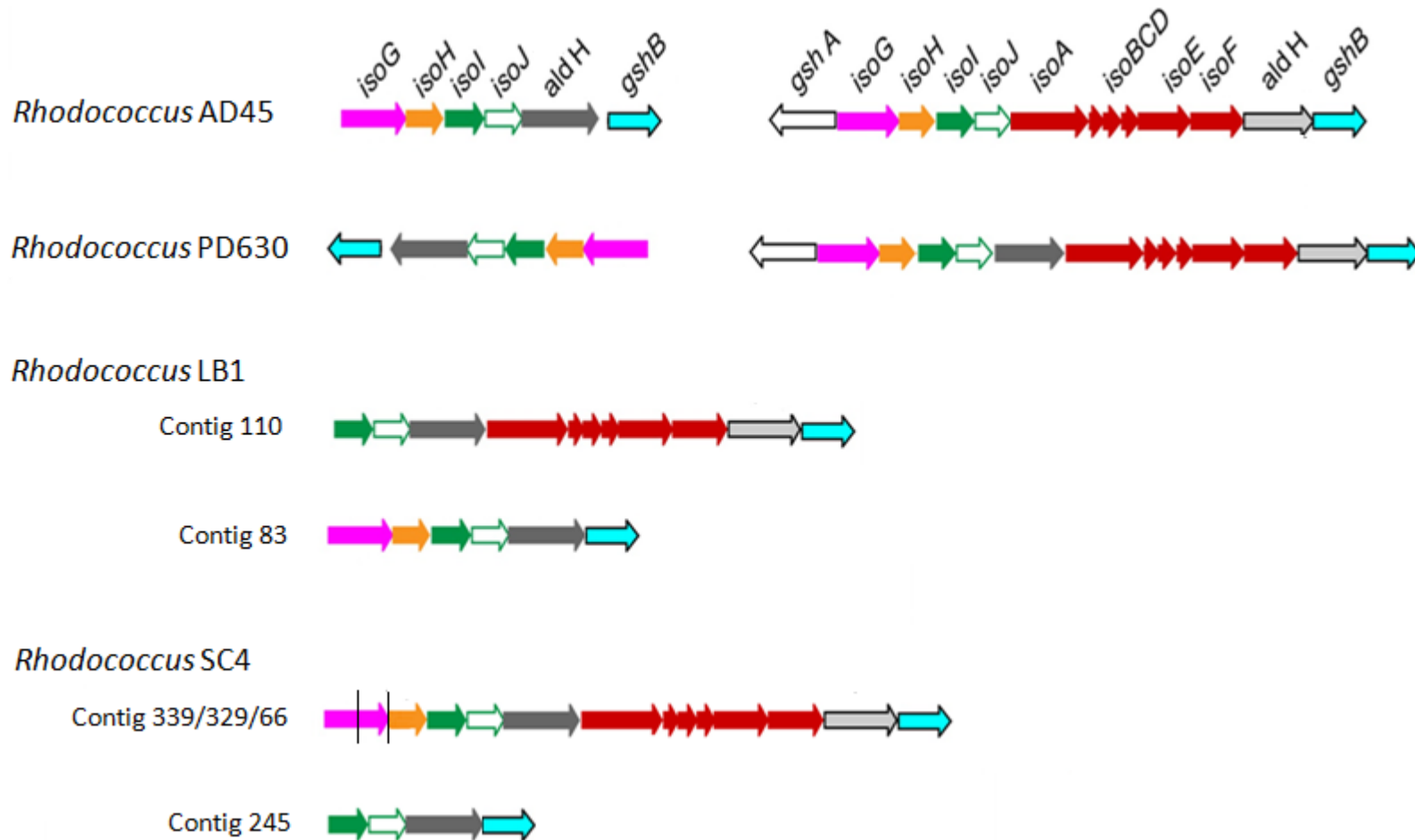


Figure 3.7 Comparison of the isoprene gene clusters across the terrestrial isoprene degrading *Rhodococcus* strains. The genes shown include *isoG*, *isoH*, *isoI*, *isoJ*, *isoA*, *isoB*, *isoC*, *isoD*, *isoE*, *isoF*, *aldH* (encoding aldehyde dehydrogenase), *gshB* (encoding glutathione synthetase), and *gshA* (encoding glutamate-cysteine ligase).

3.8 Isoprene monooxygenase is a soluble diiron centre monooxygenase

Soluble di-iron centre monooxygenase (SDIMO) enzymes (Chapter 1 section 1.5) fall into six groups based on their phylogeny and their typical substrates (Leahy *et al.*, 2003, Coleman *et al.*, 2006, Holmes & Coleman, 2008). Groups I and II are associated with alkene/aromatic monooxygenases, group III with methane monooxygenases, group IV with alkene monooxygenases, and groups V and VI with propane monooxygenases.

BLAST searches against NCBI protein database using IsoA sequences of *Rhodococcus* strains AD45, SC4, LB1 and PD630 revealed that IsoA sequences share high identity to amino acid sequences of hydroxylase α -subunits of known soluble di-iron centre monooxygenases (Figure 3.8). IsoA sequences were most similar to the hydroxylase α -subunits of group I SDIMO enzymes (Figure 3.8).

Sequence alignment of IsoA and the α -subunits of representative SDIMOs of different groups showed that IsoA contains all the residues that are absolutely conserved across the α -subunits of the SDIMO family (Figure 3.9). The conserved residues, as analyzed by Coufal and co-workers (2000), include:

- Iron cluster ligands (E114, E144, H147, E209, E243, H246 in *Methylococcus capsulatus* Bath, Rosenzweig *et al.*, 1993), highlighted in purple.
- Structural residues involved in hydrogen bonding between α -helices (D143, R146, S238, D242, R245), highlighted in blue.
- Docking residues (Y292, W371, Y376, P377), acting as a putative binding site for the reductase, highlighted in grey.
- The two protonated residues (T213, N214) associated with possible proton delivery to the active site, highlighted in green.
- The ‘handle’ forming residues (A224, G228 and D229), highlighted in orange.

The gene organization of the isoprene monooxygenase operon in *Rhodococcus* strains SC4, AD45, LB1 and PD630 is identical to that of operons encoding soluble di-iron centre monooxygenases of group I, such as toluene monooxygenase in *Pseudomonas mendocina* KR1 and alkene monooxygenase in *Xanthobacter autotrophicus* PY2 (Figure 3.10). However, it is different to the gene order of

operons encoding soluble diiron monooxygenases of other groups (Figure 3.10). This is consistent with the observations of Leahy *et al.*, (2003) that operons encoding soluble diiron monooxygenases of the same group have the same genetic organisation. Altogether, these data support the classification of the isoprene monooxygenase as a group I SDIMO.

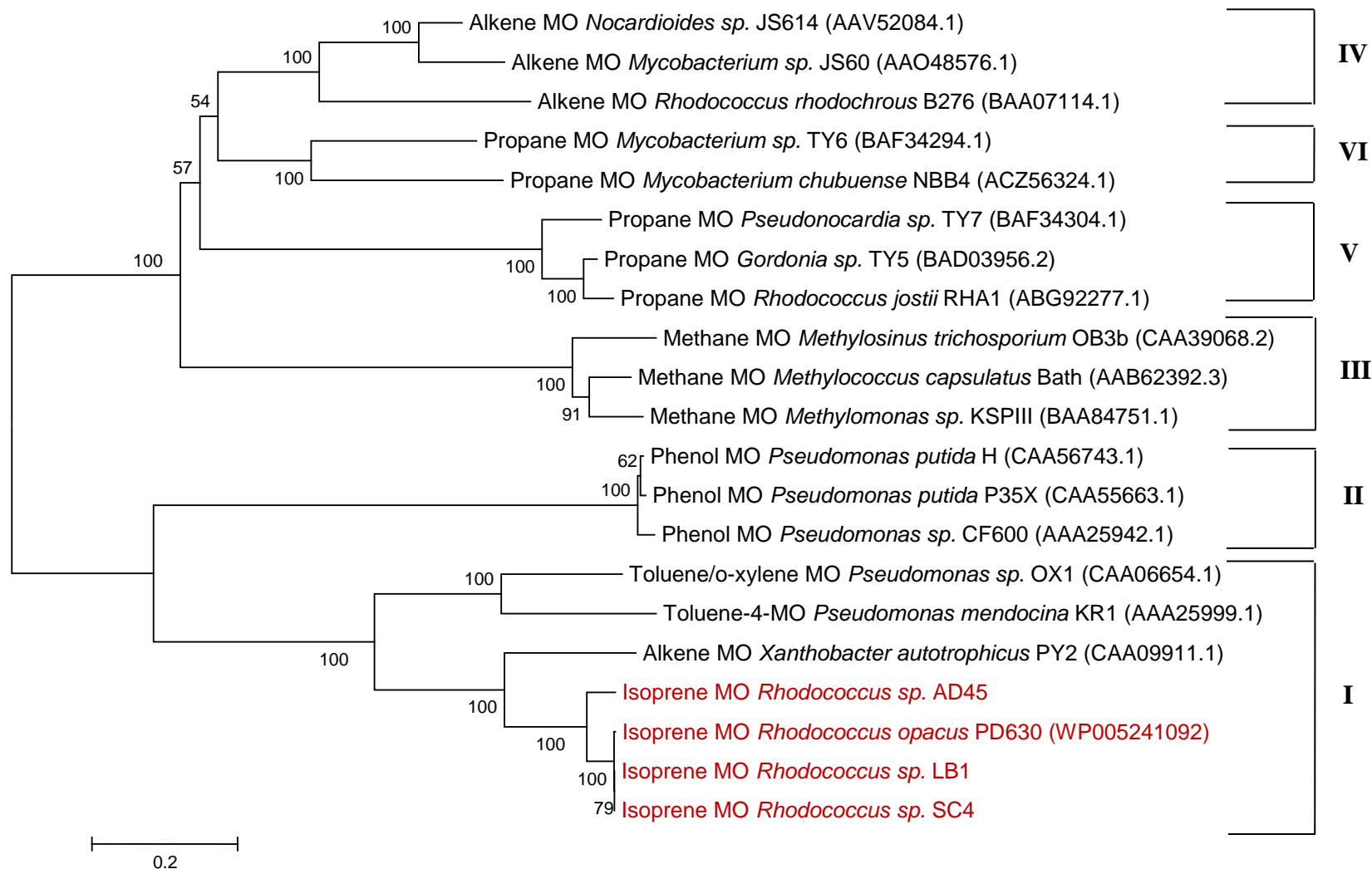


Figure 3.8 Phylogenetic relationships between IsoA (highlighted in red) and hydroxylase α -subunits of other representative SDIMOs. The amino acid sequences of the α -subunit hydroxylases of the representative SDIMOs were obtained from GenBank (The accession numbers in brackets). The SDIMO subgroups are indicated on the right of the Neighbour-joining phylogenetic tree (Bootstrap 100). 89

	10	20	30	40	50	60	70	80
<i>Methylococcus capsulatus</i> Bath MmoX	MALSTATKAATDALAANRAPTSVNAQEVHRWLQSFNWDFKNN--RTKYATKYKMANE-----TKEQFKLIAKEYARMEAVKD							
<i>Pseudomonas putida</i> H PhID	-----MTTNKKRLNLKDKYRYLTRDLGWEPYSYQKKEDVFPLEHFEGIKIT--DWDKWEDPFRLTMSYWKHQAEKE							
<i>Gordonia</i> sp. TY5 PrmA	-----MSRQSLTKAHAKITELSWEPTFATPATRFGTDYTFEKAP-----KKDPLKQIMRSYFPMEEEEKD							
<i>Rhodococcus rhodochrous</i> B276 AmoC	-----MASNPTQLHEKSKSYDWDFTSVERRPKFETKYKMPKK-----GKDPFRVLIRDYMKMEAEKD							
<i>Mycobacterium</i> sp. TY6 PrmA	-----MRNLIRAHERVKDFDWEHSYAEKPDYPTKYVMPRK-----TKDPFRHLIRDYVSMEQEKD							
<i>Rhodococcus opacus</i> PD630 IsoA	-----MLLNRDDWYDISRDLDWELSYVDPVAVAFPTSWSGAGDVPKDAWDKWDEPFRVSYRDYVRIQREKE							
<i>Rhodococcus</i> sp. AD45 IsoA	-----MLLNRDDWYDTSRDLDWELSYVDPSEAFPASWSGAGDVPTEAWDKWDEPFRVSYRDYVRIQREKE							
<i>Rhodococcus</i> sp. SC4 IsoA	-----MLLNRDDWYDISRDLDWELSYVDPVAVAFPTSWSGAGDVPKDAWDKWDEPFRVSYRDYVRIQREKE							
<i>Rhodococcus</i> sp. LB1 IsoA	-----MLLNRDDWYDISRDLDWELSYVDPVAVAFPTSWSGAGDVPKDAWDKWDEPFRVSYRDYVRIQREKE							
<i>Pseudomonas mendocina</i> KR1 TmoA	-----MAMHPRKDWYELTRATNWTPSYVTEEQLFPERMSGHMGIPLEKWEYSYDEPKTSYPEYVSIQREKD							
<i>Xanthobacter autotrophicus</i> PY2 XamoA	-----MALLNRDDWYDIARDVDWTLISYVDRAVAFPEEWKGEKDICGTAWDDWDEPFRVVSFREYVMVQRDKE							

	90	100	110	120	130	140	150	160	170
<i>Methylococcus capsulatus</i> Bath MmoX	ERQFGSLQDALTRLNAGVRVHPKWNETMKVVSNFLEVGGEYNAIAATGMLWDSAQAAEQKNGYLAQVLD E IRH T HQCAYVNYFFAKN								
<i>Pseudomonas putida</i> H PhID	KKLYAIFDAFAQNNGHQNI SDARYVNALKLFFTGVS P MEYQAFQGF S RVGRQFSGAGARVACQM Q AIDELRHVQTQVHAMSHYNKH								
<i>Gordonia</i> sp. TY5 PrmA	NRVYGAMDGAIR-GNMFRQVQERWLEWQKLF S IIPFPEISAARAMPMAIDAVPNPEIHNGLAVQMID E VRHSTIQMNLKKLYMNN								
<i>Rhodococcus rhodochrous</i> B276 AmoC	DRTHGFLDGAVR-TREATRIEPRFAEAMKIMVPQ L TNAEYQAVAGCGMIISAVENQELRQGYAAQMLD E VRHAQLEM T LRNYYAKH								
<i>Mycobacterium</i> sp. TY6 PrmA	DRQYGAMEDALARSNSAGKAQPRWMEILKIALPVVNFGEYAAMKCCGQLVD T VNNAELRQGYMAQMID E VRHTNQELYLNRYFAKH								
<i>Rhodococcus opacus</i> PD630 IsoA	SGVK-AVSSALVRS G TYEKLDPAHVAASHLHMGTTCM V EHMAV T MQSRFCRFAP T PRWRNLGVFGMLD E TRHAQLDLRF S HDLLK-								
<i>Rhodococcus</i> sp. AD45 IsoA	SGVK-AVSSALVRS G TYEKLDPAHVAASHLHMGTTCM V EHMAV T MQSRFCRFAP T PRWRNLGVFGMLD E TRHAQLDLRF S HDLLK-								
<i>Rhodococcus</i> sp. SC4 IsoA	SGVK-AVSSALVRS G TYEKLDPAHVAASHLHMGTTCM V EHMAV T MQSRFCRFAP T PRWRNLGVFGMLD E TRHAQLDLRF S HDLLK-								
<i>Rhodococcus</i> sp. LB1 IsoA	SGVK-AVSSALVRS G TYEKLDPAHVAASHLHMGTTCM V EHMAV T MQSRFCRFAP T PRWRNLGVFGMLD E TRHAQLDLRF S HDLLK-								
<i>Pseudomonas mendocina</i> KR1 TmoA	AGAY-SVKAALERAKIYENS D PGWISTLKSHYGAIAVGEYA A VTGEGRMARF S KAPGNRNMATFGMM D ELRHGQLQLFFPHEYCK-								
<i>Xanthobacter autotrophicus</i> PY2 XamoA	ASVG-AIREAMVR A KAYEKLDDGHKATSHLHMGTITM V EHMAV T MQSRFVRFAP S ARWRS L GAFGMLD E TRHTQLDLRF S HDLLN-								

114

143 144 146 147

Methylococcus capsulatus Bath MmoX
Pseudomonas putida H PhID
Gordonia sp. TY5 PrmA
Rhodococcus rhodochrous B276 AmoC
Mycobacterium sp. TY6 PrmA
Rhodococcus opacus PD630 IsoA
Rhodococcus sp. AD45 IsoA
Rhodococcus sp. SC4 IsoA
Rhodococcus sp. LB1 IsoA
Pseudomonas mendocina KR1 TmoA
Xanthobacter autotrophicus PY2 XamoA

```

      180      190      200      210      220      230      240      250
GQDPAGHNDARRTRTIGPLWKGMKRVFSDGFISGDAVECS-LNLQLVGEACFTNPLIVAVTEWAAAANGDEITPTVFLSIE
FDGLHDFAH---MYDRVWFLSVPKSFMDDARTAGPFEFL-TAVSFSFEYVLTNLLFVPPFMGAAAYNGDMATVTFGFSAQ
YIDPAGFDITEKAFAN-NYAGTIGRQFGEGFITGDAITAANIYLTVVAETAFTNTLFVAMPDEAAAANGDYLLPTVFHVSQ
WCDPSGFDIGQRGLYQ-HPAGLVSIGEFQHFNFGDPLDVI-IDLNIVAETAFTNILLVATPQVAVANGDNAMASVFLSIQ
AADPEGFHIGMKARAN-NLFGVAGRAALETFFVGDPVEGA-LNLQVVAETAYTNPIFVTLTEVAAAANGDINVTPSVFLSVQ
--QDPRFDWSQKAFHTKEWGVLAVKNFFDDAMLNADCVEAALATSLTVEHGFTNVQFVALAADAMAAGDINWSNLLSSIQ
--QDPRFDWSQKAFHTNEWGVLAVKNFFDDAMLNADCVEAALATSLTVEHGFTNVQFVALAADAMAAGDINWSNLLSSIQ
--QDPRFDWSQKAFHTKEWGVLAVKNFFDDAMLNADCVEAALATSLTVEHGFTNVQFVALAADAMAAGDINWSNLLSSIQ
--QDPRFDWSQKAFHTKEWGVLAVKNFFDDAMLNADCVEAALATSLTVEHGFTNVQFVALAADAMAAGDINWSNLLSSIQ
--KDRQFDWAWRAYHSNEWAAIAAKHFFDDIITGRDAISVAIMLTFSETGFTNMQFLGLAADAAEAAGDYTFANLISIQ
--DSPSFDWSQRAFHTDEWAVLATRNLFDDIMLNADCVEAALATSLTLEHGFTNIQFVALASDAMEAGDVNFSNLLSSIQ
                                     209   213 214           224   228 229           238
  
```

Methylococcus capsulatus Bath MmoX
Pseudomonas putida H PhID
Gordonia sp. TY5 PrmA
Rhodococcus rhodochrous B276 AmoC
Mycobacterium sp. TY6 PrmA
Rhodococcus opacus PD630 IsoA
Rhodococcus sp. AD45 IsoA
Rhodococcus sp. SC4 IsoA
Rhodococcus sp. LB1 IsoA
Pseudomonas mendocina KR1 TmoA
Xanthobacter autotrophicus PY2 XamoA

```

      260      270      280      290      300      310      320      330
TDELRHMANGYQTVVSIAN-DPASAKYLNTDLNNAFWTQQKYFTPVLGMLFEYGSKFKV---EPWVKTWDRWVYEDWGGIW
SDEARHMTLGLEVIKFMLEQHEDNVPIIQRWIDKWFWRGYRLLT-LIGMMMDYMLPNKVMS---WSEAWG-VYFEQAGGAL
SDESRRHISNGYSILLMALA-DERNRPLLERDLRYAWWNNHCVVDAAIGTFIEYGTKDRRKDRSYAEMWRRWIYDDYRSY
SDEARHMANGYGSVMALLE-NEDNLPLLNQSLDRHFWRAHKALDNAVGWCSEYGARKRP---WSYKAQWEEWVDDFVGGY
SDEARHMANGYSTLAAVVS-NEDNLKYLQADFDRAFWRQHSFLDPFLGAVYDYFQKERG---HSYLEKWTEWIEEDWVGSY
TDEARHAQQGFPTLSILME-HDP--ARAQKALDVAFWRSTRLFQTLTGPAMDYTPLDQ-----RKMSFKEFMLEWIVNHH
TDEARHAQQGFPTLSILME-HDP--ARAQKALDVAFWRSTRLFQTLTGPAMDYTPLDQ-----RKMSFKEFMLEWIVNHH
TDEARHAQQGFPTLSILME-HDP--ARAQKALDVAFWRSTRLFQTLTGPAMDYTPLDQ-----RKMSFKEFMLEWIVNHH
TDEARHAQQGGPALQLLIE-NGKR-EEAQKKVDMAIWRAWRLFAVLTGPVMDYTPLED-----RSQSFKEFMYEWIIQF
TDEARHAQLGFPTLDVMMK-HDP--KRAQQILDVAFWRSYRIFQAVTGVSMDYTPVAK-----RQMSFKEFMLEWIVKHH
242 243   245 246                                     292
  
```

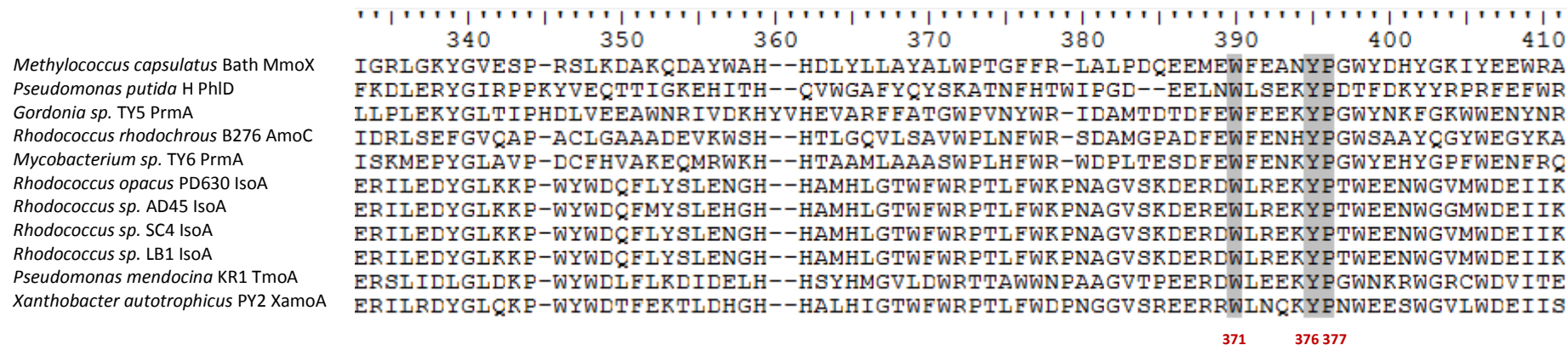
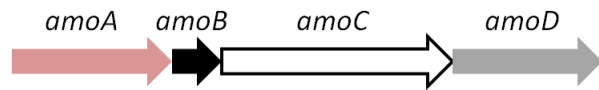


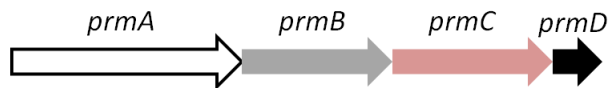
Figure 3.9 Partial alignment of deduced amino acid sequences of isoprene monooxygenase α -subunit and hydroxylase α -subunits of representative SDIMOs from different groups. Included are the methane monooxygenase from *Methylococcus capsulatus* Bath (Stainthorpe *et al.*, 1990, AAB62392.3), phenol monooxygenase from *Pseudomonas putida* H (Herrmann *et al.*, 1995, CAA56743.1), propane monooxygenase from *Gordonia sp.* TY5 (Kotani *et al.*, 2003, BAD03956.2), alkene monooxygenase from *Rhodococcus rhodochrous* B276 (Saeki & Furuhashi, 1994, BAA07114.1), propane monooxygenase from *Mycobacterium sp.* TY6 (Kotani *et al.*, 2006, BAF34294.1), isoprene monooxygenase from *Rhodococcus opacus* PD630 (Holder *et al.*, 2011, WP005241092.1), isoprene monooxygenase from *Rhodococcus sp.* AD45 (this study), isoprene monooxygenase from *Rhodococcus sp.* SC4 (this study), isoprene monooxygenase from *Rhodococcus sp.* LB1 (this study), toluene monooxygenase from *Pseudomonas mendocina* KR1 (Yen *et al.*, 1991, AAA25999.1), and alkene monooxygenase from *Xanthobacter autotrophicus* PY2 (Zhou *et al.*, 1999, CAA09911.1). The top numbering is the consensus numbering, the numbers in red correspond to the *Methylococcus capsulatus* Bath residue number.

Rhodococcus rhodochrous B276 D37875 (Saeki & Furuhashi, 1994)



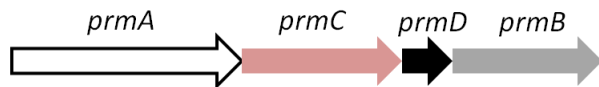
Group IV β -subunit / regulatory protein / α -subunit / reductase

Gordonia sp. TY5 AB112920 (Kotani et al., 2003)



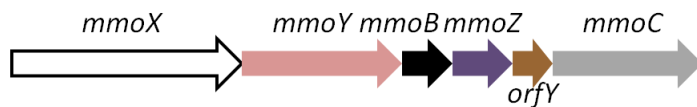
Group V α -subunit / reductase / β -subunit / regulatory protein

Mycobacterium sp. TY6 AB250938 (Kotani et al., 2006)



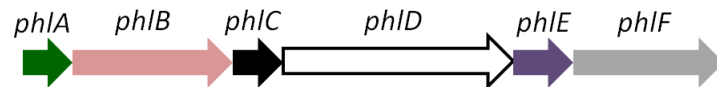
Group VI α -subunit / β -subunit / regulatory protein / reductase

Methylococcus capsulatus Bath M90050 (Stainthorpe et al., 1990)



Group III α -subunit / β -subunit / regulatory protein / γ -subunit / hypothetical protein / reductase

Pseudomonas putida H X80765 (Herrmann et al., 1995)

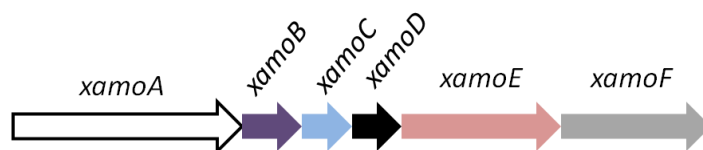


Group II hypothetical protein / β -subunit / regulatory protein / α -subunit / γ -subunit / reductase

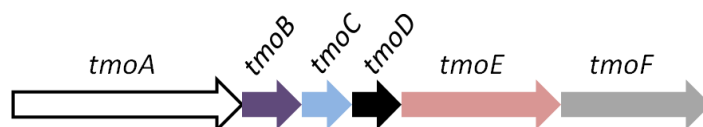
Figure 3.10 continued overleaf.

Group I α -subunit / γ -subunit / ferredoxin / regulatory protein / β -subunit / reductase

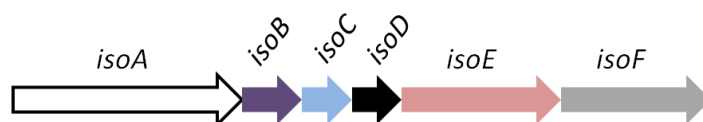
Xanthobacter autotrophicus PY2 AJ012090 (Zhou *et al.*, 1999)



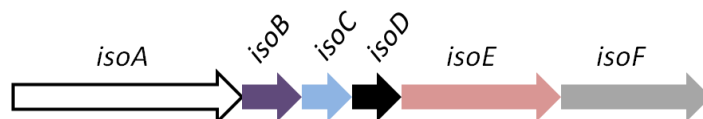
Pseudomonas mendocina KR1 M65106, M95045 (Yen *et al.*, 1991, 1992)



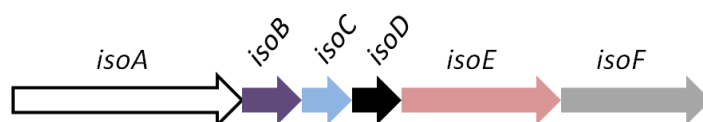
Rhodococcus sp. AD45 (This study)



Rhodococcus wratislaviensis LB1 (This study)



Rhodococcus wratislaviensis SC4 (This study)



Rhodococcus opacus PD630 (Genome information, Holder *et al.*, 2011)

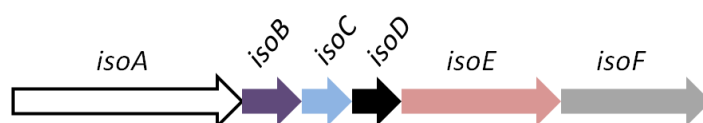


Figure 3.10 Gene organisation of operons encoding soluble diiron centre monooxygenases of different groups of SDIMO enzymes. Underlined are the GenBank accession numbers.

3.9 Glutathione as a cofactor in the isoprene oxidation pathway

The first step in the biological oxidation of an alkene results in the formation of an epoxide, a compound highly toxic for bacterial cells. The toxicity of the epoxide is generally overcome by the nucleophilic addition to the epoxide of either glutathione or coenzyme M (2-mercaptoethanesulfonate) (Krishnakumar *et al.*, 2008). A glutathione-S-transferase enzyme catalyzes the former reaction whilst the latter is catalyzed by a coenzyme M transferase. Coenzyme M (CoM) has been identified as a cofactor in the alkene oxidation pathway in *Xanthobacter autotrophicus* PY2 (Allen *et al.*, 1999), *Rhodococcus rhodochrous* B276 (Krum & Ensign, 2000), and *Nocardioides sp.* JS614 (Mattes *et al.*, 2005). The deduced amino acid sequence of coenzyme M transferase from *Xanthobacter autotrophicus* PY2 (accession number Q56837) was used as a query sequence in the BLAST searches against the genome sequences of *Rhodococcus* AD45, SC4 and LB1 strains. No homologous sequences were found in the draft genomes. However, *isoI* and *isoJ* genes encoding glutathione-S-transferase enzymes were identified in the genomes, located immediately upstream of the isoprene monooxygenase gene cluster (Tables 3.4, 3.5, 3.6, Figure 3.7). Additional copies of *isoI* and *isoJ* were identified in all three genomes.

Glutathione synthesis is not frequently found in Gram-positive bacteria (Copley & Dhillon, 2002, Fahey *et al.*, 1978, Newton *et al.*, 1996). Glutamate-cysteine ligase (EC 6.3.2.2) and glutathione synthetase (EC 6.3.2.3) are responsible for catalyzing the synthesis of glutathione (Copley & Dhillon, 2002, Figure 3.11). These two enzymes are coded by *gshA* and *gshB* respectively. The genomes of *Rhodococcus* strains LB1, AD45 and SC4 encode two putative glutathione synthetases annotated as glutathione synthetase (Figure 3.7). One copy of *gshB* was found located in close proximity to the isoprene monooxygenase gene cluster in all three draft genomes, as shown in Figure 3.7. Two copies of *gshA* were identified in all three genomes. One copy of *gshA* was located adjacent to the isoprene gene cluster only in *Rhodococcus* AD45, for the rest of the genomes both copies were located on a different contig to that of the isoprene gene cluster.

The genome sequencing information reported in this study suggests that glutathione is the cofactor in isoprene degradation pathway. This is further supported by the

experimental work of Vlieg and co-workers which led to the purification and characterization of two glutathione-S-transferases from *Rhodococcus sp.* AD45 (Vlieg *et al.*, 1998, 1999).

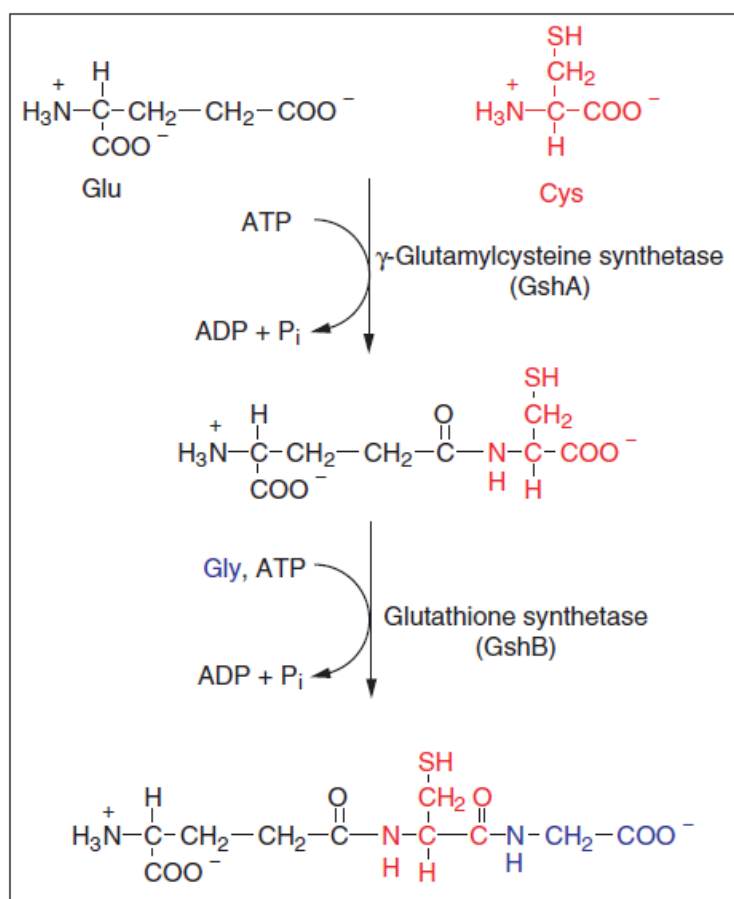


Figure 3.11 Glutathione biosynthesis pathway. Taken from Copley & Dhillon, 2002.

3.10 Pathways of alkane oxidation in *Rhodococcus* strains AD45, LB1 and SC4

Rhodococcus SC4 and *Rhodococcus* LB1 can grow on propane and their genomes encode a propane monooxygenase (Table 3.7). Propane monooxygenase genes were not found in the genome of *Rhodococcus* AD45 which cannot grow on propane (see section 3.4). The deduced amino acid sequences of the propane monooxygenase α -subunits from *Rhodococcus* SC4 and *Rhodococcus* LB1 share the highest percent identity (99%) with the amino acid sequence of the propane monooxygenase α -subunit of *Rhodococcus jostii* RHA1 (McLeod *et al.*, 2006, accession number

YP700435). The layout of the genes encoding the propane monooxygenase is identical in *Rhodococcus* strains SC4 and LB1 (Figure 3.12). A *groEL* homolog and a gene encoding a putative transcriptional regulator were also identified in the propane gene clusters in *Rhodococcus* SC4 and *Rhodococcus* LB1 genomes (Figure 3.12).

Table 3.7 Propane monooxygenase gene clusters of *Rhodococcus sp.* SC4 and *Rhodococcus sp.* LB1

	Polypeptides	Size (aa)	Size of encoding gene (bp)	Contig	Start	Finish	Homologs in <i>R. jostii</i> RHA1	% identity (aa)
<i>Rhodococcus sp.</i> SC4	Hydroxylase α -subunit	544	1,635	88	9710	11344	PrmA	99
	Reductase	347	1,044	88	11430	12473	PrmB	98
	Hydroxylase β -subunit	368	1,107	88	12525	13631	PrmC	99
	Coupling protein	113	342	88	13628	13969	PrmD	100
<i>Rhodococcus sp.</i> LB1	Hydroxylase α -subunit	544	1,635	317	15756	14122	PrmA	99
	Reductase	347	1,044	317	14036	12993	PrmB	98
	Hydroxylase β -subunit	368	1,107	317	12941	11835	PrmC	98
	Coupling protein	113	342	317	11838	11497	PrmD	100

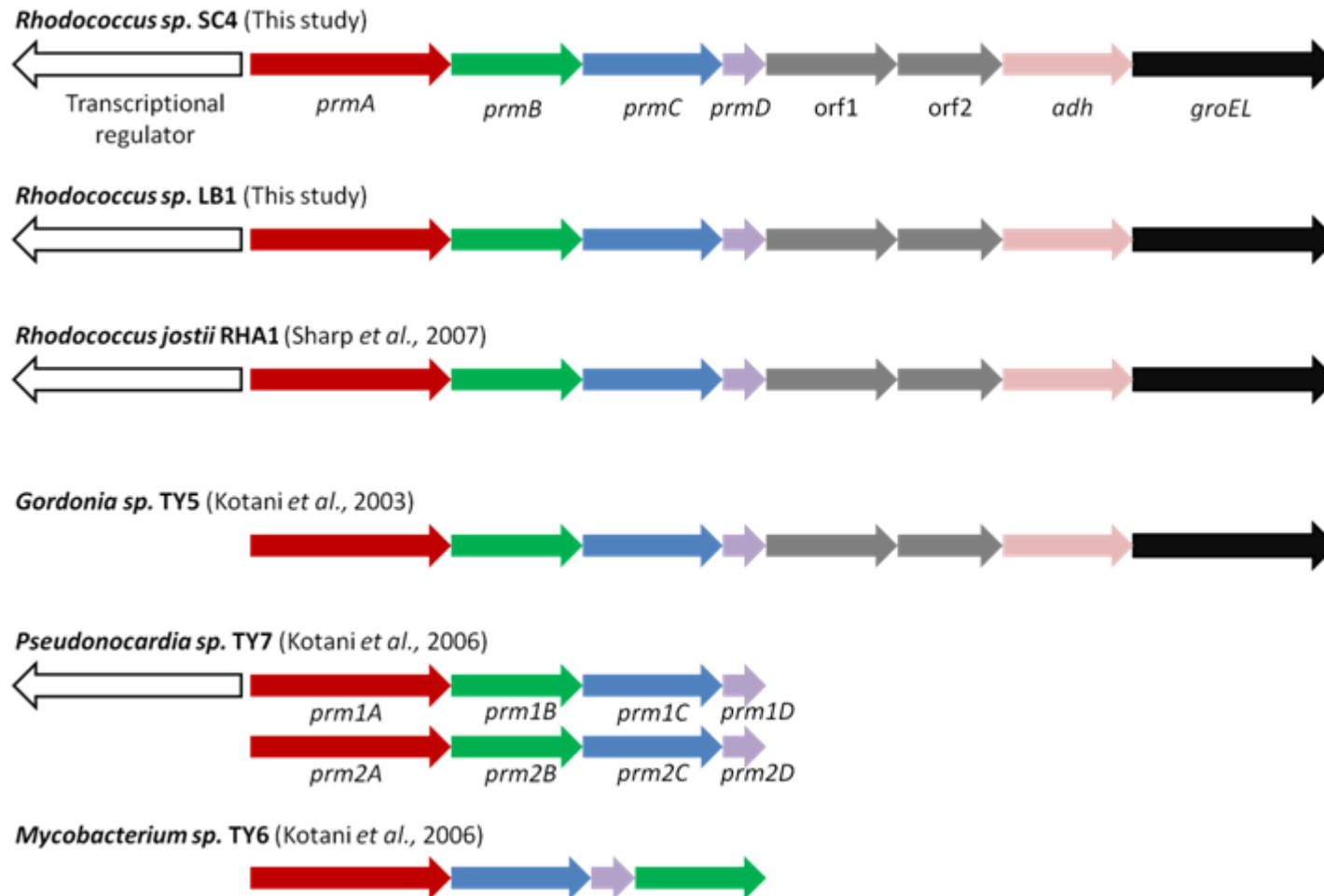


Figure 3.12 Gene organization of the propane monoxygenase gene operons in *Rhodococcus* SC4, *Rhodococcus* LB1, and other known propane-oxidizing bacteria. The proteins encoded by the propane gene cluster include PrmA: hydroxylase large subunit, PrmB: reductase, PrmC: hydroxylase small subunit, PrmD: coupling protein, Adh: alcohol dehydrogenase, chaperonin GroEL, and a putative transcriptional regulator.

Genes encoding AlkB and cytochrome P450 enzymes, responsible for the oxidation of C5-C16 alkanes, were identified in all three *Rhodococcus* draft genomes. This is consistent with the widespread ability of *Actinomycetales* bacteria to oxidize alkanes (van Beilen & Funhoff, 2007). The alkane hydroxylase systems found in *Rhodococcus* SC4 and *Rhodococcus* LB1 are likely to be functional given that they code for the transmembrane alkane monooxygenase AlkB, two cofactors rubredoxin AlkF, and rubredoxin reductase AlkG (Jurelevicius *et al.*, 2013), as shown in Figure 3.13. *alkG*, a gene coding for the rubredoxin reductase, was not identified in the genome of *Rhodococcus* AD45 which contains multiple copies of *alkB*, located on the chromosome. In *Rhodococcus* sp. SC4, *alkB* is located on contig 123 (84540-85760), the encoded monooxygenase enzyme shares 84 % identity with AlkB of *Rhodococcus* sp. BCP1 (Cappelletti *et al.*, 2011, accession number ADR72654). In *Rhodococcus* sp. LB1, *alkB* gene is located on contig 135 (32096-30864), the encoded protein shares 85 % sequence identity with AlkB of *Rhodococcus* sp. BCP1. *tetR* gene, which encodes a transcriptional regulator belonging to the TetR family, was identified adjacent to the *alkB* cluster in all three genomes (Figure 3.13).

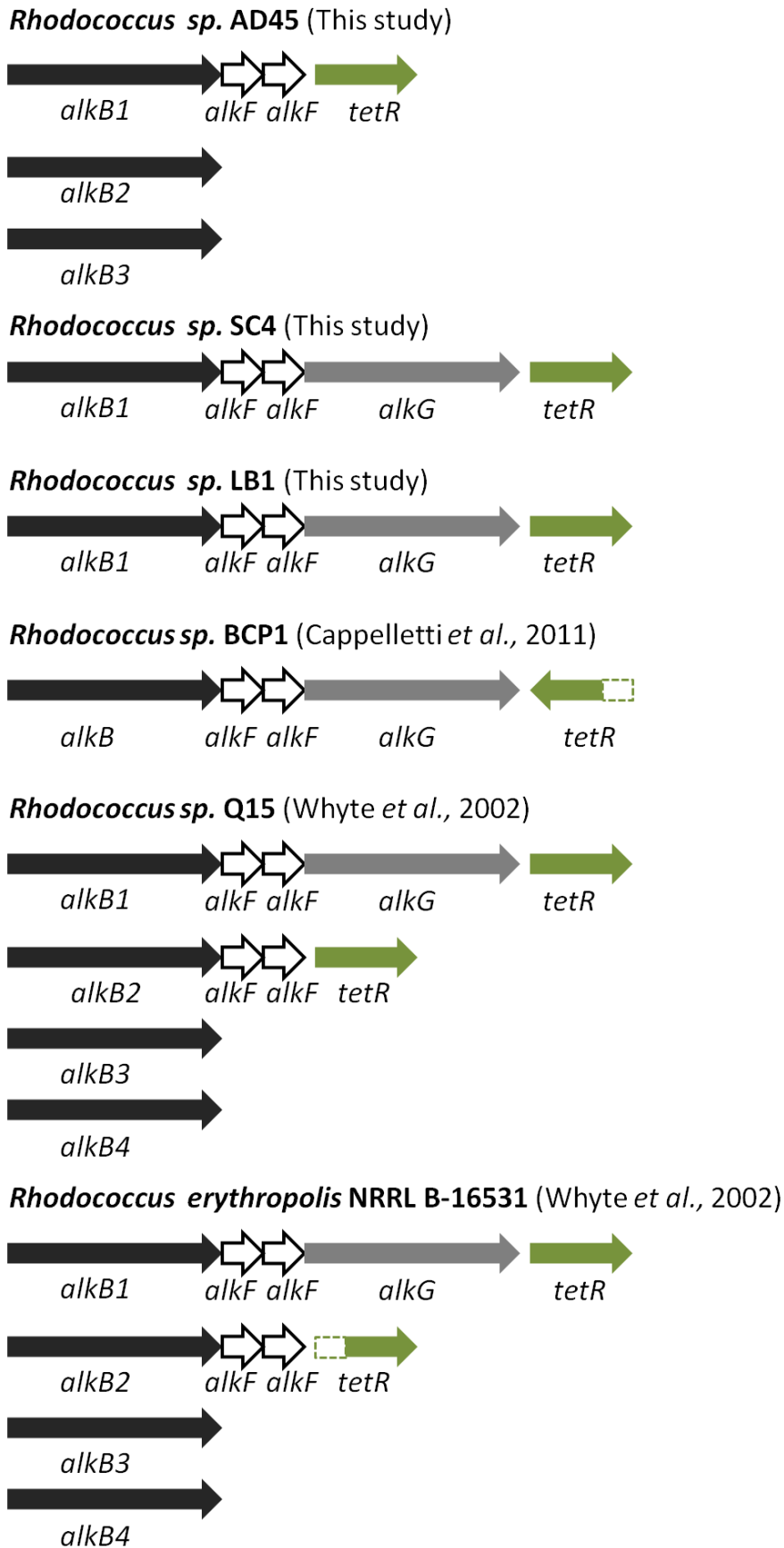


Figure 3.13 Schematic view of the *alkB* gene cluster from *Rhodococcus* strains AD45, LB1 and SC4 and other known alkane-utilizing *Rhodococcus* strains.

3.11 Terminal versus subterminal oxidation of propane in *Rhodococcus* SC4 and *Rhodococcus* LB1

Sequences with a high level of homology (over 90%) to quinone-containing alcohol dehydrogenases were found upstream of the genes encoding the propane monooxygenase in *Rhodococcus* SC4 (contig 88, 1584-2546) and *Rhodococcus* LB1 (contig 317, 23882-22920). In the propane-degrading bacterium *Gordonia* sp. TY5, propane is oxidized by monooxygenase-mediated subterminal oxidation via propan-2-ol (Kotani *et al.*, 2003). The latter is further metabolized to acetone through the activity of alcohol dehydrogenases (Adh1, Adh2 and Adh3). AcmA, FAD-dependent acetone monooxygenase, oxidizes acetone to methyl acetate, which is subsequently converted to acetic acid and methanol by the hydrolase AcmB (Kotani *et al.*, 2003, Kotani *et al.*, 2007). The pathways for propane oxidation in *Gordonia* sp. TY5 are illustrated in Figure 3.14. The *Rhodococcus* SC4 and *Rhodococcus* LB1 genomes were mined for genes homologous to *acmA* and *acmB*. *Rhodococcus* SC4 genome codes for AcmA and AcmB which have 41% and 64% amino acid identity with AcmA and AcmB from *Gordonia* sp. TY5 respectively. Similarly, AcmA and AcmB were found in *Rhodococcus* LB1 and share 44% and 64% amino acid sequence identity to AcmA and AcmB of *Gordonia* TY5 respectively. Although these findings suggest that propane is oxidized in *Rhodococcus* SC4 and *Rhodococcus* LB1 via the subterminal pathway, they do not eliminate the possibility of a terminal oxidation pathway co-occurring in the cells. For instance, *Rhodococcus* strain PNKb1 was found capable of oxidizing propane via both pathways (Woods & Murrell, 1989). Testing the growth of *Rhodococcus* strains SC4 and LB1 on terminal oxidation intermediates and testing the potential oxidation activity of propane grown *Rhodococcus* SC4 or LB1 cells towards terminal oxidation intermediates using an oxygen electrode are worthwhile considering in the future.

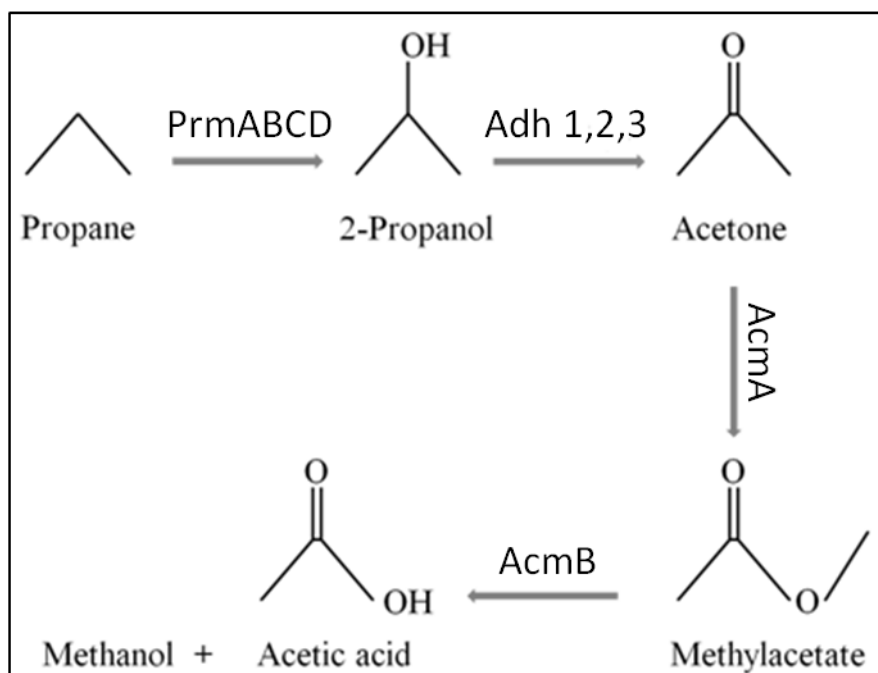


Figure 3.14 Pathway of propane oxidation in *Gordonia sp.* TY5, adapted from Hausinger *et al.*, 2007. PrmABCD: propane monooxygenase, Adh 1, 2, 3: propanol dehydrogenase, AcmA: acetone monooxygenase, AcmB: hydrolase / esterase.

3.12 Rubber degradation

Natural rubber or poly (cis-1, 4-isoprene) degradation is confined to a few bacterial genera and species, most of which belong to the *Actinomycetes* phylum (Hiessl *et al.*, 2012). The pathway for rubber degradation involves one of these two enzyme systems: rubber oxygenase A (Rox A) and latex-clearing protein (Lcp) (Yikmis & Steinbüchel, 2012). RoxA was identified in *Xanthomonas sp.* 35Y, a gram negative rubber degrading bacterium (Jendrossek & Reinhardt, 2003, Braaz *et al.*, 2004, Braaz *et al.*, 2005). Lcp seems to be more widespread amongst rubber degrading strains and was identified in *Streptomyces sp.* K30 (Rose *et al.*, 2005), *Actinoplanes sp.* OR16 (Imai *et al.*, 2011), *Streptomyces sp.* LCIC4 (Imai *et al.*, 2011) and *Gordonia polyisoprenivorans* VH2 (Hiessl *et al.*, 2012). *rox A* gene was not identified in any of the genomes. The *Rhodococcus* AD45 genome encodes a latex clearing protein (Lcp) which shares 69% amino acid identity to Lcp of *Gordonia polyisoprenivorans* strain VH2 (ABV68923). The *lcp* gene is located on the chromosome (start 4341352_stop 4340123) in *Rhodococcus* AD45. However, the *lcp* gene was not identified in the genomes of *Rhodococcus* SC4 and *Rhodococcus* LB1. The fact that these isolates are capable of degrading isoprene is a strong reason to

suggest that they are capable of degrading rubber. As a result, it is worthwhile noting that the sequence of the *lcp* gene in *Rhodococcus* SC4 and *Rhodococcus* LB1 may have not been covered by genome sequencing.

Chapter 4

Mutagenesis and regulation of *isoA* in *Rhodococcus AD45*

4.1 Introduction

Our knowledge of the genes and enzymes involved in the pathway for isoprene degradation is very limited. It is based largely on sequence data analyses rather than experimental studies. The gene cluster encoding genes involved in isoprene metabolism in *Rhodococcus* AD45 was identified following Blast searches of an 8,456 bp DNA fragment, that was cloned and sequenced by Janssen's group in the Netherlands, against several nucleotide and protein databases (Vlieg *et al.*, 2000). This DNA fragment contained 10 protein-coding genes, 6 of which encoded proteins with high sequence identity to sequences of soluble monooxygenases reported in the literature as key enzymes in the first step of many hydrocarbon oxidation pathways. This suggested that isoprene oxidation follows the same model in which an isoprene monooxygenase plays a major role in the metabolism of isoprene by bacteria. To date, no experimental data which conclusively support the previous statement have been reported. Molecular genetics experiments aimed at mutagenesis of the *isoA* gene which encodes the alpha subunit of isoprene monooxygenase was therefore a key objective to determine if the isoprene monooxygenase is responsible for isoprene degradation. *Rhodococcus* AD45, the first isolated terrestrial isoprene degrader that has been described in any detail, is a suitable model organism for the study of terrestrial isoprene degradation because it grows rapidly and efficiently on isoprene to a high optical density and its genome sequence is available (see Chapter 3). This chapter describes the construction and characterization of an *isoA* deletion mutant in *Rhodococcus* AD45. This was created by deletion of a portion of the *isoA* gene and insertion of a gentamicin cassette into *isoA*. The transcription and expression of *isoA* in *Rhodococcus* AD45 was also assayed by qRT-PCR and SDS-PAGE respectively.

4.2 Mutagenesis of *isoA* in *Rhodococcus* AD45

The mutagenesis technique used to mutate *isoA* is a marker exchange mutagenesis method which requires two homologous recombination events to occur upstream and downstream of the targeted DNA region in order to replace it with a selectable marker, in this case an antibiotic cassette. The antibiotic cassette is contained on a circular plasmid which is introduced into *Rhodococcus sp.* AD45 cells by electroporation. This plasmid cannot replicate in *Rhodococcus* AD45. Given that the second homologous recombination is a rare event, it could be ‘forced’ and selected for by the use of a counterselectable marker, for example *sacB* which provides the cells with sucrose sensitivity triggering their death when sucrose is supplied to the growth medium (Schäfer *et al.*, 1994).

4.2.1 Antibiotic sensitivity of *Rhodococcus* AD45

Rhodococcus AD45 was checked for sensitivity to selected antibiotics. Cultures were set up in triplicate in 20 ml sterile universals by inoculating 5 ml of CBS minimal medium with a fresh single colony of wild type *Rhodococcus* AD45. Glucose was used as growth substrate at a final concentration of 10 mM. Filter sterilized antibiotic solutions were separately added to the cultures at different concentrations.

Rhodococcus AD45 was first tested for sensitivity to kanamycin and gentamicin (Table 4.1) as both antibiotics are known to be stable in nutrient agar media for up to 10 days and Gm^R and Km^R cassettes have been previously used for mutagenesis experiments in our laboratory, for example with *Methylocella silvestris* BL2 (Crombie & Murrell, 2011), *Agrobacterium tumefaciens* (Chen *et al.*, 2010), and *Methylosinus trichosporium* (Martin & Murrell, 1995).

Table 4.1 Testing for antibiotic sensitivity of *Rhodococcus* AD45

Antibiotic	Concentration ($\mu\text{g/ml}$)	Growth
Kanamycin	7	Yes
	13	Yes
	17	Yes
	20	Yes
	100	No
Gentamicin	2	Yes
	5	No
	7	No

Rhodococcus AD45 is sensitive to gentamicin at a concentration of 5 $\mu\text{g/ml}$. For this reason, the gentamicin cassette (Dennis & Zylstra, 1998) was used as a selectable marker and no other antibiotics were further tested. In order to confirm the sensitivity of *Rhodococcus* AD45 to gentamicin (5 $\mu\text{g/ml}$), 50 μl of replicated overnight cultures of *Rhodococcus* AD45 grown on glucose with no added antibiotic (1.5×10^7 cells) was spread onto LB agar plates containing gentamicin (5 $\mu\text{g/ml}$). No colonies were recovered after a week of incubation at 30 °C. This also suggested that the rate of spontaneous mutagenesis was less than 1 in 1.5×10^7 .

4.2.2 Construction of a pK18*mobsacB*-based plasmid for mutagenesis of *isoA*

The various steps of the construction of the pK18*mobsacB*-based plasmid for the mutation of *isoA* are summarized in Figure 4.1. The primer set RegionAF and RegionAR (Table 4.2) was designed and used to amplify a 463 bp DNA fragment, designated region A, starting 17 bp 5' of the start codon of *isoA* to 446 bp. Another internal 469 bp DNA fragment, region B, at the 3' end of *isoA* was amplified using the primer set RegionBF and RegionBR starting at 882 bp 3' of the start codon to 1,350 bp (Table 4.2). RegionAR and RegionBF primer sequences included a *Hind*III restriction site which was added to allow the ligation of both of the separately amplified regions after a restriction digest with *Hind*III. This resulted in a 932 bp

fragment, designated the AB fragment. This fragment was then cloned into the pGEMT easy vector (Promega) and the integrity of the vector was checked by sequencing with M13 forward and reverse primers (data not shown).

Table 4.2 List of primers used in these experiments

Primers	5' to 3' sequence	Size (bp)
RegionAF	AATGGAAGGCGCAGATAATG	20
RegionAR	GCATAAGCTTTTGAGCAGGTCATGGGAGA	29
RegionBF	GCATAAGCTTGTGGATCGTCAATCATCACG	30
RegionBR	GCGGTCGATAATGTTCTGGT	20
M13F	GTAAAACGACGGCCAG	16
M13R	CAGGAAACAGCTATGAC	17
GmF	TAAGACATTCATCGCGCTTG	20
GmR	TCGTCACCGTAATCTGCTTG	20
KanF	CTGTGCTCGACGTTGCACT	20
KanR	AGCCAACGCTATGTCCTGAT	20
3723F	ATTCTCGGGACGCGAATGTG	20
5296R	AGGAAGGCGAGGCCAAGTAG	20

A 925 bp gentamicin cassette was released from plasmid p34S-Gm (Dennis & Zylstra, 1998) by cutting the plasmid with *HindIII*. The gentamicin cassette was then ligated to the pGEMT easy vector which contains the AB fragment described above, which was also cut with *HindIII*. Following transformation into *E.coli* TOP10 cells (Materials and Methods section 2.9), the vector was extracted (Materials and Methods section 2.5.2) and its integrity verified by sequencing with M13F and M13R primers. This vector was then digested with *EcoRI* which cuts it at two sites flanking the cloning region (Figure 4.1). This generated a linear construct of ~ 1,840 kbp which accounts for, in this order, region A, the gentamicin cassette and region B. The linear construct was then purified and cloned into the vector pK18*mobsaB* (Schäfer *et al.*, 1994) which contains a kanamycin resistance gene (*kanR*) and the

counter-selectable gene *sacB* (Selbitschka *et al.*, 1993), whose expression is lethal in Gram-positive bacteria when sucrose is present. pK18*mobsacB* vector can replicate in *E. coli* but not in *Rhodococcus* species, however it contains the *mob* DNA region of plasmid RP4 (Datta *et al.*, 1971) that includes the broad host range transfer elements for mobilization into different bacterial genera, including Gram-positive bacteria. The integrity of the pK18*mobsacB* vector containing the construct, referred to from now on as pMEK (Figure 4.1), was verified by sequencing with M13 primers and by *EcoRI* digest (Figure 4.2).

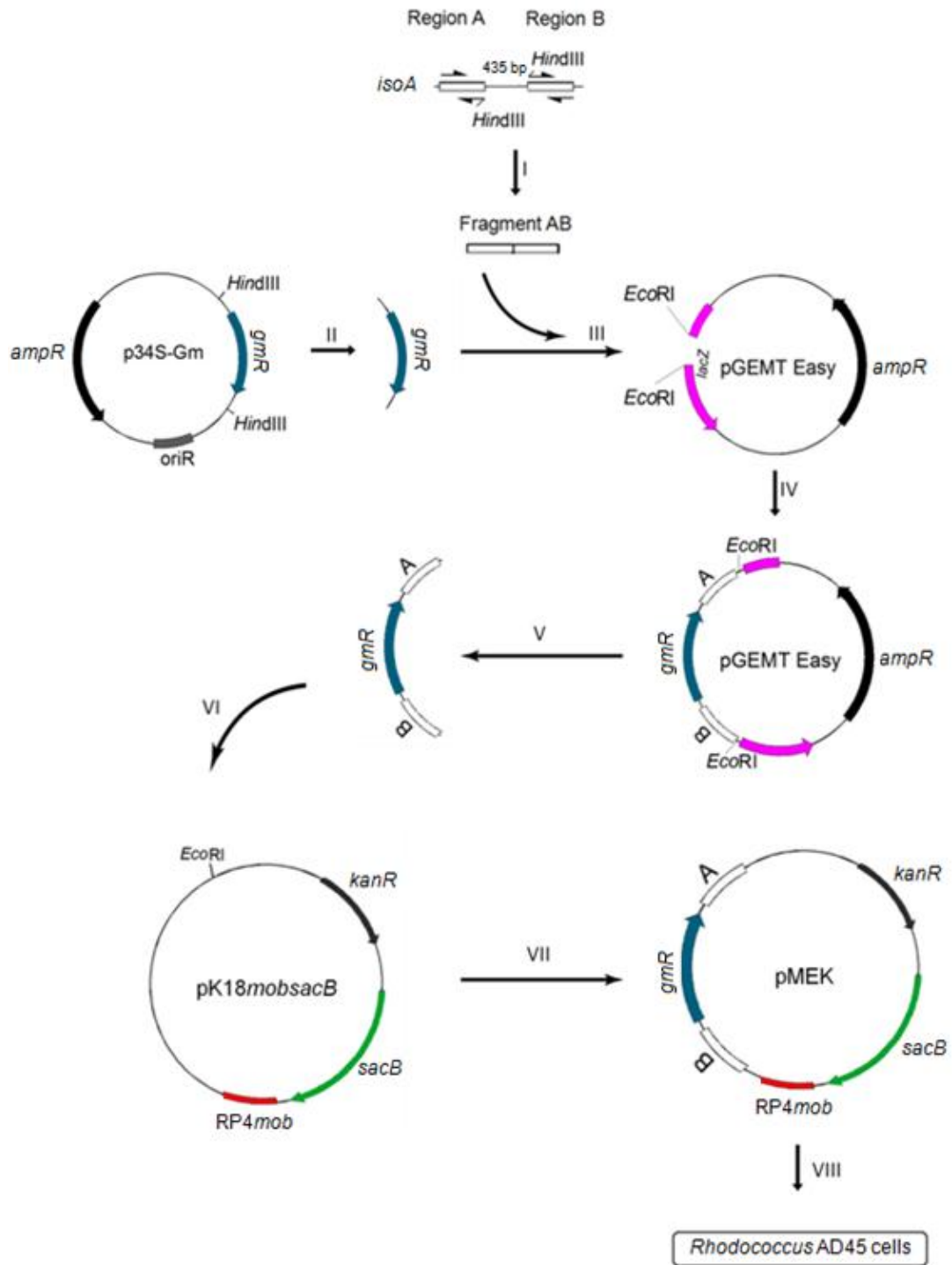


Figure 4.1 Construction of plasmid pMEK for mutagenesis of *isoA* in *Rhodococcus AD45*. Regions A and B, upstream and downstream of the 435 bp region of interest within *isoA* gene were PCR-amplified (I), ligated to the gentamicin cassette released from the p34S-Gm vector (II) and cloned into pGEMT-Easy vector (III, IV). The excision of the pGEMT-Easy vector with *EcoRI* enzymes released the linearized construct region A-Gm cassette-region B (V), which was subsequently cloned into the *EcoRI*-cut pK18mobsacB vector (VI) to give plasmid pMEK (VII). The latter was then introduced into *Rhodococcus AD45* cells (VIII).

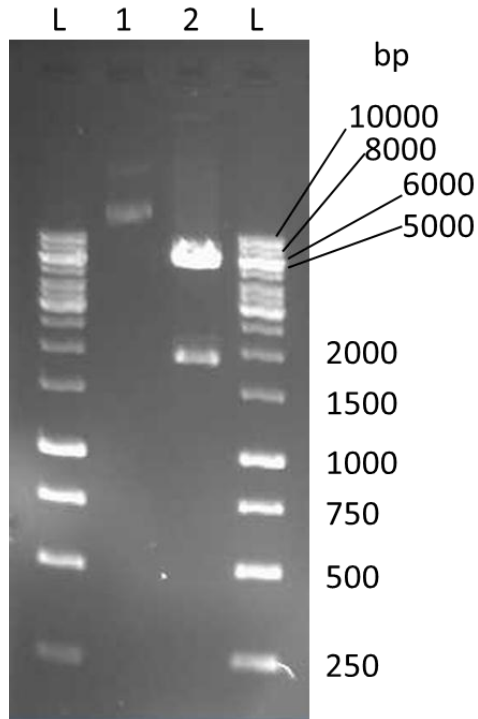


Figure 4.2 *EcoRI* digest of plasmid pMEK. Expected fragment sizes: 1,840 bp (region A- Gm cassette- region B) and 5.7 kbp (linear pK18mobsacB vector). L: Fermentas GeneRuler 1 kb ladder, lane 1: uncut pMEK vector, lane 2: *EcoRI* cut pMEK vector.

4.2.3 Transfer of DNA into *Rhodococcus* AD45

The introduction of plasmid DNA into microbial cells can be carried out through two traditional ways, conjugation and electroporation.

(i) Introduction of external DNA into *Rhodococcus* AD45 by conjugation

Conjugation of *Rhodococcus* AD45 with *E. coli* S17.1 cells (Simon *et al.*, 1983) containing the plasmid pMEK (Materials and Methods section 2.10) was carried out as follows. A fresh single colony of *E. coli* S17.1 containing the plasmid pMEK was inoculated into 5 ml of sterile LB with no added antibiotic and incubated at 37 °C, shaking at 150 rpm overnight. Similarly, a fresh single colony of *Rhodococcus* AD45 was inoculated into 5 ml sterile LB with no added antibiotic and incubated at 30 °C, shaking at 150 rpm overnight. The cells were harvested at mid-exponential phase (OD₅₄₀: 0.4 – 0.5) by centrifugation at 4,000 x g, for 15 min at 15 °C and each

of the cell pellets was washed with 5 ml of sterile LB before being mixed together in a total volume of 10 ml in a sterile Falcon tube. The mixture was then centrifuged at 4,000 x g, 15 °C for 15 min and the cells resuspended gently in 0.5 ml of LB. 0.25 ml of the resuspended pellet was spread onto a 0.2 µm sterile membrane filter (Millipore, USA) placed onto an LB agar plate and incubated at 21 °C for one hour then at 30 °C for 24 hours. The filter was removed after 24 hours and the cells from the filter were resuspended in 1 ml sterile LB, spread onto LB agar plates containing gentamicin (5 µg/ml) and nalidixic acid (NA) (10 µg/ml) then incubated at 30 °C for up to seven days. Nalidixic acid (10 µg/ml) inhibits the growth of *E. coli* S17.1 cells, whereas *Rhodococcus* AD45 cells are resistant to nalidixic acid at the same concentration as they were able to grow on LB supplemented with NA (10 µg/ml) both on agar plates and in liquid. Several trials of conjugation were carried out, each resulting in no *Rhodococcus* AD45 cells being recovered on the LB agar plates with Gm (5 µg/ml) and NA (10 µg/ml) even after 7 days of incubation at 30 °C. For this reason, electroporation was then chosen to introduce DNA into *Rhodococcus* AD45.

(ii) Transfer of plasmid DNA into *Rhodococcus* AD45 by electroporation

Given that no genetics work had previously been done with *Rhodococcus* AD45, there was a need to optimize a standard electroporation protocol in order to achieve a high electroporation frequency for *Rhodococcus* AD45. For optimization purposes, a broad host range vector, pNV18, was used. pNV18 vector (Chiba *et al.*, 2007) contains a kanamycin gene which allows the use of Kan as a selective marker at a concentration of 100 µg/ml (to which *Rhodococcus* AD45 is sensitive). Prior to electroporation, *Rhodococcus* AD45 cells were grown in 50 ml CBS medium and succinate (10 mM) to an OD₅₄₀ of 0.4 – 0.5 (mid-exponential phase) then washed, firstly with sterile water then with 10% (v/v) glycerol and resuspended in 10% (v/v) glycerol (Materials and Methods section 2.12) before being added to the pNV18 vector (25-200 ng) in 2 mm cuvettes (VWR, Taiwan) and subjected to an electric pulse (Bio-Rad GenePulser Xcell™). Many factors influence the efficiency rate of electroporation, including the settings under which the electroporation is performed and the recovery period after electroporating the cells.

To determine the optimal settings on the gene pulser (Bio-Rad GenePulser Xcell™) for electroporation, *Rhodococcus* AD45 cells were transformed with 66 ng of the vector pNV18 DNA by electroporation under different conditions (Table 4.3). The electroporation was followed by a recovery period of 4 hours in 1 ml of CBS medium containing succinate (10 mM) at 30 °C, with shaking at 150 rpm. 50 µl of cells were then spread onto LB agar plates containing Kan (100 µg/ml). This was done in triplicate and the average number of colonies recovered on the plates, together with the efficiency of DNA transfer for each setting were calculated (Table 4.3).

Table 4.3 Electroporation of *Rhodococcus* AD45 with pNV18

Cuvette	V (kV)	R (Ω)	C (µF)	Time constant (ms)	Colonies	Efficiency of DNA transfer (cfu/µg of plasmid DNA)
1	2.5	100	25	2.7	0	0
2	2.5	200	25	5.2	0	0
3	2.5	300	25	7.8	0	0
4	2.5	400	25	10.3	4000	1.3 x 10 ⁶
5	1.8	100	25	2.7	0	0
6	1.8	400	25	10	1800	0.6 x 10 ⁶

Based on the data above, it was concluded that a setting of 2.5 kV yielded a better efficiency rate of DNA transfer than 1.8 kV. For further optimization, *Rhodococcus* AD45 cells were transformed with 1 ng⁽¹⁾ of the vector pNV18 and subjected to an electric pulse with the voltage set to 2.5 kV and the capacity to 25 µF, however a range of different resistances were used: 100 Ω, 300 Ω, 400 Ω, 600 Ω, 800 Ω, and 1000 Ω. 1000 Ω was the highest resistance the gene pulser could be set to without the sample arcing. The transformation frequency was highest at 800 Ω (Table 4.4). Given that good transformation efficiency was obtained with the 2.5 kV, 25 µF, 800 Ω setting, the latter was consistently used throughout the rest of the mutagenesis experiments.

(1) We first started the downstream optimization steps using 66 ng of pNV18 plasmid DNA per reaction, as previously. However, we consistently obtained a thick bacterial lawn on the agar plates. Instead of diluting the cells prior to plating, we checked for the lowest plasmid DNA mass (1 ng) that gave good starting efficiency and a straightforward way for comparing efficiencies by easily counting colonies.

Table 4.4 Electroporation of *Rhodococcus* AD45 with pNV18

Cuvette	V (kV)	C (μ F)	R (Ω)	Time constant (ms)	Efficiency of DNA transfer (cfu/ μ g of plasmid DNA)
1	2.5	25	100	2.7	0
2	2.5	25	300	7.4	9.9×10^6
3	2.5	25	400	9.6	3.85×10^7
4	2.5	25	600	13.6	1.1×10^7
5	2.5	25	800	15.7	4.95×10^7
6	2.5	25	1000	19.5	4.84×10^7

4.2.4 Screening for *IsoA* single cross-over mutant

Rhodococcus AD45 cells were prepared as previously detailed for the transfer of the pMEK vector. 279 ng of pMEK vector DNA was added to 100 μ l of *Rhodococcus* AD45 cells and electroporation was carried out at the previously optimized settings: 2.5 kV, 800 Ω and 25 μ F. pNV18 vector was also used in this experiment as a positive control and to enable us to calculate the rate of DNA transfer efficiency which was estimated to be 1.9×10^7 cfu/ μ g of plasmid DNA. After transformation by electroporation of *Rhodococcus* AD45 cells with pMEK plasmid DNA and a recovery period of 4 hours, the cells were spread onto LB agar plates containing gentamicin (5 μ g/ml) and incubated at 30°C. 16 colonies were recovered after 3 days of incubation. These colonies were streaked with a sterile toothpick (patched) three times onto new fresh LB agar plates with gentamicin (5 μ g/ml) then screened for the isolation of single cross-over mutant colonies, by PCR using 3723F/5296R primer set located at either side of the deleted portion of the *isoA* gene (Table 4.2).

3723F primer targets a 20 bp sequence in the isoprene gene cluster at 93 nucleotides upstream of region A while 5296R primer targets a 20 bp sequence at 130

nucleotides downstream of region B. In the case of wild type *Rhodococcus* AD45 cells, this amplification reaction should yield a 1,573 bp amplicon. However, if the *Rhodococcus* AD45 cell had inserted the pMEK plasmid, no PCR product would be expected (Figure 4.3). Two colonies out of these 16 colonies, designated colony 14 and colony 15, gave no product with the 3723F / 5296R primer set (Figure 4.4).

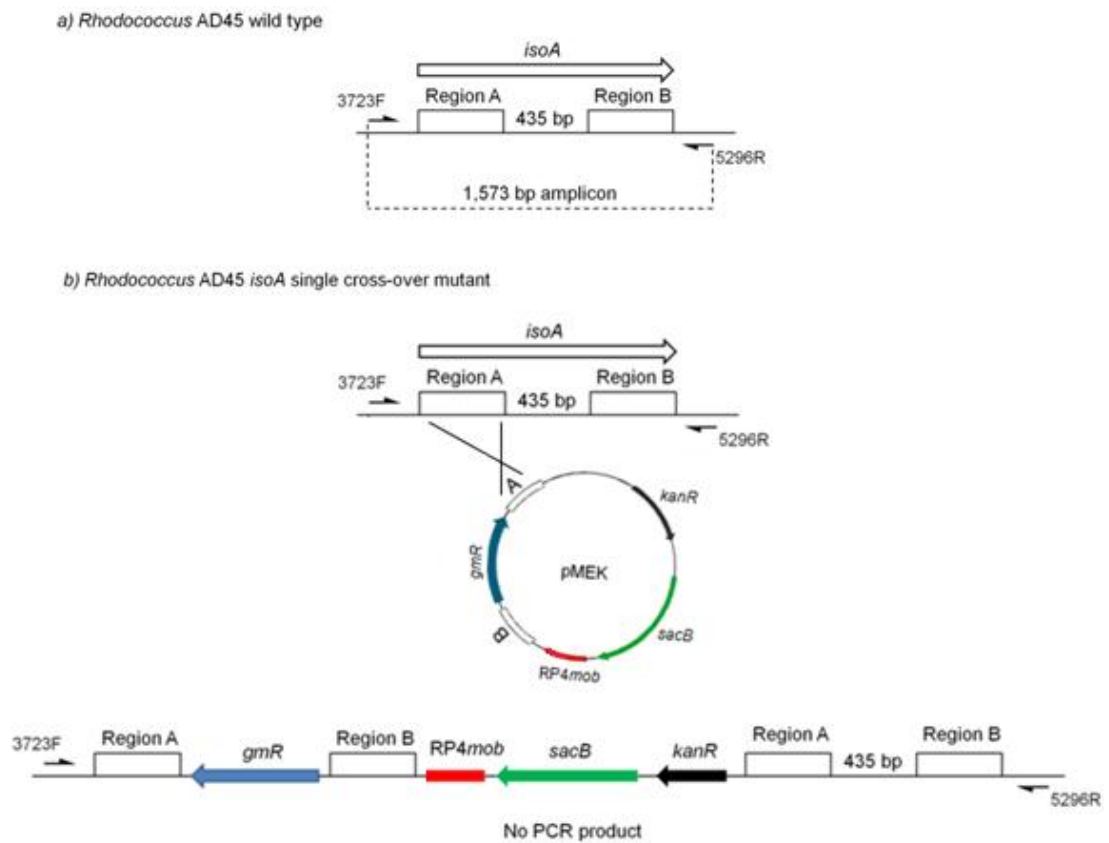


Figure 4.3 Screening for *isoA* single cross-over mutant by PCR using the primer set 3723F / 5296R.

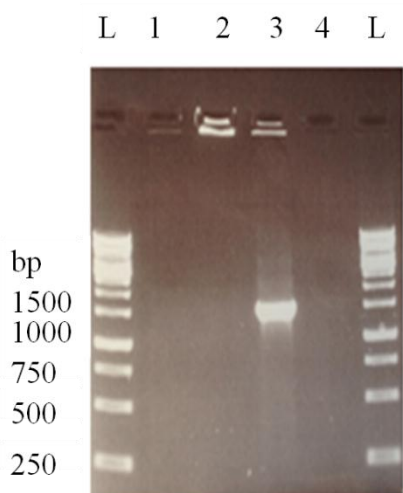


Figure 4.4 Colony PCR using primers 3723F and 5296R to screen for homologous recombination between the *Rhodococcus AD45* genome and pMEK plasmid. Lane 1: colony 14, lane 2: colony 15, lane 3: wild type *Rhodococcus AD45*, lane 4: no template control, L: GeneRuler 1 kb ladder.

Colonies 14 and 15 were further investigated to determine whether they contain the Gm cassette and the Kan gene. The GmF / GmR primer set, targeting a 234 bp fragment, was designed based on the sequence of the gentamicin cassette contained in the p34S vector (retrieved from the NCBI database) and the KanF / KanR primer set, targeting a 437 bp fragment, was designed based on the sequence of the Kan gene present in pK18mobsacB vector (also retrieved from the NCBI database) (Table 4.2). These primer sets were used respectively in the PCR amplification reactions targeting the gentamicin cassette and the kanamycin gene. As expected, the amplifications reactions yielded products of the correct size with both colonies (data not shown).

After checking that colony 14 and colony 15 had incorporated the pMEK plasmid, it was imperative to check that the latter was incorporated in the correctly targeted place in the genome. To do so, an amplification reaction was set up using the primer set 3723F / GmR. In this amplification reaction, no product was expected when using wild type *Rhodococcus AD45* colony as a template and a 1,048 bp amplicon was expected with colonies 14 and 15 (Figure 4.5). This was the case with colony 14, however no product was obtained for colony 15, suggesting that colony 15 might have incorporated the pMEK plasmid at a different place in the genome through an

illegitimate recombination (data not shown). The band corresponding to the 1,048 bp amplicon was excised from the agarose gel and checked by sequencing with 3723F/GmR primers. The analysis of the sequence confirmed that it corresponds to region A of *isoA* gene and to the gentamicin cassette. The 16S rRNA gene in colony 14 was also amplified and sequenced. The sequence had 100% identity to the 16S rRNA gene sequence of the wild type *Rhodococcus* AD45. Based on the above, colony 14 was designated as *isoA* single cross-over mutant and was used in the subsequent steps in the mutagenesis procedure.

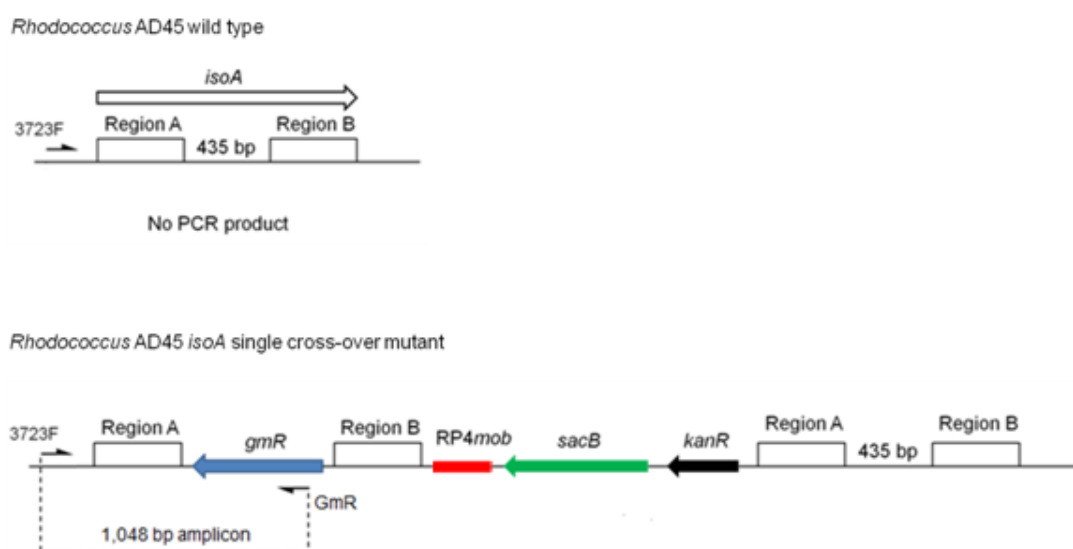


Figure 4.5 Screening for *isoA* single cross-over mutant by PCR using the primers 3723F and GmR. Homologous recombination between the genome of *Rhodococcus* AD45 and plasmid pMEK occurred at arm A.

4.2.5 Assessment of selective pressure on the single cross-over mutant

The stability of the single cross-over mutation in colony 14 and the ability of the cell to retain external DNA, were also investigated. Colony 14 was inoculated into 5 ml LB in a sterile universal with no added antibiotic and incubated at 30°C for 16 hours. Then, a 1×10^{-5} dilution of the culture was prepared and 100 μ l of the dilution was spread onto LB agar plate with no gentamicin and another 100 μ l onto LB agar plate with Gm (5 μ g/ml). This was done in triplicate and the number of colonies recovered on the LB agar plates with no gentamicin and the plates containing gentamicin was calculated (Table 4.5). T-test analysis generated a p value greater than 0.05 ($0.686 > 0.05$), suggesting that there is no significant difference in the number of colonies

recovered on the LB agar plates with or without gentamicin. This suggests that there is no selective pressure on the single cross-over mutant to revert to the wild type.

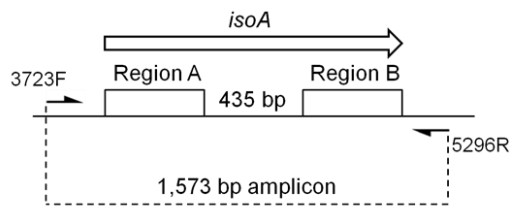
Table 4.5 Assessment of selective pressure on the single cross-over mutant

	Plates without gentamicin	Plates with gentamicin (5 µg/ml)
Replica 1	392	391
Replica 2	344	443
Replica 3	403	348

4.2.6 Selection for *isoA* double cross-over mutants

A second recombination event was forced by growing the single cross-over *isoA* mutant (colony 14) overnight in 5 ml LB with no antibiotic, then diluting the overnight culture (10^{-4} - 10^{-5}) and spreading the cells onto LB plates containing gentamicin (5µg/ml) and 10% (w/v) sucrose. Prior to this experiment, the ability of the wild type *Rhodococcus* AD45 cells to grow on 10% sucrose (w/v) was tested and *Rhodococcus* AD45 was able to grow on LB agar plates containing 10% (w/v) sucrose. After three days of incubation at 30°C, colonies were recovered on the LB+ Gm+ sucrose (10% w/v) agar plates. These colonies were patched twice onto fresh LB agar plates with Gm (5µg/ml) before being screened by PCR using the 3723F/5296R primer set (Figure 4.6). Double cross-over mutants are expected to yield a 2,063 bp PCR product which accounts for region A, Gentamicin cassette and region B, as shown in Figure 4.7.

Rhodococcus AD45 wild type



Rhodococcus AD45 *isoA* mutant

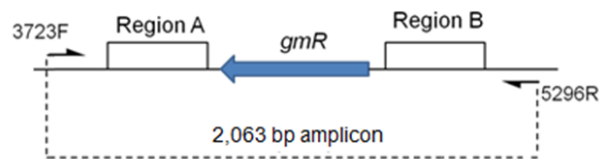


Figure 4.6 Screening for *isoA* double cross-over mutant by PCR using the primer set 3723F / 5296R.

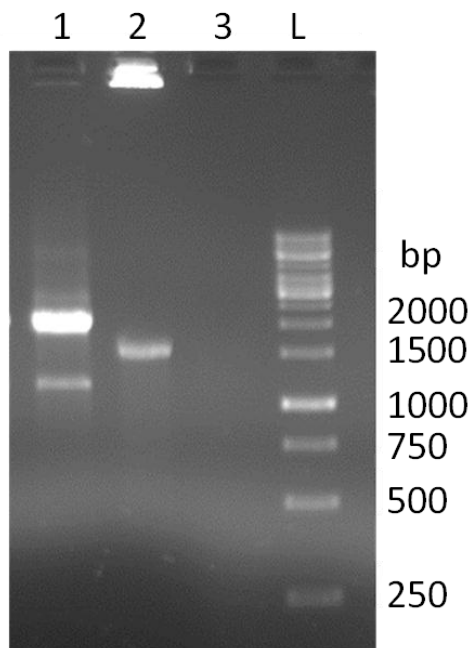


Figure 4.7 Primers 3723F and 5296R were used to screen for the replacement of the targeted *isoA* region with gentamicin resistance cassette. Lane 1: *isoA* double cross over mutant, lane 2: wild type *Rhodococcus* AD45, lane 3: no template, L: GeneRuler 1 kb ladder.

Figure 4.7 shows a 2,063 bp amplicon for a colony recovered on the LB agar plates containing gentamicin (5µg/ml) and 10% (w/v) sucrose, as opposed to a 1,573 bp

amplicon obtained in the case of wild type *Rhodococcus* AD45 colony. The band corresponding to 2,063 bp was excised and checked by sequencing with the 3723F/5296R primers. Blast searches with the sequence of the excised band confirmed that it corresponds to region A of *isoA* gene, the Gm resistance cassette and region B of *isoA* gene. The *isoA* double cross-over mutant was expected to contain the Gm cassette but not the Kan gene that was present on the pMEK vector. This is in agreement with Figures 4.8 and 4.9 which show a PCR product of the correct size (234 bp) when using the primers GmF/GmR and no PCR product with the primers KmF/KmR.

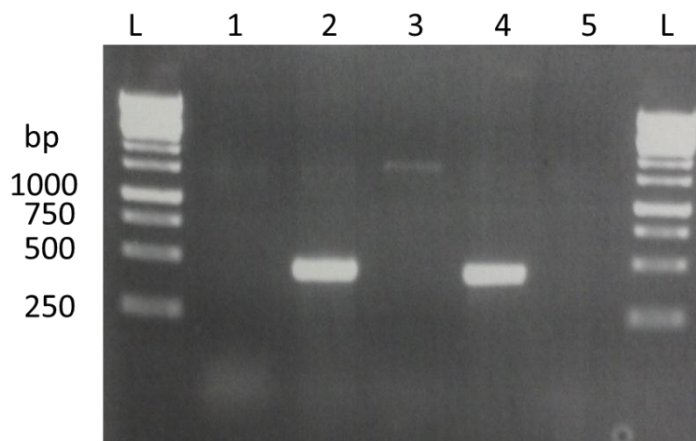


Figure 4.8 Screening for the loss of the pMEK plasmid backbone after sucrose counter selection using primers KmF and KmR (kanamycin resistance). L: GeneRuler 1 kb ladder, lane 1: $\Delta isoA$ strain, lane 2: colony14, lane 3: wild type *Rhodococcus* AD45, lane 4: pMEK vector, lane 5: no template control.

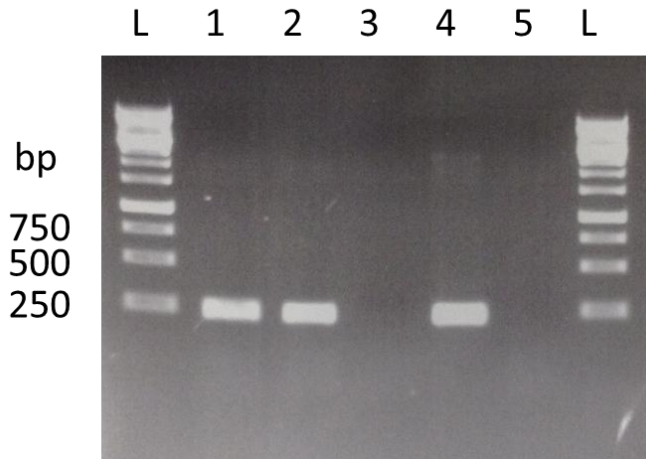


Figure 4.9 GmF and GmR primers were used to screen for the insertion of the gentamicin resistance cassette into the genome of *Rhodococcus* AD45 mutant strain. L: GeneRuler 1 kb ladder, lane 1: $\Delta isoA$ strain, lane 2: colony14, lane 3: wild type *Rhodococcus* AD45, lane 4: p34S-Gm vector, lane 5: no template control.

The *isoA* double cross-over mutant was then checked for growth on isoprene by first growing it in 10 ml CBS minimal medium with 10 mM succinate in a sterile universal. 200 μ l of that culture was then transferred separately to six sterile 125 ml serum vials containing 20 ml CBS minimal medium. 1% (v/v) isoprene was added to the first three vials as sole growth substrate. 10 mM succinate was added to the other three vials. Growth was observed in minimal medium with succinate but no growth on 1% (v/v) isoprene was observed. This experiment was repeated three times confirming that unlike wild type *Rhodococcus* AD45, the *isoA* mutant was not capable of growing on isoprene as sole source of carbon and energy (Figure 4.10). The mutagenesis experiment therefore provided solid evidence that *isoA* encodes a component of a key enzyme in isoprene metabolism in *Rhodococcus* AD45.

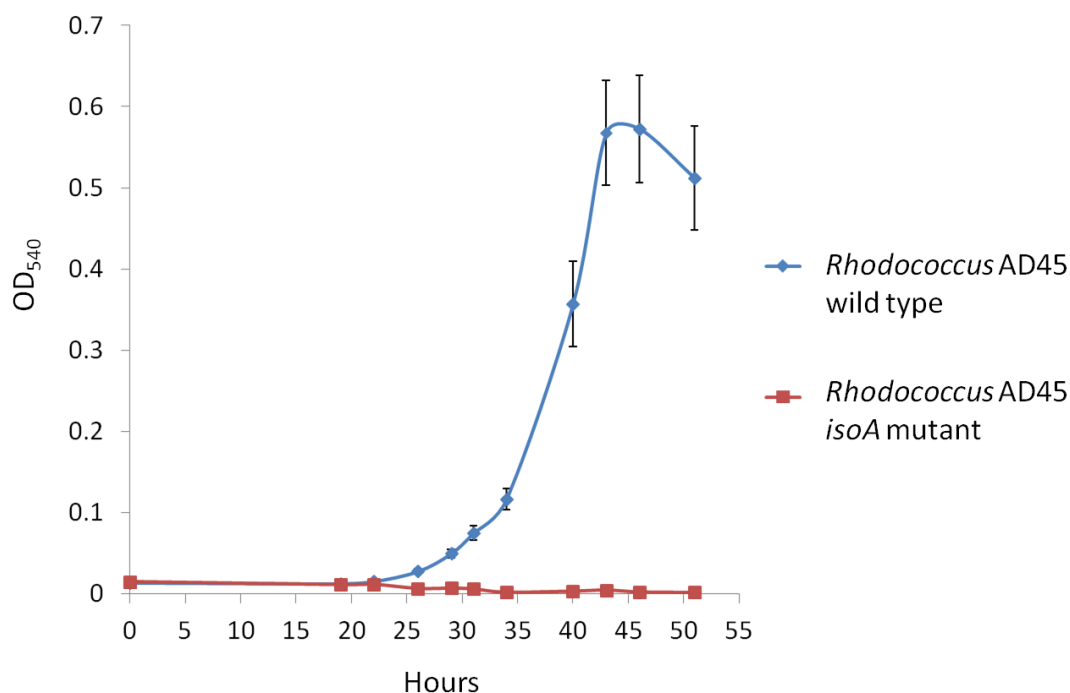


Figure 4.10 Growth curves of the *isoA* mutant strain (red) and the wild type (blue)

4.3 Assays of *isoA* transcription using quantitative RT-PCR

4.3.1 *isoA* is transcribed during growth on isoprene as shown by RT-PCR

Rhodococcus AD45 was grown on glucose (10 mM) and isoprene (1 % v/v) separately, in 50 ml CBS minimal medium in 250 ml flasks at 30 °C with shaking at 150 rpm. RNA was extracted from *Rhodococcus AD45* cells grown on glucose and *Rhodococcus AD45* cells grown on isoprene at mid-late exponential phase, using the RNeasy mini kit (Qiagen) as detailed in the Materials and Methods section 2.5.3. RNA was checked for DNA contamination by performing a standard 16S rRNA gene amplification using the purified RNA as template (data not shown). Subsequently, cDNA was generated using random hexamers and SuperScript II (Invitrogen) reverse transcriptase enzyme (Materials and Methods section 2.6.9). The synthesized cDNA from cells grown separately on isoprene and glucose was used as template in two separate sets of PCR amplification reactions targeting 16S rRNA and *isoA* genes using the primer sets 27f / 1492r (Lane, 1991) and *isoA* 494f / *isoA* 1457r, respectively (Table 4.6). *isoA* 494f and *isoA* 1457r primers were designed using Primer 3 software (available at <http://frodo.wi.mit.edu/primer3/>).

Table 4.6 List of primers used for RT-PCR

Primer name	Sequence (5'- 3')
27f	AGAGTTTGATCMTGGCTCAG
1492r	TACGGYTACCTTGTTAGGACTT
isoA 494f	AGAAGGCRTTCCACACCAAC
isoA 1457r	ACRTCCTCRCCCATCACCTC

Figure 4.11 shows a correct sized PCR band when amplifying *isoA* gene from cDNA generated from purified RNA from *Rhodococcus* AD45 cells grown on isoprene and glucose (lanes 2, 3). No reverse transcriptase (RT) controls were set up, containing purified RNA from cells grown on isoprene and glucose respectively, but no added reverse transcriptase for cDNA synthesis. No *isoA* amplification was detected in the PCR reactions that were set up with 2 ml of the no RT controls as a template (Figure 4.11, lanes 4, 5). This confirmed that the purified RNA was not contaminated with genomic DNA.

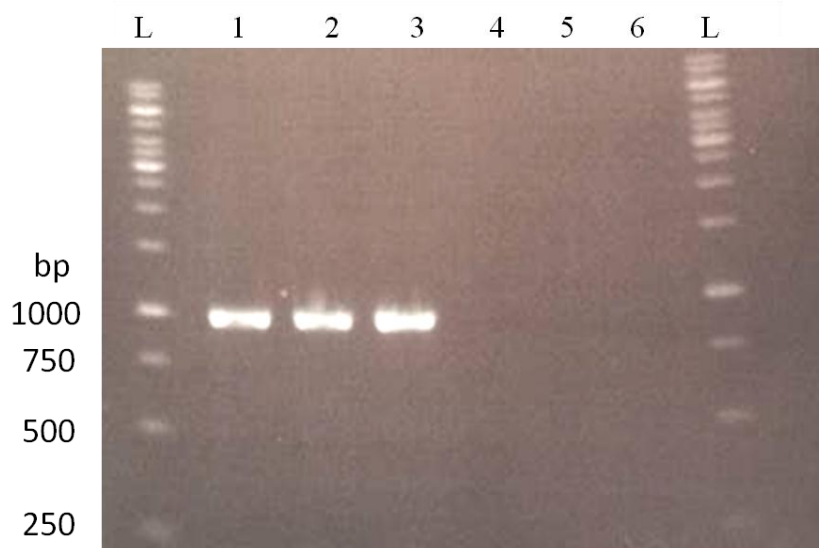


Figure 4.11 PCR of *isoA* gene from cDNA generated from mRNA and DNA control. Lane 1: *Rhodococcus* AD45 genomic DNA template, lane 2: cDNA template generated from RNA from isoprene grown *Rhodococcus* AD45 cells, lane 3: cDNA template generated from RNA from glucose grown *Rhodococcus* AD45 cells, lane 4: no RT control for isoprene grown cells, lane 5: no RT control for glucose grown cells, lane 6: no template negative control. L: GeneRuler 1kb ladder (Fermentas).

The reverse transcription assay performed in this case was not quantitative and the main conclusion that could be drawn from the data above is that *isoA* is transcribed during growth on isoprene and during growth on glucose. The fact that there was a band in the lane corresponding to cells grown on glucose justified the use of quantitative RT-PCR to determine if *isoA* transcription is regulated during growth on isoprene.

4.3.2 *isoA* transcription is upregulated during growth on isoprene as shown by quantitative RT-PCR

Rhodococcus AD45 cells were grown separately on glucose (10 mM) and isoprene (1 % v/v) in 50 ml CBS minimal medium in 250 ml sterile flasks (in triplicate) and harvested at mid-exponential phase. RNA was extracted from these cells using the RNeasy mini kit (Qiagen) (Materials and Methods section 2.5.3). The purified RNA was then checked for DNA contamination before being used as template for cDNA synthesis with SuperScript II RT (Invitrogen) (Materials and Methods section 2.6.9).

Two sets of primers were designed for qRT-PCR using the Primer Express Software (Applied Biosystems) (Table 4.7). The primer set isoA_qF / isoA_qR targets *isoA* gene, the gene of interest. The primer set rpoB_qF / rpoB_qR targets *rpoB* gene which encodes the β subunit of RNA polymerase. *rpoB* was used as a reference gene for RT-qPCR data normalization.

Table 4.7 List of primers used for quantitative RT-PCR

Primer name	Sequence (5'- 3')
isoA_qF	CGCAGAAAGCTCTCGATATCG
isoA_qR	CGGACCGGTTAACGTCTGAA
rpoB_qF	GCATCCCCGAGTCGTTCA
rpoB_qR	GAGGACAGCACCTCCACGTT

The quantitative reverse transcription reactions were set up, as described in the Materials and Methods section 2.6.10, with cDNA from three separate cultures of *Rhodococcus* AD45 grown on isoprene and three glucose grown *Rhodococcus* AD45 cultures. The negative controls consisted of purified RNA from cells grown on isoprene and glucose to which the reverse transcriptase enzyme was not added for cDNA synthesis. Standards were prepared from serial dilutions (to 10^{-4}) of cDNA generated from *Rhodococcus* AD45 cells grown on isoprene. Sybr Green was used as the fluorescent DNA probe and quantitative amplification was carried out using StepOnePlus Real - Time PCR System (Applied Biosystems).

The qRT-PCR data were analyzed by first plotting the standard curves for *isoA* and *rpoB* genes (Figures 4.12, 4.13). Based on the values of the slope of standard curves, the calculated amplification efficiencies for *isoA* and *rpoB* were 96 % and 98 %, respectively (Table 4.8). These values are within the recommended range [90 % - 105 %] for good amplification efficiency. The R^2 values were greater than 0.990, which is also recommended (Applied Biosystems StepOne and StepOnePlus Real-Time PCR Systems Guide, 2008/2010).

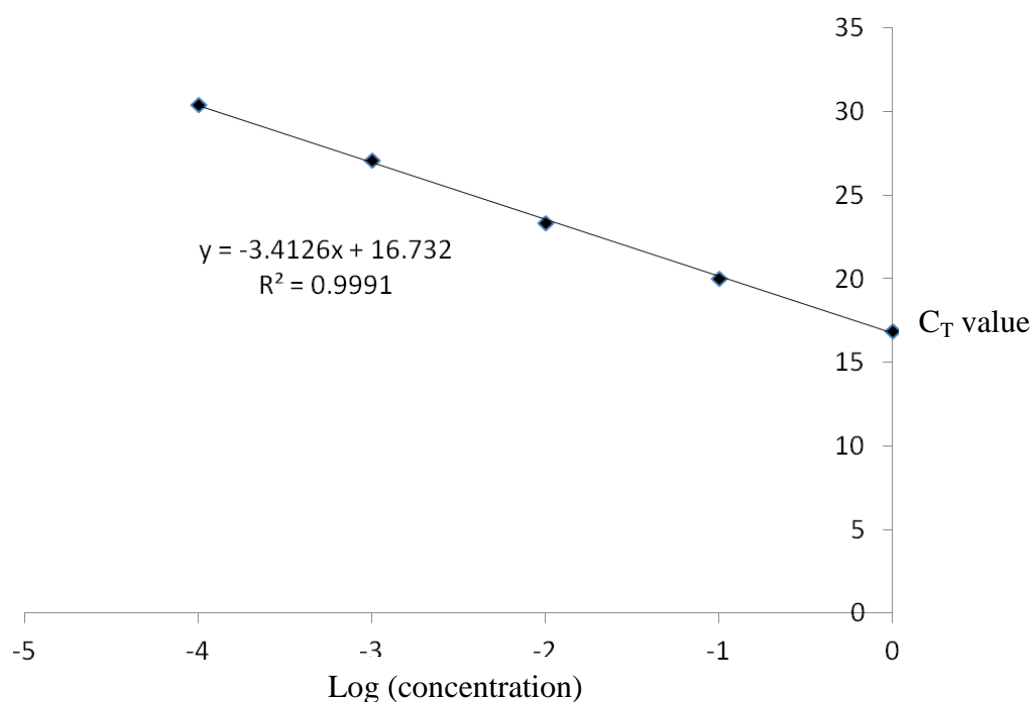


Figure 4.12 Standard curve plot for *isoA* gene showing the change in C_T values in relation to the log concentration of the standard samples.

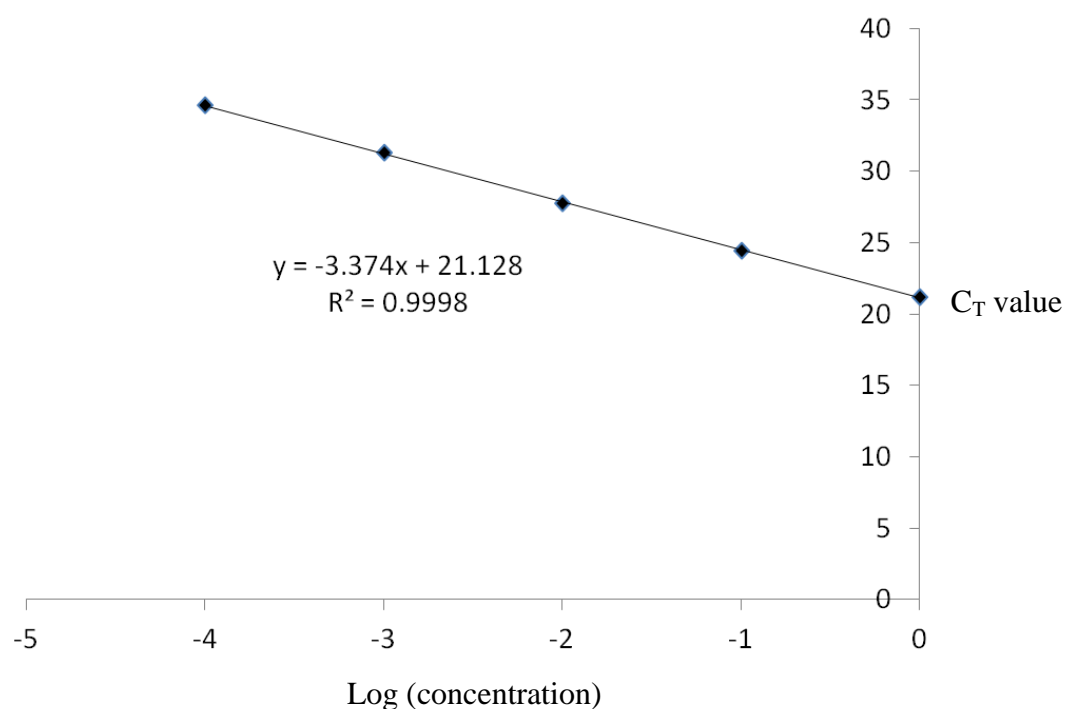


Figure 4.13 Standard curve plot for *rpoB* gene showing the change in C_T values in relation to the log concentration of the standard samples.

Table 4.8 Determination of the efficiency of the qRT-PCR amplification of *isoA* and *rpoB*

	<i>isoA</i>	<i>rpoB</i>
Slope (m)	-3.416	-3.374
Intercept (b)	16.732	21.128
% Efficiency*	96 %	98 %
R ²	0.9991	0.9998

* The % Efficiency is calculated using the following equation: $E = (10^{-1/m} - 1) \times 100$, according to the 'Guide to performing relative quantitation of gene expression using real-time quantitative PCR' published by Applied Biosystems, 2004.

T-test analysis of the relative quantity (RQ) values (Table 4.9) yielded a p value (0.02) less than 0.05. This suggests that there is a significant difference in the RQ values between growth on glucose and growth on isoprene. Therefore, the transcription of *isoA* gene is significantly different in *Rhodococcus* AD45 cells grown on isoprene compared to cells grown on glucose.

Table 4.9 qRT-PCR data

a

C a l c u l a t e	<i>isoA</i>			<i>rpoB</i>			Relative Quantity (RQ= <i>isoA/rpoB</i>)
	Ct value	Log quantity ^a	Quantity	Ct value	Log quantity ^b	Quantity	
Glucose 1	28.25	-3.37	0.00	26.59	-1.62	0.02	0.00
Glucose 2	29.36	-3.70	0.00	26.38	-1.56	0.03	0.00
Glucose 3	25.01	-2.43	0.00	20.19	0.28	1.90	0.00
Isoprene 1	20.00	-0.96	0.11	21.17	-0.01	0.98	0.11
Isoprene 2	19.02	-0.67	0.21	20.85	0.08	1.20	0.18
Isoprene 3	20.87	-1.21	0.06	23.39	-0.67	0.21	0.29

^a the equation $y = -3.4126x + 16.732$, obtained from the standard curve plot for *isoA* gene

^b Calculated using the equation $y = -3.374x + 21.128$, obtained from the standard curve plot for *rpoB* gene

4.4 The isoprene gene cluster is induced by growth on isoprene

In order to confirm, on the basis of the transcriptomics data obtained above, that the isoprene gene cluster involved in isoprene degradation in *Rhodococcus* AD45 is an inducible system, the polypeptide profiles of *Rhodococcus* AD45 grown on isoprene and glucose separately were analysed by SDS-PAGE. *Rhodococcus* AD45 cells were grown in 500 ml CBS minimal medium with 10 mM glucose or 1 % (v/v) isoprene in 2 L sterile flasks, harvested at late exponential phase (OD₅₄₀: 0.8) and subjected to three passages through a French pressure cell (American Instrument Company) followed by centrifugation at 13,000 g for 15 min at 4 °C for preparation of crude cell-free extract (Materials and Methods section 2.14.1). Proteins in cell-free extracts were quantified following the Bio-Rad Protein Assay (Bio-Rad) whereby five bovine serum albumin standards were prepared according to the manufacturer's protocol and their absorbance was measured by spectrophotometry at 595 nm. This generated a standard curve which was used to determine the unknown concentrations (x value) of the solubilized proteins in the prepared cell-free extract samples based on their absorbance measured at 595 nm (y value) (Figure 4.14).

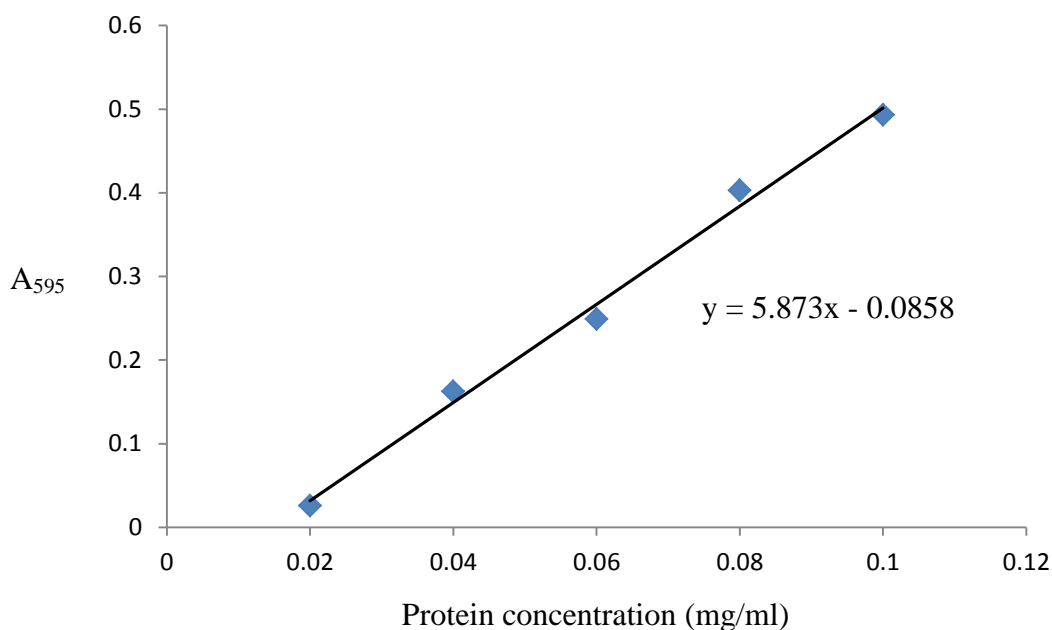


Figure 4.14 The standard curve, obtained by Bio-Rad Protein Assay, for the quantification of solubilized protein concentrations.

Both extracts were then run on a one dimension SDS denaturing polyacrylamide gel (Materials and Methods section 2.14.3), together with a prestained protein ladder (Fermentas). The polypeptide profile for cells grown on isoprene was clearly different from that of *Rhodococcus* AD45 grown on glucose (Figure 4.15). At least 8 bands were dominant only in the lane corresponding to isoprene grown cells. These bands were excised from the gel and submitted to the Proteomics Service at the University of Warwick (UK) for mass spectrometry analysis (Materials and Methods section 2.14.4). Proteomic analysis confirmed that three of the prominent bands: band 1, band 2, band 3 that appear only in cell extract from isoprene grown cells were respectively IsoH (1-hydroxy-2-glutathionyl-2-methyl-3-butene dehydrogenase), IsoE (β -subunit of the hydroxylase component of isoprene monooxygenase), IsoA (α -subunit of the hydroxylase component of isoprene monooxygenase) (Table 4.10). The finding that isoprene monooxygenase peptides were present only in isoprene grown cells suggests that the expression of the isoprene gene cluster is induced during growth on isoprene.

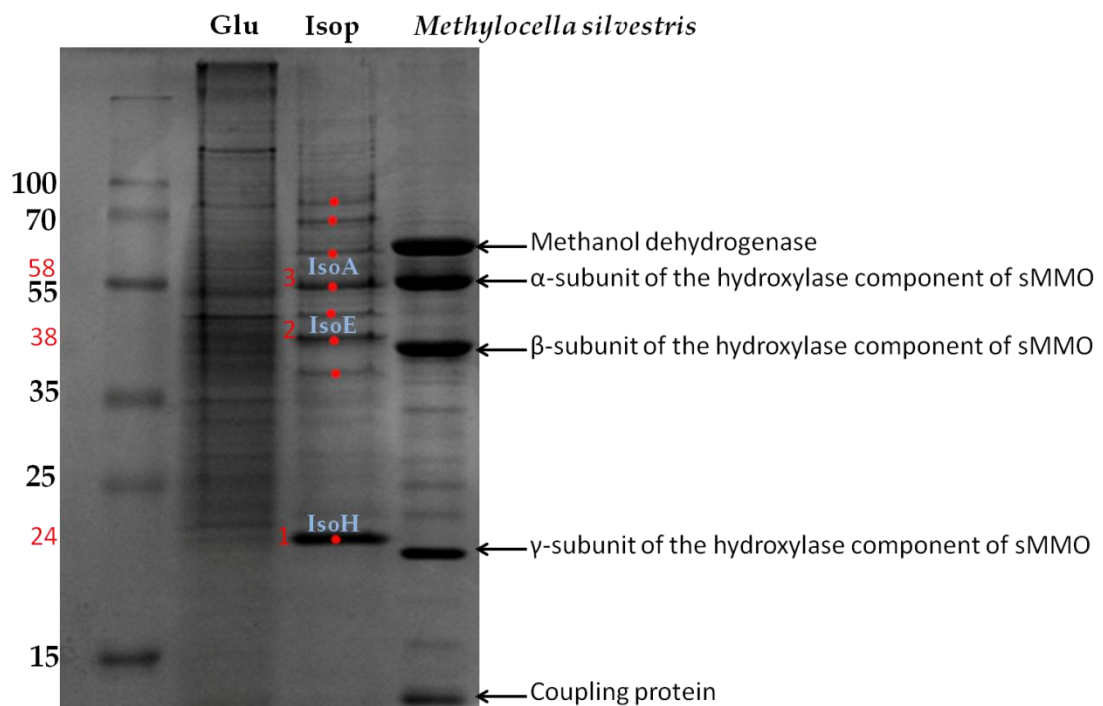


Figure 4.15 SDS-PAGE of cell-free extract, lane 1: PageRuler Plus prestained protein ladder (Fermentas), lane 2: *Rhodococcus* AD45 grown on glucose, lane 3: *Rhodococcus* AD45 grown on isoprene, lane 4: *Methylocella silvestris* grown on methane, used for reference.

Table 4.10 Polypeptides identified in the bands excised from the gel in Figure 4.15. The number of detected peptides, the percentage coverage and molecular weight of each polypeptide are reported.

Band	Peptides	Coverage (%)	Molecular Mass (kDa)	Annotation
1	13	55	24	IsoH
2	12	44	38.5	IsoE
3	14	26	59.3	IsoA

4.5 Discussion

The pathway of isoprene degradation was investigated in *Rhodococcus* AD45. The sequence information from the *Rhodococcus* AD45 genome presented the first line of evidence that the isoprene monooxygenase enzyme, a close relative to known soluble diiron centre monooxygenases (chapter 3), is potentially involved in isoprene metabolism. This pathway was tested using marker exchange mutagenesis, RT-PCR assays, and proteomics analysis that are described in this chapter. The mutation of *isoA*, coding for the alpha subunit of soluble isoprene monooxygenase, abolished growth on isoprene while it did not have an effect on growth on succinate. This conclusively indicated that isoprene monooxygenase is a key enzyme in the isoprene degradation pathway. Studies in which genes encoding other SDIMO alpha subunits were mutated, have reported a similar loss in the ability of the mutant strains to grow on the corresponding hydrocarbon substrate. For instance, the deletion of *prmA* gene, coding for the alpha subunit of soluble propane monooxygenase, resulted in the inability of *Rhodococcus jostii* RHA1 to use propane for growth (Sharp *et al.*, 2007). The insertion of a kanamycin resistance cassette into *bmoX*, that encodes the alpha subunit of soluble butane monooxygenase in the butane utilizing *Thauera butanivorans* (*Pseudomonas butanovora*), prevented the mutant from metabolizing butane and using it as a source of carbon and energy (Sayavedra-Soto *et al.*, 2005).

A basal transcription of *isoA* gene was detected in the absence of isoprene, as indicated by the *isoA* PCR product obtained with cDNA from glucose grown *Rhodococcus* AD45 cells. However, quantitative RT-PCR data showed that the

transcription of *isoA* was significantly upregulated when isoprene was supplied to the growth medium, suggesting that isoprene monooxygenase is an inducible enzyme. This observation was further supported by IsoA, IsoE, and IsoH polypeptides being exclusively expressed during growth on isoprene, as analyzed by mass spectrometry. In contrast, these polypeptides were not present in the cell-free extract prepared from *Rhodococcus* AD45 cells grown on glucose. Taken together, the results obtained in this chapter clearly suggest that isoprene is metabolized in *Rhodococcus* AD45 through the induced activity of soluble isoprene monooxygenase enzyme. However, it cannot be determined if isoprene itself, when present, induces the transcription and expression of the isoprene gene cluster or if a product of isoprene oxidation, such as the epoxide, is the inducer. An RNA sequencing experiment investigating the transcriptional regulation of the isoprene metabolic genes was conducted together with Dr Andrew Crombie, a postdoctoral fellow in our laboratory, in collaboration with Dr Gregg Whited and colleagues at DuPont Industrial Biosciences. The details of this experiment will be the subject of a separate publication. In brief, *Rhodococcus* AD45 cells were grown on 20 mM succinate in minimal medium, washed, aliquoted in equal volumes into 250 ml sterile flasks, starved for 1 hour, then incubated at 30 °C with four different carbon sources (in triplicate). The carbon sources included succinate, glucose, isoprene, and epoxyisoprene. A no substrate control was also included. Cells were removed directly prior to incubation (T_0) then at five time points throughout incubation (19, 43, 75, 240, and 1500 min) and immediately added to two volumes of RNAprotect Bacteria Reagent (Qiagen) to stop the transcriptional activity. Cells were then sent to DuPont Industrial Biosciences for RNA sequencing using Illumina HiSeq2500 platform. The analysis of mRNA data revealed that all the genes of the isoprene cluster (*isoABCDEFGHIJ*) were co-transcribed and induced in the presence of isoprene and epoxyisoprene. Incubation with the epoxide induced an immediate transcription response, in contrast, a lag period was observed for cells incubated with isoprene before transcription of the isoprene operon was activated. This suggested that epoxyisoprene is an efficient inducer of the transcription of isoprene metabolic genes. When tested, *Rhodococcus* AD45 was effectively found able to grow directly on epoxyisoprene as sole source of carbon and energy. The lag period observed for isoprene-induced cells might correspond to the reaction time necessary for epoxide

formation. However, further investigations are needed before completely ruling out a role for isoprene, albeit secondary, in activating transcription of the isoprene operon.

Chapter 5

Design and evaluation of primers for the detection of genes encoding isoprene monooxygenase alpha subunit in the environment

5.1 Introduction

The metabolic gene biomarker-based approach is a powerful tool for the study of functionally distinct bacterial groups in the environment without the need for cultivation. One advantage of using a PCR approach targeting functional gene markers over 16S rRNA gene is that the 16S rRNA gene is highly conserved across bacterial taxa, resulting in a less specific, more error prone taxonomic affiliation (Fox *et al.*, 1992, Vos *et al.*, 2012). Many studies investigating the diversity of hydrocarbon-oxidizing bacteria in the environment have been reported, using primers targeting key genes involved in the oxidation pathway. For example, *mmoX* primers which target the gene encoding the alpha subunit of soluble methane monooxygenase were used to study the diversity of methanotrophs (McDonald *et al.*, 1995). Other examples include the design of primers that target the gene encoding the large subunit of phenol hydroxylase for characterizing the phenol degrading bacterial community resident in an activated sludge ecosystem (Watanabe *et al.*, 1998). To date, such an approach has not been developed to identify isoprene degrading genes in the environment due to limited sequence and genetic information. This chapter reports the design and validation of primers targeting the *isoA* gene which codes for the alpha subunit of isoprene monooxygenase, a key enzyme in isoprene metabolism as shown previously (see Chapter 4).

5.2 Design of primers targeting *isoA* gene which encodes the alpha subunit of the isoprene monooxygenase

It is worth noting that prior to designing the *isoA* primers, we tested the degenerate primers NVC65, NVC57, NVC66, and NVC58 that were designed by Coleman and colleagues (2006) with genomic DNA from *Rhodococcus* SC4, LB1, and AD45. Although these primers were designed to target the alpha subunit of SDIMO enzymes, they did not yield a PCR product with genomic DNA from isoprene degraders. A different approach was therefore used which was based on the sequence information from the draft genomes (see Chapter 3). The genomes of *Rhodococcus* AD45, *Rhodococcus* SC4 and *Rhodococcus* LB1 contain one copy of the *isoA* gene. The amino acid sequences deduced from the *isoA* gene of each of these isolates were aligned (Figure 5.1), together with the IsoA amino acid sequences of two marine

isoprene degraders, *Mycobacterium hodleri* i29a2* and *Gordonia polyisoprenivorans* i37 which were isolated by the group of Terry McGenity at the University of Essex and extensively characterized by another PhD student in our laboratory, Antonia Johnston, working on the bacterial degradation of isoprene in the marine environment. The genomes of *Mycobacterium hodleri* i29a2* and *Gordonia polyisoprenivorans* i37 were sent by Antonia for sequencing using Illumina technology then mined for the isoprene gene cluster.

The derived amino acid sequence of *xamoA* gene, that encodes the alpha subunit of soluble alkene monooxygenase of *Xanthobacter autotrophicus* PY2 (Zhou *et al.*, 1999), was one of the top hits in BLAST searches against the NCBI database when using IsoA sequence of *Rhodococcus* AD45 as a query sequence (*XamoA* shares 70 % sequence identity with IsoA of *Rhodococcus* AD45). *Xanthobacter* PY2 does not grow on isoprene, as tested three independent times by inoculating a fresh colony of *Xanthobacter autotrophicus* PY2 (kindly provided by Professor David Leak at the University of Bath) into 50 ml CBS medium contained in a 250 ml sterile Quickfit flask and incubating the sealed flask with 1 % (v/v) isoprene at 30 °C, shaking at 150 rpm. No turbidity was observed in seven days of incubation. *XamoA* sequence was added to the alignment for the purpose of selecting amino acid regions for primer design that are conserved amongst the IsoA sequences of the isoprene utilizing isolates but contain mismatching amino acids with the corresponding *XamoA* sequence (Figure 5.1), therefore preventing *isoA* primers from binding to and amplifying *xamoA* gene. To further improve the specificity of the *isoA* primers, the deduced amino acid sequence of *mmoX*, the gene encoding the alpha subunit of soluble methane monooxygenase of *Methylosinus trichosporium* OB3b (Cardy *et al.*, 1991), was also added to the alignment (Figure 5.1) as a representative of other SDIMO alpha subunits to avoid regions covering signature residues that are conserved in all SDIMO enzymes.

In addition to screening for conserved amino acid regions between the IsoA sequences while avoiding as much as possible amino acids that have a high number of codons (codon redundancy), several criteria were also taken into consideration when designing the *isoA* primers, including primer length, GC content, melting temperature, self-complementarity and potential hairpin formation (Table 5.1).

Table 5.1 *isoA* degenerate primers

	isoAF (forward) 5' TGCATGGTCGARCAATG 3'	isoAR (reverse) 5' GRTCYTGATCGAAGCACCCTT 3'	Recommended parameters ¹
Length (bp)	18	22	18 – 28
GC content	44 to 56 %	45 to 59 %	50 % - 60 % ²
Melting temperature	45.8 to 50.3 °C	53 to 58.6 °C	55 °C - 80 °C
Potential hairpin formation ³	None	None	None
Self-complementarity ³	None	None	None

¹ According to Innis & Gelfand, 1990.

² The recommended range of GC content is between 40 % and 60 % according to Life Technologies primer design tips and tools.

³ The primers were checked for self-complementarity and potential hairpin formation on the Oligonucleotide Properties Calculator website (available at <http://www.basic.northwestern.edu/biotools/oligocalc.html>).

5.3 Optimization of PCR protocol for *isoA* amplification

Genomic DNA was extracted from *Rhodococcus* AD45, *Rhodococcus* SC4 and *Rhodococcus* LB1 cells (Materials and Methods section 2.5.1). These genomic DNAs were then challenged with the newly designed *isoA* primers by PCR using three different sets of amplification reactions. All reactions contained 10 x DreamTaq buffer (Fermentas), 0.2 mM of each dNTP, DreamTaq DNA polymerase (Fermentas), and 0.2 μ M of the forward and reverse *isoA* primers. However, one set of the reactions contained 0.07 % (w/v) BSA in the mix but lacked DMSO, one set contained 2.5 % (v/v) DMSO but lacked BSA and one set lacked both DMSO and BSA. A temperature gradient PCR was set up with annealing temperatures ranging from 50 °C to 58 °C. PCR products of correct size (1,015 bp) were obtained when the DMSO was not added and the BSA was present in the amplification reaction mix. The PCR band of the highest intensity was obtained at 54 °C, suggesting that the optimum annealing temperature to be used with the *isoA* primers is 54 °C (data not shown). However, an additional intense band corresponding to a wrong-sized amplicon also appeared, suggesting that non-specific PCR amplification was occurring.

The next step in the optimization process consisted in trying a TouchDown PCR protocol combined with a hot start (Table 5.2) to amplify *isoA* from genomic DNA of *Rhodococcus* AD45, *Rhodococcus* SC4 and *Rhodococcus* LB1. The amplification reaction was prepared as described above and contained 0.07 % (w/v) BSA. The expected PCR product of 1,015 bp was obtained with the genomic DNA from all three pure cultures of *Rhodococcus* AD45, *Rhodococcus* SC4 and *Rhodococcus* LB1 (Figure 5.2). The PCR products were purified, cloned into the pGEM-T Easy vector and sequenced with the M13 primers (Invitrogen) which span the cloning region in the pGEM-T Easy vector (Materials and Methods section 2.6.5) to confirm that the correct gene (*isoA*) was targeted and amplified. The TouchDown PCR protocol was consistently used for *isoA* amplification throughout the rest of the project.

Table 5.2 TouchDown PCR protocol for *isoA* amplification

Phase 1:

Step	Temperature	Time
1 (denature)	94 °	3 min
2 (denature)	94 °	30 s
3 (anneal)	72 °	45 s
4 (elongate)	72 °	60 s

→ Repeat steps 2 to 4, 19 times, each time decreasing the annealing temperature 1 degree to reach 53°C

Phase 2:

Step	Temperature	Time
5 (denature)	94 °	30 s
6 (anneal)	54 °	45 s
7 (elongate)	72 °	60 s

→ Repeat steps 5 to 7, 25 times

Termination phase:

Step	Temperature	Time
8 (elongate)	72 °	5 min
9 (halt reaction)	4 °	Hold infinite

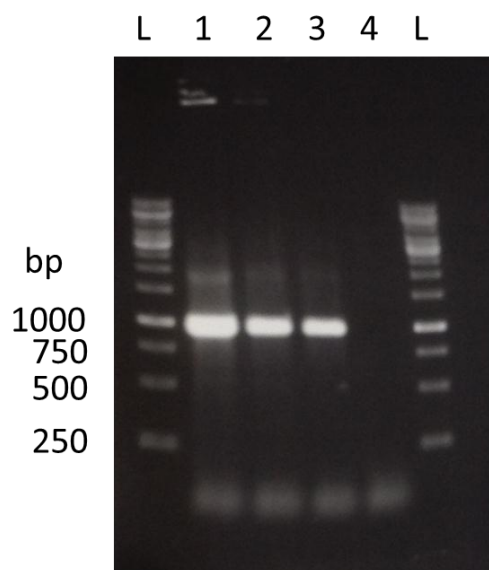


Figure 5.2 Test of the new primers using genomic DNA from *Rhodococcus* AD45, *Rhodococcus* SC4 and *Rhodococcus* LB1 strains. L: GeneRuler 1kb ladder (Fermentas), lane 1: *Rhodococcus* AD45 template DNA, lane 2: *Rhodococcus* SC4 template DNA, lane 3: *Rhodococcus* LB1 template DNA, lane 4: no template negative control.

5.4 Evaluation and validation of the primers

The *isoA* primers designed in this study were validated and evaluated by amplifying and sequencing *isoA* genes from (i) genomic DNA from pure cultures of terrestrial isoprene-degrading isolates (ii) DNA from isoprene-enriched soil samples. (iii) *isoA* primers were also tested on genomic DNA from pure cultures of non-isoprene degraders (*isoA*⁻ bacteria) which contain other soluble diiron centre monooxygenases. No PCR product was expected for the *isoA*⁻ bacteria.

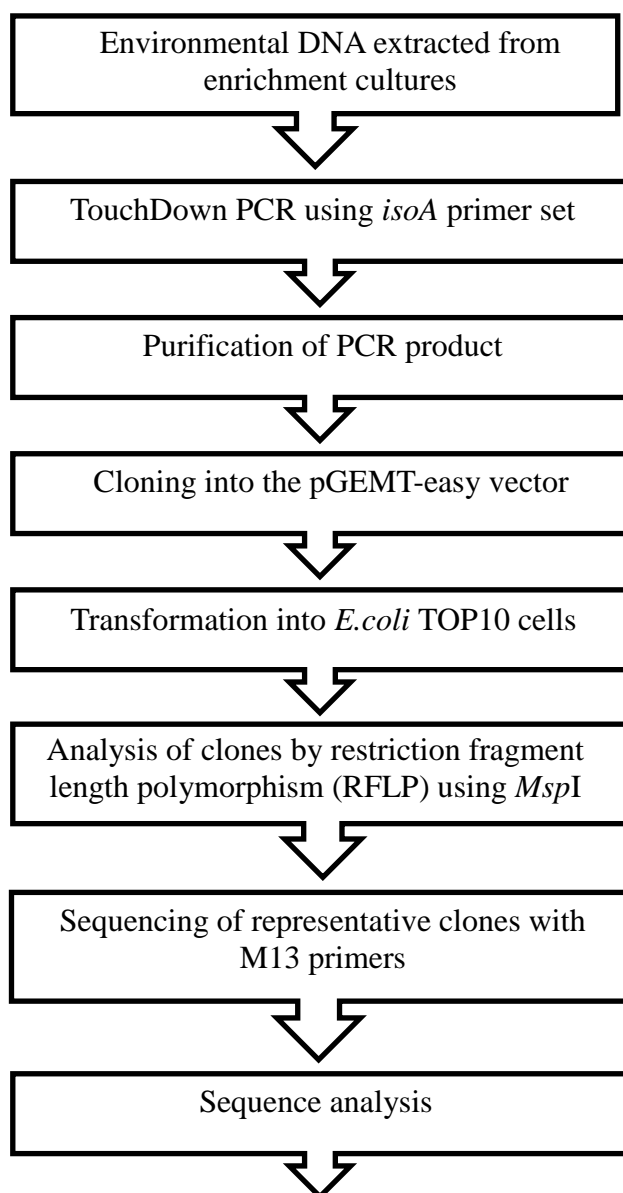
(i) Genomic DNA from pure cultures of terrestrial isoprene-degrading isolates

The *isoA* primers were tested by PCR using genomic DNA from a pure culture of *Rhodococcus opacus* PD630 whose ability to utilize isoprene for growth was recently discovered (see Chapter 3). A PCR product of the correct size was obtained (data not shown). The PCR product was then purified and cloned into the pGEM-T Easy vector (Promega) before transformation into *E.coli* TOP10 cells (materials and methods section 2.9). The plasmid was extracted (Materials and Methods section

2.5.2) and checked that it contained the *isoA* amplicon insert by PCR with the M13 primers. The amplicon was then sent for DNA sequencing using M13 forward and reverse primers. The deduced IsoA amino acid sequence of *Rhodococcus* PD630 matched the sequence that was retrieved from the genome sequence of *Rhodococcus* PD630 in the NCBI database (see Chapter 3) and shared 91 % identity to the IsoA amino acid sequence of *Rhodococcus* AD45.

(ii) Environmental DNA extracted from isoprene-enriched soil samples

Three separate isoprene enrichments were set up using soil samples collected from three different environments: an oak tree plot in Gibbet Hill wood at the University of Warwick (UK), a poplar tree plot in Gibbet Hill wood, and the garden of a house in Leamington Spa (UK). The oak and poplar tree plots were chosen for soil sampling because poplar and oak species are known to emit isoprene (see Chapter 1). The enrichment cultures were set up as follows: 0.3 g of soil, 50 ml CBS minimal medium and 1 % (v/v) isoprene in 250 ml sealed Quickfit flasks. The samples were incubated at 30 °C without shaking until all the isoprene has been consumed. Isoprene depletion in these samples was monitored by routine measurements of the headspace concentration of isoprene by gas chromatography. Isoprene was depleted in the samples within two weeks of incubation. DNA was extracted from the enrichment cultures (Materials and Methods section 2.5.1) and further processed as described in the flow chart below:



In total, 50 clones from the three different *isoA* clone libraries (oak soil clone library, poplar soil clone library and garden soil clone library) were randomly chosen, analyzed by RFLP (Materials and Methods section 2.6.6) and grouped based on their restriction pattern. Subsequently, 10 representative clones were selected for sequencing with the M13 primers. The *isoA* nucleotide sequences were checked for the forward and reverse primer sites (Figure 5.3, 5.4) and the deduced IsoA amino acid sequences were validated as authentic isoprene monooxygenase alpha subunit sequences by verifying the presence of the signature residues (see Chapter 3) (Figure 5.5). All the sequences had high shared identity (96 % and above) to IsoA of *Rhodococcus sp.* AD45 (Figure 5.6).

DNA Sequences		Translated Protein Sequences	
Species/Abbrv			
1. isoA forward primer			
2. isoA reverse primer			
3. <i>Rhodococcus</i> AD45	A	A	G
4. <i>Gordonia</i> sp.	C	A	C
5. <i>Rhodococcus</i> isolate LB1	C	A	C
6. <i>Rhodococcus</i> isolate SC4	C	A	C
7. <i>Mycobacterium</i> sp.	C	A	C
8. <i>Rhodococcus opacus</i> PD630	C	A	C
9. Garden soil clone 1	C	A	C
10. Garden soil clone 2	C	A	C
11. Garden soil clone 3	C	A	C
12. Garden soil clone 4	C	A	C
13. Garden soil clone 5	C	A	C
14. Oak soil clone 1	C	A	C
15. Oak soil clone 2	C	A	C
16. Oak soil clone 3	C	A	C
17. Poplar soil clone 1	C	A	C
18. Poplar soil clone 2	C	A	C
19. <i>Xanthobacter autotrophicus</i> PY2	T	T	C

Figure 5.4 Alignment of the *isoA* nucleotide sequences with the reverse *isoA* primer. Sequences 9-18 were from the *isoA* clone libraries. Sequence 8 was from *Rhodococcus* PD630 strain. Sequences 3-7 were retrieved from the draft genomes of the marine (*Gordonia* sp., *Mycobacterium* sp) and terrestrial (*Rhodococcus* AD45, *Rhodococcus* SC4, *Rhodococcus* LB1) isoprene-degrading isolates.

Rhodococcus sp. AD45 IsoA
Rhodococcus sp. LB1 IsoA
Rhodococcus sp. SC4 IsoA
Gordonia polyisoprenivorans i37 IsoA
Mycobacterium hodleri i29a2* IsoA
Rhodococcus opacus PD630 IsoA
Garden soil clone 1 IsoA
Garden soil clone 2 IsoA
Garden soil clone 3 IsoA
Garden soil clone 4 IsoA
Garden soil clone 5 IsoA
Oak soil clone 1 IsoA
Oak soil clone 2 IsoA
Oak soil clone 3 IsoA
Poplar soil clone 1 IsoA
Poplar soil clone 2 IsoA
Xanthobacter autotrophicus PY2 XamoA
Methylosinus trichosporium OB3b MmoX

```
PTLSILMEH--DPARAQKALDIAFWRSTRLFQTLTGPMADYYTPLDQR--KMSFKEFMLEWIVNHHHERILEDYGLKKPW  
PTLSILMEH--DPARAQKALDVAFWRSTRLFQTLTGPMADYYTPLDQR--KMSFKEFMLEWIVNHHHERILEDYGLKKPW  
PTLSILMEH--DPARAQKALDVAFWRSTRLFQTLTGPMADYYTPLDQR--KMSFKEFMLEWIVNHHHERILEDYGLKKPW  
PTLEVLMH--DPQRAQTALDVAFWRSTRLFQTLTGPMADYYTPLEQR--KMSFKEFMLEWIVNHHHERILNDYGLKKPW  
PTLAVLMEN--DPQRAQQALDVAFWRSTRLFQTLTGPMADYYTPLDQR--KMSFKEFMLEWIVNHHHERILQDYGLKKPW  
PTLSILMEH--DPARAQKALDVAFWRSTRLFQTLTGPMADYYTPLDQR--KMSFKEFMLEWIVNHHHERILEDYGLKKPW  
PTLSILMEH--DPARAQKALDIAFWRSTRLFQTLTGPMADYYTPLDQR--KMSFKEFMLEWIVNHHHERILEDYGLKKPW  
PTLSVLMH--DPARAQKALDIAFWRSTRLFQTLTGPMADYYTPLDQR--KMSYKEFMLEWIVNHHHERILEDYGLKKPW  
PTLSVLMH--DPARAQKALDIAFWRSTRLFQTLTGPMADYYTPLDQR--KMSFKEFML?WIVNHHHERILEDYGLKKPW  
PTLSILMEH--DPARAQKALDIAFWRSTRLFQTLTGPMADYYTPLDQR--KMSFKEFMLEWIVNHHHERILEDYGLKKPW  
PTLSILMEH--DPARAQKALDIAFWRSTRLFQTLTGPMADYYTPLDQR--KMSFKEFMLEWIVNHHHERILGDYGLKKPW  
PTLSILMEH--DPARAQKALDIAFWRSTRLFQTLTGPMADYYTPLDQR--KMSFKEFMLEWIVNHHHERILEDYGLKKPW  
PTLSILMEH--DPARAQKALDIAFWRSTRLFQTLTGPMADYYTPLDQR--KMSFKEFMLEWIVNHHHERILEDYGLKKPW  
PTLSILMEH--DPARAQKALDIAFWRSTRLFQTLTGPMADYYTPLDQR--KMSFKEFMLEWIVNHHHERILEDYGLKKPW  
PTLSILMEH--DPARAQKALDIAFWRSTRLFQTLTGPMADYYTPLDQR--KMSFKEFMLEWIVNHHHERILEDYGLKKPW  
PTLDVMMKH--DPKRAQQILDVAFWRSYRIFQAVTGVSMDDYYTPVAKR--QMSFKEFMLEWIVKHHHERILRDYGLQKQW  
QTIVVSIANDPASAKFLNTDLNNAFWTQQKYFTPVLGYLFEYGSKFKVEPWVKTWNRWVYEDWGGIWIWIRLQKGYGVESPA
```

330

Rhodococcus sp. AD45 IsoA
Rhodococcus sp. LB1 IsoA
Rhodococcus sp. SC4 IsoA
Gordonia polyisoprenivorans i37 IsoA
Mycobacterium hodleri i29a2* IsoA
Rhodococcus opacus PD630 IsoA
Garden soil clone 1 IsoA
Garden soil clone 2 IsoA
Garden soil clone 3 IsoA
Garden soil clone 4 IsoA
Garden soil clone 5 IsoA
Oak soil clone 1 IsoA
Oak soil clone 2 IsoA
Oak soil clone 3 IsoA
Poplar soil clone 1 IsoA
Poplar soil clone 2 IsoA
Xanthobacter autotrophicus PY2 XamoA
Methylosinus trichosporium OB3b MmoX

```
YWDQFMYSLEHGHHAMHLGTWFWRPTLFWKPNAGVSKDEREWLREKYPTWEENWGGMWDEIIKNVNTDQIEKTLPATFF  
YWDQFLYSLENGHHAMHLGTWFWRPTLFWKPNAGVSKDERDWLREKYPTWEENWGVMMWDEIIKNVNDRIEDTLPDTLP  
YWDQFLYSLENGHHAMHLGTWFWRPTLFWKPNAGVSKDERDWLREKYPTWEENWGVMMWDEIIKNVNDRIEDTLPDTLP  
YWDKFLLSLENGHHAMHIGTWFWRPTLFWKPNAGVSKDERAWLNEKYPTWEDNWGVMMWDEIIHNVNVDRIENTLPDTLP  
YWDQFMVSLENGHHAMHIGTWFWRPTLFWNPNAGVSKDERDWLREKYPTWEDNWGVWVWDEIIDNVNAGRVGMTMPETLP  
YWDQFLYSLENGHHAMHLGTWFWRPTLFWKPNAGVSKDERDWLREKYPTWEENWGVMMWDEIIKNVNDRIEDTLPDTLP  
YWDQFMYSLEHGHHAMHLGTWFWRPTLFWKPNAGVSKDEREWLREKYPTWEENWGGMWDEIIKNVNTDQIEKTLPATFF  
YWDQFMYSLENGHHAMHLGTWFWRPTLFWKPNAGVSKDEREWLREKYPTWEENWGGMWDEIFKNVNADQIENTLPATFF  
YWDQFMYSLENGHHAMHLGTWFWRPTLFWKPNAGVSKDEREWLREKYPTWEENWGGMWDEIIKNVNADQIENTLPATFF  
YWDQFMYSLEHGHHAMHLGTWFWRPTLFWKPNAGVSKDEREWLREKYPTWEENWGGMWDEIIKNVNTDQIEKTLPATFF  
YWDQFMYSLENGHHAMHLGTWFWRPTLFWKPNAGVSKDEREWLREKYPTWEENWGGMWDEIIKNVNADQIENTLPATFF  
YWDQFMYSLEHGHHAMHLGTWFWRPTLFWKPNAGVSKDEREWLREKYPTWEENWGGMWDEIIKNVNTDQIEKTLPATFF  
YWDQFMYSLEHGHHAMHLGTWFWRPTLFSWKNAGVSKDEREWLREKYPTWEENWGGMWDEIIKNVNTDQIEKTLPATFF  
YWDQFMYPLEHGHHAMHLGTWFWRPTLFWRPNAGVSKDEREWLREKYPTWEENWGGMWDEIIKNVNTDQIEKTLPATFF  
YWDQFMYSLEHGHHAMHLGTWFWRPTLFWKPNAGVSKDEREWLREKYPTWEENWGGMWDETIKNVNTDQIEKTLPATFF  
YWDTFEKTLDHGHHALHIGTWFWRPTLFWDPNGGVSREERRWLNQKYPNWEESWGVWVWDEIISNINAGNIEKTLPETLP  
SLRDAKRDAYWAHHDLALAAAYAMWPLGFAR-LALPDEEDQAWFEANYPGWADHYGKIFNEWKKLGVEDPKSGFIPYQWL
```

408

Figure 5.5 Partial alignment of deduced amino acid sequences of the α -subunit of the hydroxylases. Residues that are important for the catalytic function of the SDIMO enzymes (highlighted in blue) are conserved in the deduced IsoA sequences retrieved from the isoprene enriched soil samples. The numbers on the right correspond to the *Methylosinus trichosporium* OB3b residue number. Highlighted in red is the cysteine residue at position 151 in *Methylosinus trichosporium* OB3b soluble methane monooxygenase α -subunit which is replaced by an aspartate residue in alkene monooxygenases, including isoprene monooxygenase (Smith *et al.*, 2002).

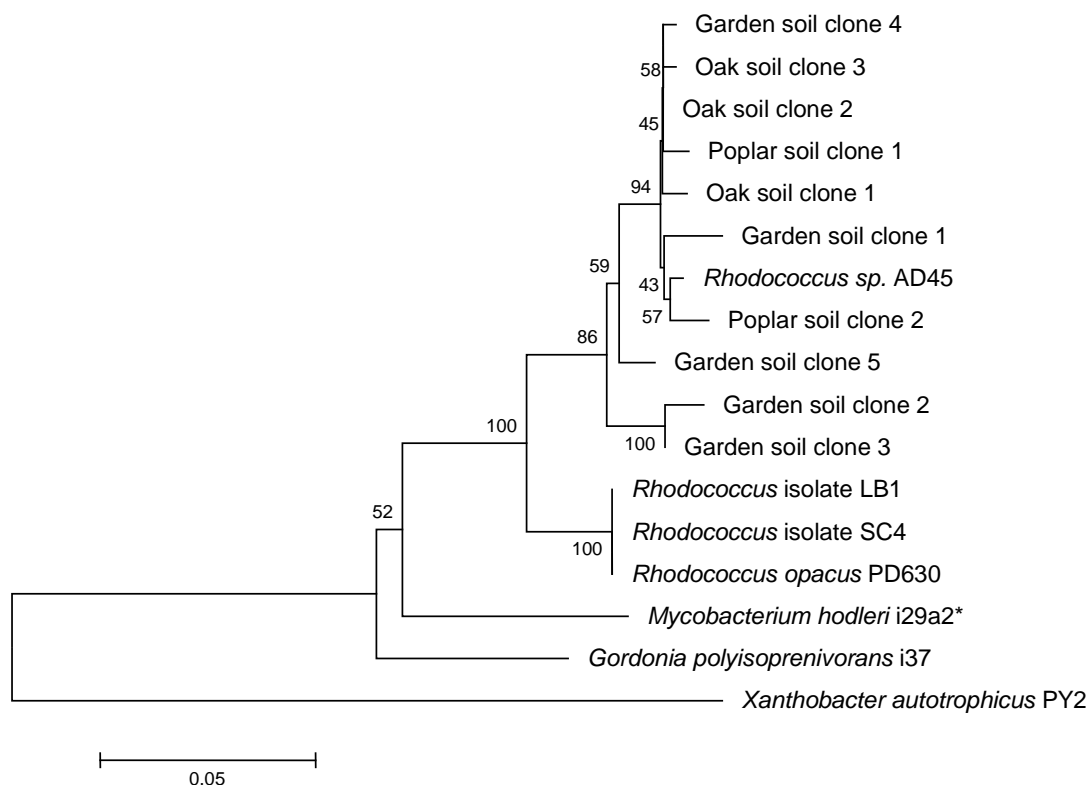


Figure 5.6 Neighbour-joining phylogenetic tree of deduced IsoA sequences (338 amino acids) from the oak, poplar and garden soil *isoA* clone libraries. XamoA from *Xanthobacter autotrophicus* PY2 (CAA09911.1) was used as the outgroup. Bootstrap values are shown (100 replicates).

(iii) Genomic DNA from pure cultures of non-isoprene degrading (*isoA*⁻) bacteria

In order to check that the primers were *isoA*-specific, they were tested with genomic DNA extracted from pure cultures of non-isoprene degrading *isoA*⁻ bacteria. The *isoA*⁻ bacteria were selected based on the fact that: (1) they are known hydrocarbon-oxidizing bacteria, (2) they do not grow on isoprene, (3) they contain a soluble diiron centre monooxygenase (Table 5.3). No *isoA* PCR product was obtained with the genomic DNA from any of these isolates, confirming the specificity of the *isoA* primers (Figure 5.7). The PCR product obtained with the genomic DNA template from *Rhodococcus jostii* RHA1 (Figure 5.7) was cloned into pGEMT-Easy vector and sequenced with the M13 primers. The sequence was analyzed and did not correspond to *isoA* gene, suggesting that a non-specific amplification had occurred with DNA from *Rhodococcus jostii* RHA1. To rule out the presence of PCR inhibitors and to check the quality of the genomic DNA extracted from these

cultures, 16S rRNA gene amplification was carried out using the universal primer set 27f/1492r (Lane *et al.*, 1991) and the genomic DNA extracted from the *isoA*⁻ bacteria as template DNA. A PCR product of the correct size (1,503 bp) was obtained for all the bacteria (Figure 5.8).

Table 5.3 List of the non-isoprene degrading *isoA*⁻ bacteria tested

Organism	Soluble diiron centre monooxygenase	Reference
<i>Methylococcus capsulatus</i> Bath	Methane monooxygenase	Stainthorpe <i>et al.</i> , 1990
<i>Methylocella silvestris</i> BL2	Methane monooxygenase Propane monooxygenase	Theisen <i>et al.</i> , 2005, Crombie & Murrell, 2014
<i>Mycobacterium sp.</i> NBB4	4 different SDIMOs (propene, ethane, propane, butane)	Coleman <i>et al.</i> , 2011
<i>Pseudomonas putida</i> ML2 *	Benzene dioxygenase	Tan <i>et al.</i> , 1993
<i>Rhodococcus aetherivorans</i> I24 *	Toluene dioxygenase	Priefert <i>et al.</i> , 2004
<i>Rhodococcus jostii</i> RHA1	Propane monooxygenase	Sharp <i>et al.</i> , 2007
<i>Rhodococcus opacus</i> DSM1069	Propane monooxygenase	Trojanowski <i>et al.</i> , 1977
<i>Rhodococcus rhodochrous</i> B276	Alkene monooxygenase	Saeki & Furuhashi, 1994
<i>Rhodococcus rhodochrous</i> PNKb1	Propane monooxygenase	Woods & Murrell, 1989

* These strains are aromatic hydrocarbon-degrading bacteria but contain a dioxygenase enzyme system and not a soluble diiron centre monooxygenase.

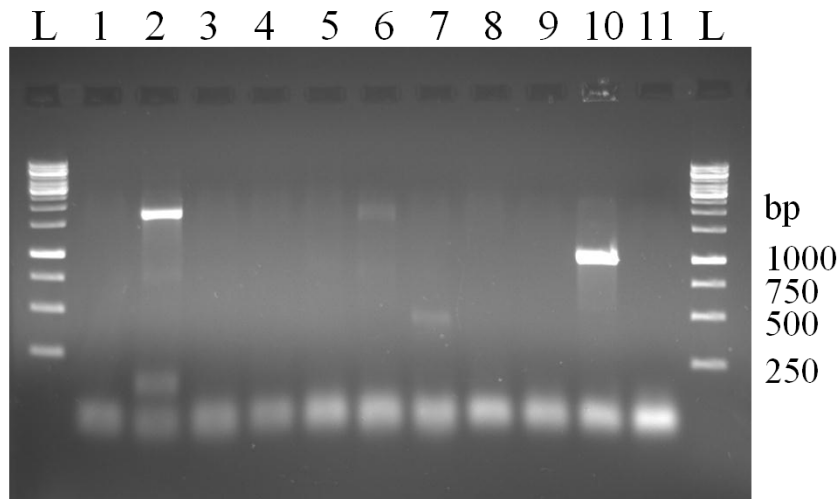


Figure 5.7 The designed primers are specific for the *isoA* gene. The *isoA* primers were tested by PCR with genomic DNA from: Lane 1: *Rhodococcus rhodochrous* PNKb1, lane 2: *Rhodococcus jostii* RHA1, lane 3: *Rhodococcus opacus* DSM1069, lane 4: *Rhodococcus aetherivorans* I24, lane 5: *Rhodococcus rhodochrous* B276, lane 6: *Methylococcus capsulatus* Bath, lane 7: *Methylocella silvestris* BL2, lane 8: *Pseudomonas putida* ML2, lane 9: *Mycobacterium sp.* NBB4. Lane 10: Positive control, Genomic DNA from *Rhodococcus* AD45, lane 11: No template negative control. L: 1 kb DNA ladder (Fermentas)

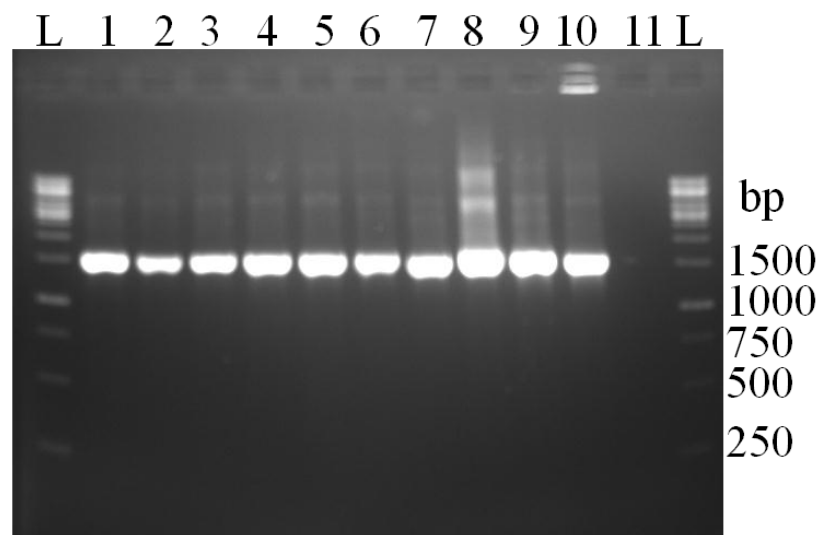


Figure 5.8 No PCR inhibitors in the genomic DNA from *isoA*⁻ bacteria. PCR amplification of 16S rRNA gene from DNA of: lane 1: *Rhodococcus rhodochrous* PNKb1, lane 2: *Rhodococcus jostii* RHA1, lane 3: *Rhodococcus opacus* DSM1069, lane 4: *Rhodococcus aetherivorans* I24, lane 5: *Rhodococcus rhodochrous* B276, lane 6: *Methylococcus capsulatus* Bath, lane 7: *Methylocella silvestris* BL2, lane 8: *Pseudomonas putida* ML2, lane 9: *Mycobacterium sp.* NBB4. Lane 10: *Rhodococcus* AD45, lane 11: No template negative control. L: 1 kb DNA ladder (Fermentas).

5.5 Discussion

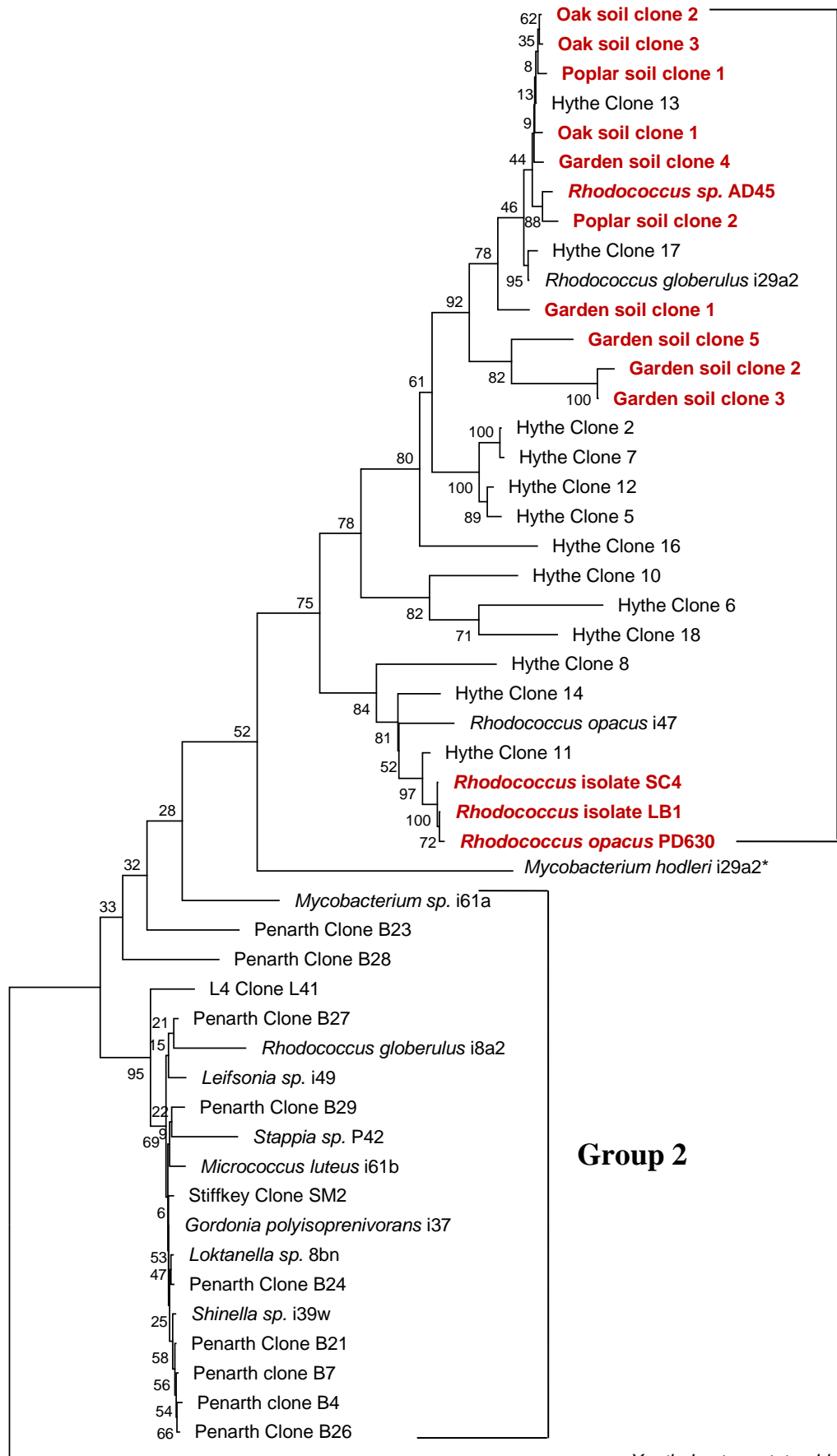
Primers targeting the *isoA* gene coding for the alpha subunit of isoprene monooxygenase were designed, tested and validated. An optimized protocol for the amplification of *isoA* from DNA from pure isolates or environmental samples was also developed. *isoA* genes were detected by PCR with DNA from three different soil samples, suggesting that isoprene degraders might be widespread in the terrestrial environment. This PCR-based approach can be applied to a variety of terrestrial environments in the future to quickly define the biogeography of the isoprene-utilizing bacteria. All *isoA* clones showed high sequence identity (91% - 99%) to the *isoA* sequence from *Rhodococcus* AD45. One possibility is that the incubation conditions that were used to set up the enrichment cultures favoured the growth of *Rhodococcus* species. In order to check that the designed *isoA* primers were not selectively biased to *Rhodococcus* isoprene-degrading strains, the primers were tested using genomic DNA from marine isoprene degraders, belonging to different taxonomic groups (Table 5.4). This work was carried out by Antonia Johnston and an *isoA* PCR product of the correct size was obtained with all the isolates. The *isoA* PCR products were cloned, sequenced, and analyzed as previously described. Based on the analysis, we confirmed that the primers designed in this study detected *isoA* in a diverse range of isoprene degraders.

Table 5.4 Marine isoprene-degrading bacteria used in the validation of *isoA* primers (done by Antonia Johnston).

Strains	Source / Reference
<i>Alphaproteobacteria</i>	
1 <i>Loktanella</i> sp. 8bn	Dr Terry McGenity
2 <i>Stappia</i> sp. P42	A. Johnston, unpublished data
<i>Gammaproteobacteria</i>	
3 <i>Shinella</i> sp. i39w	Alvarez <i>et al.</i> , 2009
<i>Actinobacteria</i>	
4 <i>Leifsonia</i> sp. i49	Dr Terry McGenity
5 <i>Micrococcus luteus</i> i61b	Dr Terry McGenity
6 <i>Rhodococcus opacus</i> i47	Dr Terry McGenity
7 <i>Rhodococcus globerulus</i> i8a2	Dr Terry McGenity
8 <i>Rhodococcus globerulus</i> i29a2	Dr Terry McGenity
9 <i>Mycobacterium</i> sp. i61a	Dr Terry McGenity

isoA primers were also tested by Antonia Johnston with DNA purified from isoprene enriched water samples, including coastal water collected from Penarth (Wales), marine water collected from two different locations: Plymouth Station L4 and Stiffkey salt marsh (Norfolk), and estuarine water sampled from the freshwater end of the Colne estuary (the Hythe, Essex). The *isoA* genes retrieved from the terrestrial and marine isolates and enrichments collectively generated an extensive *isoA* database that was analysed to define the diversity and distribution of isoprene degraders. The deduced IsoA amino acid sequences clustered into 2 main groups (Figure 5.9). Group 1 encompasses sequences closely related to IsoA of *Rhodococcus* AD45, Group 2 encompasses sequences with greatest similarity to IsoA of *Gordonia polyisoprenivorans* i37 which shares 86 % sequence identity to the IsoA sequence of *Rhodococcus* AD45. No sequences from our database were closely affiliated with IsoA of *Mycobacterium hodleri* i29a2* which shares 83 % sequence identity to IsoA of *Rhodococcus* AD45. All the terrestrial clones clustered together in group 1. Interestingly, IsoA sequences from the Hythe clone library were

more similar to the terrestrial IsoA sequences than the remaining marine sequences. This might be due to the low salinity of the water in the estuary compared to the other seawater samples or due to terrestrial bacteria being effectively washed into the estuary especially that the site chosen for sampling in the Colne estuary was close to the land. In conclusion, it is important to note that while detecting *isoA* genes in a given environmental sample indicates the presence of isoprene-degrading bacteria in this environment, it does not however determine if these bacteria are actively metabolizing isoprene. For this reason, the *isoA* PCR approach developed in this chapter should be complemented by stable isotope probing experiments which will be further exploited in the next chapter.



Xanthobacter autotrophicus PY2 (CAA09911.1)

0.05

Figure 5.9 Neighbour-joining phylogenetic tree of deduced IsoA sequences (338 amino acids) from terrestrial and marine isolates and clone libraries. Shown in red are sequences from terrestrial clones. XamoA from *Xanthobacter autotrophicus* PY2 was used as the outgroup. Bootstrap values are shown (100 replicates).

Chapter 6

Identification of active bacterial isoprene degraders in environmental soil samples

6.1 Introduction

DNA-Stable Isotope Probing (DNA-SIP) has revolutionized the field of molecular microbial ecology. Initially introduced by Radajewski *et al.*, in 2000, DNA-SIP has since been widely used in microbial studies aimed at attributing a specific metabolic activity to a taxonomically diverse group of bacteria. The Stable Isotope Probing technique is not limited to using DNA molecules as targeted cellular biomarkers. Phospholipid fatty acids (PLFAs) (Boschker *et al.*, 1998), proteins (Jehmlich *et al.*, 2008a, 2008b), rRNA (Manefield *et al.*, 2002), and mRNA (Huang *et al.*, 2009) are also suitable biomarkers for SIP experiments as they successfully incorporate the stable isotopes and can be used in downstream analyses. Environmental samples or mixed bacterial cultures are incubated with the substrate of interest which is usually labelled with either ^{13}C or ^{15}N (Uhlik *et al.*, 2013, Murrell & Whiteley, 2011), depending on whether the substrate is used as a carbon or nitrogen source. The ^{13}C and ^{15}N labels will be retrieved exclusively in the cellular material of bacteria that were capable of metabolizing the labelled substrate. Active substrate utilisers are therefore identified without the need for cultivation. A well recognized example of the successful application of the DNA-SIP technique is the characterization of the diversity and identity of methylotrophic bacteria. Several research groups have employed this powerful tool to investigate the composition of methylotrophic populations involved in methane, methanol or methylamine metabolism in diverse environments, including peat soil and caves (Morris *et al.*, 2002, Hutchens *et al.*, 2004, Nercessian *et al.*, 2005, Dumont *et al.*, 2006, Cébron *et al.*, 2007, Chen *et al.*, 2008, Neufeld *et al.*, 2008).

This chapter aims to identify active isoprene degraders in soil samples. While this information is already available for marine environmental samples, including sediments and water, no study investigating active terrestrial isoprene-degrading populations has been reported to date.

6.2 DNA-SIP experiments with partially labelled ^{13}C -isoprene

6.2.1 Experimental set-up

The partially labelled ^{13}C -isoprene (2 out of 5 carbons were labelled) was a kind gift from DuPont Industrial Biosciences (California, USA) (Dr Gregg Whited *et al.*). The microcosms for the SIP experiments were set up in 2 L sterile Quickfit flasks. 5 g of wet soil collected from the garden of a house in Leamington Spa (UK) were placed into the flasks without any added nutrient supplements. The soil was acidic with a pH of 6.0. Either ^{12}C -isoprene or partially labelled ^{13}C -isoprene was added to the samples as specified in Figure 6.1. Controls with 5 g of autoclaved soil were also set up to link the depletion of isoprene in the rest of the samples to biological activity and rule out leakage of isoprene from flasks. The sealed flasks were incubated at 30°C without shaking for 2 weeks (T_1) for samples 3, 5, 6 and for 18 days (T_2) for samples 4, 7, and 8. $8\mu\text{l}$ of isoprene was initially added to all samples, setting the initial concentration of isoprene to 1000 ppmv. Upon depletion of isoprene in the samples, as determined by GC measurements of the headspace concentration, the microcosms were re-spiked with another $8\mu\text{l}$ of isoprene. In total, microcosms sacrificed at T_1 were spiked three times with $8\mu\text{l}$ isoprene and had consumed $48\mu\text{mol}$ of isoprene / 1 g of soil, whereas samples sacrificed at T_2 were spiked four times with $8\mu\text{l}$ isoprene and had consumed $64\mu\text{mol}$ of isoprene / 1 g of soil.

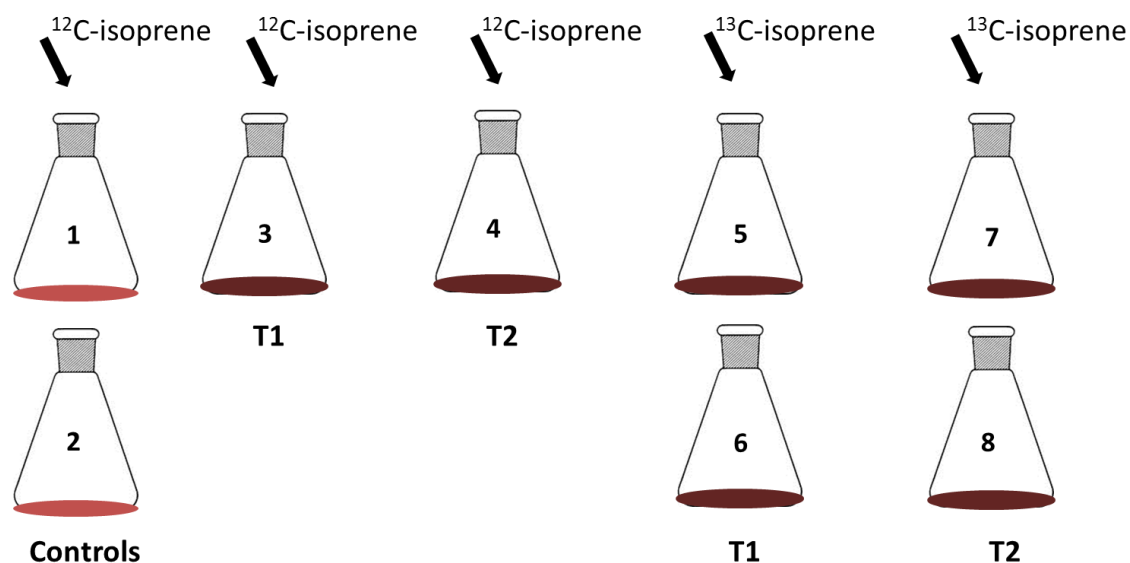


Figure 6.1 Experimental set up of the SIP incubations. The SIP experiment consisted of three samples for each time point (T_1 and T_2), including one sample incubated with ^{12}C -isoprene and duplicate samples incubated with partially labelled ^{13}C -isoprene. Control flasks 1 and 2 contained autoclaved soil.

6.2.2 DNA extraction from soil, density gradient ultracentrifugation and fractionation

Total DNA was extracted from the soil samples using the FastDNA spin kit for soil (MP Biomedicals), as described in the Materials and Methods section 2.5.1. 1 µg of extracted DNA was subjected to density gradient ultracentrifugation followed by fractionation according to Neufeld *et al.*, (2007) in order to separate the ¹³C-labelled DNA contained in the heavy fractions from unlabelled DNA contained in the light fractions. The formation of a correct density gradient was verified using a Reichart AR200 digital refractometer (Figure 6.2).

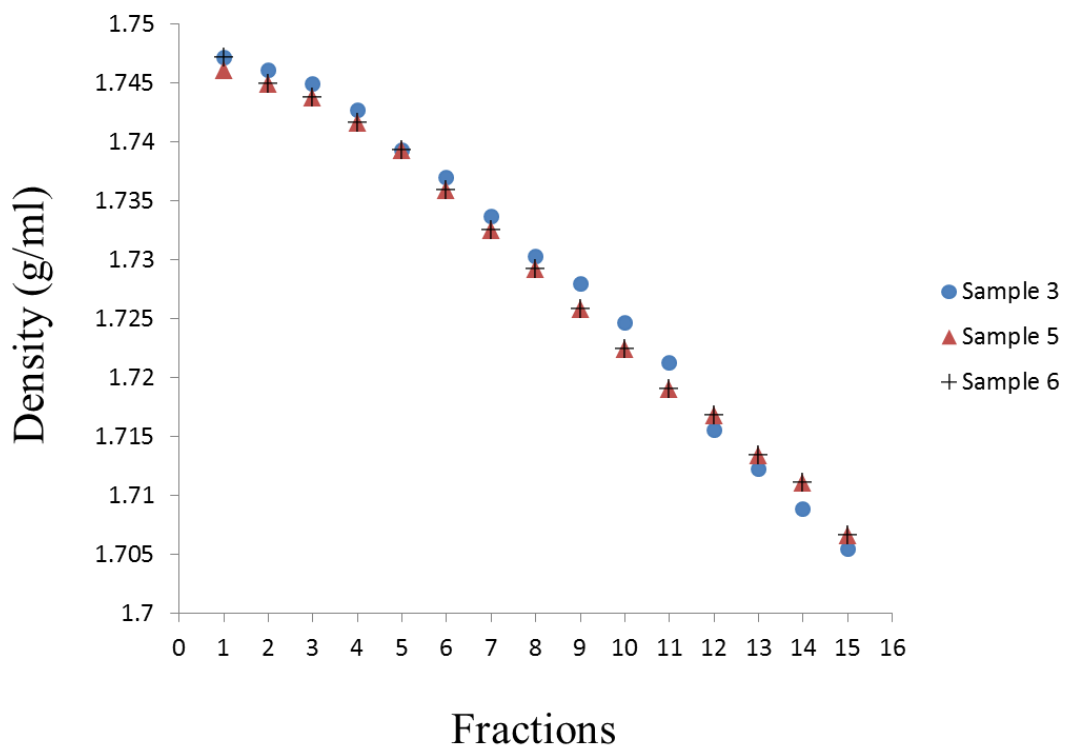


Figure 6.2 Density gradients of CsCl measured from each fraction of T₁ samples 3, 5 and 6.

6.2.3 Analysis of the bacterial community profile by 16S rRNA gene profiling using Denaturing Gradient Gel Electrophoresis (DGGE)

DNA from SIP experiments was then precipitated from each fraction (Materials and Methods section 2.15) and used as a template in PCR amplification reactions

targeting 16S rRNA genes using primers 341F-GC (Muyzer *et al.*, 1993) and 907R (Lane 1991) (Table 6.1).

Table 6.1 Primers used for the amplification of 16S rRNA genes from the fractionated samples

Primer name	5'-3' sequence
341F-GC	CGCCCGCCGCGCGCGGGCGGGGCGGGGGCACGGGGG GCCTACGGGAGGCAGCAG
907R	CCGTCAATTCMTTTRAGTTT

The PCR products were then run on an 8% polyacrylamide denaturing gel, 30% - 70% denaturant concentrations, for 16 h at 80 V using the DCode™ Universal Mutation Detection System (Bio-Rad).

(i) DGGE analysis of T₁ samples

DGGE analysis of sample 5 (¹³C-isoprene) showed at least two dominant bands appearing only in the heavy DNA fractions 8 (density 1.729) and 9 (density 1.7258) (Figure 6.3). These bands correspond to the 16S rRNA genes of bacteria capable of metabolizing isoprene, thus incorporating ¹³C into their DNA molecules. As expected, the duplicate sample 6 (¹³C-isoprene) showed the same DGGE profile to that of sample 5 (data not shown). Sample 3 incubated with unlabelled ¹²C-isoprene showed no difference in the bacterial community profile across the fractions with most of the DNA retrieved in the light fractions (Figure 6.4). The shift in microbial community profiles between heavy and light DNA in microcosms 5 and 6, as analyzed by DGGE, suggests that ¹³C-isoprene was successfully assimilated by isoprene utilizing bacteria.

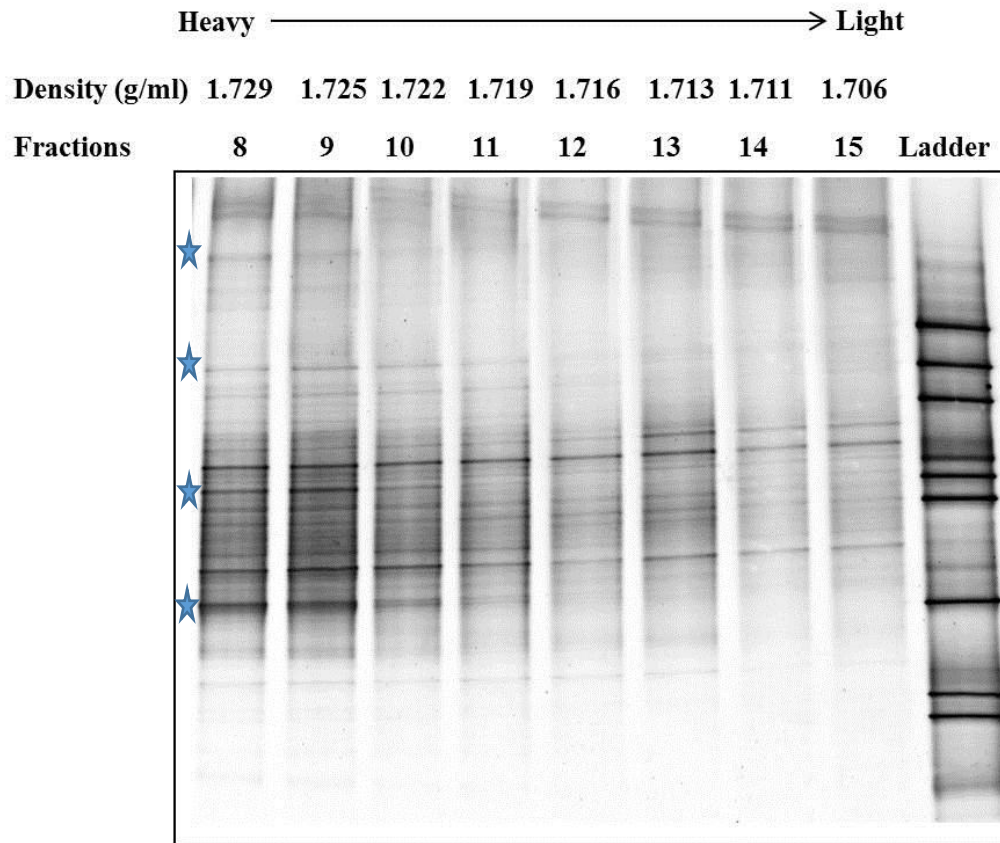


Figure 6.3 DGGE analysis of 16S rRNA genes in fractions 8 to 15 from microcosm 5 incubated with ^{13}C -isoprene.

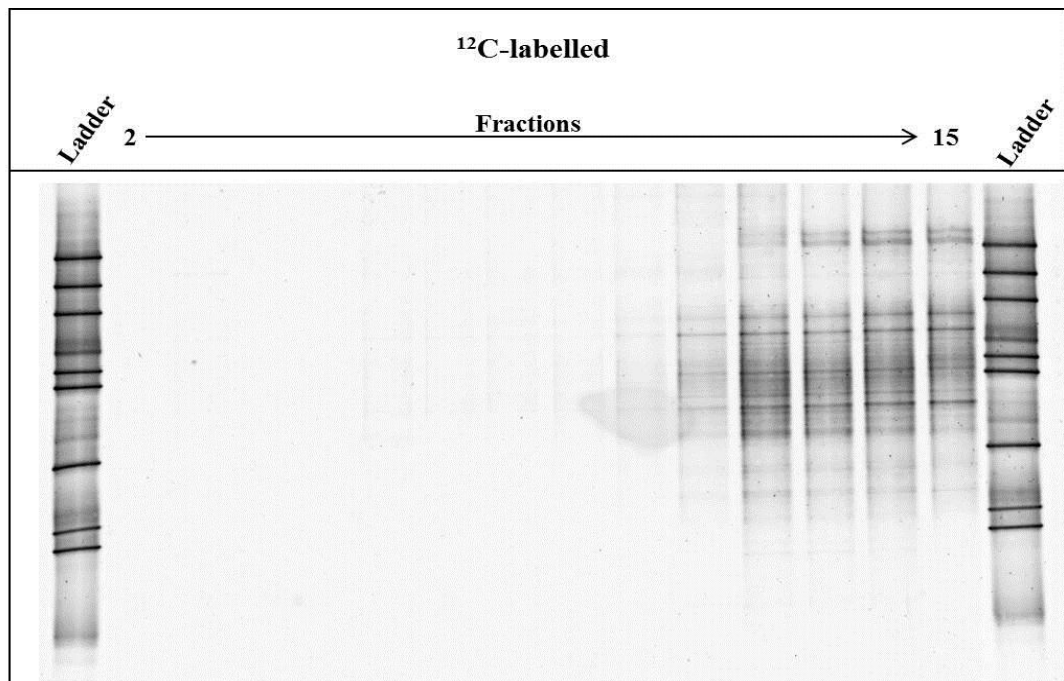


Figure 6.4 DGGE analysis of 16S rRNA genes in fractions 2 to 15 from microcosm 3 incubated with ^{12}C -isoprene. The arrow indicating the density going from heavy (left) to light (right).

(ii) DGGE analysis of T₂ samples.

Samples 4, 7 and 8 were processed using the same approach as described above.

There was no difference in the bacterial community profiles of the ¹³C-microcosms at T₁ and T₂, as revealed by the DGGE analysis (Figure 6.5). For this reason, samples 4, 7, 8 were not further analysed.

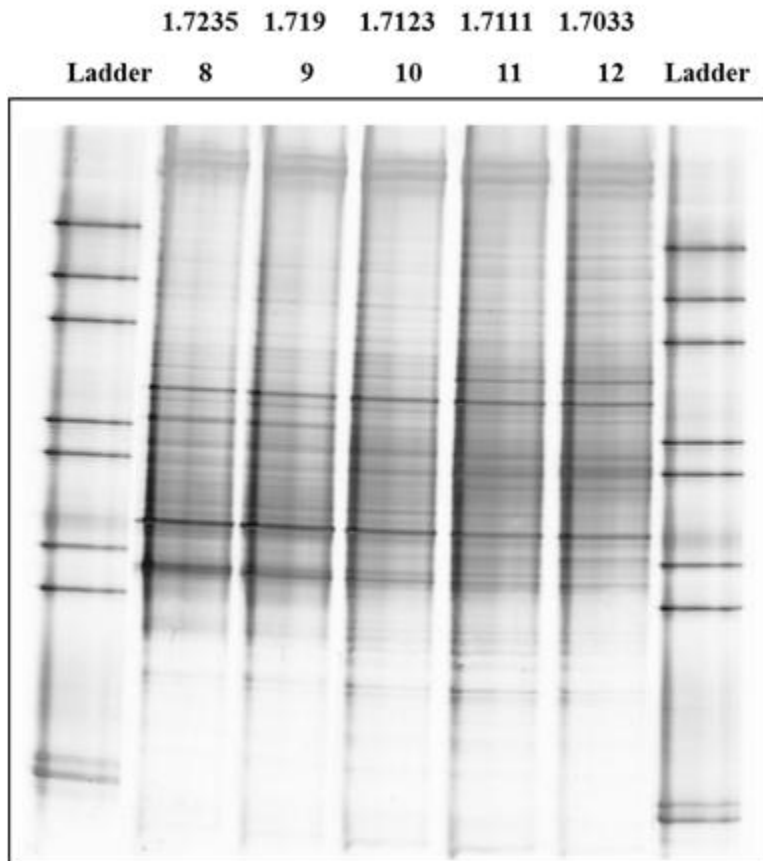


Figure 6.5 DGGE analysis of 16S rRNA genes in fractions 8 to 12 from microcosm 8 (T₂) incubated with ¹³C-isoprene. The top numbers refer to the density (g.ml⁻¹) and the bottom numbers refer to the fraction number.

6.2.4 Identification of active isoprene degraders by 454 16S rRNA amplicon sequencing

16S rRNA genes were amplified from ‘heavy’ (fraction 9) and ‘light’ (fraction 14) DNA from the ¹³C-isoprene enrichment samples 5 and 6 using the primer set 27Fmod/519R modbio (Table 6.2). The amplicon was then purified and sent for 454 pyrosequencing at MrDNA (Texas, USA).

Table 6.2 Primers used for 454 16S rRNA amplicon sequencing

Primer name	5' - 3' sequence
27Fmod	AGRGTTTGATCMTGGCTCAG
519Rmodbio	GTNTTACNGCGGCKGCTG

Data were processed using Qiime pipeline provided by Bio-Linux. The sequences were quality checked prior to any further analysis. Only sequences with read length between 200 and 1000 bp, an average base quality score above 25, and zero mismatch in primer, were considered in the analysis. The number of 16S rRNA gene sequences that passed quality control was 3,996 from the heavy DNA of sample 5; 11,992 from light DNA of sample 5; 4,563 from heavy DNA of sample 6; and 3,714 from light DNA of sample 6.

As expected, the microbial communities of the duplicate ^{13}C -isoprene enrichment samples 5 and 6 showed similar profiles (Figure 6.6). *Proteobacteria* dominated the enrichment cultures, accounting for ~ 50% of the 16S rRNA gene sequences from the heavy fractions (Table 6.3). *Actinobacteria*, *Bacteroidetes* and *Firmicutes* were also detected in the heavy fractions of both samples, showing an increase in their relative abundance compared to the light fraction. This suggests that bacteria belonging to these phyla are active within the community. The bacterial population that incorporated the ^{13}C label also included TM7 bacteria (Hugenholtz *et al.*, 2001) which represented more than 1% of the community (Table 6.3).

In the context of *Proteobacteria*, *Rhizobiales* order was by far the most represented within the isoprene-degrading community, accounting on average for 26% of the sequences (Table 6.4). 16S rRNA gene sequences from the heavy fraction of the ^{13}C -isoprene incubations also included other *Proteobacteria* representatives such as *Caulobacterales*, *Burkholderiales*, and *Sphingomonadales* (Table 6.4). Phylotypes affiliated with the genera *Phenylobacterium* (*Caulobacterales*), *Hyphomicrobium* (*Rhizobiales*) and *Brevundimonas* (*Caulobacterales*) were identified in the heavy fractions.

The number of 16S rRNA gene sequences which affiliated with *Actinomycetales* (*Actinobacteria*) in the heavy fractions represented 23% of the total sequences (Table 6.4). This implies that a large population of bacteria belonging to this group have incorporated the ^{13}C label into their genomes. The *Actinomycetales* population was mainly composed of members from the *Nocardiaceae*, *Mycobacteriaceae* and *Nocardioideaceae* families. At the genus level, *Rhodococcus* phylotypes were identified, accounting for 7% of the sequences from the heavy fraction compared to 4% of those from the light fraction (Table 6.4). *Bacteroidetes* bacteria that were labelled with ^{13}C belonged mostly to the *Chitinophagaceae* family of the *Sphingobacteriales* order.

Table 6.3 Bacterial composition of the light fraction (^{12}C -DNA) and heavy fraction (^{13}C -DNA) of the ^{13}C -isoprene enriched microcosms, at the phylum level. The numbers represent the relative abundance (%) of the corresponding phylum within the community. Only phyla representing > 0.5% of the community in any of the four samples are shown. Other: includes unclassified bacteria as well as phyla representing less than 0.5% of the community.

Phylum	Sample 5 ^{12}C -DNA	Sample 5 ^{13}C -DNA	Sample 6 ^{12}C -DNA	Sample 6 ^{13}C -DNA
<i>Acidobacteria</i>	1.21	0.95	2.42	1.34
<i>Actinobacteria</i>	16.27	26.45	17.69	26.45
<i>Armatimonadetes</i>	0.23	0.30	0.38	0.64
<i>Bacteroidetes</i>	0.78	3.60	1.00	9.18
<i>Firmicutes</i>	0.43	2.33	0.46	1.31
<i>Planctomycetes</i>	1.16	0.73	1.05	0.53
<i>Proteobacteria</i>	65.51	52.80	61.20	45.96
TM7	1.13	1.15	1.18	3.94
<i>Verrucomicrobia</i>	0.13	0.15	0.75	0.24
<i>Deinococcus-Thermus</i>	–	–	0.59	–
Other	13.16	11.54	13.27	10.41
Total	100	100	100	100

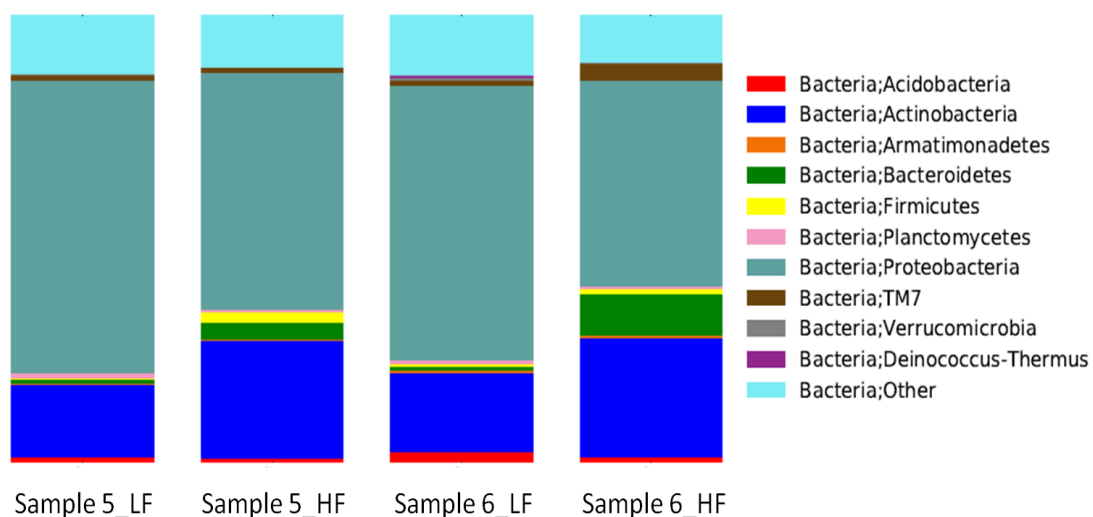


Figure 6.6 Bar graphs displaying the bacterial community composition at the phylum level of the light fraction (LF, ^{12}C -DNA) and heavy fraction (HF, ^{13}C -DNA) of the ^{13}C -isoprene incubations. Only phyla representing $> 0.5\%$ of the community in any of the four samples are shown.

Table 6.4 Bacterial composition of the isoprene-enriched microcosms at the order, family or genus level. The numbers represent the relative abundance (%) of the corresponding taxonomic group within the community. Only groups representing > 0.5% of the community in any of the four samples, are shown. Other: includes unclassified bacteria as well as taxonomic groups representing less than 0.5% of the community.

Taxon	Sample 5 ¹² C-DNA	Sample 5 ¹³ C-DNA	Sample 6 ¹² C-DNA	Sample 6 ¹³ C-DNA
ORDER				
<i>Actinobacteria; Actinobacteria; Acidimicrobiales</i>	0.58	0.48	0.40	0.46
<i>Actinobacteria; Actinobacteria; Actinomycetales</i>	11.75	23.12	14.81	23.30
<i>Actinobacteria; Actinobacteria; Solirubrobacterales</i>	2.72	1.65	1.32	1.78
<i>Proteobacteria; Alphaproteobacteria; Caulobacterales</i>	1.52	3.48	2.21	2.54
<i>Proteobacteria; Alphaproteobacteria; Rhizobiales</i>	39.50	29.15	37.51	23.89
<i>Proteobacteria; Alphaproteobacteria; Sphingomonadales</i>	1.36	1.00	1.48	1.80
<i>Proteobacteria; Alphaproteobacteria; Rhodobacterales</i>	0.04	0.03	0.11	1.47
<i>Proteobacteria; Alphaproteobacteria; Rhodospirillales</i>	1.54	0.50	1.59	0.88
<i>Proteobacteria; Betaproteobacteria; Burkholderiales</i>	1.55	1.55	1.32	1.40
<i>Proteobacteria; Deltaproteobacteria; Myxococcales</i>	0.55	1.03	0.94	0.68
<i>Proteobacteria; Gammaproteobacteria; Xanthomonadales</i>	0.75	0.40	0.92	0.96
<i>Firmicutes; Bacilli; Bacillales</i>	0.37	0.65	0.43	1.14
<i>Firmicutes; Clostridia; Clostridiales</i>	0.04	1.28	0.00	0.02
<i>Bacteroidetes; Sphingobacteria; Sphingobacteriales</i>	0.61	2.08	0.73	6.88
<i>Planctomycetes; Planctomycetacia; Planctomycetales</i>	1.13	0.73	1.05	0.53
<i>Deinococcus-Thermus; Deinococci; Deinococcales</i>			0.59	
Other	36	32.88	34.6	32.28

FAMILY				
<i>Actinobacteria; Actinobacteria; Actinomycetales; Geodermatophilaceae</i>	0.35	0.58	0.22	0.20
<i>Actinobacteria; Actinobacteria; Actinomycetales; Microbacteriaceae</i>	0.54	0.63	1.05	0.35
<i>Actinobacteria; Actinobacteria; Actinomycetales; Mycobacteriaceae</i>	0.18	0.73	0.43	1.49
<i>Actinobacteria; Actinobacteria; Actinomycetales; Nocardiaceae</i>	3.57	7.86	4.42	7.25
<i>Actinobacteria; Actinobacteria; Actinomycetales; Nocardiodaceae</i>	1.38	1.80	1.21	2.54
<i>Actinobacteria; Actinobacteria; Actinomycetales; Pseudonocardiaceae</i>	0.48	0.05	1.05	0.46
<i>Actinobacteria; Actinobacteria; Solirubrobacterales; Solirubrobacteraceae</i>	0.52	0.38	0.24	0.20
<i>Proteobacteria; Alphaproteobacteria; Caulobacterales; Caulobacteraceae</i>	1.49	3.40	2.21	2.54
<i>Proteobacteria; Alphaproteobacteria; Rhizobiales; Bradyrhizobiaceae</i>	3.08	3.23	1.97	1.29
<i>Proteobacteria; Alphaproteobacteria; Rhizobiales; Hyphomicrobiaceae</i>	4.47	3.13	6.17	3.79
<i>Proteobacteria; Alphaproteobacteria; Rhizobiales; Phyllobacteriaceae</i>	1.71	1.25	0.65	1.67
<i>Proteobacteria; Alphaproteobacteria; Rhizobiales; Xanthobacteraceae</i>	0.43	0.65	0.08	0.33
<i>Proteobacteria; Alphaproteobacteria; Rhodobacterales; Rhodobacteraceae</i>	0.04	0.03	0.11	1.47
<i>Proteobacteria; Alphaproteobacteria; Rhodospirillales; Rhodospirillaceae</i>	1.16	0.38	1.40	0.66
<i>Proteobacteria; Alphaproteobacteria; Sphingomonadales; Sphingomonadaceae</i>	1.08	0.73	0.65	1.23
<i>Proteobacteria; Gammaproteobacteria; Pseudomonadales; Pseudomonadaceae</i>	0.11	0.13	0.08	0.85
<i>Proteobacteria; Gammaproteobacteria; Xanthomonadales; Xanthomonadaceae</i>	0.71	0.35	0.89	0.96
<i>Bacteroidetes; Sphingobacteria; Sphingobacteriales; Chitinophagaceae</i>	0.53	1.85	0.30	6.51
<i>Firmicutes; Clostridia; Clostridiales; Peptostreptococcaceae</i>	0.02	0.60		
<i>Planctomycetes; Planctomycetacia; Planctomycetales; Planctomycetaceae</i>	1.13	0.73	1.05	0.53
<i>Deinococcus-Thermus; Deinococci; Deinococcales; Deinococcaceae</i>			0.59	
Other	77.06	71.55	75.26	65.68
GENUS				
<i>Actinobacteria; Actinobacteria; Actinomycetales; Mycobacteriaceae; Mycobacterium</i>	0.18	0.73	0.43	1.49

<i>Actinobacteria; Actinobacteria; Actinomycetales; Nocardiaceae; Rhodococcus</i>	3.31	7.18	4.12	6.68
<i>Actinobacteria; Actinobacteria; Actinomycetales; Nocardioideae; Nocardioides</i>	0.41	0.63	0.19	0.90
<i>Actinobacteria; Actinobacteria; Solirubrobacterales; Solirubrobacteraceae; Solirubrobacter</i>	0.52	0.38		
<i>Actinobacteria; Actinobacteria; Actinomycetales; Nocardioideae; Aeromicrobium</i>			0.67	0.09
<i>Actinobacteria; Actinobacteria; Actinomycetales; Nocardioideae; Marmoricola</i>			0.19	1.07
<i>Actinobacteria; Actinobacteria; Actinomycetales; Pseudonocardiaceae; Pseudonocardia</i>			1.02	0.44
<i>Proteobacteria; Alphaproteobacteria; Caulobacterales; Caulobacteraceae; Brevundimonas</i>	0.73	0.73	1.10	0.92
<i>Proteobacteria; Alphaproteobacteria; Caulobacterales; Caulobacteraceae; Phenylobacterium</i>	0.38	2.15	0.51	1.01
<i>Proteobacteria; Alphaproteobacteria; Rhizobiales; Hyphomicrobiaceae; Hyphomicrobium</i>	1.16	0.95	1.53	0.85
<i>Proteobacteria; Alphaproteobacteria; Rhizobiales; Hyphomicrobiaceae; Pedomicrobium</i>	1.46	1.15	0.57	0.11
<i>Proteobacteria; Alphaproteobacteria; Rhizobiales; Xanthobacteraceae; Pseudolabrys</i>	0.43	0.65		
<i>Proteobacteria; Alphaproteobacteria; Rhizobiales; Hyphomicrobiaceae; Devosia</i>			0.97	1.51
<i>Proteobacteria; Gammaproteobacteria; Pseudomonadales; Pseudomonadaceae; Pseudomonas</i>			0.05	0.81
<i>Bacteroidetes; Bacteroidetes" _incertae_sedis; Ohtaekwangia; Ohtaekwangia; Ohtaekwangia</i>			0.13	0.79
<i>Bacteroidetes; Sphingobacteria; Sphingobacteriales; Chitinophagaceae; Terrimonas</i>				1.07
<i>Deinococcus-Thermus; Deinococci; Deinococcales; Deinococcaceae; Deinococcus</i>			0.59	
Other	91.43	85.46	87.91	82.25

6.2.5 Analysis of *isoA* amplicon sequences

‘Heavy’ DNA from fraction 9 of sample 5 and ‘Heavy’ DNA from fraction 9 of sample 6 were pooled then used as template in the amplification reactions of the *isoA* gene. An amplicon of the correct size (1,015 bp) was obtained, purified and sent for 454 sequencing. Only 45 *isoA* sequences passed the quality control and were greater than 200 bp in length with an average quality score above 25. These sequences grouped into seven different Operational Taxonomic Units (OTUs) with the cut-off value set to 97% sequence similarity. Representative sequences from each OTU were aligned using MEGA6. The Neighbour-joining phylogenetic tree based on the representative deduced IsoA amino acid sequences of the different OTUs revealed that 96% of the sequences (43 out of 45 total sequences) were affiliated to IsoA of *Rhodococcus* AD45 (> 91% amino acid sequence identity) (Figure 6.7).

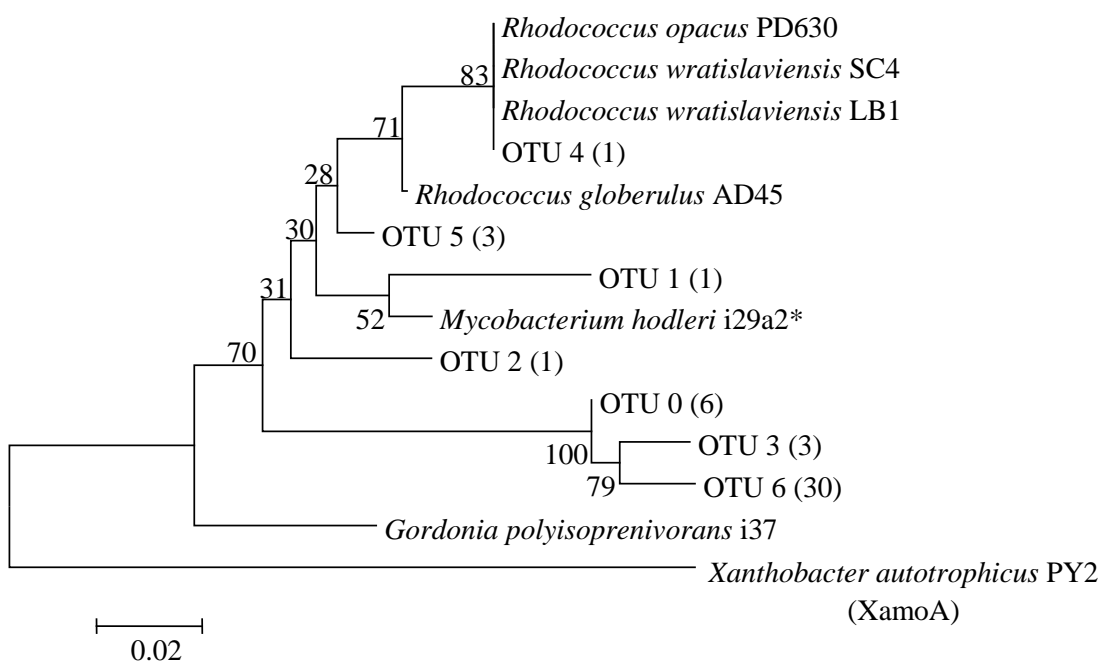


Figure 6.7 Neighbour-joining phylogenetic tree of deduced IsoA sequences (111 amino acids) from the 454 pyrosequencing of *isoA* amplicons from the ‘heavy DNA’ of the ^{13}C -isoprene SIP incubations. The number in bracket represents the number of sequences assigned to the respective OTU. XamoA from *Xanthobacter autotrophicus* PY2 (Zhou *et al.*, 1999), was used as the outgroup. Bootstrap values are shown (100 replicates).

6.3 DNA-SIP experiments with fully labelled ^{13}C -isoprene

6.3.1 Experimental set-up

The fully labelled ^{13}C -isoprene was a kind gift from DuPont Industrial Biosciences (California, USA). Another SIP experiment was set up in 120 ml sterile serum vials. The vials contained 5 g of soil collected on the 31st of May, 2013 from the path to John Innes Center (Norwich, UK) from a 10 cm depth. The sampling site was covered with wild grasses and willow trees. The pH of the soil sample were estimated to be 7.4. Isoprene was added to the samples as liquid in a volume of 2.5 μl , setting the initial headspace concentration of isoprene to 0.5% (v/v). Samples 1, 2 and 3 were incubated with ^{13}C -isoprene whereas samples 4 and 5 were incubated with ^{12}C -isoprene. Three replicate controls were set up with 5 g of autoclaved soil and incubated with 2.5 μl of ^{12}C -isoprene. The sealed serum vials were incubated without shaking in the dark at room temperature, with no added nutrient supplements. Isoprene was entirely depleted on the 7th day of incubation, as monitored by GC measurements of the headspace concentration of isoprene (Figure 6.8). 1%, 0.5% and 0.2% isoprene standards were set up for accurate GC measurements. All 5 samples were then re-spiked with 2.5 μl of isoprene, again to 0.5% isoprene (v/v). The samples were sacrificed after 15 days of incubation with an overall consumption of 10 μmol of isoprene per 1 g of soil.

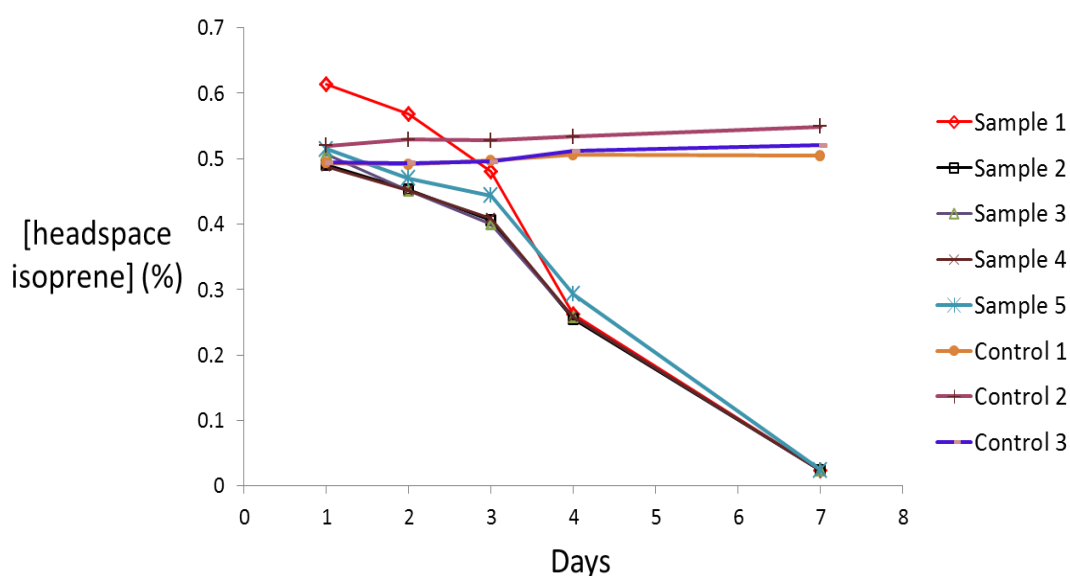


Figure 6.8 Consumption of isoprene in the SIP incubations spiked for the first time with 8 μl of isoprene i.e. 0.5% isoprene (v/v).

6.3.2 Processing of the SIP incubations

Once the SIP-microcosms were sacrificed at t=15 days, total DNA was extracted using the FastDNA spin kit for soil (MP Biomedicals), similarly to above. 2 µg of DNA extracted from each sample was added to caesium chloride solutions then subjected to a density gradient ultracentrifugation and fractionation following the instructions of Neufeld *et al.*, (2007). The CsCl density of each fraction was determined using a Reichart AR200 refractometer and the formation of good gradients was confirmed for all samples. DNA was then extracted from the fractions and was used in downstream analyses.

6.3.3 DGGE profiles of 16S rRNA genes amplified from DNA extracted from heavy and light fractions of the ¹³C-incubated microcosms

DGGE profiles of 16S rRNA genes amplified from DNA extracted from heavy and light fractions of the ¹³C-incubated microcosms were analysed. The triplicate enrichment samples 1, 2 and 3 yielded similar DGGE profiles, all showing a clear change in microbial communities between the heavy and light fractions (Figures 6.9, 6.10). The reason for this change is that members of the microbial community actively metabolised isoprene and incorporated the ¹³C label into their now ‘heavy’ genomic DNA. By contrast, the bacterial community in the ¹²C-isoprene SIP incubation displayed similar profile across the fractions, with most of the bacterial DNA being retrieved in the light fractions (Figure 6.11). In order to identify the isoprene-degrading bacterial community, DNA-SIP and DGGE analyses were complemented by 454 pyrosequencing of partial 16S rRNA genes from ¹³C-DNA in the heavy fractions.

	Fractions	Heavy	—————→					Light
Density (g.ml ⁻¹)		1.730	1.726	1.722	1.719	1.714	1.711	1.706
Ladder		6	7	8	9	10	11	12

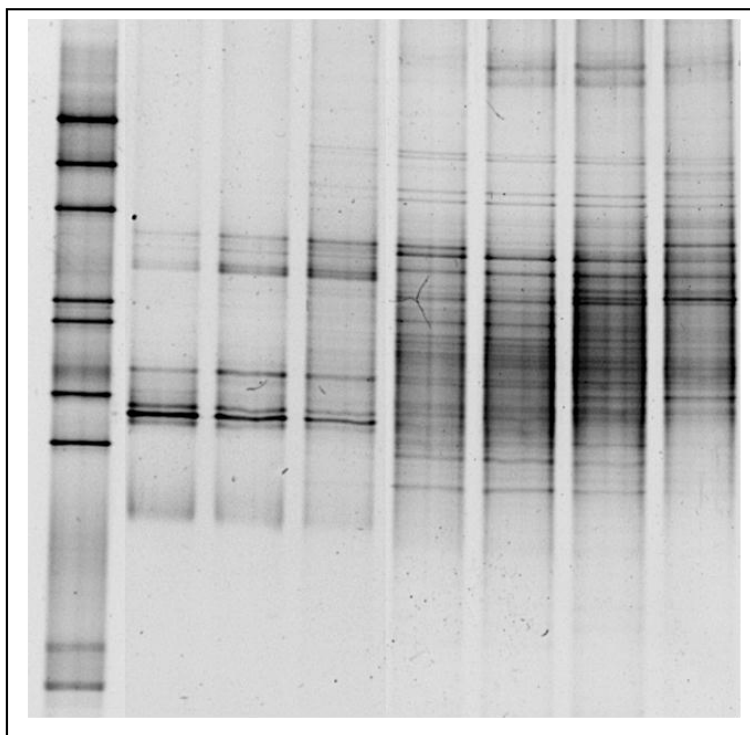


Figure 6.9 DGGE profile of 16S rRNA genes amplified from DNA extracted from heavy and light fractions (6 to 12) of ¹³C-incubated sample 2.

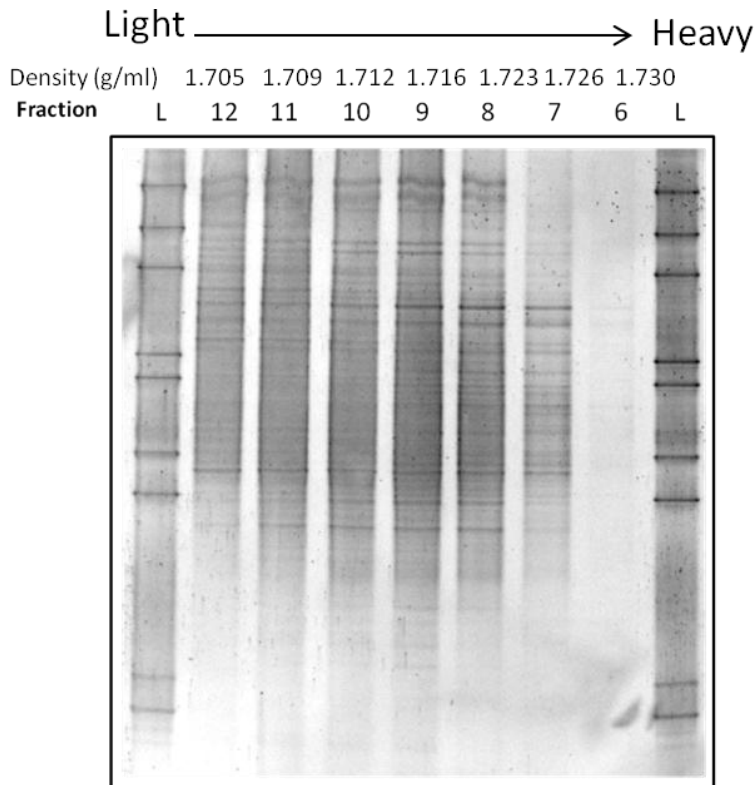


Figure 6.11 DGGE profile of 16S rRNA genes amplified from DNA extracted from fractions 12 to 6 of ^{12}C -isoprene incubated sample 4.

6.3.4 Analysis of 454 pyrosequencing data

16S rRNA genes were amplified using the primer set 27Fmod/519R modbio (refer to Table 6.2) from:

- DNA extracted from the soil sample prior to incubation with isoprene (referred to from now on as T_0)
- Pooled unfractionated DNA extracted from the triplicate ^{13}C -isoprene incubated microcosms 1, 2 and 3 after 15 days of incubation (T_1)
- DNA extracted from the heavy fraction 7 of the ^{13}C -isoprene incubated sample 1 (S1F7)
- DNA extracted from the heavy fraction 7 of the ^{13}C -isoprene incubated sample 2 (S2F7)
- DNA extracted from the heavy fraction 7 of the ^{13}C -isoprene incubated sample 3 (S3F7)
- Pooled DNA extracted from the light fraction 11 of the ^{13}C -isoprene incubated samples 1, 2 and 3 (S1/2/3F11)

- Pooled DNA extracted from fraction 7 of the ^{12}C isoprene incubated samples 4 and 5 (S4/5F7)
- Pooled DNA extracted from fraction 11 of the ^{12}C isoprene incubated samples 4 and 5 (S4/5F11)

A correct sized amplicon (493 bp) was obtained for all samples and was sent for 454 pyrosequencing at MrDNA (Texas, USA). 454 data were analyzed using Qiime (BioLinux). Only the sequences that passed the quality control (Table 6.5) were used in the analysis of the microbial community composition.

Table 6.5 Number of 454 reads that passed quality control for each sample

Sample							
T ₀	T ₁	S1F7	S2F7	S3F7	S1/2/3F11	S4/5F7	S4/5F11
1,895	3,458	3,871	7,550	3,109	1,687	698	2,020

The bacterial community profiles of T₀ and T₁ microcosms show an increase in the population of *Actinobacteria* in the microcosm of T₁ (Figure 6.12). This suggests that *Actinobacteria* were enriched in the presence of isoprene as the sole source of carbon and energy in the SIP incubations. The microbial profiles of the heavy fractions of the ^{13}C -isoprene incubations strongly support the observation that *Actinobacteria* were actively involved in isoprene metabolism. *Actinobacteria* largely dominated the heavy fractions, accounting on average for 84% of the 16S rRNA gene sequences as opposed to 9% in the light fraction (Table 6.6).

Proteobacteria phylotypes were also detected in the heavy fractions of the ^{13}C -isoprene incubated microcosms 1, 2 and 3, accounting for ~8%, 11% and 16% of the sequences, respectively (Table 6.6).

Actinomycetales bacteria seem to be major players in isoprene degradation. Members of this group showed a 10 fold increase in their relative abundance when comparing the bacterial population composition at T₀ to that at T₁, i.e. after 15 day incubation with isoprene (Figure 6.13). The *Actinomycetales* order was represented on average by 83% of the 16S rRNA gene sequences from the heavy fractions of the ^{13}C -isoprene incubations, compared to 4% of the sequences from the light fraction. The

remaining sequences in the heavy fractions were mostly affiliated with the *Burkholderiales* (*Proteobacteria*) order (Figure 6.13).

In the context of *Actinobacteria*, members belonging to the *Rhodococcus* genus were by far the most abundant within the isoprene-degrading bacterial community (Table 6.7). Members of the *Nocardiaceae* family, other than *Rhodococcus*, were also detected by ~ 5 % of the sequences from the ¹³C- heavy fractions. The taxonomic classification of these members was, however, not resolved beyond the family level. The increase of the initial population of *Comamonadaceae* bacteria after incubation with isoprene and the incorporation of the ¹³C label by representatives of this family (Table 6.7) are strong evidence of the participation of the *Comamonadaceae* family in the isoprene degradation process.

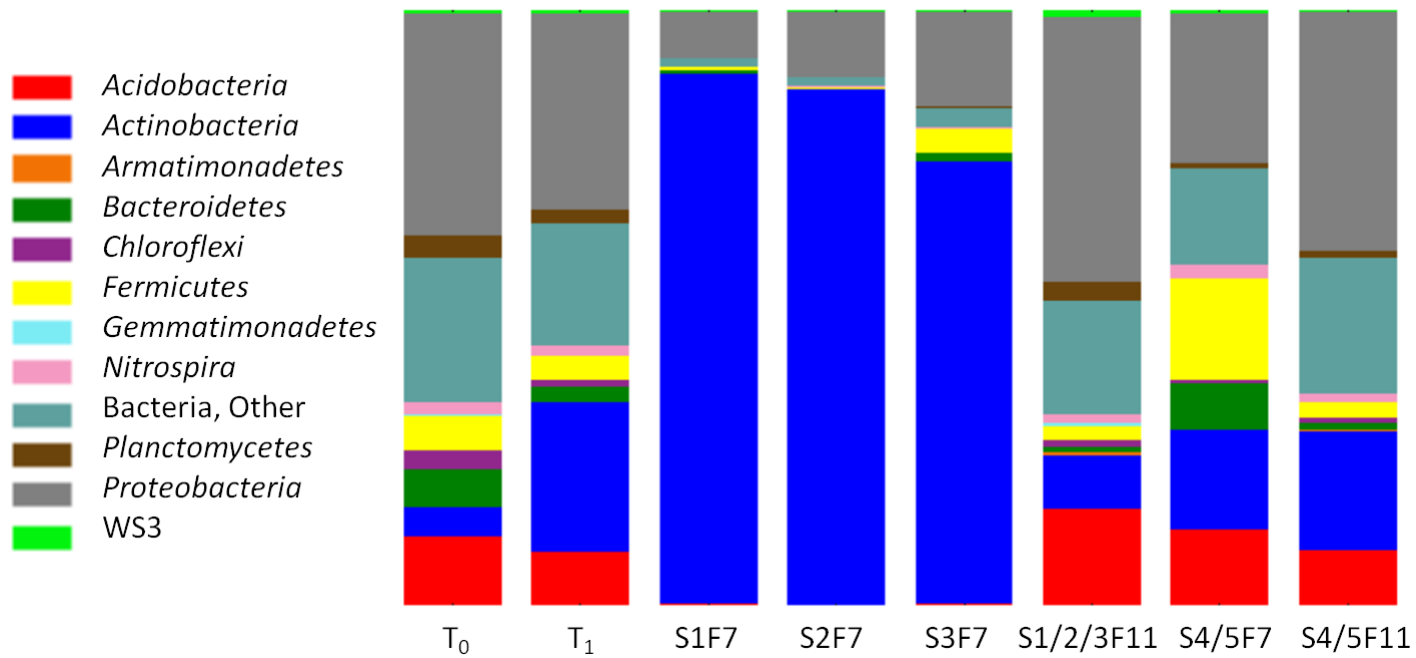


Figure 6.12 Bar graphs displaying the bacterial community composition at the phylum level. Only phyla representing > 0.5% of the community in any of the samples are shown.

Table 6.6 Bacterial composition of T₀ and T₁ microcosms as well as the heavy and light fractions of the SIP incubations, at the phylum level. The numbers represent the relative abundance (%) of the corresponding phylum within the community. Only phyla representing > 0.5% of the community in any of the samples, are shown. Other: includes unclassified bacteria as well as phyla representing less than 0.5% of the community.

Phylum	T0	T1	S1F7	S2F7	S3F7	S1/2/3F11	S4/5F7	S4/5F11
<i>Acidobacteria</i>	11.66	9.14	0.34	0.09	0.35	16.18	12.75	9.41
<i>Actinobacteria</i>	4.85	25.01	89.23	86.77	74.53	9.07	16.91	20.00
<i>Armatimonadetes</i>	-	0.12	-	-	-	0.53	-	0.10
<i>Bacteroidetes</i>	6.33	2.57	0.39	0.09	1.25	1.07	7.74	1.34
<i>Chloroflexi</i>	3.27	1.19	-	-	0.03	0.89	0.57	0.84
<i>Firmicutes</i>	5.91	3.88	0.77	0.37	4.21	2.37	17.05	2.57
<i>Gemmatimonadetes</i>	0.21	0.14	-	-	-	0.59	-	0.10
<i>Nitrospira</i>	2.06	1.62	0.03	0.03	0.03	1.54	2.44	1.44
<i>Planctomycetes</i>	3.59	2.49	-	0.05	0.10	3.20	0.86	1.29
<i>Proteobacteria</i>	37.47	32.88	7.88	11.14	16.11	44.64	25.21	40.10
WS3	0.37	0.40	-	-	-	0.83	0.29	0.20
Bacteria; Other	24.27	20.56	1.37	1.46	3.38	19.09	16.19	22.62
Total	100	100	100	100	100	100	100	100

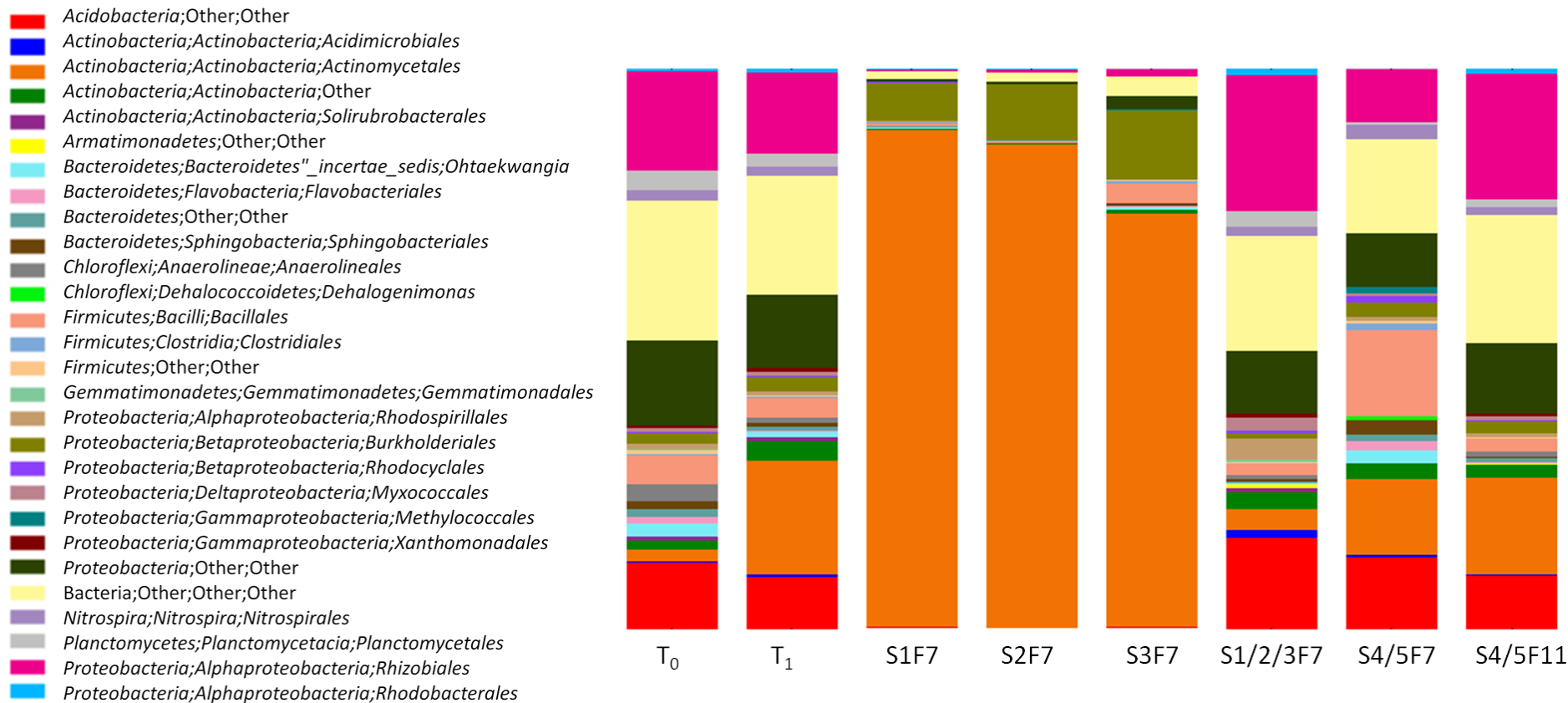


Figure 6.13 Bar graphs displaying the bacterial community composition at the Order level. Only bacterial Orders representing > 0.5% of the community in any of the samples are shown. Other: includes unclassified bacteria as well as orders representing less than 0.5% of the community.

Table 6.7 Bacterial composition of the samples, at the genus level. The numbers represent the relative abundance (%) of the genera within the community. Only genera representing > 0.5% of the community in any of the samples, are shown. Highlighted in red are those representing more than 5% of the community in the heavy fraction of the ¹³C-isoprene SIP incubations. Other: includes unclassified bacteria as well as genera representing less than 0.5% of the community.

Genus	T0	T1	S1F7	S2F7	S3F7	S1/2/3F11	S4/5F7	S4/5F11
Unclassified <i>Acidobacteria</i>	11.66	9.14	0.34	0.09	0.35	16.18	12.75	9.41
Unclassified Acidimicrobiales	0.42	0.46	-	0.03	0.10	1.42	0.57	0.25
<i>Actinobacteria</i>; <i>Actinobacteria</i>; <i>Actinomycetales</i>; <i>Nocardiaceae</i>; <i>Rhodococcus</i>	0.11	11.74	77.01	75.76	61.11	0.24	8.17	10.15
<i>Actinobacteria</i>; <i>Actinobacteria</i>; <i>Actinomycetales</i>; <i>Nocardiaceae</i>	-	0.87	5.61	4.81	4.79	0.12	1.00	1.04
<i>Actinobacteria</i> ; <i>Actinobacteria</i> ; <i>Actinomycetales</i> ; <i>Nocardioidaceae</i> ; <i>Nocardioides</i>	0.11	0.03	-	0.04	0.03	1.01	0.14	
<i>Actinobacteria</i> ; <i>Actinobacteria</i> ; <i>Actinomycetales</i> ; <i>Propionibacteriaceae</i> ; <i>Propionibacterium</i>	-	-	-	-	-	-	0.57	-
Unclassified <i>Actinomycetales</i>	1.79	8.13	6.35	5.95	8.17	2.38	3.58	6.19
Unclassified <i>Solirubrobacterales</i>	0.74	0.52		0.03		0.83	0.14	0.10
Unclassified <i>Actinobacteria</i>	1.69	3.47	0.26	0.15	0.61	3.08	2.72	2.28
Unclassified <i>Armatimonadetes</i>	-	0.12	-	-	-	0.53	-	0.10
<i>Nitrospira</i> ; <i>Nitrospira</i> ; <i>Nitrospirales</i> ; <i>Nitrospiraceae</i> ; <i>Nitrospira</i>	2.06	1.62	0.03	0.03	0.03	1.54	2.44	1.44
<i>Gemmatimonadetes</i> ; <i>Gemmatimonadetes</i> ; <i>Gemmatimonadales</i> ; <i>Gemmatimonadaceae</i> ; <i>Gemmatimonas</i>	0.21	0.14	-	-	-	0.59	-	0.10
<i>Planctomycetes</i> ; <i>Planctomycetacia</i> ; <i>Planctomycetales</i> ; <i>Planctomycetaceae</i> ; <i>Gemmata</i>	0.58	0.46	-	0.04	-	0.89	-	0.20
<i>Planctomycetes</i> ; <i>Planctomycetacia</i> ; <i>Planctomycetales</i> ; <i>Planctomycetaceae</i>	2.80	1.88	-	0.01	0.01	2.02	0.43	1.09
<i>Chloroflexi</i> ; <i>Dehalococcoidetes</i> ; <i>Dehalogenimonas</i> ; <i>Dehalogenimonas</i> ; <i>Dehalogenimonas</i>	0.05	-	-	-	-	-	0.57	-
<i>Chloroflexi</i> ; <i>Anaerolineae</i> ; <i>Anaerolineales</i> ; <i>Anaerolineaceae</i>	3.06	0.93	-	-	0.03	0.53	-	0.84
Unclassified WS3	0.37	0.40	-	-	-	0.83	0.29	0.20

<i>Proteobacteria; Alphaproteobacteria; Rhizobiales; Bradyrhizobiaceae</i>	1.79	0.95	0.13	0.29	0.42	2.07	0.72	2.48
<i>Proteobacteria; Alphaproteobacteria; Rhizobiales; Hyphomicrobiaceae; Pedomicrobium</i>	0.53	0.81	-	0.01	0.16	4.56	0.29	0.89
<i>Proteobacteria; Alphaproteobacteria; Rhizobiales; Hyphomicrobiaceae; Hyphomicrobium</i>	0.63	0.64	-	-	-	0.71	0.29	1.04
<i>Proteobacteria; Alphaproteobacteria; Rhizobiales; Hyphomicrobiaceae</i>	0.42	0.35	-	-	0.16	0.47	0.14	0.89
<i>Proteobacteria; Alphaproteobacteria; Rhizobiales; Methylobacteriaceae; Methylobacterium</i>	-	-	-	-	-	-	0.57	-
<i>Proteobacteria; Alphaproteobacteria; Rhizobiales; Phyllobacteriaceae; Aminobacter</i>	0.11	0.20	-	-	-	0.36	0.29	0.74
<i>Proteobacteria; Alphaproteobacteria; Rhizobiales; Phyllobacteriaceae</i>	0.47	0.38	-	-	-	0.18	-	0.50
Unclassified <i>Rhizobiales</i>	13.88	11.07	0.08	0.16	0.16	15.95	7.16	16.09
<i>Proteobacteria; Alphaproteobacteria; Rhodobacterales; Rhodobacteraceae</i>	0.16	0.52	0.03	0.01	-	0.95	-	0.64
<i>Proteobacteria; Alphaproteobacteria; Rhodospirillales; Rhodospirillaceae</i>	0.90	0.52	-	-	-	3.56	0.57	0.69
Unclassified <i>Alphaproteobacteria</i>	4.27	4.19	0.13	0.11	0.55	2.73	1.15	4.16
<i>Proteobacteria; Betaproteobacteria; Burkholderiales; Comamonadaceae; Variovorax</i>	-	0.03	0.39	0.58	1.70	-	-	-
<i>Proteobacteria; Betaproteobacteria; Burkholderiales; Comamonadaceae</i>	0.11	0.55	5.22	8.15	9.13	0.06	0.29	0.64
Unclassified <i>Burkholderiales</i>	1.79	1.97	1.29	1.26	2.21	0.89	2.44	1.44
<i>Proteobacteria; Betaproteobacteria; Rhodocyclales; Rhodocyclaceae</i>	0.32	0.29	0.18	0.04	-	0.36	1.00	0.10
Unclassified <i>Betaproteobacteria</i>	2.32	1.94	0.03	0.09	0.45	2.13	2.15	2.57
<i>Proteobacteria; Deltaproteobacteria; Myxococcales; Polyangiaceae</i>	0.16	0.12	-	-	-	0.65	0.14	0.25
<i>Proteobacteria; Deltaproteobacteria; Myxococcales; Cystobacteraceae</i>	0.05	0.23	-	-	0.06	0.53	0.29	-
Unclassified <i>Myxococcales</i>	0.42	0.35	-	-	0.06	1.24	0.14	0.54
Unclassified <i>Deltaproteobacteria</i>	2.43	1.36	-	-	0.13	2.02	0.86	1.24
<i>Proteobacteria; Gammaproteobacteria; Methylococcales; Methylococcaceae; Methylococcus</i>	-	-	-	0.01	0.23	-	1.15	-
<i>Proteobacteria; Gammaproteobacteria; Xanthomonadales; Xanthomonadaceae</i>	0.47	0.67	0.03	-	-	0.59	-	0.50
Unclassified <i>Gammaproteobacteria</i>	1.48	1.24	0.05	0.01	0.06	2.07	2.44	0.99
Unclassified <i>Proteobacteria</i>	5.02	4.92	0.36	0.41	1.13	2.85	3.15	3.86
<i>Firmicutes; Bacilli; Bacillales; Bacillaceae 1; Bacillus</i>	1.27	0.95	0.18	0.05	2.16	1.13	8.31	0.45
<i>Firmicutes; Bacilli; Bacillales; Pasteuriaceae; Pasteuria</i>	1.95	1.07	-	0.01	-	0.59	0.57	0.84
<i>Firmicutes; Bacilli; Bacillales; Planococcaceae; Paenisporosarcina</i>	0.05	-	-	-	-	-	0.72	-
Unclassified <i>Bacillales</i>	1.74	1.42	0.36	0.04	1.22	-	5.87	-
<i>Firmicutes; Clostridia; Clostridiales; Clostridiaceae; Clostridium sensu strict</i>	0.05	0.06	0.05	0.12	0.23	-	0.86	-
Unclassified <i>Firmicutes</i>	0.79	0.35	0.08	0.13	0.48	0.12	0.57	0.05

<i>Bacteroidetes; Bacteroidetes" _incertae_sedis; Ohtaekwangia; Ohtaekwangia; Ohtaekwangia</i>	2.37	0.87	0.03	0.01	0.45	0.24	2.29	0.15
<i>Bacteroidetes; Flavobacteria; Flavobacteriales; Flavobacteriaceae; Flavobacterium</i>	0.95	0.20	0.13	0.04	0.26	0.00	1.58	0.15
<i>Bacteroidetes; Sphingobacteria; Sphingobacteriales; Chitinophagaceae</i>	0.90	0.40	0.03	0.01	0.23	0.24	0.86	0.25
Unclassified <i>Sphingobacteriales</i>	0.53	0.26	0.05	-	0.16	0.36	1.86	0.15
Unclassified <i>Bacteroidetes</i>	1.58	0.84	0.15	0.03	0.13	0.24	1.15	0.64
Other	24.43	20.38	1.45	1.47	2.84	19.43	16.76	22.57

6.3.5 Analysis of *isoA* amplicon sequences

The unfractionated DNA, which was extracted from each of the triplicate ¹³C-isoprene SIP incubations at t= 15 days, was pooled and used as template in the amplification of *isoA* gene. The amplification reaction yielded a product of the correct size (1,015 bp) which was purified and sent for 454 pyrosequencing. Unfortunately, low sequence coverage was obtained and only 223 reads were considered of good quality. These grouped into 39 different OTUs (Table 6.8). The representative nucleotide and deduced amino acid sequences from each OTU were aligned. Some of the sequences displayed frameshift errors as a result of an insertion or deletion. These were manually corrected and the amino acid sequences were re-aligned.

Table 6.8 Analysis of 454 *isoA* sequences from the ¹³C-isoprene enriched microcosms and comparison of representative IsoA sequences with IsoA of *Rhodococcus* AD45.

OTU	Number of assigned sequences for each OTU	Size of representative <i>isoA</i> (bp)	Size of deduced IsoA (aa)	% aa identity to IsoA of <i>Rhodococcus</i> AD45
OTU 1	1	180	60	88
OTU 2	2	352	117	96
OTU 3	4	391	130	93
OTU 4	1	235	ND	ND
OTU 5	2	412	136	93
OTU 6	3	388	130	98
OTU 7	16	282	94	97
OTU 8	4	391	130	99
OTU 9	2	233	77	97
OTU 10	1	304	100	99
OTU 11	4	247	ND	ND
OTU 12	14	234	77	97
OTU 13	1	247	83	92
OTU 14	4	241	ND	ND
OTU 15	4	226	75	95
OTU 16	1	407	135	96
OTU 17	3	298	98	96
OTU 18	3	245	ND	ND
OTU 19	4	369	123	98
OTU 20	2	307	102	100
OTU 21	49	356	118	97
OTU 22	1	262	86	95
OTU 23	3	328	106	96
OTU 24	2	403	134	93

OTU 25	5	198	ND	ND
OTU 26	1	454	151	93
OTU 27	11	448	148	99
OTU 28	1	252	82	96
OTU 29	1	270	88	97
OTU 30	1	194	63	97
OTU 31	1	259	83	96
OTU 32	1	206	ND	ND
OTU 33	39	389	129	96
OTU 34	1	252	84	93
OTU 35	1	391	129	92
OTU 36	13	312	103	96
OTU 37	9	250	82	98
OTU 38	1	324	106	98
OTU 39	6	379	124	99

ND: The derived amino acid sequence could not be determined nor correctly aligned as the read contained many deletions.

6.4 Discussion

In this study, ^{13}C -isoprene DNA-SIP experiments were used in tandem with 454 pyrosequencing of 16S rRNA and *isoA* genes for characterizing the diversity of bacterial isoprene degraders.

16S rRNA gene based analysis of the isoprene degrading community after incubation with fully labelled ^{13}C -isoprene revealed a low diversity. About 70% of the 16S rRNA gene sequences, which were amplified from the ^{13}C -DNA, affiliated with the genus *Rhodococcus*, known to be abundant in isoprene-enriched water and marine sediments from a previous study conducted by the group of Terry McGenity at the University of Essex (Alvarez *et al.*, 2009). Several *Rhodococcus* strains have already been isolated that grow on isoprene as source of carbon and energy (Alvarez *et al.*, 2009, Ewers *et al.*, 1990, Vlieg *et al.*, 1998, this study Chapter 3)

Betaproteobacteria 16S rRNA gene phylotypes were also detected in the heavy fractions of the ^{13}C -isoprene SIP incubations. Representatives of *Proteobacteria* phylum accounted for a large proportion of the microbial population in the isoprene - enriched Indonesian seawater (Alvarez *et al.*, 2009). They were identified, however, as *Alphaproteobacteria*. Members of the Gamma-subclass of *Proteobacteria* were also present in the marine isoprene enrichments, in considerably lower abundance. This study is the first indication that *Betaproteobacteria* (*Comamonadaceae*) are likely to be involved in isoprene metabolism. Further metabolic and growth tests are required in order to rule out the possibility of a cross-feeding phenomenon taking place in the ^{13}C -isoprene incubated microcosms. This calls for serious attempts to isolate and cultivate isoprene-degrading *Comamonadaceae* strains.

The low diversity of the isoprene utilizing community from the fully labelled ^{13}C -isoprene incubation was confirmed by the *isoA* gene based analysis. The deduced representative IsoA sequences from all 39 OTUs, with the exception of OTU 1, shared over 90% amino acid sequence identity with IsoA of *Rhodococcus* AD45.

454 pyrosequencing of 16S rRNA genes from the partially labelled ^{13}C -isoprene SIP incubations revealed that the ^{13}C label was incorporated by bacteria belonging to more diverse phylogenetic groups, including *Proteobacteria*, *Actinobacteria*,

Bacteroidetes, and *Firmicutes*. The ability of these phyla to metabolize isoprene has already been suggested (Alvarez *et al.*, 2009).

The analysis of the 16S rRNA gene sequences from ^{13}C -DNA at the family level gave a similar result to that obtained from the analysis of 454 16S rRNA amplicon sequences from marine samples incubated with isoprene. For instance, *Caulobacteraceae*, *Hyphomicrobiaceae*, *Phyllobacteriaceae*, *Nocardiaceae* sequences were identified among the 16S rRNA gene sequences. The order *Rhizobiales*, commonly found in plant-associated environments, was highly represented in the sequences from both the heavy and light fractions of the partially labelled ^{13}C -isoprene incubations. While it is tempting to suggest a role for *Rhizobiales* bacteria in isoprene degradation in the environment, especially in soils covered with isoprene-emitting vegetation, the fully labelled ^{13}C -isoprene SIP experiment shows no enrichment of *Rhizobiales* bacteria at T_1 , i.e. after incubation with isoprene. *Rhizobiales* sequences were also virtually only found in the light fraction. This suggests that *Rhizobiales* bacteria, which were already present in the soil in association with willow trees, were not active within the isoprene-degrading microbial community. *Bacteroidetes* bacteria which metabolized isoprene, as revealed by the 16S rRNA gene sequences from the heavy fraction, belonged to the order *Sphingobacteriales*, previously not associated with isoprene metabolism. The amplification of *isoA* gene from ^{13}C -DNA further confirmed the presence of isoprene utilizers within the bacterial community. However, the low number of *isoA* sequences makes it difficult to draw diversity related conclusions.

Chapter 7

Final discussion

This study successfully tested and supported two main hypotheses: (1) isoprene degradation by bacteria is widespread in the terrestrial environment (2) bacterial isoprene degradation is catalysed by an induced SDIMO enzyme system.

Isoprene-degrading bacteria were readily enriched and isolated from soil and leaves, suggesting that these bacteria are widely distributed in the terrestrial environment. Plants represent the largest source of biogenic isoprene flux to the atmosphere (Guenther *et al.*, 2006). The isolation of an isoprene-utilizing *Rhodococcus* strain from leaves suggest that leaf surfaces might represent an ideal niche for isoprene-degrading bacterial communities, potentially feeding on a portion of the isoprene that exits the leaf through the stomata. This challenges the current rate of isoprene consumption used for global models of isoprene cycling which is based solely on isoprene uptake by soils (Cleveland & Yavitt, 1997). This rate is therefore likely to increase, given the large number of isoprene emitting plants.

The physiology of *Rhodococcus* SC4 and LB1 isolates was characterized, showing that these strains were capable of growing on other carbon sources such as acetate, propane, and butane. *Rhodococcus* SC4 and LB1 are therefore facultative isoprene-utilizing bacteria, similarly to the marine isoprene degraders that were isolated by Alvarez and colleagues (2009). It was not determined if these bacteria, when inoculated into culture media containing isoprene and another carbon source (e.g. glucose), prefer utilizing isoprene for growth. This could be easily addressed by supplementing 10 mM glucose and 1 % (v/v) isoprene to 250 ml Quickfit flasks containing CBS minimal medium inoculated with *Rhodococcus* SC4 or LB1 cells then incubating the flasks at 30 °C and measuring the growth density and headspace concentration of isoprene during incubation.

The identification of the isoprene gene cluster in the genome sequences of *Rhodococcus* AD45, SC4 and LB1 was relatively straightforward and was guided by the work of Vlieg *et al.*, (2000). The organisation of the genes within the isoprene cluster was in perfect agreement with that reported by Vlieg and colleagues. With the exception of *isoA*, the gene sequences were also a perfect match. The deduced soluble isoprene monooxygenase sequence contained all the important amino acid residues that are conserved across all SDIMO enzymes and showed the highest level of homology to the SDIMO enzymes of group 1 which includes the alkene

monooxygenase of *Xanthobacter autotrophicus* PY2. The genes involved in isoprene degradation in *Rhodococcus sp.* AD45 were located on a plasmid, further indicating that the capacity for isoprene degradation might be widespread in nature due to potential horizontal gene transfer. An operon encoding soluble propane monooxygenase was identified in the draft genomes of *Rhodococcus* SC4 and LB1, suggesting that these bacteria oxidize propane and isoprene via two independent SDIMO enzyme systems.

The genome sequence of *Rhodococcus sp.* AD45 provided a robust database for mapping and identifying the polypeptides that *Rhodococcus* AD45 expresses during growth on isoprene. Polypeptides identified, by mass spectrometry analysis, as the active site polypeptides of soluble isoprene monooxygenase were present in cells grown on isoprene, but not expressed in cells grown on glucose. This suggested that *Rhodococcus* AD45 expresses isoprene monooxygenase enzyme selectively when isoprene is used for growth. The qRT-PCR data further showed that isoprene monooxygenase gene expression was activated at the transcriptional level given that *isoA* transcripts were significantly more abundant in cells grown on isoprene compared to cells grown on glucose. The regulatory mechanism of isoprene degradation remains largely unknown. However, there is a growing body of evidence that the SDIMO enzyme system responsible for isoprene degradation by bacteria is induced by the epoxide, the first intermediate in the isoprene oxidation pathway (Crombie *et al.*, manuscript in preparation).

Several lines of evidence were presented in support of the hypothesis that isoprene is metabolized in bacteria primarily by acting as a substrate for the isoprene monooxygenase enzyme. The deletion and replacement of a DNA fragment within the *isoA* gene with a gentamicin resistance cassette completely impaired the ability of *Rhodococcus sp.* AD45 to utilize isoprene as a source of carbon and energy. Furthermore, using primers that were developed to selectively amplify *isoA* from pure isolates and environmental samples, we showed that all the isoprene-degrading bacteria (terrestrial and marine) that are in culture to date contain the *isoA* gene encoding the alpha subunit of soluble isoprene monooxygenase. It is worth noting however that these results do not preclude the possibility of an alternative pathway, albeit secondary, for isoprene degradation. The *isoA* PCR-approach developed in this study allows one not only to swiftly screen any newly isolated isoprene degrader for

the hydroxylase alpha subunit gene, but also allows one to generate information on which terrestrial ecosystems (in terms of pH, moisture content, temperature, biomass cover) are rich with isoprene-degrading bacteria, thus expanding our currently limited understanding of the biogeography of isoprene degraders in the terrestrial environment.

DNA- stable isotope probing experiments combined with 454 pyrosequencing of 16S rRNA and *isoA* gene amplicons allowed us to identify bacteria that are capable of metabolizing isoprene, which can otherwise be overlooked in cultivation-dependent methods. As expected, 16S rRNA gene sequences affiliated with the genus *Rhodococcus* were retrieved in the heavy (^{13}C) DNA of the SIP enrichments and accounted for a substantial fraction of the total sequences. Interestingly, 16S rRNA sequences affiliated with species previously not known to metabolize isoprene, such as members of the *Comamonadaceae* family, were also retrieved. This finding can guide future isolation work of isoprene degraders by tailoring the enrichment conditions (e.g temperature, medium, pH) in favour of the growth of these bacteria. In light of the widely recognized limitations of the stable isotope probing method, we conducted a time-course microcosm experiment (with the partially labelled ^{13}C -isoprene) and shortened the incubation period of the SIP enrichments to reduce the occurrence of a cross-feeding phenomenon. Although isoprene concentrations used in the SIP experiments were higher than those to which bacteria are exposed in nature, they were lowered to the minimum required concentration for sufficient labelling. Raman-FISH can be used in tandem with the DNA-SIP experiments in the future to analyze bacteria that incorporated the ^{13}C label at the single-cell level (Huang *et al.*, 2010, Murrell & Whiteley, 2011). This method relies on the fact that the cells that have metabolized isoprene and incorporated the ^{13}C -isotope in their cellular molecules will show different Raman spectra to unlabelled cells. The individual labelled cells can then be identified using FISH probes specific for major isoprene degraders. The 16S rRNA gene sequence database generated in this study from the isolates, enrichment soil samples, and SIP microcosms will provide a solid platform for designing the FISH probes.

Future studies could focus on assaying the rate of isoprene oxidation by the isoprene monooxygenase enzyme. Using an oxygen electrode, whole fresh cells of *Rhodococcus sp.* AD45 can be incubated with isoprene or another substrate of

interest in a closed chamber where oxygen concentration can be monitored. We expect glucose-grown *Rhodococcus sp.* AD45 not to show any oxidation activity with isoprene given the inducible nature of the isoprene monooxygenase enzyme. We can also assay whether isoprene-grown *Rhodococcus sp.* SC4 or LB1 cells are capable of oxidizing propane, although this seems unlikely given that the genomes of *Rhodococcus* SC4 and *Rhodococcus* LB1 encode two SDIMO enzymes. The purification of the soluble isoprene monooxygenase enzyme is also well worth considering in the future. This will require the development of an *in vitro* assay for the isoprene monooxygenase.

References

- Affek, H.P., and Yakir, D. (2003) Natural abundance carbon isotope composition of isoprene reflects incomplete coupling between isoprene synthesis and photosynthetic carbon flow. *Plant Physiol* 131: 1727-1736.
- Allen, J.R., Clark, D.D., Krum, J.G., and Ensign, S.A. (1999) A role for coenzyme M (2-mercaptoethanesulfonic acid) in a bacterial pathway of aliphatic epoxide carboxylation. *Proc Natl Acad Sci USA* 96: 4832-4837.
- Alvarez, H.M., Mayer, F., Fabritius, D., and Steinbüchel, A. (1996) Formation of intracytoplasmic lipid inclusions by *Rhodococcus opacus* strain PD630. *Arch Microbiol* 165: 377-386.
- Alvarez, L.A., Exton, D.A., Timmis, K.N., Suggett, D.J., and McGenity, T.J. (2009) Characterization of marine isoprene-degrading communities. *Environ Microbiol* 11: 3280-3291
- Anderson, L.J., Harley, P.C., Monson, R.K., and Jackson, R.B. (2000) Reduction of isoprene emissions from live oak (*Quercus fusiformis*) with oak wilt. *Tree Physiol* 20: 1199-1203
- Arneth, A., Niinemets, Ü., Pressley, S., Bäck, J., Hari, P., Karl, T., Noe, S., Prentice, I.C., Serça, D., Hickler, T., Wolf, A., and Smith, B. (2007) Process-based estimates of terrestrial ecosystem isoprene emissions: incorporating the effects of a direct CO₂-isoprene interaction. *Atmos Chem Phys* 7: 31-53.
- Arneth, A., Monson, R.K., Schurgers, G., Niinemets, Ü., and Palmer, P.I. (2008) Why are estimates of global terrestrial isoprene emissions so similar (and why is this not so for monoterpenes)? *Atmos Chem Phys* 8: 4605-4620.
- Arneth, A., Schurgers, G., Lathiere, J., Duhl, T., Beerling, D.J., Hewitt, C.N., Martin, M., and Guenther, A. (2011) Global terrestrial isoprene emission models: sensitivity to variability in climate and vegetation. *Atmos Chem Phys* 11: 8037-8052.
- Atkinson, R., and Arey, J. (1998) Atmospheric chemistry of biogenic organic compounds. *Acc Chem Res* 31: 574-583.
- Atkinson, R., and Arey, J. (2003) Gas-phase tropospheric chemistry of biogenic volatile organic compounds: a review. *Atmos Environ* 37: 197-219
- Atkinson, R., Baulch, D.L., Cox, R.A., Crowley, J.N., Hampson, R.F., Hynes, R.G., Jenkin, M.E., Rossi, M.J., Troe, J., and IUPAC subcommittee. (2006) Evaluated kinetic and photochemical data for atmospheric chemistry: Volume II – gas phase reactions of organic species. *Atmos Chem Phys* 6: 3625-4055.
- Baker, A.R., Turner, S.M., Broadgate, W.J., Thompson, A., McFiggans, G.B., Vesperini, O., Nightingale, P.D., Liss, P.S., and Jickells, T.D. (2000) distribution and sea-air fluxes of biogenic trace gases in the eastern atlantic ocean. *Global Biogeochem Cycles* 14: 871-886.

- Banerjee, A., and Sharkey, T.D. (2014) Methylerythritol 4-phosphate (MEP) pathway metabolic regulation. *Nat Prod Rep* 31: 1043-1055.
- Behnke, K., Ehling, B., Teuber, M., Bauerfeind, M., Louis, S., Hänsch, R., Polle, A., Bohlmann, J., and Schnitzler, J.P. (2007) Transgenic, non-isoprene emitting poplars don't like it hot. *Plant J* 51: 485-499.
- Bell, K.S., Philip, J.C., Aw, D.W., and Christofi, N. (1998) The genus *Rhodococcus*. *J Appl Microbiol* 85: 195-210.
- Boden, R., Thomas, E., Savani, P., Kelly, D.P., Wood, A.P. (2008) Novel methylotrophic bacteria isolated from the River Thames (London, UK). *Environ Microbiol* 10: 3225-3236.
- Bonsang, B., Polle, C., and Lambert, G. (1992) Evidence for the marine production of isoprene, *Geophys Res Lett* 19: 1129-1132.
- Bonsang, B., Gros, V., Peeken, I., Yassaa, N., Bluhm, K., Zoellner, E., Sarda-Esteve, R., and Williams, J. (2010) Isoprene emission from phytoplankton monocultures: the relationship with chlorophyll-a, cell volume and carbon content. *Environ Chem* 7: 554-563.
- Borbon, A., Fontaine, H., Veillerot, M., Locoge N., Galloo, J.C., and Guillermo, R. (2001) An investigation into the traffic-related fraction of isoprene at an urban location. *Atmos Environ* 35: 3749-3760.
- Bos, L.D., Sterk, P.J., and Schultz, M.J. (2013) Volatile metabolites of pathogens: a systematic review. *PLoS Pathog* 9: e1003311.
- Boschker, H.T.S., Nold, S.C., Wellsbury, P., Bos, D., de Graaf, W., Pel, R., Parkes, R.J., and Cappenberg, T.E. (1998). Direct linking of microbial populations to specific biogeochemical processes by ¹³C-labeling of biomarkers. *Nature* 392: 801-805.
- Braaz, R., Fischer, P., and Jendrossek, D. (2004) Novel type of heme-dependent oxygenase catalyses oxidative cleavage of rubber (poly-cis-1,4-isoprene). *Appl Environ Microbiol* 70: 7388-7395.
- Braaz, R., Armbruster, W., and Jendrossek, D. (2005) Heme-dependent rubber oxygenase RoxA of *Xanthomonas* sp. Cleaves the carbon backbone of poly(cis-1,4-isoprene) by a dioxygenase mechanism. *Appl Environ Microbiol* 71: 2473-2478.
- Broadgate, W.J., Liss, P.S., and Penkett, S.A. (1997) Seasonal emissions of isoprene and other reactive hydrocarbon gases from the ocean. *Geophys Res Lett* 24: 2675-2678.
- Broadgate, W.J., Malin, G., Küpper, F.C., Thompson, A., and Liss, P.S. (2004) Isoprene and other non-methane hydrocarbons from seaweeds: a source of reactive hydrocarbons to the atmosphere. *Mar Chem* 88: 61-73.
- Cailleux, A., and Allain, P. (1989) Isoprene and sleep. *Life Sci* 44: 1877-1880.
- Cappelletti, M., Fedi, S., Frascari, D., Ohtake, H., Turner, R.J., and Zannoni, D. (2011) Analyses of both the alkB gene transcriptional start site and alkB promoter-inducing properties of *Rhodococcus* sp. strain BCP1 grown on n-alkanes. *Appl Environ Microbiol* 77: 1619-1627.

- Cardy, D.L.N., Laidler, V., Salmond, G.P.C., and Murrell, J.C. (1991) Molecular analysis of the methane monooxygenase (MMO) gene cluster of *Methylosinus trichosporium* OB3b. *Mol Microbiol* 5: 335-342.
- Carlton, A.G., Wiedinmyer, C., and Kroll, J.H. (2009) A review of Secondary Organic Aerosol (SOA) formation from isoprene. *Atmos Chem Phys* 9: 4987-5005.
- Cébron, A., Bodrossy, L., Stralis-Pavese, N., Chen, Y., and Murrell, J.C. (2007) DNA stable isotope probing of active methane-oxidizing bacteria in Roscommon landfill biocover soil. *FEMS Microbiol Ecol* 62: 12-23.
- Chen, Y., Dumont, M.G., Neufeld, J.D., Bodrossy, L., Stralis-Pavese, N., McNamara, N.P., Ostle, N., Briones, M.J., and Murrell, J.C. (2008) Revealing the uncultivated majority: combining DNA stable-isotope probing, multiple displacement amplification and metagenomic analyses of uncultivated Methylocystis in acidic peatlands. *Environ Microbiol* 10: 2609-2622.
- Chen, Y., McAleer, K.L., and Murrell, J.C. (2010) Monomethylamine as a nitrogen source for a nonmethylophilic bacterium, *Agrobacterium tumefaciens*. *Appl Environ Microbiol* 76: 4102-4104.
- Chiba, K., Hoshino, Y., Ishino, K., Kogure, T., Mikami, Y., Uehara, Y., and Ishikawa, J. (2007) Construction of a pair of practical *Nocardia-Escherichia coli* shuttle vectors. *Jpn J Infect Dis* 60: 45-47.
- Claeys, M., Graham, B., Vas, G., Wang, W., Vermeylen, R., Pashynska, V., Cafmeyer, J., Guyon, P., Andreae, M.O., Artaxo, P., and Maenhaut, W. (2004) Formation of secondary organic aerosols through photooxidation of isoprene. *Science* 303: 1173-1176.
- Cleveland, C.C., and Yavitt, J.B. (1997) Consumption of atmospheric isoprene. *Geophys Res Lett* 24: 2379-2382.
- Cleveland, C.C., and Yavitt, J.B. (1998) Microbial consumption of atmospheric isoprene in a temperate forest soil. *Appl Environ Microbiol* 64: 172-177.
- Coleman, N.V., Bui, N.B., and Holmes, A.J. (2006) Soluble di-iron monooxygenase gene diversity in soils, sediments and ethene enrichments. *Environ Microbiol* 8: 1228-1239.
- Coleman, N.V., Yau, S., Wilson, N.L., Nolan, L.M., Migocki, M.D., Ly, M.-a., Crossett, B., and Holmes, A.J. (2011) Untangling the multiple monooxygenases of *Mycobacterium chubuense* strain NBB4, a versatile hydrocarbon degrader. *Environ Microbiol Rep* 3: 297-307.
- Conkle, J.P., Camp, B.J., and Welch, B.E. (1975) Trace composition of human respiratory gas. *Arch Environ Health* 30: 690-695.
- Copley, S.D. and Dhillon, J.K. (2002) lateral gene transfer and parallel evolution in the history of glutathione biosynthesis genes. *Genome Biol* 3: research 0025.1-0025.16.
- Cordoba, E., Salmi, M., and León, P. (2009) Unravelling the regulatory mechanisms that modulate the MEP pathway in higher plants. *J Exp Bot* 60: 2933-2943.

- Coufal, D.E., Blazyk, J.L., Whittington, D.A., Rosenzweig, A.C., and Lippard, S.J. (2000) Sequencing and analysis of the *Methylococcus capsulatus* (Bath) soluble methane monooxygenase genes. *Eur J Biochem* 267: 2174-2185.
- Crombie, A., and Murrell, J.C. (2011) Development of a system for genetic manipulation of the facultative methanotroph *Methylocella silvestris* BL2. *Methods Enzymol* 495: 119-133.
- Datta, N., Hedges, R.W., Shaw, E.J., Sykes, R.B., and Richmond, M.H. (1971) Properties of an R factor from *Pseudomonas aeruginosa*. *J Bacteriol* 108: 1244-1249.
- Delwiche, C.F., and Sharkey, T.D. (1993) Rapid appearance of ¹³C in biogenic isoprene when ¹³CO₂ is fed to intact leaves. *Plant Cell Environ* 16: 587-591.
- DeMaster, E.G., and Nagasawa, H.T. (1978) Isoprene, an endogenous constituent of human alveolar air with a diurnal pattern of excretion. *Life Sci* 22: 91-97.
- Deneris, E.S., Stein, R.A., and Mead, J.F. (1984) In vitro biosynthesis of isoprene from mevalonate utilizing a rat liver cytosolic fraction. *Biochem Biophys Res Commun* 123: 691-696.
- Dennis, J.J., and Zylstra, G.J. (1998) Plasposons: modular self-cloning minitransposon derivatives for rapid genetic analysis of Gram-negative bacterial genomes. *Appl Environ Microbiol* 64: 2710-2715.
- DeSantis, T.Z., Hugenholtz, P., Larsen, N., Rojas, M., Brodie, E.L., Keller, K., Huber, T., Dalevi, D., Hu, P., and Andersen, G.L. (2006) Greengenes, a Chimera-Checked 16S rRNA Gene Database and Workbench Compatible with ARB. *Appl Environ Microbiol* 72: 5069-5072
- Dlugokencky, E.J., Nisbet, E.G., Fisher, R., and Lowry, D. (2011) Global atmospheric methane: budget, changes and dangers. *Philos Trans A Math Phys Eng Sci* 369: 2058-2072.
- Donoso, L., Romero, R., Rondon, A., Fernandez, E., Oyola, P., and Sanhueza, E. (1996) Natural and anthropogenic C₂ to C₆ hydrocarbons in the central-eastern Venezuelan atmosphere during the rainy season. *J Atmos Chem* 25: 201-214.
- Dumont, M.G., Radajewski, S.M., Miguez, C.B., McDonald, I.R., and Murrell, J.C. (2006). Identification of a complete methane monooxygenase operon from soil by combining stable isotope probing and metagenomic analysis. *Environ Microbiol* 8: 1240-1250.
- Ekberg, A., Arneth, A., Hakola, H., Hayward, S., and Holst, T. (2009) Isoprene emission from wetland sedges. *Biogeosci* 6: 601-613.
- Engelhart, G.J., Moore, R.H., Nenes, A., and Pandis, S.N. (2011) Cloud condensation nuclei activity of isoprene secondary organic aerosol. *J Geophys Res* 116: D02207.
- Ensley, B.D. (1991) Biochemical diversity of trichloroethylene metabolism. *Annu Rev Microbiol* 45: 283-299.

- Euler, D.E., Davé, S.J., and Guo, H. (1996) Effect of cigarette smoking on pentane excretion in alveolar breath. *Clin Chem* 42: 303-308.
- Evans, R.C., Tingey, D.T., Gumpertz, M.L., and Burns, W.F. (1982) Estimates of isoprene and monoterpene emission rates in plants. *Bot Gaz* 143: 304-310.
- Ewers, J., Freier-Schroder, D. and Knackmuss, H.J. (1990) Selection of trichloroethene (TCE) degrading bacteria that resist inactivation by TCE. *Arch Microbiol* 154: 410-413.
- Fahey, R.C., Brown, W.C., Adams, W.B., and Worsham, M.B. (1978) Occurrence of glutathione in bacteria. *J Bacteriol* 133: 1126-1129.
- Fall, R., and Wildermuth, M.C. (1998) Isoprene synthase: From biochemical mechanism to emission algorithm. *J Geophys Res* 103: 25599–25609.
- Fall, R., and Copley, S.D. (2000) Bacterial sources and sinks of isoprene, a reactive atmospheric hydrocarbon. *Environ Microbiol* 2: 123-130.
- Fan, J., and Zhang, R. (2004) Atmospheric oxidation mechanism of isoprene. *Environ Chem* 1: 140-149.
- Fehsenfeld, F., Calvert, J., Fall, R., Goldan, P., Guenther, A.B., Hewitt, C.N., Lamb, B., Liu, S., Trainer, M., Westberg, H., and Zimmerman, P. (1992) Emissions of volatile organic compounds from vegetation and the implications for atmospheric chemistry. *Global Biogeochem Cycles* 6: 389-430.
- Fenske, J.D., and Paulson, S.E. (1999) Human breath emissions of VOCs. *J Air Waste Manag Assoc* 49: 594-598.
- Filipiak, W., Sponring, A., Baur, M.M., Filipiak, A., Ager, C., Wiesenhofer, H., Nagl, M., Troppmair, J., and Amann, A. (2012) Molecular analysis of volatile metabolites released specifically by *Staphylococcus aureus* and *Pseudomonas aeruginosa*. *BMC Microbiol* 12: 113.
- Fox, B.G., Borneman, J.G., Wackett, L.P., and Lipscomb, J.D. (1990) Haloalkene oxidation by the soluble methane monooxygenase from *Methylosinus trichosporium* OB3b: mechanistic and environmental implications. *Biochemistry* 29: 6419-6427.
- Fox, G.E., Wisotzkey, J.D., and Jurtshuk, P.Jr. (1992) How close is close: 16S rRNA sequence identity may not be sufficient to guarantee species identity. *Int J Syst Bacteriol* 42: 166-170.
- Fuentes, J. D., Wang, D., and Gu, L. (1999) Seasonal variations in isoprene emissions from a Boreal Aspen forest. *J Appl Meteorol* 38: 855-869.
- Funk, J.L., Jones, C.G., Baker, C.J., Fuller, H.M., Giardina, C.P., and Lerdau, M.T. (2003) Diurnal Variation in the Basal Emission Rate of Isoprene. *Ecol Appl* 13: 269-278.
- Gao, B., and Gupta, R.S. (2012) Phylogenetic framework and molecular signatures for the main clades of the phylum *Actinobacteria*. *Microbiol Mol Biol Rev* 76 (1): 66-112.

- Gelmont, D., Stein, R.A., and Mead, J.F. (1981) Isoprene-the main hydrocarbon in human breath. *Biochem Biophys Res Commun* 99: 1456-1460.
- Geron, C., Guenther, A., Sharkey, T., and Arnts, R.R. (2000) Temporal variability in basal isoprene emission factor. *Tree Physiol* 20: 799-805.
- Gershenson, J. (2008) Insects turn up their noses at sweating plants. *Proc Natl Acad Sci USA* 105: 17211-17212.
- Goldstein, A.H., Goulden, M.L., Munger, J.W., Wofsy, S.C., and Geron C.D. (1998) Seasonal course of isoprene emissions from a midlatitude deciduous forest. *J Geophys Res* 103: 31045-31056.
- Gounaris, K., Brain, A.R.R., Quinn, P.J., and Williams, W.P. (1984) Structural reorganisation of chloroplast thylakoid membranes in response to heat-stress. *Biochim Biophys Acta* 766: 198-208.
- Greenberg, J.P., Guenther, A.B., Pétron, G., Wiedinmyer, C., Vega, O., Gatti, L.V., Tota, J., and Fisch, G. (2004) Biogenic VOC emissions from forested Amazonian landscapes. *Glob Change Biol* 10: 651-662.
- Guenther, A., Hewitt, C.N., Erickson, D., Fall, R., Geron, C., Graedel, T., Harley, P., Klinger, L., Lerdau, M., McKay, W.A., Pierce, T., Scholes, B., Steinbrecher, R., Tallamraju, R., Taylor, J., and Zimmerman, P. (1995) A global model of natural volatile organic compound emissions. *J Geophys Res* 100: 8873-8892.
- Guenther, A., Karl, T., Harley, P., Wiedinmyer, C., Palmer, P.I., and Geron, C. (2006) Estimates of global terrestrial isoprene emissions using MEGAN (Model of Emissions of Gases and Aerosols from Nature). *Atmos Chem Phys* 6: 3181-3210.
- Haapanala, S., Rinne, J., Pystynen, K.-H., Hellén, H., Hakola, H., and Riutta, T. (2006) Measurements of hydrocarbon emissions from a boreal fen using the REA technique. *Biogeosci* 3: 103-112.
- Hallquist, M., Wenger, J.C., Baltensperger, U., Rudich, Y., Simpson, D., Claeys, M., Dommen, J., Donahue, N.M., George, C., Goldstein, A.H., Hamilton, J.F., Herrmann, H., Hoffmann, T., Iinuma, Y., Jang, M., Jenkin, M.E., Jimenez, J.L., Kiendler-Scharr, A., Maenhaut, W., McFiggans, G., Mentel, Th.F., Monod, A., Prévôt, A.S.H., Seinfeld, J.H., Surratt, J.D., Szmigielski, R., and Wildt, J. (2009) The formation, properties and impact of secondary organic aerosol: current and emerging issues. *Atmos Chem Phys* 9: 5155-5236.
- Hanson, D.T., Swanson, S., Graham, L.E., and Sharkey, T.D. (1999) Evolutionary significance of isoprene emission from mosses. *Am J Bot* 86: 634-639.
- Harley, P., Guenther, A., and Zimmerman, P. (1996) Effects of light, temperature and canopy position on net photosynthesis and isoprene emission from sweetgum (*Liquidambar styraciflua*) leaves. *Tree Physiol* 16: 25-32.
- Harley, P.C., Monson, R.K., and Lerdau, M.T. (1999) Ecological and evolutionary aspects of isoprene emission from plants. *Oecologia* 118: 109-123.
- Hausinger, R.P. (2007) New insights into acetone metabolism. *J Bacteriol* 189: 671-673.

Heald, C.L., Wilkinson, M.J., Monson, R.K., Alo, C.A., Wang, G., and Guenther, A. (2009) Response of isoprene emission to ambient CO₂ changes and implications for global budgets. *Global Change Biol* 15: 1127-1140.

Hellén, H.; Hakola, H.; Pystynen, K. H.; Rinne, J.; and Haapanala, S. (2006) C₂-C₁₀ hydrocarbon emissions from a boreal wetland and forest floor. *Biogeosci* 3: 167-174.

Herrmann, H., Müller, C., Schmidt, I., Mahnke, J., Petruschka, L., Hahnke, K. (1995) Localization and organization of phenol degradation genes of *Pseudomonas putida* strain H. *Mol Gen Genet* 247: 240-246.

Hewitt, C.N., MacKenzie, A.R., Di Carlo, P., Di Marco, C.F., Dorsey, J.R., Evans, M., Fowler, D., Gallagher, M.W., Hopkins, J.R., Jones, C.E., Langford, B., Lee, J.D., Lewis, A.C., Lim, S.F., McQuaid, J., Misztal, P., Moller, S.J., Monks, P.S., Nemitz, E., Oram, D.E., Owen, S.M., Phillips, G.J., Pugh, T.A., Pyle, J.A., Reeves, C.E., Ryder, J., Siong, J., Skiba, U., and Stewart, D.J. (2009) Nitrogen management is essential to prevent tropical oil palm plantations from causing ground-level ozone pollution. *Proc Natl Acad Sci USA* 106: 18447-18451.

Hiessl, S., Schuldes, J., Thurmer, A., Halbsguth, T., Broker, D., Angelov, A., Liebl, W., Daniel, R., and Steinbuchel, A. (2012) Involvement of two latex-cleaning proteins during rubber degradation and insights into the subsequent degradation pathway revealed by the genome sequence of *Gordonia polyisoprenivorans* strain VH2. *Appl Environ Microbiol* 78: 2874-2887.

Holder, J.W., Ulrich, J.C., DeBono, A.C., Godfrey, P.A., Desjardins, C.A., Zucker, J., Zeng, Q., Leach, A.L., Ghiviriga, I., Dancel, C., Abeel, T., Gevers, D., Kodira, C.D., Desany, B., Affourtit, J.P., Birren, B.W., and Sinskey, A.J. (2011) Comparative and functional genomics of *Rhodococcus opacus* PD630 for biofuels development. *PLoS Genet* 7: e1002219.

Holmes, A.J., and Coleman, N.V. (2008) Evolutionary ecology and multidisciplinary approaches to prospecting for monooxygenases as biocatalysts. *Antonie Van Leeuwenhoek* 94: 75-84.

Holmes, A. (2009). The diversity of soluble di-iron monooxygenases with bioremediation applications. In *Advances in Applied Bioremediation, Soil Biology* 17. Ajay Singh, Ramesh C. Kuhad, Owen P. Ward (eds.), Germany: Springer, pp. 91-102.

Huang, W.E., Ferguson, A., Singer, A.C., Lawson, K., Thompson, I.P., Kalin, R.M., Larkin, M.J., Bailey, M.J., Whiteley, A.S. (2009) Resolving genetic functions within microbial populations: in situ analyses using rRNA and mRNA stable isotope probing coupled with single-cell raman-fluorescence in situ hybridization. *Appl Environ Microbiol* 75: 234-241.

Huang, W.E., Li, M., Jarvis, R.M., Goodacre, R., and Banwart, S.A. (2010). Shining light on the microbial world: the application of Raman microspectroscopy. *Adv Appl Microbiol* 70: 153-186.

Hugenholtz, P., Tyson, G.W., Webb, R.I., Wagner, A.M., and Blackall, L.L. (2001) Investigation of candidate division TM7, a recently recognized major lineage of the

- domain Bacteria with no known pure culture representatives. *Appl Environ Microbiol* 67: 411-419.
- Hutchens, E., Radajewski, S., Dumont, M.G., McDonald, I.R., and Murrell, J.C. (2004) Analysis of methanotrophic bacteria in Movile Cave by stable isotope probing. *Environ Microbiol* 6: 111-120.
- Imai, S., Ichikawa, K., Muramatsu, Y., Kasai, D., Masai, E., and Fukuda, M. (2011) Isolation and characterization of *Streptomyces*, *Actinoplanes*, and *Methylibium* strains that are involved in degradation of natural rubber and synthetic poly(cis-1,4-isoprene). *Enzyme Microb Technol* 49: 526-531.
- Innis, M.A. and Gelfand, D.H. (1990) Optimization of PCRs. In PCR Protocols: A Guide to Methods and Applications. Gelfand, D.H., Sninsky, J.J., Innis, M.A., and White, H. (eds.), Academic Press, San Diego, CA, pp. 3-12.
- Jehmlich, N., Schmidt, F., Hartwich, M., von Bergen, M., Richnow, H.H., and Vogt, C. (2008a) Incorporation of carbon and nitrogen atoms into proteins measured by protein-based stable isotope probing (Protein-SIP). *Rapid Commun Mass Spectrom* 22: 2889-2897.
- Jehmlich, N., Schmidt, F., von Bergen, M., Richnow, H.H., and Vogt, C. (2008b) Protein-based stable isotope probing (Protein-SIP) reveals active species within anoxic mixed cultures. *ISME J* 2: 1122-1133.
- Jendrossek, D., and Reinhardt, S. (2003) Sequence analysis of a gene product synthesized by *Xanthomonas sp.* during growth on natural rubber latex. *FEMS Microbiol Lett* 224: 61-65.
- Jones, C.A., and Rasmussen, R.A. (1975) Production of isoprene by leaf tissue. *Plant Physiol* 55: 982-987.
- Julsing, M.K., Rijpkema, M., Woerdenbag, H.J., Quax, W.J., and Kayser, O. (2007) Functional analysis of genes involved in the biosynthesis of isoprene in *Bacillus subtilis*. *Appl Microbiol Biotechnol* 75: 1377-1384.
- Jurelevicius, D., Alvarez, V.M., Peixoto, R., Rosado, A.S., and Seldin, L. (2013) The use of a combination of alkB primers to better characterize the distribution of alkane-degrading Bacteria. *Plos One* 8: e66565.
- Karl, T., Prazeller, P., Mayr, D., Jordan, A., Rieder, J., Fall, R., and Lindinger, W. (2001) Human breath isoprene and its relation to blood cholesterol levels: new measurements and modeling. *J Appl Physiol* 91: 762-770.
- King, J., Kupferthaler, A., Unterkofler, K., Koc, H., Teschl, S., Teschl, G., Miekisch, W., Schubert, J., Hinterhuber, H., and Amann, A. (2009) Isoprene and acetone concentration profiles during exercise on an ergometer. *J Breath Res* 3: 027006.
- King, J., Kupferthaler, A., Frauscher, B., Hackner, H., Unterkofler, K., Teschl, G., Hinterhuber, H., Amann, A., and Högl, B. (2012) Measurement of endogenous acetone and isoprene in exhaled breath during sleep. *Physiol Meas* 33: 413-428.

Kirschke, S., Bousquet, P., Ciais, P., Saunois, M., Canadell, J.G., Dlugokencky, E.J., Bergamaschi, P., Bergmann, D., Blake, D.R., Bruhwiler, L., Cameron-Smith, P., Castaldi, S., Chevallier, F., Feng, L., Fraser, A., Heimann, M., Hodson, E.L., Houweling, S., Josse, B., Fraser, P.J., Krummel, P.B., Lamarque, J-F., Langenfelds, R.L., Le Quere, C., Naik, V., O'Doherty, S., Palmer, P.I., Pison, I., Plummer, D., Poulter, B., Prinn, R.G., Rigby, M., Ringeval, B., Santini, M., Schmidt, M., Shindell, D.T., Simpson, I.J., Spahni, R., Steele, L.P., Strode, S.A., Sudo, K., Szopa, S., Van Der Werf, G.R., Voulgarakis, A., Van Weele, M., Weiss, R.F., Williams, J.E., and Zeng, G. (2013) Three decades of global methane sources and sinks. *Nat Geosci* 6: 813-823.

Köksal, M., Zimmer, I., Schnitzler, J.P., and Christianson, D.W. (2010) Structure of isoprene synthase illuminates the chemical mechanism of teragram atmospheric carbon emission. *J Mol Biol* 402: 363-373.

Kotani, T., Yamamoto, T., Yurimoto, H., Sakai, Y., and Kato, N. (2003) Propane monooxygenase and NAD⁺-dependent secondary alcohol dehydrogenase in propane metabolism by *Gordonia sp.* strain TY-5. *J Bacteriol* 185: 7120-7128.

Kotani, T., Kawashima, Y., Yurimoto, H., Kato, N., and Sakai, Y. (2006) Gene structure and regulation of alkane monooxygenases in propane-utilizing *Mycobacterium sp.* TY-6 and *Pseudonocardia sp.* TY-7. *J Biosci Bioeng* 102: 184-192.

Kotani, T., Yurimoto, H., Kato, N., and Sakai, Y. (2007) Novel acetone metabolism in a propane-utilizing bacterium, *Gordonia sp.* strain TY-5. *J Bacteriol* 189: 886-893.

Kreuzwieser, J., Graus, M., Wisthaler, A., Hansel, A., Rennenberg, H., and Schnitzler, J-P. (2002) Xylem-transported glucose as an additional carbon source for leaf isoprene formation in *Quercus robur*. *New Phytologist* 156: 171-178.

Krishnakumar, A.M., Sliwa, D., Endrizzi, J.A., Boyd, E.S., Ensign, S.A., and Peters, W. (2008) Getting a handle on the role of coenzyme M in alkene metabolism. *Microbiol Mol Biol Rev* 72: 445-456.

Kriszt, B., Tánácsics, A., Cserhádi, M., Tóth, Á., Nagy, I., Horváth, B., Nagy, I., Tamura, T., Kukolya, J., and Szoboszlai, S. (2012) De novo genome project for the aromatic degrader *Rhodococcus pyridinivorans* strain AK37. *J Bacteriol* 194: 1247-1248.

Krum, J.G. and Ensign, S.A. (2000) Heterologous expression of bacterial epoxyalkane: coenzyme M transferase and inducible coenzyme M biosynthesis in *Xanthobacter autotrophicus* PY2 and *Rhodococcus rhodochrous* B276. *J Bacteriol* 182: 2629-2634.

Krum, J.G., and Ensign, S.A. (2001) Evidence that a linear megaplasmid encodes enzymes of aliphatic alkene and epoxide metabolism and coenzyme M (2-mercaptoethanesulfonate) biosynthesis in *Xanthobacter* strain Py2. *J Bacteriol* 183: 2172-2177.

- Kushch, I., Arendacká, B., Stolc, S., Mochalski, P., Filipiak, W., Schwarz, K., Schwentner, L., Schmid, A., Dzien, A., Lechleitner, M., Witkovský, V., Miekisch, W., Schubert, J., Unterkofler, K., and Amann, A. (2008) Breath isoprene-aspects of normal physiology related to age, gender and cholesterol profile as determined in a proton transfer reaction mass spectrometry study. *Clin Chem Lab Med* 46: 1011-1018.
- Kuzma, J., Fall, R. (1993) Leaf Isoprene Emission Rate Is Dependent on Leaf Development and the Level of Isoprene Synthase. *Plant Physiol* 101: 435-440.
- Kuzma, J., Nemecek-Marshall, M., Pollock, W.H., and Fall, R. (1995) Bacteria produce the volatile hydrocarbon isoprene. *Curr Microbiol* 30: 97-103.
- Lane, D.J. (1991) 16S/23S rRNA sequencing, pp. 115-147. In Stackebrandt E., and Goodfellow M. (Eds.), *Nucleic acid techniques in bacterial systematics*. JohnWiley & Sons, Inc., New York, N.Y.
- Laothawornkitkul, J., Paul, N.D., Vickers, C.E., Possell, M., Taylor, J.E., Mullineaux, P.M., and Hewitt, C.N. (2008) Isoprene emissions influence herbivore feeding decisions. *Plant Cell Environ* 31: 1410-1415.
- Larkin, M.J., Kulakov, L.A., and Allen, C.C. (2005) Biodegradation and *Rhodococcus* – masters of catabolic versatility. *Curr Opin Biotechnol* 16: 282-290.
- Leahy, J.G., Batchelor, P.J., and Morcomb, S.M. (2003) Evolution of the soluble diiron monooxygenases. *FEMS Microbiol Rev* 27: 449-479.
- Lechner, M., Moser, B., Niederseer, D., Karlseder, A., Holzknecht, B., Fuchs, M., Colvin, S., Tilg, H., and Rieder, J. (2006) Gender and age specific differences in exhaled isoprene levels. *Respir Physiol Neurobiol* 154: 478-483.
- Letek, M., Gonzalez, P., MacArthur, I., Rodriguez, H., Freeman, T.C., Valero-Rello, A., Blamco, M., Buckley, T., Cherevach, I., et al., (2010) The genome of a pathogenic *Rhodococcus*. Cooptive virulence underpinned by key gene acquisitions. *Plos Genet* 6: e1001145.
- Lewis, A.C.; Mcquaid, J.B.; Carslaw, N.; Pilling, M.J. (1999) Diurnal cycles of short-lived tropospheric alkenes at a North Atlantic coastal site. *Atmosph Environ* 33: 2417-2422.
- Lewis, A.C., Carpenter, L.J., and Pilling, M.J. (2001) Nonmethane hydrocarbons in Southern Ocean boundary layer air. *J Geophys Res* 106: 4987-4994.
- Lichtenthaler, H.K. (1999) The 1-deoxy-D-xylulose-5-phosphate pathway of isoprenoid biosynthesis in plants. *Annu Rev Plant Physiol Plant Mol Biol* 50: 47-65.
- Lindberg, P., Park, S., and Melis, A. (2010) Engineering a platform for photosynthetic isoprene production in cyanobacteria, using *Synechocystis* as the model organism. *Metab Eng* 12: 70-79.
- Logan, B.A., Monson, R.K., and Potosnak, M.J. (2000) Biochemistry and physiology of foliar isoprene production. *Trends Plant Sci* 5: 477-481.

- Loivamäki, M., Louis, S., Cinege, G., Zimmer, I., Fischbach, R.J., and Schnitzler, J.P. (2007) Circadian rhythms of isoprene biosynthesis in grey poplar leaves. *Plant Physiol* 143: 540-551.
- Loivamäki, M., Mumm, R., Dicke, M., and Schnitzler, J.P. (2008) Isoprene interferes with the attraction of bodyguards by herbaceous plants. *Proc Natl Acad Sci USA* 105:17430-17435.
- Loreto, F., and Sharkey, T.D. (1990) A gas-exchange study of photosynthesis and isoprene emission in *Quercus rubra* L. *Planta* 182: 523-531.
- Loreto, F., Mannozi, M., Maris, C., Nascetti, P., Ferranti, F., and Pasqualini, S. (2001) Ozone quenching properties of isoprene and its antioxidant role in leaves. *Plant Physiol* 126: 993-1000.
- Loreto, F., and Velikova, V. (2001) Isoprene produced by leaves protects the photosynthetic apparatus against ozone damage, quenches ozone products, and reduces lipid peroxidation of cellular membranes. *Plant Physiol* 127: 1781-1787
- Loreto, F., Pinelli, P., Brancaleoni, E., and Ciccioli, P. (2004) ¹³C labeling reveals chloroplastic and extrachloroplastic pools of dimethylallyl pyrophosphate and their contribution to isoprene formation. *Plant Physiol* 135: 1903-1907.
- Manefield, M., Whiteley, A.S., Griffiths, R.I., and Bailey, M.J. (2002) RNA stable isotope probing, a novel means of linking microbial community function to phylogeny. *Appl Environ Microbiol* 68: 5367-5373.
- Marmur, J. (1961) A procedure for the isolation of deoxyribonucleic acid from micro-organisms. *J Mol Biol* 3: 208-218.
- Martin, H., and Murrell, J.C. (1995) Methane monooxygenase mutants of *Methylosinus trichosporium* constructed by marker-exchange mutagenesis. *FEMS Microbiol Lett* 127: 243-248.
- Mattes, T.E., Coleman, N.V., Spain, J.C., and Gossett, J.M. (2005) Physiological and molecular genetic analyses of vinyl chloride and ethane degradation in *Nocardioides* sp. Strain JS614. *Arch Microbiol* 183: 95-106.
- Merkx, M., Kopp, D.A., Sazinsky, M.H., Blazyk, J.L., Müller, J., and Lippard, S.J. (2001) Dioxygen activation and methane hydroxylation by soluble methane monooxygenase: a tale of two irons and three proteins. *Angew Chem Int Ed Engl* 40: 2782-2807.
- McDonald, I.R., Kenna, E.M., and Murrell, J.C. (1995) Detection of methanotrophic bacteria in environmental samples with the PCR. *Appl Environ Microbiol* 61: 116-121.
- McLeod, M.P., Warren, R.L., Hsiao, W.W., Araki, N., Myhre, M., Fernandes, C., Miyazawa, D., Wong, W., Lillquist, A.L., Wang, D., Dosanjh, M., Hara, H., Petrescu, A., Morin, R.D., Yang, G., Stott, J.M., Schein, J.E., Shin, H., Smailus, D., Siddiqui, A.S., Marra, M.A., Jones, S.J., Holt, R., Brinkman, F.S., Miyauchi, K., Fukuda, M., Davies, J.E., Mohn, W.W., and Eltis, L.D. (2006) The complete genome

of *Rhodococcus sp.* RHA1 provides insights into a catabolic powerhouse. *Proc Natl Acad Sci USA* 103: 15582-15587.

Miller, B., Oschinski, C., and Zimmer, W. (2001) First isolation of an isoprene synthase gene from poplar and successful expression of the gene in *Escherichia coli*. *Planta* 213: 483-487.

Milne, P.J., Riemer, D.D., Zika R.G., and Brand, L.E. (1995) Measurement of vertical distribution of isoprene in seawater, its chemical fate, and its emission from several phytoplankton monocultures. *Mar Chem* 48: 237-244.

Miyoshi, A., Hatakeyama, S., and Washida, N. (1994) OH radical-initiated photooxidation of isoprene: an estimate of global CO production. *J Geophys Res* 99: 18779-18787.

Monson, R.K., and Fall, R. (1989) Isoprene emission from aspen leaves: influence of environment and relation to photosynthesis and photorespiration. *Plant Physiol* 90: 267-274.

Monson, R.K., Jaeger, C.H., Adams, W.W., Driggers, E.M., Silver, G.M., and Fall, R. (1992) Relationships among isoprene emission rate, photosynthesis, and isoprene synthase activity as influenced by temperature. *Plant Physiol* 98: 1175-1180.

Monson, R.K., Trahan, N., Rosenstiel, T.N., Veres, P., Moore, D., Wilkinson, M., Norby, R.J., Volder, A., Tjoelker, M.G., Briske, D.D., Karnosky, D.F., and Fall, R. (2007) Isoprene emission from terrestrial ecosystems in response to global change: minding the gap between models and observations. *Philos Trans A Math Phys Eng Sci* 365: 1677-1695.

Monson, R.K., Jones, R.T., Rosenstiel, T.N., and Schnitzler, J.P. (2013) Why only some plants emit isoprene. *Plant Cell Environ* 36: 503-516.

Moore, R.M., Oram, D.E., and Penkett, S.A. (1994) Production of isoprene by marine phytoplankton cultures. *Geophys Res Lett* 21: 2507-2510.

Morris, S.A., Radajewski, S., Willison, T.W., and Murrell, J.C. (2002) Identification of the functionally active methanotroph population in a peat soil microcosm by stable-isotope probing. *Appl Environ Microbiol* 68: 1466-1452.

Murrell, J.C., and Whiteley, A. (eds) (2011) Stable isotope probing and related technologies. Washington, DC: ASM press.

Muyzer, G., de Waal, E.C., and Uitterlinden, A.G. (1993) Profiling of complex microbial populations by denaturing gradient gel electrophoresis analysis of polymerase chain reaction-amplified genes coding for 16S rRNA. *Appl Environ Microbiol* 59: 695-700.

Nakicenovic, N. et al., (2000). Special report on emissions scenarios: a special report of working group III of the intergovernmental panel on climate change, Cambridge University Press, pp. 239–292.

- Nedwell D.B., (1996) Methane production and oxydation in soils and sediments, pp. 33–50. In: Murrell J.C., Kelly D.P. (Eds.), *Microbiology of Atmospheric Trace Gases*, Springer.
- Nelson, N., Lagesson, V., Nosratabadi, A.R., Ludvigsson, J., and Tagesson, C. (1998) Exhaled isoprene and acetone in newborn infants and in children with diabetes mellitus. *Pediatr Res* 44: 363-367.
- Nercessian, O., Noyes, E., Kalyuzhnaya, M.G., Lidstrom, M.E., and Chistoserdova, L. (2005) Bacterial populations active in metabolism of C1 compounds in the sediment of Lake Washington, a freshwater lake. *Appl Environ Microbiol* 71: 6885-6899.
- Neufeld, J.D., Vohra, J., Dumont, M.G., Lueders, T., Manefield, M., Friedrich, M.W., and Murrell, J.C. (2007) DNA stable-isotope probing. *Nat Protoc* 2: 860-866.
- Neufeld, J.D., Chen, Y., Dumont, M.G., and Murrell, J.C. (2008) Marine methylotrophs revealed by stable-isotope probing, multiple displacement amplification and metagenomics. *Environ Microbiol* 10: 1256-1535.
- Newton, G.L., Arnold, K., Price, M.S., Sherrill, C., Delcardayre, S.B., Aharonowitz, Y., Cohen, G., Davies, J., Fahey, R.C., and Davis, C. (1996) Distribution of thiols in microorganisms: mycothiol is a major thiol in most actinomycetes. *J Bacteriol* 178: 1990-1995.
- Notomista, E., Lahm, A., Di Donato, A., and Tramontano, A. (2003) Evolution of bacterial and archaeal multicomponent monooxygenases. *J Mol Evol* 56: 435-445.
- Pacifico, F., Harrison, S.P., Jones, C.D., and Sitch, S. (2009) Isoprene emission and climate. *Atmos Environ* 43: 6121-6135.
- Pacifico, F., Folberth, G.A., Jones, C.D., Harrison, S.P., and Collins, W.J. (2012) Sensitivity of biogenic isoprene emissions to past, present, and future environmental conditions and implications for atmospheric chemistry. *J Geophys Res* 117: D22302.
- Palmer, P. I., and Shaw, S.L. (2005) Quantifying global marine isoprene fluxes using MODIS chlorophyll observations. *Geophys Res Lett* 32: L09805.
- Partensky, F., Hess, W.R., and Vaultot, D. (1999) *Prochlorococcus*, a marine photosynthetic prokaryote of global significance. *Microbiol Mol Biol Rev* 63: 106-127.
- Peter, H., Wiegand, H.J., Bolt, H.M., Greim, H., Walter, G., Berg, M., and Filser, J.G. (1987) Pharmacokinetics of isoprene in mice and rats. *Toxicol Lett* 36: 9-14.
- Poisson, N., Kanakidou, M., and Crutzen, P.J. (2000) Impact of non-methane hydrocarbons on tropospheric chemistry and the oxidizing power of the global troposphere: 3-dimensional modelling results. *J Atmos Chem* 36: 157-230.
- Potosnak, M.J., Baker, B.M., LeSturgeon, L., Disher, S.M., Griffin, K.L., Bret-Harte, M.S., and Starr, G. (2013) Isoprene emissions from a tundra ecosystem. *Biogeosciences* 10: 871-889.

- Priefert, H., O'Brien, X.M., Lessard, P.A., Dexter, A.F., Choi, E.E., Tomic, S., Nagpal, G., Cho, J.J., Agosto, M., Yang, L., Treadway, S.L., Tamashiro, L., Wallace, M., and Sinsky, A.J. (2004) Indene bioconversion by a toluene inducible dioxygenase of *Rhodococcus* sp. I24. *Appl Microbiol Biotechnol* 65: 168-176.
- Pulido, P., Perello, C., and Rodriguez-Concepcion, M. (2012) New insights into plant isoprenoid metabolism. *Mol Plant* 5: 964-967.
- Radajewski, S., Ineson, P., Parekh, N.R., and Murrell, J.C. (2000) Stable-isotope probing as a tool in microbial ecology. *Nature* 403: 646-649.
- Rasmussen, R.A., and Went, F.W. (1965) Volatile organic material of plant origin in the atmosphere. *Proc Natl Acad Sci USA* 53: 215-220.
- Rasmussen, R.A. (1970) Isoprene: identified as a forest-type emission to the atmosphere. *Environ Sci Technol* 4: 667-671.
- Rasulov, B., Hüve, K., Vålbe, M., Laisk, A., Niinemets, U. (2009) Evidence that light, carbon dioxide, and oxygen dependencies of leaf isoprene emission are driven by energy status in hybrid aspen. *Plant Physiol* 151: 448-460.
- Rasulov, B., Hüve, K., Bichele, I., Laisk, A., and Niinemets, U. (2010) Temperature response of isoprene emission in vivo reflects a combined effect of substrate limitations and isoprene synthase activity: a kinetic analysis. *Plant Physiol* 154: 1558-1570.
- Reimann, S., Calanca, P., and Hofer, P. (2000) The anthropogenic contribution to isoprene concentrations in a rural atmosphere. *Atmos Environ* 34: 109-115.
- Rinne, H.J.I., Guenther, A.B., Greenberg, J.P., and Harley, P.C. (2002) Isoprene and monoterpene fluxes measured above Amazonian rainforest and their dependence on light and temperature. *Atmos Environ* 36: 2421-2426
- Rose, K., Tenberge, K.B., and Steinbuchel, A. (2005) Identification and characterization of genes from *Streptomyces* sp. Strain K30 responsible for clear zone formation on natural rubber latex and poly(cis-1,4-isoprene) rubber degradation. *Biomacromolecules* 6: 180-188.
- Rosenstiel, T.N., Fisher, A.J., Fall, R., and Monson, R.K. (2002) Differential accumulation of dimethylallyl diphosphate in leaves and needles of isoprene- and methylbutenol-emitting and nonemitting species. *Plant Physiol* 129: 1276-1284.
- Rosenstiel, T.N., Potosnak, M.J., Griffin, K.L., Fall, R., and Monson, R.K. (2003) Increased CO₂ uncouples growth from isoprene emission in an agriforest ecosystem. *Nature* 421: 256-259.
- Rosenzweig, A.C., Frederick, C.A., Lippard, S.J., and Nordlund, P. (1993) Crystal structure of a bacterial non-haem iron hydroxylase that catalyses the biological oxidation of methane. *Nature* 366: 537-543.
- Saeki, H., and Furuhashi, K. (1994) Cloning and characterization of a *Nocardia corallina* B-276 gene cluster encoding alkene monooxygenase. *J Ferment Bioeng* 78: 399-406.

- Salerno-Kennedy, R., and Cashman, K.D. (2005) Potential applications of breath isoprene as a biomarker in modern medicine: a concise overview. *Wien Klin Wochenschr* 117: 180-186.
- Sanadze, G.A. (1957) Emission of organic matters by leaves of Robinia pseudoacacia L. *Soobsh Acad Nauk GSSR* 19:83.
- Sanadze, G.A. (1991) Isoprene effect: light dependent emission of isoprene by green parts of plants pp. 135–152. In: Sharkey T.D., Holland E.A., Mooney H.A., editors. Trace gas emissions by plants. San Diego, CA: Academic Press.
- Sanadze, G.A. (2004) Biogenic isoprene (a review) *Russian Journal of Plant Physiology* 51: 729-741.
- Sanderson, M.G., Jones, C.D., Collins, W.J., Johnson, C.E., and Derwent, R.G. (2003) Effect of climate change on isoprene emissions and surface ozone levels. *Geophys Res Lett* 30: 1936.
- Sasaki, K., Ohara, K., and Yazaki, K. (2005) Gene expression and characterization of isoprene synthase from *Populus alba*. *FEBS Lett* 579: 2514-2518.
- Sayavedra-Soto, L.A., Doughty, D.M., Kurth, E.G., Bottomley, P.J., and Arp, D.J. (2005) Product and product-independent induction of butane oxidation in *Pseudomonas butanovora*. *FEMS Microbiol Lett* 250: 111-116.
- Sazinsky, M.H., and Lippard, S.J. (2006) Correlating structure with function in bacterial multicomponent monooxygenases and related diiron proteins. *Acc Chem Res* 39: 558-566
- Schäfer, A., Tauch, A., Jäger, W., Kalinowski, J., Thierbach, G., and Pühler, A. (1994) Small mobilizable multi-purpose cloning vectors derived from the *Escherichia coli* plasmids pK18 and pK19: selection of defined deletions in the chromosome of *Corynebacterium glutamicum*. *Gene* 145: 69-73.
- Schnitzler, J.P., Graus, M., Kreuzwieser, J., Heizmann, U., Rennenberg, H., Wisthaler, A., and Hansel, A. (2004) Contribution of different carbon sources to isoprene biosynthesis in poplar leaves. *Plant Physiol* 135: 152-160.
- Schöller, C., Molin, S., and Wilkins, K. (1997) Volatile metabolites from some gram-negative bacteria. *Chemosphere* 35: 1487-1495.
- Schöller, C.E., Gürtler, H., Pedersen, R., Molin, S., and Wilkins, K. (2002) Volatile metabolites from actinomycetes. *J Agric Food Chem* 50: 2615-2621.
- Schrader, S.M., Wise, R.R., Wacholtz, W.F., Ort, D.R., and Sharkey, T.D. (2004) Thylakoid membrane responses to moderately high leaf temperature in Pima cotton. *Plant Cell Environ* 27: 725-735.
- Seemann, T. (2014) Prokka: rapid prokaryotic genome annotation. *Bioinformatics* 30: 2068-2069.
- Selbitschka, W., Niemann, S., and Pühler, A. (1993) Construction of gene replacement vectors for Gram - bacteria using a genetically modified *sacRB* gene as a positive selection marker. *Appl Microbiol Biotechnol* 38: 615-618.

- Sharkey, T.D., Holland, E.A., Mooney, H.A., eds (1991) Trace Gas Emissions by Plants. Academic Press, San Diego, CA.
- Sharkey, T.D., and Loreto, F. (1993) Water stress, temperature, and light effects on the capacity for isoprene emission and photosynthesis of kudzu leaves. *Oecologia* 95: 328–333.
- Sharkey, T.D. (1996a) Isoprene synthesis by plants and animals. *Endeavour* 20: 74-78.
- Sharkey, T.D., Singaas, E.L., Vanderveer, P.J., and Geron, C. (1996b) Field measurements of isoprene emission from trees in response to temperature and light. *Tree Physiol* 16: 649-654.
- Sharkey, T.D., Chen, X.Y., and Yeh, S. (2001) Isoprene increases thermotolerance of fosmidomycin-fed leaves. *Plant Physiol* 125:2001-2006.
- Sharkey, T.D., and Yeh, S. (2001) Isoprene emission from plants. *Annu Rev Plant Physiol Plant Mol Biol* 52: 407-436.
- Sharkey, T.D., Wiberley, A.E., and Donohue, A.R. (2008) Isoprene emission from plants: why and how. *Ann Bot* 101: 5-18.
- Sharp, J.O., Sales, C.M., LeBlanc, J.C., Liu, J., Wood, T.K., Eltis, L.D., Mohn, W.W., and Alvarez-Cohen, L. (2007) An inducible propane monooxygenase is responsible for N-nitrosodimethylamine degradation by *Rhodococcus sp.* strain RHA1. *Appl Environ Microbiol* 73: 6930-6938.
- Shaw, S.L., Chisholm, S.W., and Prinn, R.G. (2003) Isoprene production by *Prochlorococcus*, a marine cyanobacterium, and other phytoplankton. *Mar Chem* 80: 227-245.
- Shaw, S.L., Gantt, B., and Meskhidze, N. (2010) Production and emissions of marine isoprene and monoterpenes: a review. *Adv Meteorol* 2010: ID408696.
- Silver, G.M., and Fall, R. (1991) Enzymatic synthesis of isoprene from dimethylallyl diphosphate in aspen leaf extracts. *Plant Physiol* 97: 1588-1591.
- Silver, G.M., and Fall, R. (1995) Characterization of aspen isoprene synthase, an enzyme responsible for leaf isoprene emission to the atmosphere. *J Biol Chem* 270: 13010-13016.
- Simon, R., Priefer, U., and Pühler, A. (1983) A broad host range mobilization system for in-vivo genetic engineering - Transposon mutagenesis in Gram-negative bacteria. *Bio-Technology* 1: 784-791.
- Singaas, E.L., Lerdau, M., Winter, K., and Sharkey, T.D. (1997) isoprene increases thermotolerance of isoprene-emitting species. *Plant Physiol* 115: 1413-1420
- Singaas, E.L., and Sharkey, T.D. (2000) The effect of high temperature on isoprene synthesis in oak leaves. *Plant Cell Environ* 23: 751-757.

- Sivy, T.L., Shirk, M.C., and Fall, R. (2002) Isoprene synthase activity parallels fluctuations of isoprene release during growth of *Bacillus subtilis*. *Biochem Biophys Res Commun* 294: 71-75.
- Siwko, M.E., Marrink, S.J., de Vries, A.H., Kozubek, A., Schoot Uiterkamp, A.J., and Mark, A.E. (2007) Does isoprene protect plant membranes from thermal shock? A molecular dynamics study. *Biochim Biophys Acta* 1768: 198-206.
- Smith, T.J., Slade, S.E., Burton, N.P., Murrell, J.C., and Dalton, H. (2002) An improved system for protein engineering of the hydroxylase component of soluble methane monooxygenase. *Appl Env Microbiol* 68: 5265-5273.
- Stainthorpe, A.C., Lees, V., Salmond, G.P.C., Dalton, H., and Murrell, J.C. (1990) The methane monooxygenase gene cluster of *Methylococcus capsulatus* (Bath). *Gene* 91: 27-34.
- Stone, D., Whalley, L.K., Heard, D.E. (2012) OH and HO₂ radicals: field measurements and model comparisons. *Chem Soc Rev* 41: 6348-6404.
- Sun, Z., Niinemets, Ü., Hüve, K., Rasulov, B., and Noe, S.M. (2013) Elevated atmospheric CO₂ concentration leads to increased whole-plant isoprene emission in hybrid aspen (*Populus tremula* × *Populus tremuloides*). *New Phytol* 198: 788-800.
- Taalman, R.D. (1996) Isoprene: background and issues. *Toxicology* 113: 242-246.
- Tamura, K., Dudley, J., Nei, M., and Kumar, S. (2007) MEGA4: Molecular evolutionary genetics analysis (MEGA) software version 4.0. *Mol Biol Evol* 24: 1596-1599.
- Tamura, K., Stecher, G., Peterson, D., Filipski, A., and Kumar, S. (2013) MEGA6: Molecular evolutionary genetics analysis (MEGA) software version 6.0. *Mol Biol Evol* 30: 2725-2729.
- Tan, H.M., Tang, H.Y., Joannou, C.L., Abdel-Wahab, N.H. and Mason, J.R. (1993) The *Pseudomonas putida* ML2 plasmid-encoded genes for benzene dioxygenase are unusual in codon usage and low in G+C content. *Gene* 130: 33-39.
- Taucher, J., Hansel, A., Jordan, A., Fall, R., Futrell, J.H., and Lindinger, W. (1997) Detection of isoprene in expired air from human subjects using proton-transfer-reaction mass spectrometry. *Rapid Commun Mass Spectrom* 11: 1230-1234.
- Taylor, R.T., Hanna, M.L., Shah, N.N., Shonnard, D.R., Duba, A.G., Durham, W.B., Jackson, K.J., Knapp, R.B., Wijesinghe, A.M., Knezovich, J.P., and Jovanovich, M.C. (1993) In situ bioremediation of trichloroethylene-contaminated water by a resting-cell methanotrophic microbial filter. *Hydrol Sci J* 38: 323-342.
- Theisen, A.R., Ali, M.H., Radajewski, S., Dumont, M.G., Dunfield, P.F., McDonald, I.R. et al. (2005) Regulation of methane oxidation in the facultative methanotroph *Methylocella silvestris* BL2. *Mol Microbiol* 58: 682-692.
- Tingey, D.T., Evans, R., and Gumpertz, M. (1981) Effects of environmental conditions on isoprene emission from live oak. *Planta* 152: 565-570.

- Tingey, D.T., Evans, R.C., Bates, E.H., and Gumpertz, M.L. (1987) Isoprene emissions and photosynthesis in three ferns – the influence of light and temperature. *Physiol Plant* 69: 609-616.
- Trojanowski, J., Haider, K., and Sundman, V. (1977) Decomposition of ¹⁴C-labelled lignin and phenols by a *Nocardia* sp. *Arch Microbiol* 114: 149-153.
- Trowbridge, A.M., Asensio, D., Eller, A.S., Way, D.A., Wilkinson, M.J., Schnitzler, J.P., Jackson, R.B., and Monson, R.K. (2012) Contribution of various carbon sources toward isoprene biosynthesis in poplar leaves mediated by altered atmospheric CO₂ concentrations. *PLoS One* 7: e32387.
- Uhlik, O., Leewis, M-C., Strejcek, M., Musilova, L., Mackova, M., Leigh, M.B., and Macek, T. (2013) Stable isotope probing in the metagenomics era: a bridge towards improved bioremediation. *Biotechnol Adv* 31: 154-165.
- van Beilen, J.B, and Funhoff, E.G. (2007) Alkane hydroxylases involved in microbial alkane degradation. *Appl Microbiol Biotechnol* 74: 13-21.
- van Ginkel, C.G., de Jong, E., Tilanus, J.W.R. and de Bont, J.A.M. (1987) Microbial oxidation of isoprene, a biogenic foliage volatile and of 1,3-butadiene, an anthropogenic gas. *FEMS Microbiol Lett* 45: 275-279.
- van Hylckama Vlieg, J.E., Kingma, J., vandenWijngaard, A.J., and Janssen, D.B. (1998) A glutathione S-transferase with activity towards cis-1,2-dichloroepoxyethane is involved in isoprene utilization by *Rhodococcus* sp. strain AD45. *Appl Environ Microbiol* 64: 2800-2805.
- van Hylckama Vlieg, J.E., Kingma, J., Kruizinga, W., and Janssen, D.B. (1999) Purification of a glutathione S-transferase and a glutathione conjugate-specific dehydrogenase involved in isoprene metabolism in *Rhodococcus* sp. strain AD45. *J Bacteriol* 181: 2094-2101.
- van Hylckama Vlieg, J.E.T., Leemhuis, H., Spelberg, J.H.L. and Janssen, D.B. (2000) Characterization of the gene cluster involved in isoprene metabolism in *Rhodococcus* sp. strain AD45. *J Bacteriol* 182: 1956-1963.
- Velikova, V., Várkonyi, Z., Szabó, M., Maslenkova, L., Nogues, I., Kovács, L., Peeva, V., Busheva, M., Garab, G., Sharkey, T.D., and Loreto, F. (2011) Increased thermostability of thylakoid membranes in isoprene-emitting leaves probed with three biophysical techniques. *Plant Physiol* 157: 905-916.
- Vickers, C.E., Possell, M., Cojocariu, C.I., Velikova, V.B., Laothawornkitkul, J., Ryan, A., Mullineaux, P.M., and Nicholas, N.C. (2009) Isoprene synthesis protects transgenic tobacco plants from oxidative stress. *Plant Cell Environ* 32: 520-531.
- Vickers, C.E., Possell, M., Hewitt, N.C., and Mullineaux, P.M. (2010) Genetic structure and regulation of isoprene synthase in Poplar (*Populus* spp.). *Plant Mol Biol* 73: 547-558.
- Vos, M., Quince, C., Pijl, A.S., de Hollander, M., and Kowalchuk, G.A. (2012) A comparison of rpoB and 16S rRNA as markers in pyrosequencing studies of bacterial diversity. *PLoS One* 7: e30600.

- Wagner, W.P., Nemecek-Marshall, M., and Fall, R. (1999) Three distinct phases of isoprene formation during growth and sporulation of *Bacillus subtilis*. *J Bacteriol* 181: 4700-4703.
- Wagner, W.P., Helmig, D., and Fall, R. (2000) Isoprene biosynthesis in *Bacillus subtilis* via the methylerythritol phosphate pathway. *J Nat Prod* 63: 37-40.
- Wagner, P., and Kuttler, W. (2014) Biogenic and anthropogenic isoprene in the near-surface urban atmosphere--a case study in Essen, Germany. *Sci Total Environ* 475: 104-115.
- Wang, W., and Lippard, S.J. (2014) Diiron oxidation state control of substrate access to the active site of soluble methane monooxygenase mediated by the regulatory component. *J Am Chem Soc* 136: 2244-2247.
- Watanabe, K., Teramoto, M., Futamata, H., and Harayama, S. (1998) Molecular detection, isolation, and physiological characterization of functionally dominant phenol-degrading bacteria in activated sludge. *Appl Environ Microbiol* 64: 4396-402.
- Watson, W.P., Cottrell, L., Zhang, D., and Golding, B.T. (2001) Metabolism and molecular toxicology of isoprene. *Chem Biol Interact* 135-136: 223-238.
- Whyte, L.G., Smits, T.H., Labbé, D., Witholt, B., Greer, C.W., and van Beilen, J.B. (2002) Gene cloning and characterization of multiple alkane hydroxylase systems in *Rhodococcus* strains Q15 and NRRL B-16531. *Appl Environ Microbiol* 68: 5933-5942.
- Wiberley, A.E., and Donohue, A.R. (2008) Isoprene emission from plants: why and how. *Ann Bot* 101: 5-18.
- Wiberley, A.E., Donohue, A.R., Westphal, M.M., and Sharkey, T.D. (2009) Regulation of isoprene emission from poplar leaves throughout a day. *Plant Cell Environ* 32: 939-947.
- Wiedinmyer, C., Tie, X., Guenther, A., Neilson, R., and Granier, C. (2006) Future changes in biogenic isoprene emissions: how might they affect regional and global atmospheric chemistry?. *Earth Interact* 10: 1-19.
- Wolfertz, M., Sharkey, T.D., Boland, W., and Kühnemann, F. (2004) Rapid regulation of the methylerythritol 4-phosphate pathway during isoprene synthesis. *Plant Physiol* 135: 1939-1945.
- Woods, N.R., and Murrell, J.C. (1989) The metabolism of propane in *Rhodococcus rhodochrous* PNKb1. *J Gen Microbiol* 135: 2335-2344.
- Yang, X., Xue, R., Shen, C., Li, S., Gao, C., Wang, W., and Zhao, X. (2011) Genome sequence of *Rhodococcus* sp. strain R04, a polychlorinated-biphenyl biodegrader. *J Bacteriol* 193: 5032-5033.
- Yen, K.M., Karl, M.R., Blatt, L.M., Simon, M.J., Winter, R.B., Fausset, P.R., Lu, H.S., Harcourt, A.A., and Chen, K.K. (1991) Cloning and characterization of a *Pseudomonas mendocina* KR1 gene cluster encoding toluene-4-monooxygenase. *J Bacteriol* 173: 5315-5327.

Yen, K.M., and Karl, M.R. (1992) Identification of a new gene, *tmoF*, in the *Pseudomonas mendocina* KR1 gene cluster encoding toluene-4-monooxygenase. *J Bacteriol* 174: 7253-7261.

Yikmis, M., and Steinbüchel, A. (2012) Historical and recent achievements in the field of microbial degradation of natural and synthetic rubber. *Appl Environ Microbiol* 78: 4543-4551

Zeidler, J., Schwender, J., Mueller, C., Wiesner, J., Weidemeyer, C., Beck, E., Jomaa, H., and Lichtenthaler, H.K. (1998) Inhibition of the non-mevalonate 1-deoxy-D-xylulose-5-phosphate pathway of plant isoprenoid biosynthesis by fosmidomycin. *Z Naturforsch C* 53: 980-986.

Zhao, Y., Yang, J., Qin, B., Li, Y., Sun, Y., Su, S., and Xian., M. (2011) Biosynthesis of isoprene in *Escherichia coli* via methylerythritol phosphate (MEP) pathway. *Appl Microbiol Biotechnol* 90: 1915-1922.

Zhao, L., Chang, W-C., Xiao, Y., Liu, H-W., Liu, P. (2013) Methylerythritol phosphate pathway of isoprenoid biosynthesis. *Ann Rev Biochem* 82: 497-530.

Zhou, N.Y., Jenkins, A., Chan Kwo Chion, C.K. and Leak, D.J. (1999) The alkene monooxygenase from *Xanthobacter* strain Py2 is closely related to aromatic monooxygenases and catalyzes aromatic monohydroxylation of benzene, toluene, and phenol. *Appl Environ Microbiol* 65: 1589-1595.

Ziemann, P.J., and Atkinson, R. (2012) Kinetics, products, and mechanisms of secondary organic aerosol formation. *Chem Soc Rev* 41: 6582-6605.